CHARACTERISATION OF HUMAN HOLOCARBOXYLASE SYNTHETASE

by

LISA MARIE BAILEY, B.Biotech(Hons)

A thesis submitted to the University of Adelaide, South Australia in fulfilment of the requirements for the degree of Doctor of Philosophy

School of Molecular and Biomedical Science
The University of Adelaide
Adelaide, South Australia, 5005

December 2008

Abstract

Biotin (also known as vitamin H or vitamin B7) is an essential micronutrient that is utilised by all living organisms. A key enzyme in the lifecycle of biotin is biotin protein ligase (BPL). BPL catalyses the attachment of biotin onto the biotin-requiring enzymes, a family of enzymes that play important roles in essential pathways such as fatty acid synthesis, gluconeogenesis and amino acid metabolism. Whilst there is a catalytic core conserved among the BPLs of all species, the N-terminal region of the molecule varies considerably in length and function. Mammalian BPL, commonly referred to as holocarboxylase synthetase, contains a large N-terminal extension not present in prokaryotes. The function and significance of this N-terminal extension is not understood. The aim of this project was to examine the function of the N-terminal portion of human holocarboxylase synthetase (referred to as HCS).

To date, no crystal structure for HCS has been reported. Insights into the enzyme have come from mutagenesis and proteolytic mapping of eukaryotic BPLs. For example, yeast BPL has a large N-terminal extension analogous to HCS. Previous work in our laboratory has investigated yeast BPL by mapping the domain structure using limited proteolysis. It has been shown that the N-terminus plays a critical role in catalysis as its removal renders the enzyme inactive (Polyak *et al.*, 1999). A similar approach has been applied to map the domain boundaries in HCS. Work by others in our laboratory showed the N-terminal extension of HCS consisted of up to three domains: Met^{1}-Ala^{80}, Ala^{80}-Glu^{151} and Lys^{160}-Asp^{311}, joined by two protease sensitive linker regions between Glu^{151} to Lys^{160}, and Lys^{312} to Glu^{336}.

In this study four polyclonal antibodies, raised against peptide epitopes from different regions of HCS, were affinity purified for characterisation. All antibodies detected multiple

isoforms of HCS by Western Blot analysis upon extracts of human embryonic kidney cells. Mass spectrometry determined that these isoforms varied at their N-terminus.

To investigate if the HCS isoforms are subjected to differential localisation into subcellular compartments, three approaches were attempted: immunocytochemistry, overexpression of GFP-tagged HCS and subcellular fractionation followed by Western Blotting. All methods showed all isoforms of HCS localised primarily in the cytosolic fraction, implying that processing of the protein alone is not responsible for determining HCS localisation.

A novel approach to examine potential protein binding partners, based on the work of Choi-Ree *et al*. (2004), using an engineered HCS variant was attempted. Whilst no novel binding partners were identified, studies with this HCS variant revealed intramolecular interactions occurring between the N- and C-terminal portions of the enzyme, which was confirmed by Yeast Two Hybrid Assay.

Multiple Carboxylase Deficiency (MCD) is a disease caused by a defect in biotin metabolism. The more severe neonatal form of the disease is caused by reduced HCS activity, which subsequently affects biotinylation of all the biotin-dependent enzymes.
To examine the critical role of the N-terminus of HCS in biotin metabolism, two fibroblast cell lines isolated from MCD patients who responded poorly to biotin therapy were investigated. Genotyping revealed that the patients were homozygous for the L216R mutation in the N-terminal extension. The patients' fibroblasts had a reduced proliferation rate compared to wildtype cells, and when grown in biotin-deficient media, were less able to respond to the re-addition of biotin. Whilst the HCS mRNA transcript was readily detected in MCD cell lines, protein and enzyme activity could not be detected, implying mutation of this single residue does have drastic effects on protein stability and function. Overexpression studies revealed that wildtype and mutant proteins localise to the same cellular compartments but enzyme activity was severely compromised for HCS-L216R

and could not be elevated by additional biotin. Furthermore, the turn-over rate for the mutant protein was double that of wildtype HCS. These results help to provide a molecular explanation for the incomplete biotin responsiveness of the MCD condition in patients with the HCS-L216R mutation, and imply that this region of the enzyme is critical for HCS function.

Finally, HCS has been implicated in other cellular processes, such as histone modification. Biotinylation is a new class of histone modification which has been reported in the literature. The most common method of analysis of histone biotinylation is the use of streptavidin as a probe, exploiting the strong non-covalent interaction of avidin for biotin. However studies presented in the thesis show that streptavidin should not be used for analysis of histone biotinylation, as it binds to histones independently of biotin. In a biotin-depletion cell culture system, the amount of streptavidin-reactive material in histone extracts, as examined by Western Blotting, was not affected by biotin availability. This was despite the biotin-depletion treatment reducing cell viability and biotinylation of biotin-dependent carboxylases. Blocking biotin binding sites on streptavidin with free biotin prior to Western Blot analysis did not affect histone binding. In contrast, the biotin-containing protein Pyruvate Carboxylase, was not detected by streptavidin that was pre-incubated with biotin. Finally, cells grown in biotin deficient media supplemented with ^{14}C labelled biotin failed to incorporate biotin onto histone proteins, whereas biotin incorporation onto biotin-dependent carboxylases was readily detected. These results suggest that histone biotinylation may be an artefactual observation, and that streptavidin is not an appropriate tool to measure the dynamics of biotin transfer on and off histone proteins. Analysis with methods which do not rely on secondary detection systems, such as mass spectrometry, will provide the most powerful evidence for histone biotinylation occurring as a physiologically relevant modification.

Statement of Originality

This work contains no material which has been accepted for the award of any other degree or diploma in any university or other tertiary institution and, to the best of my knowledge and belief, contains no material previously published or written by another person, except where due reference has been made in the text.

I give consent to this copy of my thesis when deposited in the University Library, being made available for loan and photocopying, subject to the provisions of the Copyright Act 1968.

Signed

…….....

Lisa Marie Bailey

Acknowledgments

My sincerest gratitude goes to my supervisors Prof. John Wallace, Dr Steven Polyak and Dr Grant Booker for their never-ending guidance, encouragement and support.

It's been an honour to work with John, who was always supportive and gave me the freedom to explore and develop ideas. I'm grateful to him for sharing his patience, persistence, extensive knowledge, and occasional glass of red wine with me. I'd like particularly to thank Steven, who gave me my first opportunity, hiring me to work initially as a research assistant in the lab. It was my first taste of the mysterious world of a vitamin until then I'd barely heard of! I'd like to thank you Steven, for encouraging me to continue studying and take up my PhD. Over the subsequent years, no matter how the experiments were going at the time, I always felt so much more enthused and confident after talking things through with you. I'll be forever grateful for that, and none of this work would have been possible without your patience, guidance and friendship.

I'd like to thank Sarawut "Yui" Jitrapakdee for all his helpful comments and reading of manuscripts, and introducing me to the world of Korean BBQ cuisine. I'd also like to thank Prof Murray Whitelaw for advice on manuscripts, and for providing the plasmids and cell lines necessary for the tetracycline-repressible expression studies.

I'm grateful to Dr Callum Wilson, Starship Childrens Hospital, Auckland NZ, for providing MCD fibroblasts and his advice on manuscripts, and to Dr Tim Rayner for encouragement through my honours year and for donating wild-type fibroblasts for use in this study.

I'd also like to thank Dr Roy Gravel and Shannon Healy, at the University Of Calgary, Canada for their assistance with histone extraction and biotin-depletion methods, and for kindly hosting me in their lab for a short time.

Of course it's the people you work with that make life in the lab liveable. Big thanks go out to all the past and present BPL crew. To Nicole Pendini, thanks for letting me use your hard-purified ligases and biotin domains, and for being my BPL buddy. I'll drink a toast (with red champagne of course!) to you finding those crystals! Thanks to Daniel Bird for all his help with the work on the chimera proteins, and for always being there to play with the dry ice when it came in. My thanks to Ruby Ivanov for all her help with work on the L216R mutant, to Lungisa Mayende for continuing the yeast two hybrid work, and to Belinda Ng for continuing the BPL assay development. I'd like to thank past lab members, including Fiona Whelan, Rachel Swift and Lisa Clarke. Particulary for their early work on the domain mapping of HCS and promiscuous biotinylation mutant, that were of great assistance to my project.

Of course that was only half the Wallace lab, and I'd like to thank "the dark side", everyone involved in the IGF work, for making it such a great place to work, and for never ending supplies of cake for morning tea. To Dr Briony Forbes, Kerrie McNeil, Carlie Delaine, Clair Alvino, Dr Kathy Surinya-Johnson, SheeChee Ong, and to past members, Mehrnaz Keyhanfer, Thirajit "O" Boonsaen, Teerakul "Gap" Arpornsuwan, Adam Denley, "Wau" Kuang and to honorary lab members Gemma Brierley, Michelle Zucker, Tamara Cooper, it's been a pleasure. Thanks also to the Booker lab for fun times and particularly to Cvetan Stojkoski for assistance with molecular modelling.

Working in the School of Molecular and Biomedical Sciences has been fantastic, and there are so many people I need to thank. John MacKrill, for assistance with antibody production and showing me the ropes in tissue culture, Serge Volgin in the store, Chris Cursaro for general helping out and of course everyone in CSU! I'd like to thank Velta Vingelis for all her encouragement and sharing her love of teaching with me.

I’m grateful to Dr Meredith Wallwork at Adelaide Microscopy for her expert advice and instruction in microscopy, and of course The Adelaide Proteomics Facility including Prof Peter Hoffman, Dr Chris Bagley, Dr Megan Retallick for mass spectrometry and protein sequencing services.

A big thanks to everyone else I have ever begged, borrowed (but never stole!) things from. You are too numerous to mention, but particularly thanks to Alix Farrell and Dr Edwina Ashby for antibodies I borrowed.

I’d like to acknowledge the Department of Molecular and Biomedical Science, the Faculty of Health Sciences and The Federation of University Women for travel fellowships. I was the recipient of a University of Adelaide Postgraduate Award.

Lastly, I need to thank my friends and family. To all my friends, thanks for keeping me sane. To Kelly, thanks for always being up for coffee and cake at Rumours at the drop of a hat, I wish you all the best in your PhD and whatever comes after that. Thanks for all your support. To Dave, look- I made it! Thanks for all your love and support (and the neck rubs while I was writing this up!) I couldn’t have done it without you. Finally, I’d like to dedicate this thesis to my Mum and Dad, for their never-ending love, encouragement and belief in me that made this possible.

Table of Contents

List of Figures

List of Tables

List of publications

Publications

LM Bailey, RA Gravel, JC Wallace & SW Polyak. (2008) Production and characterisation of polyclonal antibodies to examine isoforms of holocarboxylase synthetase. *Manuscript in preparation.*

NR Pendini[†], **L Bailey**[†], GW Booker, MC Wilce, JC Wallace & SW Polyak. (2008) Microbial Biotin Protein Ligases aid in understanding holocarboxylase synthetase deficiency. *BBA Protein and Proteomics. 1784(7-8):973-82.*

[†]Equal first authorship.

L Bailey, RA Ivanov, S Jitrapakdee, CJ Wilson, JC Wallace and SW Polyak.(2008) Reduced half-life of Holocarboxylase Synthetase from patients with severe multiple carboxylase deficiency. *Human Mutation 29(6):E47-57.*

L Bailey, RA Ivanov, JC Wallace, and SW Polyak. (2008) Artifactual detection of biotin on histones by streptavidin. *Analytical Biochemistry 373(1):71-7.*

Ng B, Polyak SW, Bird D, **Bailey L**, Wallace JC, Booker GW. (2008) *Escherichia coli* biotin protein ligase: Characterisation and development of a high throughput assay. *Analytical Biochemistry 376(1):131-6*.

NR Pendini[†], **LM Bailey**[†], GW Booker, MC Wilce, JC Wallace, and SW Polyak, Ph.D. (2008) Biotin Protein Ligase from *Candida albicans*: Expression, purification and development of a novel assay. *Archives of Biochemistry and Biophysics. 479(2):163-9.*

[†]Equal first authorship.

Conference Proceedings

L Bailey, RA Ivanov, SW Polyak and JC Wallace (2007) Artefactual detection of biotin on histones: non specific binding by streptavidin. *Proceedings of Annual Scientific Meeting of Australian Society for Medical Research South Australia 2007.* Oral Presentation.

L Bailey, SW Polyak and JC Wallace (2007) Subcellular Distribution of HCS Isoforms. *Proceedings of the 32nd Lorne Proteins Conference, Poster 276.*

L Bailey, N Pendini, RD Swift, C Wilson, JC Wallace and SW Polyak (2006) The N-terminal Domain of Holocarboxylase Synthetase (HCS) is critical for correct biotin metabolism in human cells. *New Frontiers Of Biotin Biochemistry, A satellite meeting of the 20th IUBMB International Congress of Biochemistry and Molecular Biology and 11th FAOBMB Congress, Kumamoto Prefecture, Japan June 2006.* Oral Presentation.

L Bailey, N Pendini, RD Swift, C Wilson, JC Wallace and SW Polyak (2006) The N-terminal Domain of Holocarboxylase Synthetase (HCS) is critical for correct biotin metabolism in human cells. *Proceedings of Annual Scientific Meeting of Australian Society for Medical Research South Australia 2006* Oral Presentation, Ross Wishart Finalist Session.

L Bailey, SW Polyak, C Wilson and JC Wallace (2006) A cell culture model of Multiple Carboxylase Deficiency: Examining N-terminal mutations of holocarboxylase synthetase. *Proceedings of the 31st Lorne Proteins Conference*, Poster 222.

L Bailey, SW Polyak and JC Wallace (2005) Production of polyclonal antibodies for functional analysis of human biotin protein ligase (holocarboxylase synthetase), *Proceedings of ComBio 2005*, Poster number POS-MON-01.

L Bailey, SW Polyak and JC Wallace (2005) Characterisation of human biotin protein ligase (holocarboxylase synthetase EC 6.3.4.10). *East Coast Protein Meeting June 2005*. Poster number 1.

L Bailey, SW Polyak and JC Wallace (2005) Characterisation of human biotin protein ligase (holocarboxylase synthetase EC 6.3.4.10) *Proceedings of Annual Scientific Meeting of Australian Society for Medical Research South Australia 2005* Poster number 12.

List of Abbreviations

aa	amino acid
Ab	antibody
ACC	acetyl CoA carboxylase
AD	activation domain
Amp	ampicillin
AP	alkaline phosphatase
APS	ammonium persulphate
ATP	adenosine triphosphate
BirA	biotin inducible repressor A
BCA	bicinchoninic acid
BCCP	biotin carboxyl carrier protein
BLAST	basic local alignment search tool
BME	beta-mercaptoethanol
bp	base pair
BPL	biotin protein ligase
BSA	bovine serum albumin
C-	carboxyl-
Cα	central carbon atom
cDNA	complementary deoxyribonucleic acid
cGMP	cyclic guanosine monophosphate
cHCS	C-terminal amino acids 315-726 of HCS
C-HCS	C-terminal antibody to holocarboxylase synthetase
DAPI	4’,6-diamidino-2-phenylindole
Daxx	Death domain associated protein
DBD	DNA binding domain
DEPC	diethyl pyrocarbonate
DMEM	Dulbecco’s modified eagles medium
DMSO	dimethyl sulfoxide
DNA	deoxynucleotide triphosphate
dNTPs	deoxynucleotide triphosphates
DTT	dithiothreitol
E. coli	*Escherichia coli*
ECL	enhanced chemiluminescence
EDTA	ethylene diamine tetra-acetic acid
EGTA	ethylene glycol-O,O’-bis-[2-amino-ethyl]-N,N,N’,N’,-tetraacetic acid
ELISA	enzyme linked immunosorbent assay
Eu	europium
FCS	fetal calf serum
G418	geneticin

GFP	green fluorescent protein
hr	hour
HCS	human holocarboxylase synthetase
HEPES	4-(2-hydroxyethyl)-1-piperazine-ethanesulphonic acid
3-HIA	3-hydroxyisovaleric acid
hPC107	107 amino acids encoding the biotin domain of human pyruvate carboxylase
HRP	horseradish peroxidase
IP	immunoprecipitation
K_a	affinity constant
K_M	Michaelis constant
kb	kilobase pair
kDa	kilodalton
LB	Luria broth
LC-ESI-MS	Liquid chromatography electrospray ionisation tandem mass spectrometry
LplA	lipoyl ligase
m	metre
M	molar
μ	micron
mA	milliampere
MAb	monoclonal antibody
Min	minute, minutes
MCC	methylcrotonyl-CoA carboxylase
MCD	multiple carboxylase deficiency
MOPS	3-morpholinopropanesulfonic acid
MS	mass spectrometry
MW	molecular weight
MWCO	molecular weight cut-off
n	nano
N-	amino-
N1	n-terminal antibody 1 to holocarboxylase synthetase
N2	n-terminal antibody 2 to holocarboxylase synthetase
N3	n-terminal antibody 3 to holocarboxylase synthetase
nHCS	N-terminal amino acids 1-314 of holocarboxylase synthetase
NHS-	N-succinimidyl ester
NLS	nuclear localisation sequence
NMR	nuclear magnetic resonance
$OD_{x\ nm}$	optical density at x nm wavelength
p	pico
PAb	polyclonal antibody
PCC	propionyl-CoA carboxylase
PBS	phosphate buffered saline
PBS-T	phosphate buffered saline and 0.1% (v/v) Tween-20

PBMC	peripheral blood mononuclear cells
PC	pyruvate carboxylase
PCR	polymerase chain reaction
PDB	protein data bank
PFA	paraformaldehyde
PhBPL	*P.horikoshii* BPL
PKG	protein kinase G
PMSF	phenylmethylsulfonylfluoride
PVDF	polyvinyl difluoride
RNA	ribonucleic acid
RNase	ribonuclease
rpm	revolutions per minute
RT	room temperature
SDS	sodium dodecyl sulphate
SDS-PAGE	sodium dodecyl sulphate polyacrylamide gel electrophoresis
s	second
SEM	standard error of the mean
TBS	tris buffered saline
TBS-T	tris buffered saline and 0.1% (v/v) Tween-20
TEMED	N,N.N,N'N'-tetramethylethylene-diamine
Tris	2-amino-2-hydroxymethylpropane-1,3-diol
Tween-20	polyoxyethylene-sorbitan monolaurate
U	units (active)
UTR	untranslated region
V_{max}	maximum velocity
UV	ultra violet
WB	Western blot
WT	wild type
yBPL	Yeast (*S.cerevisiae*) biotin protein ligase
yPC104	104 amino acids encoding the biotin domain of yeast pyruvate carboxylase

Introduction

1 Introduction

1.1 Biotin

Biotin, also known as vitamin H or vitamin B7 (Ames *et al.*, 2002) is a small 244Da water soluble molecule essential for life. Biotinylation is a post-translational modification essential for the activity of several important metabolic enzymes known collectively as the biotin-dependent enzymes (Jitrapakdee and Wallace, 2003, Samols *et al.*, 1988). The biotin moiety is attached to a specific lysine residue within a structured biotin domain, and here it acts to transfer carboxyl groups between donor and acceptor molecules during carboxylation reactions via a “swinging arm” mechanism (Pacheco-Alvarez *et al.*, 2002, Samols *et al.*, 1988, Perham, 2000).

This classical function has been long known and well studied, yet there remain many areas of biotin metabolism that are poorly understood. In recent years there has been a growing interest in other roles biotin may play in the cell, such as transcriptional regulation, demonstrating there may be more to this vitamin than previously thought.

1.2 The biotin cycle

Whilst bacteria and plants are able to synthesise their own biotin, higher eukaryotes must obtain biotin from exogenous sources. In humans biotin may be utilised from dietary sources or generated by microflora of the gut (Said, 1999b). Dietary biotin can exist in either a free or protein bound form. Gastric proteases cleave the protein-bound form into small peptide fragments. The activity of biotinidase releases free biotin from these peptide fragments (Hymes and Wolf, 1999). Free biotin can then be attached to apo-biotin enzymes in an enzymatic reaction catalysed by Biotin Protein Ligase (BPL), also known as holocarboxylase synthetase in mammals (HCS, E.C. 6.3.4.10).

1.3 Biotin-dependent enzymes

Biotin enzymes are categorised into three classes, carboxylases (class I, the class to which all eukaryotic biotin enzymes belong), decarboxylases (class II, typical of anaerobic prokaryotes) and transcarboxylase. (Samols *et al.*, 1988).

In mammals there are 5 biotin-dependent enzymes which catalyse a variety of metabolically important reactions (figure 1.1). Acetyl CoA Carboxylase (ACC) catalyses the carboxylation of acetyl-CoA to form malonyl Co-A. There are two isoforms of ACC, ACC1 and ACC2 that both have enzymatic activities in the cytoplasm. The main difference between these two isoforms is a 114 amino acid extension at the N-terminus of ACC2, targeting this form to the outer mitochondrial membrane (Abu-Elheiga *et al.*, 2000). Here, it is proposed to regulate fatty acid oxidation by controlling the shuttling of long chain fatty acids into the mitochondria (Kim, 1997). ACC1 is the only biotin dependent enzyme present in the cytosol and is predominantly expressed in lipogenic tissue, where it controls the *de novo* synthesis of long chain fatty acids. As fatty acids are a pre-requisite of membrane biosynthesis it is clear that ACC1 is an essential enzyme. This is supported by recent work showing that ACC1 knock-out mice are embryonic lethal, embryos do not develop past day 8.5 (Abu-Elheiga *et al.*, 2005). The ACC2 enzyme is predominantly found in heart and skeletal muscle (Kim, 1997).

The three remaining biotin enzymes are located in the mitochondria. Pyruvate Carboxylase (PC) forms oxaloacetate, an intermediate of the Krebs cycle, from the carboxylation of pyruvate. (Wallace *et al.*, 1998) Oxaloacetate is required for gluconeogenesis, fatty acid synthesis, and the synthesis of some neurotransmitters. Propionyl-CoA carboxylase (PCC) is involved in the metabolism of branched chain amino acids and the breakdown of odd-chain fatty acids and cholesterol by catalysing the formation of methylmalonyl-CoA from propionyl-CoA. β-methylcrotonyl CoA carboxylase (MCC) catalyses a key step in leucine catabolism (Pacheco-Alvarez *et al.*, 2002).

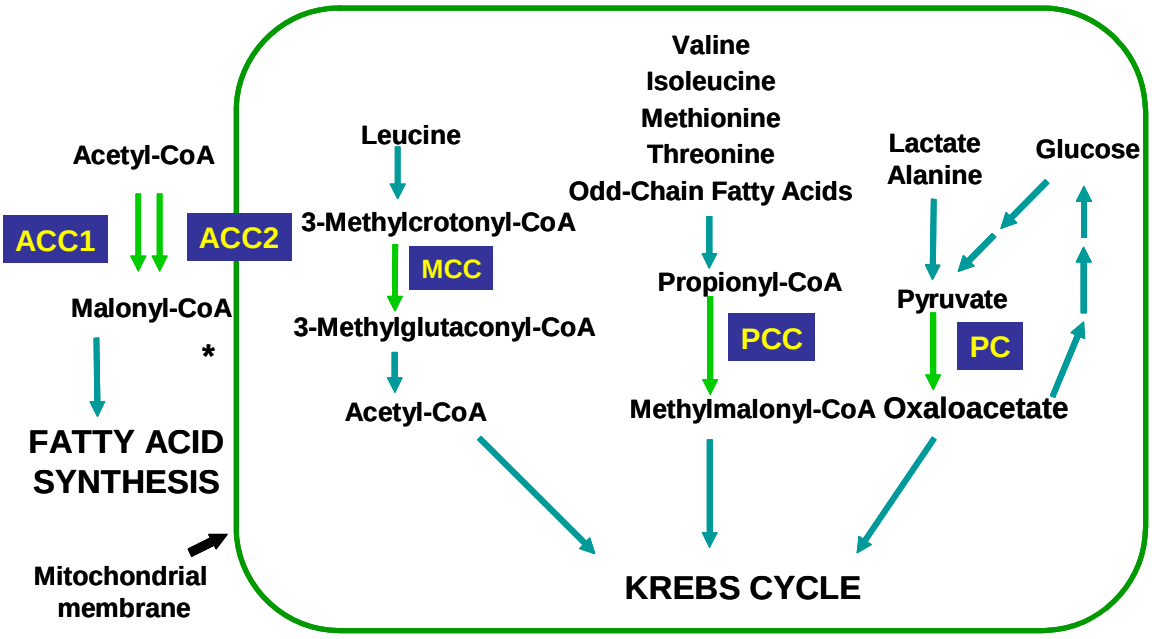

Figure 1-1 The role of biotin-dependent carboxylases in human metabolism.
Adapted from (Pacheco-Alvarez *et al.*, 2002). *ACC2 is situated in the mitochondrial membrane where in controls import of long chain fatty acids into the mitochondria.

1.4 Biotin domains

The attachment of biotin by BPL occurs at a specific lysine residue presented within the context of a folded biotin domain. The first characterised structure of a biotin domain was the biotin carboxyl carrier protein (BCCP), a subunit of the *E.coli* acetyl CoA carboxylase (Atthappilly and Hendrickson, 1995) . The structure consists of two four-stranded β-sheets forming a flattened β-barrel with the N and C terminal residues brought close together in 3 dimensional space in one sheet and the biotinyl-lysine residue located within a highly conserved MKM sequence in an exposed β-turn in the other sheet (figure 1.2) (Reche *et al.*, 1998, Waldrop *et al.*, 1994, Roberts *et al.*, 1999). The correct positioning of this target residue on the hairpin loop is critical, as moving the lysine residue by just one position to the N or C terminal side abolishes biotinylation *in vitro* and *in vivo* (Reche *et al.*, 1998).

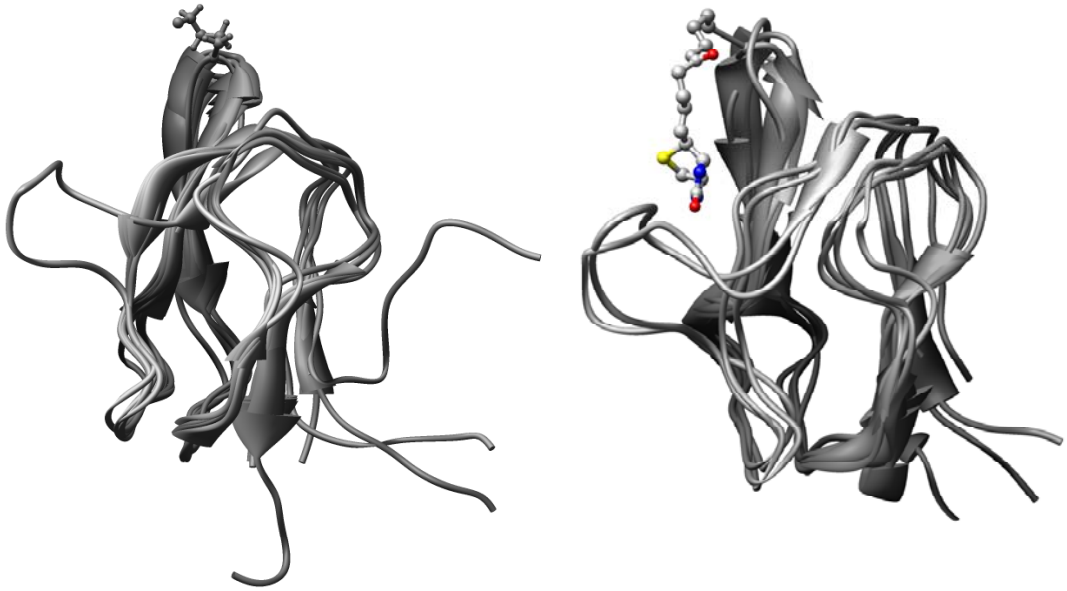

Figure 1-2 Structural conservation of the biotin-accepting domain.
Coordinates deposited in the PBD were downloaded and overlayed against other biotin domains to demonstrate the structural conservation across species. The structures of apo (left panel) and holo (right panel) biotin domains are shown. Left: Apo domains of *E.coli* BCCP (3BDO), *P.shermanii* TC (1DCZ), *B.subtilis* BCCP (1Z7T) and *P.horikoshii* BCCP (2D5D) and TC (2EVB) are overlayed. Right: Biotinylated domains from *E.coli* BCCP, determined by x-ray crystallography (1DBO) and NMR (2BDO), and *P.shermanii* TC (1O78) are overlayed. The target lysine side chain either free (left) or covalently bonded to biotin (right) are represented in ball and stick mode. Model generated by Dr Steven Polyak, University of Adelaide.

The biotin domain is structurally analogous to the lipoyl domain of lipoic acid dependent enzymes, where lipoic acid is attached to a specific lysine residue within a highly conserved DKA motif by lipoyl ligase (LplA) (Reche and Perham, 1999, Perham, 2000). Mutation of the MKM biotinylation sequence in the *E.coli* BCCP to the DKA motif resulted in loss of biotinylation and a low level of lipoylation *in vitro* (Reche *et al.*, 1998). One of the structural cues preventing lipoylation of BCCP in *E.coli* is the presence of a “protruding thumb” structure, consisting of 8 amino acids between the β2 and β3 strands (Reche and Perham, 1999) (figure 1). Amino acid sequence alignments suggest that this feature is absent in eukaryotic biotin domains. It is not known how eukaryotic BPLs distinguish the specific lysine in the biotin domain as opposed to lipoyl domains for modification.

Truncation studies of the BCCP domain show that 35-40 residues either side of the biotinyl-lysine are required to specify modification (Li and Cronan, 1992). Further truncation abolishes biotinylation by removing residues essential for forming the hydrophobic core (Athappilly and Hendrickson, 1995).

The target lysine for biotinylation usually resides approximately 30 amino acids from the C-terminus. One notable exception to this is found in mammalian ACC where the target residue resides in the centre of the protein (figure 1.3). *In vivo* studies have shown that the biotin domain of ACC1 is a poorer substrate for BPL than PC. Mutational studies to change residues in the biotin domain to make it more PC or ACC2 like failed to increase the rate of biotinylation (Polyak *et al.*, 2002). It may be that other regions of the ACC1 enzyme are involved in biotinylation or that some cofactor or post translational modification is necessary for BPL to recognise ACC1. ACC is regulated at many levels possibly including biotinylation by BPL.

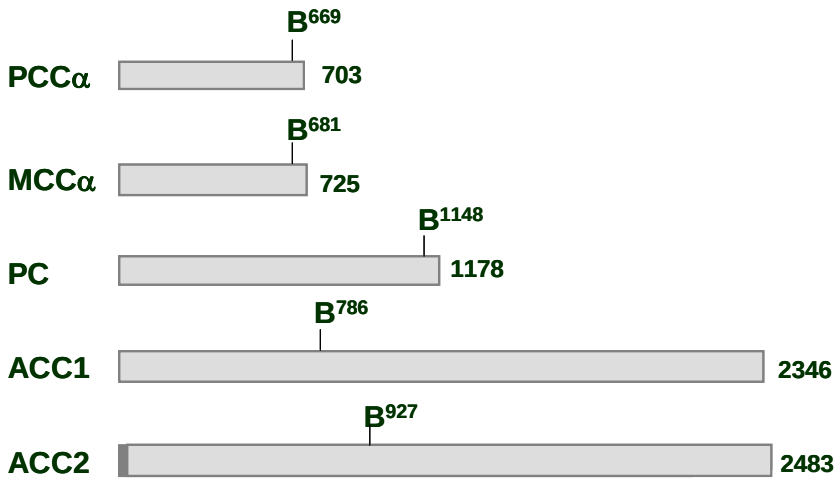

Figure 1-3 Schematic representation of the relative position of the biotin attachment site (indicated by B) in the five mammalian carboxylases.

There is a high degree of sequence similarity and functional conservation of biotin domains between enzymes and also between species (Chapman-Smith and Cronan, 1999a, Samols *et al.*, 1988). Thus BPLs from bacteria are able to recognise and biotinylate biotin domains from eukaryotic substrates and vice versa. The interaction

between BPL and biotin domains is an example of an exquisitely precise protein:protein interaction that has remained conserved throughout evolution.

1.5 Biotin protein ligases

1.5.1 Reaction mechanism

Enzymatic biotinylation proceeds through a conserved two step reaction. (figure 1.4). In the first reaction ATP is utilised to form the adenylated intermediate biotinyl-AMP. The biotinyl group is then attached via an amide linkage to the ε-amino group of a specific lysine of the apo-biotin domain (Chapman-Smith *et al.*, 1999).

Step 1: Biotin + ATP ↔ Biotinyl-AMP + PPi

Step 2: Biotinyl-AMP+ apoprotein → biotinyl-protein + AMP

Figure 1-4 Two step reaction mechanism of biotinylation (Chapman-Smith *et al.*, 1999)

The biotinylation reaction is analogous to the mechanism of amino acyl-tRNA synthetases and lipoyl ligases, where the reaction proceeds though an adenylated intermediate (Chapman-Smith and Cronan, 1999a). These enzymes share a common core fold in their catalytic domains, despite divergent amino acid sequences (Reche, 2000). This has led to the suggestion of a common ancestral enzyme consisting of an ATP binding domain able to activate the carboxyl group of small metabolites through adenylation (Artymiuk *et al.*, 1994).

1.5.2 Prokaryotic BPLs

The best characterised BPL is that of *Escherichia coli*, also known as BirA (Biotin Inducible Repressor A). BirA is a truly remarkable enzyme, with dual functions as a biotin ligase and also as the transcriptional regulator of biotin biosynthesis (Cronan, 1989). The crystal structure was resolved to 2.5Å in 1992 by Wilson and colleagues, who showed the enzyme consists of three domains. The C-terminal domain, which bears structural resemblance to SH3 domains, is essential for enzyme function and is implicated in ATP binding (Chapman-Smith *et al.*, 2001). The central catalytic domain contains all the known biotin contacting residues and is the domain most highly conserved across species (Tissot *et al.*, 1997). The N-terminal domain is a classical helix-turn-helix structure required by DNA binding proteins (Wilson *et al.*, 1992).

By linking biotin ligase activity with DNA binding BirA is a dual function molecule that allows bacterial cells to tightly regulate biotin metabolism. In the presence of apo-biotin enzymes BirA adopts a biotin ligase activity. Conversely, when biotin is not required BirA functions as a transcriptional repressor to prevent further synthesis of the biotin biosynthetic enzymes (Chapman-Smith and Cronan, 1999a). Here, BirA dimerisation facilitates a co-operative interaction with DNA to form the transcription repressor. Competing protein:protein interactions between BirA dimerisation and BCCP control the transcription of the biotin synthesis genes of the *bio* operon (Weaver *et al.*, 2001a). It is the biotinyl-AMP that acts as the co-repressor that triggers DNA binding by BirA. (Weaver *et al.*, 2001a, Cronan, 1989, Samols *et al.*, 1988). In the absence of apo-BCCP substrate and presence of free biotin, biotinyl-AMP-BirA accumulates in the cell and dimerises, binding to the *bio* operon and blocking biotin synthesis. The binding of biotinyl-AMP to BirA causes a disorder-to-order transition in the three flexible surface loops in the central domain required for dimerisation. Ordering of these loops favours dimer formation, in

which the β-sheets of the central domain of each monomer are arranged side-by-side forming an extended β-sheet (Weaver *et al.*, 2001b). In low biotin conditions any biotinyl-AMP synthesized is rapidly used to biotinylate apo-BCCP and hence the operator is not occupied and biotin is synthesised. (figure 1.5).

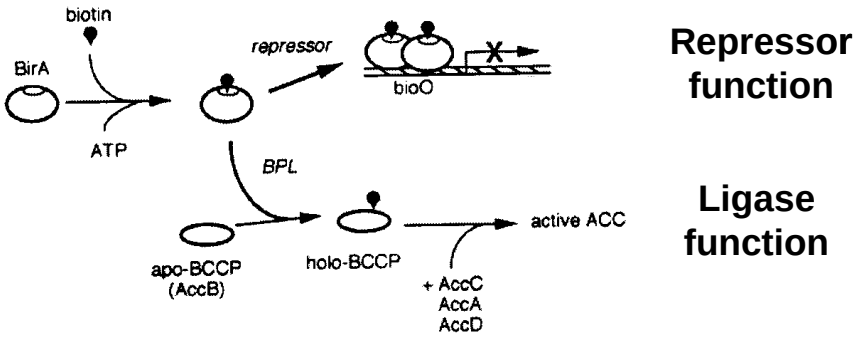

Figure 1-5 Model of the dual functions of BirA.
In the absence of apo-BCCP substrate, holo-BirA dimerises and binds to the BioO operon, repressing biotin synthesis. Adapted from (Chapman-Smith and Cronan, 1999a).

The BirA binding sites upstream of *bio* operons are conserved among eubacterial and archaeal genomes (Rodionov *et al.*, 2002). This suggests a common mechanism among these species for the regulation of biotin metabolism.

The BirA N-terminal DNA binding domain has also been shown to play some role in catalysis (Xu and Beckett, 1996). Deletion of the N-terminus abolished DNA binding to the *bio* operon as expected, but did not alter the synthesis of biotinyl-5'-AMP or the transfer of biotin to the BCCP substrate. However, the affinities for the ligands biotin and biotinyl-5'-AMP were reduced 100 to 1000 fold respectively. It was proposed by Xu and Beckett that the interaction of the N and C terminal domains is crucial for the kinetic stability of the BirA-biotinyl-5'-AMP complex. Interestingly they note that the function of the N-terminal DNA binding domain is dependent on binding of the adenylate intermediate, and that concurrently the binding of the the adenylate is dependent on the N-terminal domain.

1.5.3 Eukaryotic BPLs

Unlike *E.coli* BirA, which has only one substrate to modify, BPLs of eukaryotes must be able to biotinylate multiple substrates within the cell. It is not known if there is a hierarchy of importance for the biotin dependent enzymes and which, if any, would be preferentially biotinylated. Although the BPL recognises the folded biotin domain within each enzyme, it is not known if or how, substrate specificity between enzymes occurs.

Figure 1-6 Diagrammatic comparison of BPLs from different classes.
The catalytic core is conserved across kingdoms, with variation in the N-terminal domain. Adapted from (Denis *et al.*, 2002).

The catalytic core of BPLs is highly conserved across kingdoms (figure 1.7), suggesting a common catalytic mechanism conserved through evolution. There is significant sequence variation in the N-terminal portions of BPLs across kingdoms (figure 1.6). Prokaryotic BPLs may or may not bear an N-terminal DNA biotin domain, such as that discussed for BirA in the previous section. The large N-terminal extensions of yeast and mammalian BPLs are not believed to be involved in DNA binding (as in BirA). The function of this N-terminal extension is currently unknown, although information critical for BPL targeting in plants (Tissot *et al.*, 1997), and enzyme activity in human HCS (Campeau and Gravel, 2001) and yeast BPL (Polyak *et al.*, 1999), have been shown.

1.5.4 Plant BPLs

The first plant BPL (HCS1) was isolated from *Arabidopsis thaliana* by functional complementation of a BirA conditional lethal bacterial strain (Tissot *et al.*, 1997). The cDNA encoded a 367 amino acid protein containing a 30 amino acid N-terminal putative chloroplast targeting sequence. Subsequent genome analysis in *Arabidopsis* revealed a second BPL gene (HCS2) (Denis *et al.*, 2002). This lacked the targeting sequence and was therefore proposed to encode a cytosolic form of the enzyme. The HCS2 form undergoes alternative splicing to give rise to several different isoforms with unknown function, although it is speculated these different isoforms may have altered subtrate specificities and cellular locations (Denis *et al.*, 2002).

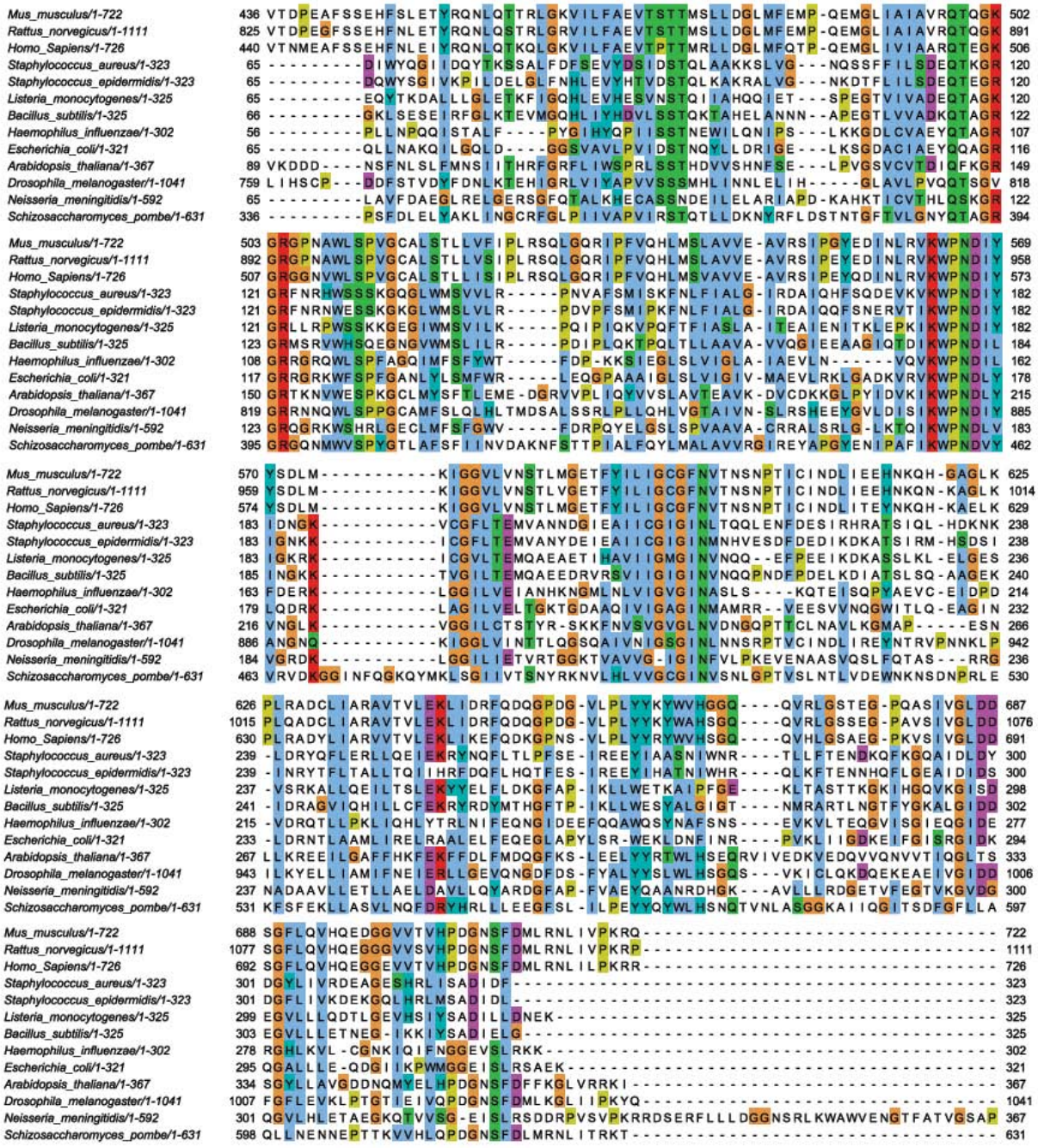

Figure 1-7 Conservation of the catalytic core of BPLs through evolution.
A multiple sequence alignment was performed in ClustalW using mouse, rat, human, *S.aureus*, *S.epidermidis*, *L.monocytogenes*, *B.subtilis*, *H.influenzae*, *E.coli*, *A.thaliana*, *D.melongaster*, *N.meningitidis* and *S.pombe* BPL sequences. Colours indicate conservation of amino acids with similar physico-chemical properties.

Control of biotin synthesis in plants is not well understood. Plant HCS1 was unable to complement the repressor function of BirA in a BirA depressed mutant of *E.coli* (Alban, 2000). The high biotin content of plant cells compared to bacteria suggests there may not be a strong repression system in the plant kingdom (Tissot *et al.*, 1997). Although the mechanism is unknown it has been shown that biotin synthesis is dependent on factors such as development, exposure to light, and biotin availability (Patton *et al.*, 1996).

1.5.5 Yeast BPLs

The BPL from *Saccharomyces cerevisiae* contains 690 amino acids with a predicted molecular weight of 76.4 kDa (Cronan and Wallace, 1995). Like mammalian BPLs, yeast BPL contains a large N-terminal extension of unknown function (Chapman-Smith and Cronan, 1999b). Whilst the X-ray structure for this enzyme has not yet been reported, protein chemistry experiments have provided some detail about the enzyme. Limited proteolysis data indicate the presence of a flexible linker separating the first 27 kDa and the C-terminal 50 kDa (Polyak *et al.*, 1999). Susceptibility to proteolysis was decreased by the addition of ligands, suggesting that substrate binding caused a global conformational change in structure, affecting regions at a distance from the catalytic site (Polyak *et al.*, 1999). A series of N-terminal truncations were catalytically inactive both *in vivo* (unable to complement a conditional lethal BirA *E.coli* strain, figure 1.8) and in *in vitro* biotinylation assays (Polyak *et al.*, 1999). Thus, demonstrating that this N-terminal domain is essential for catalysis.

Figure 1-8 The N-terminus of yeast BPL is critical for enzyme function.
The yeast N-terminal domain was found to contain a protease sensitive linker region by limited proteolysis (indicated by scissors, left). Truncations past this linker region resulted in inactive enzyme, which was unable to resuce growth of BirA deficient *E.coli* (strain Cy918). (Polyak *et al.*, 1999).

1.5.6 Human HCS

Mammalian BPL is commonly referred to as holocarboxylase synthetase (HCS) in the literature due to all mammalian biotin-dependent enzymes being class I carboxylases. In this thesis I will refer to the human BPL enzyme as HCS.

The cDNA encoding HCS was independently isolated by two groups. The Narisawa group used a probe generated from bovine BPL sequence against a human cDNA library to obtain the cDNA (Suzuki *et al.*, 1994). Concurrently the Gravel group employed functional complementation of a BirA conditional lethal strain of *E.coli* to isolate the cDNA (Leon-Del-Rio *et al.*, 1995). Both encode a 726 amino acid protein with a predicted mass of 80.8 kDa (Suzuki *et al.*, 1994). Observations that patients with multiple carboxylase deficiency (discussed in section 1.7 following) have a reduced biotinylation of all five carboxylases supports the notion that there is only one BPL enzyme in humans (Feldman *et al.*, 1981).

The HCS gene spans approximately 240 kb and is comprised of 14 exons (Yang *et al.*, 2001). The first methionine codon is found in exon 6 and the stop codon in exon 14. Three mRNA species have been identified which start in different exons(Yang *et al.*, 2001). Two transcripts have been reported in a variety of human tissues, one starting at exon 1, the second at exon 3. One mRNA starting at exon 2 was found in a KG-1 myeloid cell line. As exon 3 contains a stop codon, the 5' UTR variation does not appear to have an effect on the amino acid sequence. In addition various splicing patterns of exons 3-6 were observed. None of these created new initiation codons, but one splice variant that lacked both exons 5 and 6 skipped the first two in-frame methionine residues, thereby encoding only the shortest form of the enzyme starting at Met^{58} (Yang *et al.*, 2001). The factors controlling transcription and mRNA splicing and possible effects this has on BPL in the cell are currently unknown.

Three potential initiation of translation sites have been proposed for HCS at Met^{1}, Met^{7} and Met^{58} (Hiratsuka *et al.*, 1998). The methionine at 234 is not likely to be a start site as this protein has shown to be catalytically inactive *in vitro* in human fibroblasts (Sakamoto *et al.*, 1999). It has also been demonstrated that proteins corresponding to all three initiation start sites are translated *in vivo* (Hiratsuka *et al.*, 1998). Kinetic studies on the different isoforms found that the Met^{58} isoform showed a 40% reduction in activity compared to the Met^{1} isoform (Sakamoto *et al.*, 1999).

The existence of multiple isoforms of HCS was suggested by the study by Hiratsuka *et al*. (1998), who reported proteins of 86KDa, 82KDa, and 76KDa in the cytosol of the placenta. The same study showed an immunoreactive band of approximately 62KDa in the mitochondrial fraction. A recent study by Narang and colleagues (2004) reported a 66KDa immunoreactive band in both nuclear and cytosolic fractions. Early studies showed partially purified rat cytosolic and mitochondrial preparations were able to catalyse holocarboxylase formation, indicating that both active HCS and apo-enzymes were present in each compartment (Kosow *et al.*, 1962). Fractionation studies on mouse

3T3-L1 cells reported over 70% of all HCS activity in the cytosolic fraction (Chang and Cohen, 1983). In another study on the subcellular distribution of HCS in rat liver, 18% of HCS activity was in the nuclear fraction, 18% in the mitochondrial fraction, 5% in the microsomal fraction and the majority (59%) in the cytoplasm. (Cohen *et al.*, 1985). The significance of nuclear HCS will be discussed in detail (section 1.8). No recognisable mitochondrial or nuclear targeting sequence has yet been determined for HCS, and it is not understood how the enzyme is compartmentalised within the cell. There have not been any studies examining the regulation or distribution of different BPL isozymes in different cellular compartments or within different tissue types. Furthermore, post-translational modifications and processing of HCS have not been investigated. I propose that there is information in the N-terminal region of HCS which aids in compartmentalisation or post-translational processing of the enzyme.

1.5.7 Human HCS structure

The human HCS protein is over twice the size of BirA, with the central catalytic domain showing the highest sequence similarity across species (Campeau and Gravel, 2001, Tissot *et al.*, 1997) (see also figure 1.7). The X-ray structure for HCS has not been reported but information about the enzyme has come from other studies. Deletion studies by Campeau and Gravel (2001), showed that the minimal functional protein consists of the last 349 residues. There was an absolute requirement for the C-terminus for functional enzyme, similar to results seen with the BirA enzyme (Chapman-Smith *et al.*, 2001). Although the N-terminal domain was not essential for activity the N-terminal extension was implicated in the catalytic mechanism (figure 1.9). Deletions up to Ala^{80} resulted in fully functional enzyme, whereas deletions up to Leu^{166} were able to rescue BirA deficient *E.coli* but were unstable and unable to be detected by Western blotting. Of particular significance were N-terminal deletions up to Ala^{235} or Thr^{266} which were inactive or only weakly active, but further deletions up to Lys^{378} restored activity. Deletions into the

catalytic domain (up to Leu^{460} or Pro^{569}) were inactive as expected. This indicates that the region between Leu^{166}-Arg^{290} is a structured domain required for catalysis (Campeau and Gravel, 2001). This agreed with an independent report where deletions up to Ile^{117} produced a functional HCS that was 40% more active than the full-length protein (Sakamoto *et al.*, 1999).

Recent work in our laboratory has shown that the N-terminus consists of 3 distinct structural domains as determined by limited proteolysis experiments (Swift, 2003). These three domains are Met^{1}-Ala^{80}, Ala^{80}-Glu^{151} and Lys^{160}-Asp^{311} (figure 1.9). These results agree with the observations of Campeau and Gravel, with the third domain (Lys^{160}-Glu^{311}) corresponding to the region that interacts with the catalytic domain. Analysis of truncated HCS forms has shown that domain III is required for catalysis and its removal reduces HCS activity by at least 100-fold. (Pendini *et al.*, 2006).

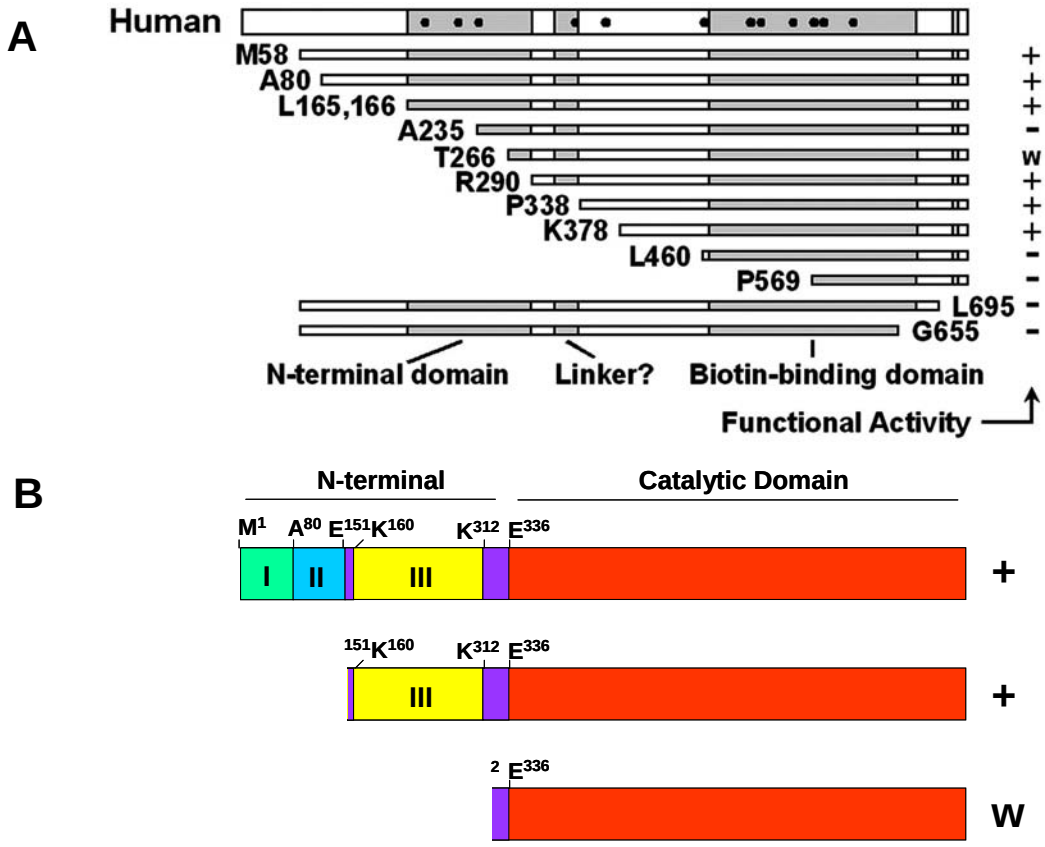

Figure 1-9 Schematic of domain configuration of human HCS.

(A) Truncation studies of Campeau and Gravel (2001). The N-terminal domain critical for enzyme function (Leu^{166}-Arg^{290}) is shaded grey. The C-terminal biotin binding domain is also shaded grey. Circles indicate point mutations in MCD patients. Functional activity of each construct is indicated by +, w (weak) or – and represents the ability of each construct to complement *E.coli* birA104.

(B) Domain mapping of HCS by Swift et. al (2004). The N-terminus of HCS consists of three domains separated by protease sensitive linker regions, domain I (Met^{1}-Ala^{80}), domain II (Ala^{80}-Glu^{151}) and domain III (Lys^{160}-Asp^{311}). Activity of two variants of HCS, Gly^{159}-Arg^{726} (domain III + catalytic domain) and Met^{314}-Arg^{726} (catalytic domain) are indicated by + or w (weak). Activity was measured by assay on lysates of *E.coli* overexpressing constructs (Swift *et al.*, 2004) or on purified HCS (Pendini *et al.*, 2006).

1.6 Biotin in human health

The Dietary Reference Intake for biotin, based on indicators of biotin deficiency, is 30 μg/day (Ames *et al.*, 2002). It is estimated that the dietary intake in Western populations is between 35 and 70 μg/day (Peters *et al.*, 2002). Despite the essential role of this

vitamin, an estimated average requirement and recommended dietary intake for biotin are yet to be determined (Said, 1999a). This is because frank biotin deficiency is rare, but may be induced by the consumption of raw egg white containing avidin, which binds biotin tightly ($Ka=10^{15}$ mol/L). The symptoms of biotin deficiency include dermatitis, conjunctivitis, alopecia, ataxia, hypotonia, keto-lactic acidosis/organic aciduria, seizures and developmental delay in adults and children (Zempleni and Mock, 1999).

Whilst clinical biotin deficiency may be rare, small scale clinical studies have indicated that marginal biotin deficiency is common during pregnancy (Mock *et al.*, 1997a, Mock and Stadler, 1997). Whilst there were no clinical symptoms of deficiency, increased urinary excretion of 3-hydroxyisovaleric acid (3-HIA) was observed in 26 of 29 women in early pregnancy and 21 out of 26 women in late pregnancy (Mock *et al.*, 1997a, Mock and Stadler, 1997). 3-HIA excretion increases as a result of decreased MCC activity, causing shuttling of methylcrotonyl CoA to an alternative pathway. Excretion of 3-HIA is the preferred biochemical test for measuring biotin status (Mock *et al.*, 1997b). Biotin supplementation restored 3-HIA excretion to normal levels (Mock *et al.*, 2002). This is concerning as several studies have shown biotin deficiency to be teratogenic (Zempleni and Mock, 2000). In mice, maternal biotin deficiency induced by avidin consumption caused congenital defects in more than 90% of offspring, with the most common defects micrognathia, cleft palate and micromelia (Mock *et al.*, 2003, Watanabe and Endo, 1990, Watanabe, 1983). This occurred even when there were no signs of biotin deficiency in the dams (Watanabe and Endo, 1984). Similar results have been reported in hamsters (Mock *et al.*, 2003). Hen and turkey eggs have a higher embryonic mortality and reduced hatchability when the hens are biotin deficient (Zempleni and Mock, 2000). Whilst a link between biotin deficiency in mothers and deleterious effects on the foetus is yet to be proven in humans, clearly there is an important role for biotin in early development and hence presumably even marginal biotin deficiency should be avoided in pregnant women.

1.7 Multiple carboxylase deficiency (MCD)

Multiple carboxylase deficiency (MCD) is the condition arising from the lack of activity of all the biotin-dependent enzymes. It can be caused by either a defect in biotinylation of carboxylases (HCS deficiency, OMIM 253270), a deficit in recycling of biotin in the cell (biotinidase deficiency, OMIM 253260) or failure of biotin transport. Whilst there are numerous clinically and biochemically common features, individual cases are extremely variable. Symptoms include ketoacidosis, feeding difficulties, hypotonia, seizures, developmental delay and dermal abnormalities such as rashes, dryness of the skin and alopecia. In severe or untreated cases this can lead to coma and death (Baumgartner and Suormala, 1997).

(Saunders *et al.*, 1979) first implicated HCS in MCD when it was observed that biotin-carboxylase activities in patients' fibroblasts were severely reduced in low biotin media but could be rescued by biotin-rich media. These cells could not be rescued by complementation with known carboxylase mutants, suggesting a requirement for a common holocarboxylase synthetase. The involvement of HCS was confirmed by (Burri *et al.*, 1981), who developed an HCS assay using apo-PCC partially purified from the livers of biotin-deficient rats. In this assay, the K_M for biotin was elevated 60 fold in extracts from patients fibroblasts relative to normal controls. This study was the first to conclusively show a defect in HCS in an MCD patient.

Subsequently it was shown that defects in biotinidase can also give rise to MCD (Wolf *et al.*, 1983). Initially, age of onset was used to define the defect giving rise to MCD. HCS deficiency usually presents with ketoacidosis in neonates within the first few days of life, and is associated with a poor prognosis if left untreated. Biotinidase deficiency generally presents with a gradual onset of symptoms including audio visual pathologies (which are not associated with HCS deficiency), limb muscle weakness and progressive neurologic abnormalities (Baumgartner and Suormala, 1997). Additionally, biotinidase deficiency

does not present until initial biotin stores are depleted, and is also dependent on the amount of biotin in the diet and residual biotinidase activity. Generally, biotinidase deficiency presents at a later age (average onset at 3 months, (Wolf *et al.*, 1985)). However, HCS deficiency has been known to present as late as 8 years (Sakamoto *et al.*, 2000). Hence the clinical relevance of age of onset has decreased as a diagnostic tool with diagnosis relying on either DNA assay for known mutations (summarised in table 1.1) or enzyme activity assay. Neonatal screening by tandem mass spectroscopy for HCS deficiency is now available using filter paper dried blood spot samples (Lund *et al.*, 2007), and pre-natal molecular diagnosis by DNA analysis can be achieved through chorionic villus sampling at 11 weeks gestation in families with a history of the disease (Malvagia *et al.*, 2005).

There are many mutations in the HCLS gene that give rise to MCD (figure 1.10, table 1.1). The severity of disease varies greatly with the genotype of each individual. Broadly, the mutations can be classified into two groups. First are the K_M mutants, for which the mutation results in an enzyme with a decreased affinity for biotin. Second are the V_{max} mutants, where the affinity for biotin is essentially unchanged but the activity of the enzyme is compromised and response to biotin therapy varies. For most patients with mutations in the biotin binding region of HCS pharmacological doses of biotin (10 mg/day) are sufficient to treat both clinical and biochemical symptoms (Zempleni and Mock, 1999). However, there have been several mutations observed which map to the N-terminal domain (domain III, see figure 1.10), providing further evidence that this is a functionally important portion of the enzyme. Patients with these N-terminal mutations (L237P and L216R) respond poorly to biotin therapy and generally have a poor long-term prognosis (discussed further detail in Chapter 5).

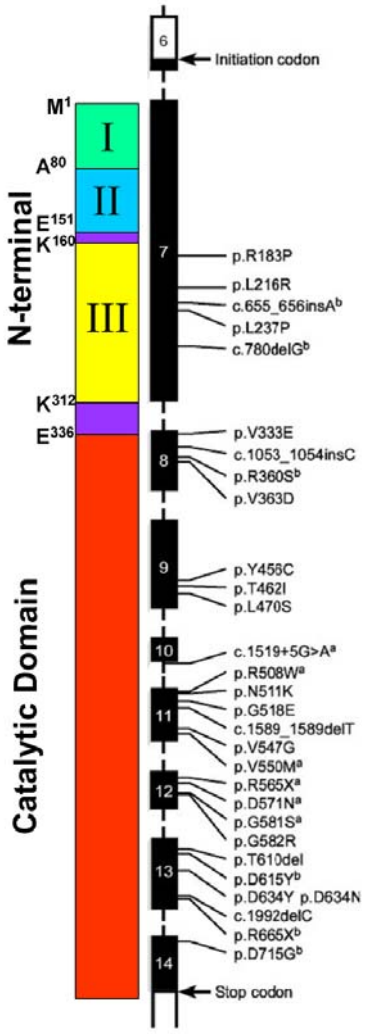

Figure 1-10 Schematic diagram showing location of mutations that give rise to MCD.

Left, a diagram showing the boundaries of protein domains as determined by limited proteolysis (Swift, 2003). Right, the black boxes represent exons of the HCLS gene. Positions of mutations arising in MCD are indicated (adapted from Suzuki *et al*., 2005).

Exon / Intron	Nucleotide change in cDNA	Effect on coding region	Number of Alleles	Patient Origin	References
Mutations					
Exon 7	c.548G>C	R183R	2	Unknown	(Sakamoto *et al.*, 1999)
Exon 7	c. 647T>G	L216R	14	Australian Maori Samoan	(Dupuis *et al.*, 1996) (Morrone *et al.*, 2002)(Wilson *et al.*, 2005)
Exon 7	c. 655-656insA	pI219NfsX58 (truncation)	2	Japanese	(Yang *et al.*, 2001)
Exon 7	c.710T>C	L237P	9	Japanese	(Aoki *et al.*, 1995) (Yang *et al.*, 2001)
Exon 7	c.780delG	G261VfsX20 (truncation)	7	Japanese	(Aoki *et al.*, 1995) (Yang *et al.*, 2001)
Exon 8	c.1053_1054insC	L353AfsX7 (truncation)	1	Spanish	(Yang *et al.*, 2001, Briones *et al.*, 1989)
Exon 8	c.1080A>C	R360S	2	Japanese	(Yang *et al.*, 2001)
Exon 8	c.1088T>A	V363D	2	Unknown	(Dupuis *et al.*, 1996)
Exon 9	c.1367A>G	Y456C	1	Malaysian	(Yang *et al.*, 2001)
Exon 9	c.1385C>T	T462I	1	Spanish	(Yang *et al.*, 2001, Aoki *et al.*, 1999)
Exon 9	c.1409T>C	L470S	1	Japanese	(Yang *et al.*, 2001)
Intron 10	c.1519+5G>A	IVS10+5G>A Splice Defect	32 *carrier frequency 1:20 in Faroese	Spanish Danish Faroese Swedish French German	(Holme *et al.*, 1988, Sakamoto *et al.*, 2000, Yang *et al.*, 2001, Suzuki *et al.*, 2005, Lund *et al.*, 2007)
Exon 11	C.1522C>T	R508W	15	Japanese Taiwanese Chinese Iranian Other	(Dupuis *et al.*, 1996, Sakamoto *et al.*, 1998, Yang *et al.*, 2001, Morrone *et al.*, 2002)
Exon 11	c.1533T>A	N511K	1	Italian	(Morrone *et al.*, 2002)
Exon 11	c.1553G>A	G518E	1	Unknown	(Dupuis *et al.*, 1996)
Exon 11	c.1589delT	L529RfsX15 truncated	1	German	(Aoki *et al.*, 1999)
Exon 11	c.1640T>G	V547G	1	German	(Yang *et al.*, 2001)
Exon 11	c.1648G>A	V550M	8	Japanese African Other	(Dupuis *et al.*, 1996, Aoki *et al.*, 1997, Morrone *et al.*, 2002, Tang *et al.*, 2003)
Exon 12	c.1693C>T	R565X truncated	2	Japanese African	(Sakamoto *et al.*, 1998, Yang *et al.*, 2001, Tang *et al.*, 2003)
Exon 12	c.1711G>A	D571N	3	German Spanish	(Aoki *et al.*, 1999, Dupuis *et al.*, 1996, Suzuki *et al.*, 2005)
Exon 12	c.1741G>A	G581S	4	Italian Turkish	(Fuchshuber *et al.*, 1993, Suormala *et al.*, 1997, Morrone *et al.*, 2002)
Exon 12	c.1744G>A	G582R	1	Italian	(Morrone *et al.*, 2002)
Exon 13	c.1828_1830del	T610deletion	2	Lebanese	(Aoki *et al.*, 1999, Touma *et al.*, 1999)
Exon 13	c.1843G>T	D615Y	1	Spanish	(Suzuki *et al.*, 2005)
Exon 13	c.1990G>T	D634Y	1	German	(Suormala *et al.*, 1997)
Exon 13	c.1990G>A	D634N	2	Japanese Chinese	(Suzuki *et al.*, 2005, Tang *et al.*, 2003)
Exon 13	c.1992delC	R665DfsX41 truncation	1	French	(Suormala *et al.*, 1997)
Exon 13	c.1993C>T	R665X truncation	1	Japanese	(Suzuki *et al.*, 2005)
Exon 14	c.2144A>G	D715G	1	Japanese	(Suzuki *et al.*, 2005)
Polymorphisms					
Exon 6	c.285C>T	P95P			dbSNP #rs2230182
Exon 7	c.126G>T	E42D		Malaysian	(Yang *et al.*, 2001, Aoki *et al.*, 1999) dbSNP #rs1065758
Exon 7	c.971G>A	R324H		Spanish	(Suzuki *et al.*, 2005)
Exon 8	c.1053T>C	N351N			dbSNP #rs1065759

Table 1-1 Summary of known mutations and polymorphisms of the HCLS gene adapted from Suzuki *et al.*, 2005.

1.8 A new role for biotin?

For many years it was believed that biotin was only biologically active when attached to the biotin enzymes. However, there is increasing evidence that biotin may have more than a co-factor role as it has been implicated in regulating gene expression. Even early studies showed the presence of biotin in the nuclei of cells, despite the lack of biotin-dependent enzymes in the nucleus (Dakshinamurti and Mistry, 1963b). An experiment, in which biotin fed to biotin-deficient rats resulted in increased incorporation of ^{14}C labelled amino acids into specific polypeptides, was the first study to show biotin associated with a transcriptional or translational process (Dakshinamurti and Mistry, 1963a). Recent DNA microarray studies have suggested that biotin supplementation affects expression of ~300 genes in peripheral blood mononuclear cells (Wiedmann *et al.*, 2004). Biotin appears to modulate a wide variety of genes, including those involved in glucose metabolism, the immune system and also the biotin-dependent enzymes themselves (Rodriguez-Melendez and Zempleni, 2003).

Examples of modulation by biotin include glucokinase, which had increased activity in cultured hepatocytes after biotin administration (Spence and Koudelka, 1984). It was later demonstrated that an increase in mRNA preceded the increase in enzyme activity (Romero-Navarro *et al.*, 1999). Pharmacological concentrations (10 nM) of biotin decreased secretion of Interleukin-2 (IL-2) in Jurkat cells (Manthey *et al.*, 2002), but a later study showed that expression of IL-2 and IL-2 receptor were actually increased with biotin supplementation, and lower secretion of IL-2 was attributed to increased biotin-mediated endocytosis (Rodriguez-Melendez *et al.*, 2003). Biotin supplementation has also been shown to increase expression of interferon-γ, IL-1β and decrease expression of IL-4 in peripheral blood mononuclear cells (Wiedmann *et al.*, 2003).

Several studies have shown that biotin modulates expression of enzymes involved in its function as a co-factor. Biotin depletion in *Arabidopsis* caused by a mutation in the *Bio1* biotin synthesis gene, regulates expression of MCC at the translational or post-translational level (Che *et al.*, 2003). Biotin deficiency in rats reduced total protein and enzyme activity of PCC and PC and importantly reduced levels of HCS mRNA (Rodriguez-Melendez *et al.*, 2001). Similarly, low biotin content of colorectal cancer cells compared to normal cells was correlated with lower levels of PCC mRNA (Cherbonnel-Lasserre *et al.*, 1997).

A key study by Solorzano-Vargas and co-workers (2002), examined one of the potential mechanisms by which biotin may exert these effects. They showed that biotin depletion of HepG2 cells resulted in a decrease in mRNA for ACC1, ACC2, PCC and HCS. Addition of 1μM biotin to biotin-depleted cells restored mRNA levels to normal. Addition of cGMP resulted in restoration of mRNA levels. However mRNA levels were not restored when cells were incubated with an inhibitor of guanylate cyclase and biotin (Solorzano-Vargas *et al.*, 2002). This implied a signalling pathway involving cGMP, the best known of which is the protein kinase G (PKG) pathway. When activated by cGMP, PKG migrates to the nucleus where it is involved in the transcription of early response genes such as c-fos (Gudi *et al.*, 1996). This was confirmed by incubating deficient HepG2 cells with a PKG inhibitor which blocked biotin induced restoration of mRNA levels. Importantly, HCS itself was critical in this biotin responsive expression, as fibroblasts from an MCD patient with defective HCS enzyme were unable to restore mRNA levels at low biotin concentrations. This is supported by an independent study which showed the biotin-dependent expression of the asialoglycoprotein receptor in cultured hepatocytes (Collins *et al.*, 1988), was the result of the increased levels of cGMP due to stimulation of guanylate cyclase by biotin (Stockert and Ren, 1997, Li and Cronan, 1992, Singh and Dakshinamurti, 1988). A signalling cascade involving cGMP, guanylate cyclase, HCS and PKG is one mechanism by which biotin modulated gene expression may occur.

Another mechanism comes from recent observations that histones are biotinylated (Hymes *et al.*, 1995). Biotinylation of histones is increased by UV irradiation (Peters *et al.*, 2002) and also increases during cellular proliferation (Stanley *et al.*, 2001). It was originally proposed that biotinidase was responsible for the attachment and removal of biotin to histones via a biotinyl-transferase mechanism (Hymes *et al.*, 1995, Ballard *et al.*, 2002). However biotinidase expression levels and enzymatic activity did not correspond to increased biotinylation of histones seen in proliferating cells, and biotinidase activity has not been detected in the nucleus (Stanley *et al.*, 2001). Narang and collegues (2004) showed that HCS is capable of biotinylating histones *in vitro* and that fibroblasts from MCD patients show decreased histone biotinylation *in vivo*. This is despite the lack of any recognisable biotinylation sequence within histones, although there are an abundance of lysine residues present. Previous studies have shown that HCS activity can be detected in the nuclear fraction (Cohen *et al.*, 1985). Narang and colleagues also showed by immunohistochemistry that the majority of HCS protein localised in the nucleus in several cell lines, and that only the catalytic domain was required to target the enzyme to the nucleus. HCS was also shown to co-localise with lamin-B, a component of the nuclear membrane. This implied that HCS may be involved in directly controlling global gene expression through the modification of histones, analogous to other histone modifications such as acetylation, methylation, phosphorylation and ubiquitination that have been shown to cause changes in chromatin structure which affect gene expression (Berger, 2002). Another recent observation has shown that biotin modulated gene expression may occur through the Sp1 and Sp3 transcription factors. There is an increased nuclear abundance of these factors in biotin supplemented Jurkat cells compared to biotin deficient cells (Griffin *et al.*, 2003).

Two of the mechanisms by which biotin affects gene expression involve HCS as a key enzyme. This suggests that, like its bacterial counterpart, human BPL may also be a multi-functional protein.

I propose that HCS, like bacterial BirA, plays a central role in controlling biotin utilisation within the cell, and that this is achieved through activities associated with the N-terminal domain. The aims of this thesis are to investigate the role of the N-terminal domain of human HCS and to determine if it plays a part in novel protein:protein interactions, enzyme subcellular localisation, or regulation of gene expression, for example through biotinylation of histones.

General Methods and Materials

2 General materials and methods

2.1 Materials

2.1.1 General materials

Materials	Supplier
Amicon® Centrifugal Filter Devices (10,000 NWML)	Millipore, MA, USA
BioTrace™ nitrocellulose membrane	Pall Gelman Laboratory, MI, USA
Cryotube™ vials	Nunc, Roskilde, Denmark
Durapore Membrane Filter	Millipore, MA, USA
Econo-columns (glass) for chromatography	Bio-Rad Laboratories Inc., CA, USA
Econo-Pac (plastic) columns for chromatography	Bio-Rad Laboratories Inc., CA, USA
Griener Lumitrac 600 White 96 well plate	Stennick Scientific
HiTrap Protein A HP	GE Healthcare, Buckinghamshire, England
Minisart syringe filter 0.2 μm or 0.45 μm	Sartorious, Goettingen, Germany
Nunc MaxiSorpTM flat-bottom 96 well plate	Nunc, Roskilde, Denmark
PVDF membrane (Hybond P)	GE Healthcare, Buckinghamshire, England
Streptavidin Sepharose High Performance	GE Healthcare, Buckinghamshire, England
SulfoLink® Coupling Gel	Pierce Biotechnology, Rockford, IL, USA
Tissue Culture plasticware	Falcon, NJ, USA
Trans-blot Transfer Medium, 0. 2 μm supported nitrocellulose membrane	Bio-Rad Laboratories Inc., CA, USA.
X-ray film (Curix ortho HT-G)	Agfa, Belgium
ZipTip with 0.6 μL C18 resin	Millipore, MA, USA

2.1.2 Chemical reagents

All chemicals and reagents were of analytical grade, or of the highest purity available. Most common laboratory chemicals were purchased from Sigma Aldrich Inc (St Louis, MO, USA) or BDH Chemicals Ltd. (Victoria, Australia). Specialised reagents and their suppliers are listed below.

Reagents	Supplier
1kb, 100bp and 2-log DNA ladders	New England Biolabs, MA, USA
Acrylamide and Bis-Acrylamide Solutions	Bio-Rad Laboratories Inc., CA, USA
Antarctic Phosphatase	New England Biolabs, MA, USA
Avidin, Alkaline Phosphatase Conjugated	Sigma, St Louis, MO, USA
Biotinylated Protein Ladder Detection Pack	Cell Signalling Technologies, MA, USA
Bradford Protein Reagent Concentrate	Bio-Rad Laboratories Inc., CA, USA
d-[8,9-^{3}H] Biotin	GE Healthcare, Buckinghamshire, England

d-[*carbonyl*-^{14}C] Biotin	GE Healthcare, Buckinghamshire, England
(+)-Biotin N-succinimidyl ester (NHS Biotin)	Sigma, St Louis, MO, USA
Deoxynucleotide Solution Set	New England Biolabs, MA, USA
Dulbecco's Modified Eagle Medium (DMEM)	Invitrogen Life Technologies Inc, NY, USA
Enhancement Solution (for DELFIA)	Wallac (Perkin Elmer) MA, USA
Fetal Calf Serum (FCS)	GibcoBRL, NY, USA
Horse Serum	Agnieszka Stokowski, University of Adelaide
Lipofectamine™ 2000	Invitrogen Life Technologies Inc, NY, USA
MagicMark™ XP Marker	Invitrogen Life Technologies Inc, NY, USA
Mark 12 Unstained Standard	Invitrogen Life Technologies Inc, NY, USA
O-Phenylenediamine (OPD)	Sigma, St Louis, MO, USA
Optiphase Hi Safe Scintillation Fluid	Wallac (Perkin Elmer), MA, USA
Penicillin and streptomycin (for tissue culture)	Gibco, Melbourne, Australia
Prestained Protein Marker, Broad Range	New England Biolabs, MA, USA
Protease Inhibitor Cocktail	Sigma, St Louis, MO, USA
Protein A Agarose Immunoprecipitation Reagent	Santa Cruz Biotechnology, Inc., CA, USA
Protein G Plus Agarose Immunoprecipitation Reagent	Santa Cruz Biotechnology, Inc., CA, USA
Random Primers	Promega, NSW, Australia
RNAse free DNAseI	Roche, Basel, Switzerland
Skim Milk Powder for blocking	Diploma
Streptavidin Dynabeads	Invitrogen Life Technologies Inc, NY, USA
Streptavidin, Europium conjugated	Wallac (Perkin Elmer) MA, USA
Streptavidin, Peroxidase conjugated	Chemicon, Vic, Australia
SUPERaseIn RNAse Inhibitor	Ambion Inc., TX, USA
SuperScript III Reverse Transcriptase	Invitrogen Life Technologies Inc, NY, USA
T4 DNA ligase	New England Biolabs, MA, USA
Taq DNA polymerase	New England Biolabs, MA, USA
TEMED	Bio-Rad Laboratories Inc., CA, USA
Thermopol Buffer (10x)	New England Biolabs, MA, USA
Trizol Reagent	GibcoBRL , NY, USA
Trypsin, Modified, sequencing grade	Roche, Basel, Switzerland
Trypsin/EDTA	Gibco, Melbourne, Australia
VENT DNA polymerase	New England Biolabs, MA, USA

2.1.3 Restriction endonucleases

All restriction endonucleases, provided with appropriate buffer concentrates, were purchased from New England Biolabs, MA, USA.

2.1.4 Antibodies

Antibodies were reconstituted and stored as per manufacturers instructions. Antibodies were used at the manufacturers recommended dilutions.

Antibody	Supplier
Cy3 conjugated AffiniPure Donkey Anti-rabbit IgG	Jackson ImmunoResearch Laboratories, Inc., PA, USA
Rabbit Anti-chicken PC (anti-PC) antibody	(Rohde *et al.*, 1991)
Rat anti-alpha tubulin antibody	Acris antibodies, GmbH, Germany
Polyclonal anti-biotin HRP conjugated antibody	Cell Signalling Technologies, MA, USA
Goat anti-GFP antibody	Santa Cruz Biotechnology, Inc., CA, USA
Peroxidase conjugated Affinity purified anti-rat antibody	Rockland, PA, USA
Peroxidase conjugated Affinity purified donkey anti-rabbit IgG	Rockland, PA, USA
Peroxidase conjugated Affinity purified donkey anti-rat IgG	Rockland, PA, USA

2.1.5 Bacterial strains

E. coli DH5α (New England Biolabs, MA, USA) were used for routine molecular cloning.

2.1.6 Bacterial media

Luria Broth: 1% (w/v) tryptone, 0.5% (w/v) yeast extract, 1% NaCl, adjusted to pH 7.0 with NaOH.

LB agar: LB supplemented with 1.5% (w/v) bacto-agar.

Bacterial selection: Selection of bacteria bearing plasmid was achieved through addition of appropriate antibiotics to both liquid and solid media. Ampicillin was used at 100 μg/mL and Kanamycin at 50 μg/mL.

2.1.7 Tissue culture cell lines

293T: (Human embryonic kidney) Suzanne Cory, WEHI, obtained from John Heath, Oxford University, UK

HeLa: (Cervical carcinoma) American Type Culture Collection, VA, USA

HepG2: (Hepatocellular liver carcinoma), American Type Culture Collection, VA, USA

HFF: (Primary foreskin fibroblasts), Dr Tim Rayner, TGR Biosciences, Adelaide Australia

MCD-PM: (MCD patient fibroblasts), Dr Callum Wilson, Starship Childrens Hospital, Auckland, New Zealand.

MCD-JW: (MCD patient fibroblasts), Dr Callum Wilson, Starship Childrens Hospital, Auckland, New Zealand.

CHO-AA8-Tet Off: Clontech, CA, USA

2.1.8 Tissue culture media

Complete media consisted of Dulbecco's Modified Eagles Medium (DMEM) High Glucose with 25mM HEPES supplemented with 10% FCS and 1% Penicillin/Streptomycin. Modified media are outlined in the specific methods sections of chapter 6.

2.1.9 Primers

All primers were purchased from Geneworks Pty Ltd., Hindmarsh, South Australia. All primers used were of sequencing grade.

Primer Name	Sequence 5'→3'	Use
B16	cttacgagtgaagtggcccaacg	Internal HCS sequencing (forward for C-terminus)
B20	tggtagcaatgaccaacagc	Internal HCS sequencing (reverse for N-terminus)
B72	tcatgattgagtcagtcaagtttgc	Internal HCS sequencing (forward across *BglII* site)
B80	tactttccccaactgcttggtc	Internal HCS sequencing (reverse across *PstI* site)
B86	atctacgaattccatggaagatagactccacatgg	Forward HCS Met1 primer with *NcoI* and *EcoRI* sites
B88	atctacaccggtccctcgagccgccgtttggggaggatgagg	Full length HCS reverse with *EcoRI* and *HindIII* sites
B92	tacatctaccccgggctcgagttaccgccgtttggggagg	Full length HCS reverse primer with *XhoI* and *XmaI* sites
B93	atctacgaattccatggataatggactggtaccc	Forward HCS Met7 primer with *NcoI* and *EcoRI* sites
B99	atctacgaattccaagcttccgccgtttggggaggatgagg	Full length HCS reverse with *EcoRI* and *HindIII* sites
B100	atctacgaattccaagcttcctgtccttgtcctcattctcc	N-terminal HCS reverse primer with *EcoRI* and *HindIII* sites
B103	atctacgaattccatggagcatgttggcagag	Forward HCS Met58 primer with *NcoI* and *EcoRI* sites
B104	atagcggtttgactcacgg	Forward pEGFP-N1 sequencing primer
B105	gtcgtgctgcttcatgtgg	Reverse pEGFP-N1 sequencing primer

B106	gctctctcttagatttgtttcatcc	Internal HCS sequencing primer (used for RT-PCR)
B107	gagataatcggctcttaagg	Internal HCS sequencing primer (used for RT-PCR)
B117	atctacgaattcatggaagatagactccacatgg	Forward Met1HCS with *EcoRI* site in frame for pLexA
B118	atctacctcgagttacctgtccttgtcctcattctcc	Reverse HCS^{1-314} with *XhoI* and stop codon
B122	atctcagaattcatgattgtgcatgtgccttttgg	Forward $HCS^{315-726}$ primer with *EcoRI* site in frame for pLexA
B123	atcctagaattcatgcggccgcgtcgac	Forward primer to correct Y2H AD plasmids with out of frame inserts
B124	atctcaatccatatctagccttatgatgtgccagattatgcctct	pB42AD forward with HA tag and *NdeI* site
B125	atcctatctagactggcgaagaagtccaaagc	pB42AD reverse with *XbaI* site
B126	atcctagaattccatatggtgaagctgagcaaaga	Tom7 forward with EcoRI and NdeI sites
B127	atcctagaattccatatggcaaaaatctccagccc	SC100C forward with EcoRI and NdeI sites
B132	gctggccgtggtggtcggggtcggaaatgg	Forward BirA mutagenic oligo R118→ G
B133	ccatttccgaccccgaccaccacggccagc	Reverse BirA mutagenic oligo R118→ G
B134	ccgagggcaaaggaggtggagggaatgtgtgg	Forward HCS mutagenic oligo R508→ G
B135	ccacacattccctccacctcctttgccctcgg	Reverse HCS mutagenic oligo R508 → G
B137	atcctagaattccatatgacatctacaagtttcacaaaag	TPT1 forward with EcoRI and NdeI sites
B149	ggagaatgaggacaaggacaggcctgagcctatccagttacttaatgc	To make HCS-BirA chimera overlap extension primer
B150	gcattaagtaactggataggctcaggcctgtccttgtcctcattctcc	To make HCS-BirA chimera overlap extension primer
B151	gatcgatcaagcttctcgagttattaatgatgatgatgatgtcc	To make HCS-BirA chimera overlap extension primer
B156	cggacaactgtctgcggttggtcattgc	Forward HCS mutagenic oligo L216→ R
B157	gcaatgaccaaccgcagacagttgtccg	Reverse HCS mutagenic oligo L216→ R
B176	ccgtggacggacaactgtctcc	Forward primer for analysis of L216R genotype
B177	ctgcagccactgctcaagacgct	Reverse primer for analysis of L216R genotype
β-actin-For	ctggcaccacaccttctac	Forward β-actin primer
β-actin-Rev	gggcacagtgtgggtgac	Reverse β-actin primer
pEF-For	ggtcttactgacatccactttgc	pEFIRES sequencing primer forward
pEF-Rev	gacaaacgcacaccggcctt	pEFIRES reverse sequencing primer
pLexA-5'	cgtcagcagagcttcaccattg	pLexA sequencing primer forward
pLexA-3'	cgcccggaattagcttggctg	pLexA sequencing primer reverse
pB42AD-5'	ccagcctcttgctgagtggagatg	pB42AD sequencing primer forward
pB42AD-3'	atttctggcaaggtagacaagccg	pB42AD sequencing primer reverse

USP	cgccagggttttcccagtcacgac	Universal sequencing primer forward (pGEM-T plasmids)
RSP	cacacaggaaacagctatgaccatc	Universal sequencing primer reverse (pGEM-T plasmids)

2.1.10 Commercial kits

Kit	Supplier
BCA Protein Assay Kit	Pierce, IL, USA
Beta-Glo Assay Kit	Promega, WI, USA
CellTiter 96® AQ_{ueous} One Solution Cell Proliferation Assay	Promega, WI, USA
DNAEasy Tissue Kit	QIAGEN, GmbH, Germany
pGEM-T Easy Vector System I Kit	Promega, WI, USA
QIAGEN Plasmid Midi Kit	QIAGEN, GmbH, Germany
QIAprep Miniprep Kit	QIAGEN, GmbH, Germany
QIAquick Gel Extraction Kit	QIAGEN, GmbH, Germany
QIAquick PCR Purification Kit	QIAGEN, GmbH, Germany
Qproteome Cell Compartment Kit	QIAGEN, GmbH, Germany
QuikChange Site-Directed Mutagenesis Kit	Stratagene, CA, USA
UltraClean GelSpin DNA Purification Kit	MO BIO Laboratories, Inc. CA, USA
UltraClean Mini Plasmid Prep Kit	MO BIO Laboratories, Inc. CA, USA

2.1.11 Buffers and solutions

Antifade: 70% glycerol, 30 mM Tris pH 9.0, 2.5% n-propyl gallate.

Blocking Solution (for Westerns): 3% Skim Milk Powder (w/v) in PBS.

BSA Blocking Solution (for histone blots): 10% BSA (w/v) in PBS.

CAS Buffer (ELISA): PBS containing 0.1% (v/v) Tween20 and 1% (w/v) sodium caseinate.

Coomassie Blue stain: 0.2% (w/v) Coomassie brilliant blue, 10% (v/v) Methanol , 10% (v/v) Acetic Acid.

Coomassie Destain: 10% (v/v) Methanol, 10% (v/v) Acetic Acid.

ELISA Coating Buffer: 0.1 M carbonate / bicarbonate pH 9.6.

Enhanced Chemiluminescent Reagent (ECL) #1: 100 mM Tris pH 8.5, 2.5 mM luminol, 400 mM coumaric acid.

Enhanced Chemiluminescent Reagent (ECL) #2: 100 mM Tris pH 8.5, 0.2% (v/v) H_2O_2.

Gel Drying Solution: 50% Ethanol, 5% glycerol.

GTS (SDS Gel Running Buffer), 10X : 25 mM Tris-glycine pH 8.3, 0.1% (w/v) SDS.

Hypotonic Extract Buffer (HEB Buffer): 10 mM Tris pH 8, 1.5 mM $MgCl_2$, 10 mM NaCl, 10% (v/v) glycerol and 1 mM DTT, 1 mM PMSF, 1x Sigma Protease Inhibitor Cocktail added immediately before use.

Immuno Blocking Solution: PBS containing 5% Horse serum.

Immunoprecipitation Lysis Buffer: 50 mM HEPES pH 7.5, 100 mM NaCl, 10 mM EDTA, 1% (v/v) Triton X-100. Just prior to use 1x Sigma Protease Inhibitor Cocktail and 1 mM PMSF were added.

Loading Buffer (for DNA) 6X: 0.5x TBE, 40% (v/v) glycerol, 1 mg/mL bromophenol blue.

O-phenylenediamine (OPD) Buffer: 24.3 mM Citric Acid, 51.4 mM Na_2HPO_4 , pH 5.0

OPD Solution: 0.012% H_2O_2, 7.4 mM OPD in OPD Buffer.

PAT: PBS containing 0.1% (v/v) Tween20 and 0.1% (w/v) sodium azide.

PBS: 0.137 M NaCl, 2.7 mM KCl, 1.46 mM KH_2PO_4, 8.1 mM Na_2HPO_4 (pH 7.4).

PBS-Tween (PBS/T): PBS, 0.1% (v/v) Tween20.

RIPA Buffer: 10 mM Tris-Cl pH 7.4, 100 mM NaCl, 1 mM EDTA, 0.1% SDS, 0.5% Sodium deoxycholate, 10% glycerol, 1% NP-40, 25 mM $Na_2P_2O_4$. PMSF 0.5 mM and 1x Sigma Protease Inhibitor Cocktail were added immediately prior to use.

SDS-PAGE Sample Buffer (for Proteins) 5X: 0.25 M Tris (pH 6.8), 10% (w/v) SDS, 0.5% (w/v) bromophenol blue, 50% (w/v) glycerol.

SDS-PAGE, 10% Polyacrylamide Resolving Gel (GTS running buffer): 0.375 M Tris pH 8.8, 0.1% (v/v) SDS, 10% Acrylamide, 0.325% Bis-Acrylamide, 0.05% Ammonium Persulphate, 0.25% TEMED.

SDS-PAGE, 4.4% Polyacrylamide Stacking Gel (GTS running buffer): 0.125 M Tris pH 6.8, 0.1% (v/v) SDS, 4.4% Acrylamide, 0.098% Bis-Acrylamide, 0.05% Ammonium Persulphate, 0.25% TEMED.

SDS-PAGE, 15% Polyacrylamide Resolving Gel (Tricine running buffer): 1 M Tris pH 8.3, 15% Acrylamide, 0.57% Bis-Acrylamide, 0.1% Ammonium Persulphate, 0.01% TEMED.

SDS-PAGE, 2.87% Polyacrylamide Stacking Gel (Tricine running buffer) : 1.25 M Tris pH 8.3, 2.87% Acrylamide, 0.12% Bis-Acrylamide, 0.1% Ammonium Persulphate, 0.01% TEMED.

Sequencing Buffer (for DNA sequencing): 200 mM Tris pH 9.0, 5 mM EDTA.

TBE: 216 g Trizma base, 100 g boric acid, 18.6 g EDTA to 1L with MilliQ H_2O.

TBS: 100 mM Tris pH 7.5, 150 mM NaCl.

TE: 10 mM Tris pH 7.5, 1 mM EDTA.

Towbin Transfer Buffer: 20 mM Tris-HCl pH 7.5, 1.15 M Glycine, 20% Methanol, 0.1% (w/v) SDS.

Transformation Buffer 1: 30 mM KAc, 100 mM RbCl, 10 mM $CaCl_2$, 50 mM $MnCl_2$, 18.7% (v/v) glycerol.

Transformation Buffer 2: 10 mM MOPS, 10 mM RbCl, 75 mM $CaCl_2$, 15% (v/v) glycerol

Tricine Gel Running Buffer: 17.875 g Tricine, 12.125 g Tris, 1 g SDS up to 1 L with MilliQ H_2O.

2.1.12 Plasmids and vectors

Plasmids obtained for use in this study:

Yeast Two Hybrid

pLexA	Matchmaker Yeast Two Hybrid System, Clontech, CA, USA.
pLexA-Pos	Matchmaker Yeast Two Hybrid System, Clontech, CA, USA.
pLexA-53	Matchmaker Yeast Two Hybrid System, Clontech, CA, USA.
pLexA-Lam	Matchmaker Yeast Two Hybrid System, Clontech, CA, USA.
pB42AD	Matchmaker Yeast Two Hybrid System, Clontech, CA, USA.
pB42AD-T	Matchmaker Yeast Two Hybrid System, Clontech, CA, USA.

Mammalian Expression

pEFIRES	(Hobbs *et al.*, 1998)
pTR-EYFP	Prof. Murray Whitelaw, University of Adelaide, Australia. A derivative of the pTRE plasmid from Clontech, CA, USA.

HCS/BPL Plasmids (not made in this study)

pK (hBPL-his6)	Dr. Steven Polyak, University of Adelaide, Australia.
pGEX(hPC107)	Dr. Steven Polyak, University of Adelaide, Australia.
pK(yPC104)	(Polyak *et al.*, 2001)

GFP

pEGFP-N1	Clontech, CA, USA
pEGFP-C1	Clontech, CA, USA

2.1.13 Computer software

Data were analysed using GraphPad Prism and Microsoft Excel 2003 software. Images were manipulated with LeicaAS and Photoshop version 6.0. Chromatograms (from DNA sequencing) were viewed with Chromas. ApE was used a plasmid map drawing software. Protein structures were generated in Chimera (Pettersen *et al.*, 2004).

2.1.14 Web resources

NCBI was used to access protein, nucleotide and PubMed databases (http://www.ncbi.nlm.nih.gov/) and the BLAST (Basic Local Alignment Search Tool) databases. Multiple sequence alignments were performed using ClustalW (http://www.ebi.ac.uk/clustalw/). The ExPasy Proteomics Tools server (http://au.expasy.org/tools/) provided access to protein prediction (localisation, motif searches, predicted MW and PI) programs and DNA→ Protein Translation programs.

2.2 General methods

2.2.1 Culture of mammalian cells

Cells were grown in complete medium unless otherwise indicated. Cells were kept at 37˚C and 5% CO_2.

2.2.1.1 Passaging cells

When cells reached >80% confluence cells were washed twice in PBS then 1 mL trypsin/EDTA added per 75cm^2 dish. After 3-5 minutes at 37˚C, 5% CO_2 cells were collected in PBS and centrifuged at 200 g for 2 minutes. Cells were resuspended in DMEM and plated out as appropriate.

2.2.1.2 Counting cells

For cell counting cells were first trypsinised as described above. 20 μL of the resuspended cells was mixed with 20 μL trypan blue and viable (white) cells counted using a haemocytometer grid and inverted microscope.

2.2.1.3 Freezing cells

For long term storage of cell lines, cells were trypsinised and rinsed in PBS. Cells were then resuspended in 1 mL FCS + 10% DMSO per 100 mm dish. Cells were transferred to cryogenic vials before being placed in an isopropanol bath at -80˚C for controlled freezing. Once frozen, vials of cells were transferred to liquid nitrogen for long term storage.

2.2.1.4 Transfection of mammalian cells

Cells were transfected using Lipofectamine™ 2000 (Invitrogen) according to manufacturers instructions. Transfections were performed in complete media in the absence of antibiotics in a ratio of DNA:lipofectamine 1:2.

2.2.2 Protein techniques

2.2.2.1 Preparation of cell lysates

For preparation of whole cell lysates for Western Blot analysis cells were lysed in RIPA buffer unless otherwise indicated. One millilitre of chilled RIPA buffer was added per 100 mm dish of cells and incubated on ice for 30 minutes. Lysate was collected into a 1.5 mL eppendorf tube and centrifuged for 5 minutes at 17,500 g at 4˚C. The supernatant was recovered and stored at -20˚C until use.

For HCS activity assays whole cell lysates were prepared in Hypotonic Extract Buffer. To do this adherent cells were scraped into PBS with a cell scraper, pelleted by centrifugation (400 g 5 min 4˚C), resuspended in Hypotonic Extract Buffer and incubated at 4˚C with shaking for 30 minutes. Cells were then cracked by freezing at -80˚C for one hour, thawed, followed by shaking for 30 minutes at 4˚C after the addition of 4 M NaCl to a final concentration of 420 mM. Soluble protein was then collected by centrifugation (17,500 g, 30 minutes, 4˚C).

2.2.2.2 Determination of protein concentration

Protein concentration was assayed using either the Bradford Reagent (Bio-Rad Laboratories Inc., CA, USA) or BCA Assay (Pierce, IL, USA) method depending on sample buffer compatibility. A standard curve of bovine serum albumin (BSA) was generated from 0 to 1 mg/mL. For the Bradford assay 10 μL of sample was mixed with 200 μL of 1x Bradford Reagent in a 96 well plate (Falcon). Absorbance at 600 nm wavelgenth was measured on a microplate reader (Molecular Devices, CA, USA).

For the BCA assay 25 μL of sample was mixed with 200 μL of BCA working reagent and incubated at 37˚C for 30 minutes. Absorbance at 580 nm wavelength was measured on a PolarStar Galaxy microplate reader (BMG Labtech, Vic, Australia). In both instances

standard curves were generated and linear regression used to calculate protein concentration using Microsoft Excel 2003.

2.2.2.3 SDS-PAGE electrophoresis and gel staining

Proteins were separated under reducing conditions by gel electrophoresis using a Mini-Protean III gel tank (Bio-Rad, USA). One millimetre thick gels were used. Glycine based gels were used for routine separation of cell lysates (Laemmli, 1970) . Tricine gels were used for resolution of proteins less than 25 kDa (ie, histones) (Schagger and von Jagow, 1987). The resolving gel was covered with isopropanol whilst polymerising to prevent gel shrinkage. After the gel was set the isopropanol was removed and the gel rinsed with distilled water. The stacking gel was then poured and a comb inserted. Once the stacking gel was set the comb was removed and the apparatus was assembled according to the manufacturer's instructions. Protein samples containing 1x Protein Sample Buffer were boiled for 5 minutes and then centrifuged briefly to collect condensation. Protein samples were loaded onto the gel using gel loading tips (Quality Scientific Plastics, USA). Glycine gels were electrophoresed in GTS buffer at 100V until the dye front reached the bottom of the gel. Tricine gels were electrophoresed under the same conditions in Tricine Running Buffer. For resolution of high molecular weight proteins (such as HCS) gels were electrophoresed for a further 15 minutes after the dye front left the gel.

2.2.2.4 Western Blotting

Proteins were transferred onto a nitrocellulose membrane using a semi-dry transfer unit (Hoefer SemiPhor, Amersham Pharmacia Biotech, CA, USA). Six sheets of Whatman filter paper and the nitrocellulose membrane were pre-soaked in Towbin Transfer Buffer prior to assembly of the gel sandwhich. Proteins were transferred for 2-4 hours at 40 mA per gel. The membranes were then blocked in the appropriate blocking buffer (routinely, 3% milk for HCS Westerns, 10% BSA for histone blots).

2.2.3 Immunoprecipitation

Cells were harvested from 15 cm petri dishes. After washing cells in ice-cold PBS cells, 300 μL of immunoprecipitation lysis buffer was added and cells scraped off using a cell scraper and collected in an eppendorf. Cells were lysed on ice for 30 minutes (at 4°C). Soluble material was collected by centrifugation at 17,500 g for 15 minutes at 4°C.

Lysate was pre-cleared by addition of 20 μL of each protein A and protein G agarose beads (40 μL total), followed by incubation on a rotating wheel for 30 minutes at 4°C. Soluble, pre-cleared lysate was collected by centrifugation at 17,500 g for 30 seconds at 4°C. Pre-cleared lysate was assayed for protein concentration, and then 2 mg of lysate added to an eppendorf tube. Five micrograms of primary antibody was added and incubated overnight at 4°C on a rotating wheel. The next day, 30 μL of protein A agarose and 30 μL of protein G agarose (60 μL total) were added and incubated for a further 4 hours at 4°C on a rotating wheel. Immunoprecipitates were collected by centrifugation at 5,000 rpm for 30 seconds at 4°C. Immunoprecipitates were washed three times in 1 mL PBS, and then the pellet resuspended in SDS sample buffer and boiled for 5 minutes prior to fractionation by SDS-PAGE.

2.2.4 HCS activity assays

For *in vitro* HCS assays, the apo-biotin domain consisting of the C-terminal 104 amino acids of yeast PC (yPC-104) was used as a substrate. This was kindly provided by Dr S. Polyak and was purified as described previously (Polyak *et al.*, 1999). Holo-yPC104 was also provided as a positive control.

2.2.4.1 *In vitro* ^{3}H-biotin biotinylation assay

In vitro biotinylation assays were carried out as described previously (Chapman-Smith *et al.*, 1999). Briefly, cells were harvested and lysates prepared in HEB buffer. To quantitate HCS activity an *in vitro* biotinylation reaction was performed for one hour at 37°C in a 100 μL reaction mix containing 50 mM Tris pH 8.0, 3 mM ATP, 5.5 mM $MgCl_2$, 0.1 mg/mL BSA, 0.1 μM DTT, 5 μM apo-yPC104, 10 μM ^{3}H biotin and 100 μg lysate. At completion of the assay aliquots were spotted onto Whatman filter paper pre-treated with 10% TCA and 0.1 mg/mL biotin. Filter papers were washed twice in ice cold 10% TCA and once in ice-cold ethanol (100%), dried, and added to 2 mL Optiphase HiSafe Scintillation fluid. Radioactivity measurements were obtained using a Rackbeta Liquid Scintillation Counter (Perkin Elmer, MA, USA).

2.2.4.2 Time-resolved fluorescence Eu^{3+}-Streptavidin assay

Apo-yPC104 was diluted in TBS and 100 ng/well added to white Greiner 96 well plates. A standard curve of holo-yPC104 (0 -100 ng) was added to each plate as positive control and to allow comparison between plates. After coating the plate overnight at 4°C, the plate was blocked in 1% BSA in TBS for one hour, followed by five washes in TBS 0.1% Tween. For the biotinylation assay, 50 μL of master mix containing 50 mM Tris pH 8.0, 3 mM ATP, 5.5 mM $MgCl_2$, 5 μM biotin, 0.1 mg/mL BSA and 0.1 μM DTT was added to each well. Cellular lysates, prepared in HEB buffer, were diluted to appropriate concentrations in 50 mM Tris pH 8.0. Addition of 50 μL of lysate marked commencement of the assay. After one hour at 37°C the plate was washed five times in TBS 0.1% Tween. Europium-labelled Streptavidin was diluted 1:1000 in TBS containing 0.1% Tween and 100 μM Diethylenetriaminepentaacetic acid (DPTA). 50 μL of Eu^{3+} Streptavidin was added per well and incubated one hour at 37°C, followed by washing five times in TBS 0.1% Tween containing 100 μM DPTA followed by three washes in sterile water. 50 μL of Enhancement Solution (Perkin-Elmer) was added per well and incubated for 10 minutes

before reading the plate using time-resolved fluorescence on a PolarStar Galaxy microplate reader (BMG Labtech, Vic, Australia).

2.2.5 Mass spectrometry

Mass Spectrometry was performed at the Adelaide Proteomics Facility, University of Adelaide.

2.2.5.1 MALDI mass spectrometry (MS and MS/MS)

One microliter of each sample was applied to a 600 μm AnchorChip (Bruker Daltonik GmbH, Bremen, Germany) according to the alpha-cyano-4-hydroxycinnamic acid (HCCA) thin-layer method. MALDI TOF mass spectra were aquired using a Bruker ultralfex II MALDI TOF/TOF mass spectrometer (Bruker Daltonic, GmbH) operating in reflection mode under the control of the flexControl software (version 3.0, Bruker Daltonik GmbH). External calibration was performed using peptide standards (Bruker Daltonik, GmbH) that were analysed under the same conditions. Spectra were obtained at random locations over the surface of the matrix spot.

MS spectra were subjected to smoothing, background subtraction and peak detection using flexAnalysis (Version 3.0, Bruker Daltonik GmbH). The spectra and mass lists were exported to BioTools (Version 3.0, Bruker Daltonik GmbH). Here, the MS spectra were submitted to the in-house Mascot database-searching engine (Matrix Science: http://www.matrixscience.com).

2.2.5.2 Liquid chromatography-ESI mass spectrometry (MS and MS/MS)

Three microlitres of the trypsin digested sample was diluted to 5.5 μL with 1% formic acid in an autosampler vial and 5 μL analysed. The samples were chromatographed using an Agilent Protein ID Chip column assembly (40 nL trap column with 0.075 x 43 mm C-18 analytical column) housed in an Agilent HPLC-Chip Cube Interface connected to an HCT ultra 3D-Ion-Trap mass spectrometer (Bruker Daltonik GmbH). The column was equilibrated with 4% acetonitirile / 0.1% formic acid at 0.5 μL/min and the samples eluted with an acetonitrile gradient (4%-30% in 30 minutes). Ionizable species (300 < m/z < 1,200) were trapped and one or two of the most intense ions eluting at the time were fragmented by collision-induced dissociation (CID).

The resulting spectra were subjected to peak detection using DataAnalysis (Version 3.4, Bruker Daltonik, GmbH). The combined MS and MS/MS lists were exported in Mascot generic format and submitted to Mascot database search engine.

2.2.6 Molecular biology techniques

2.2.6.1 Agarose gel electrophoresis

Analysis of DNA and separation of DNA fragments was performed using agarose gel electrophoresis. Gel slabs were poured by melting 0.8-2% (w/v) agarose in TBE buffer. Prior to loading into wells DNA samples were mixed with an appropriate volume of 6X DNA Loading Buffer. Samples were electrophoresed in TBE buffer at 100-150V and then stained in Ethidium bromide solution (1 μg/mL) for 10 minutes followed by destaining in distilled water. DNA was visualised on a UV transilluminator and photographed using a Mitsubishi Video Processor.

2.2.6.2 Preparation of DH5-α competent cells

A single colony picked off a plate was used to inoculate a 2 mL overnight culture of DH5α in Luria Broth. After incubation overnight at 37˚C with rotation, 330 μL was subcultured into 10 mL of LB and the culture grown until it reached log phase (as indicated by an OD_{600nm} of 0.5-0.6). Five mL of log phase culture was then added to 100 mL pre-warmed LB and incubated for a further 1.5 hours. The culture was split into 4 x 50 mL centrifuge tubes and placed on ice for 5 minutes. Cells were pelleted by centrifugation at 3,200 g for 5 minutes at 4˚C. The cells were then resuspended in a total of 40 mL of Transformation Buffer 1 and incubated on ice for 5 minutes, then collected by centrifugation at 3,200 g for 5 minutes at 4˚C. This was followed by resuspension in Transformation Buffer 2 to a final volume of 4 mL. Cells were chilled on ice for 5 minutes prior to aliquoting and storing at -80˚C until required.

2.2.6.3 Restriction digest of DNA

Routinely, 1-5 μg of DNA was digested with 1-10 U of restriction enzyme in the appropriate NEB buffer for 2 hours at 37˚C. In the instance of double digests the buffer conditions for the more sensitive enzyme were used (as recommended by NEB). For cloning, DNA fragments were separated by agarose gel electrophoresis before purification from the excised gel slice using either a QIAGEN or MOBIO Gel Purification Kit.

2.2.6.4 Ligation of DNA fragments

Prior to ligation, endonuclease treated vector DNA was treated with Antarctic Phosphatase (New England Biolabs, CA, USA), according to manufacturer's instructions, to prevent vector re-ligation. Ligation was carried out in a 10 μL volume in an insert:vector ratio of 3:1 in 1X ligase buffer and 2 U of T4 DNA ligase for 1-4 hours at room temperature or 16 hours at 4˚C.

2.2.6.5 Transformation of competent cells

Five μL of ligation mixture was added to 100 μL of competent cells and incubated on ice for 30 minutes. Cells were incubated at 42˚C for 5 minutes then allowed to recover for 5 minutes on ice. Cells were immediately plated onto pre-warmed LB agar plates for ampicillin selection, otherwise a 1 hr recovery step with 1 mL LB was performed prior to plating.

2.2.6.6 Glycerol stocks

For long term storage of *E. coli* strains, equal volumes of an overnight culture and 80% glycerol were mixed and stored at -80˚C.

2.2.6.7 Purification of plasmid DNA

For purification of small (<10 μg) amounts of plasmid DNA the QIAGEN QIAprep Miniprep Kit was employed. For larger scale purification the QIAGEN Midi prep Kit was used according to manufacturers instructions. For transfection quality DNA, purified material from the kits was precipitated in 70% (v/v) isopropanol, pelleted by centrifugation at 17,500 g for 30 minutes and then washed in 70% (v/v) ethanol before resuspension in sterile MilliQ water.

2.2.6.8 Quantification of DNA

DNA was quantified by measuring absorbance at 260 nm using a CARY WinUV Spectrophotometer. A measure of 1 OD_{260} unit is equal to 50 μg/mL.

2.2.6.9 DNA sequencing

Plasmid DNA or PCR products were used as templates for DNA sequencing. A 20 μL reaction containing 200 ng DNA, 100 ng of appropriate primer, and 2 μL BigDye (version

3) reaction mix (Perkin Elmer, Applied Biosystems, CA, USA) was prepared in Sequencing Buffer for PCR. The PCR profile consisted of 30 cycles of denaturation at 96˚C for 30 seconds, annealing at 50˚C for 15 seconds and extension at 60˚C for 4 minutes. After thermocycling, 80 μL of 75% (v/v) isopropanol and 1 μL glycogen (20 mg/mL) were added to the PCR products, vortexed and left at room temperature for 30 minutes. Precipitated DNA was isolated by centrifugation at 17,500 g for 20 minutes. The pellet was washed twice in 75% isopropanol followed by centrifugation for 5 minutes at 17,500 g. The pellet was then dried in a 37˚C heating block prior to being submitted to the Molecular Pathology Sequencing Service at the Institute of Medical and Veterinary Science, Adelaide. Sequencing was carried out on a 3700 Applied Biosystems Analyser. Upon upgrade to the 3730 Analyser the protocol was identical but the reaction consisted of 200 ng DNA, 100 ng primer, 1 μL of BigDye (version 3) and 3 μL of 5X sequencing buffer (Perkin Elmer, Applied Biosystems, CA, USA).

2.2.6.10 PCR protocols

PCR reactions routinely consisted of the following in a 50 μL reaction: 1x ThermoPol Buffer, 250 ng oligonucleotide primers, 400 μM dNTP mixture and 1 U VENT DNA polymerase. Reactions were routinely carried out under the following cycling conditions: 30 seconds denaturation at 95˚C, 30 seconds annealing at 60˚C, 90 seconds extension at 72˚C for 25-35 cycles. All reactions were carried out on a MJ Research PTC 2000 Thermal Cycler (GMI Inc., MN, USA).

Colony PCR was carried out using the conditions outlined above but whole bacteria were used as template. A single colony was picked from an agar plate using a 200 μL pipette tip, the tip used to streak a fresh agar plate and then aspirated in master mix in the reaction tube.

2.3 Molecular cloning HCS constructs.

2.3.1.1 HCS constructs with GFP tag

Refer to figure 2.1 for the cloning strategy employed for generation of GFP tagged HCS constructs. Primers were designed to engineer appropriate restriction sites into the cDNA to allow for in-frame cloning of HCS or HCS fragments into pEGFP vectors. Refer to 2.1.11 for a full list of primers.

Construct	Forward Primer	5' Restriction site added	Reverse Primer	3' Restriction site added
pEGFPN1 (Met1-HCS)	B86	EcoRI	B100	EcoRI
pEGFPN1 (Met7-HCS)	B93	EcoRI	B100	EcoRI
pEGFPN1 (Met58-HCS)	B103	EcoRI	B100	EcoRI
pEGFPN1 (Met1-nHCS)	B86	EcoRI	B99	EcoRI
pEGFPN1 (Met7-nHCS)	B93	EcoRI	B99	EcoRI
pEGFPN1 (Met58-nHCS)	B103	EcoRI	B99	EcoRI
pEGFPC1 (Met1-HCS)	B86	EcoRI	B92	XmaI

Table 2-1Primer sets used to amplify HCS fragments for cloning into pEGFP vectors.

pET(HCS) (provided by Dr Steven Polyak, University of Adelaide) was used as the template DNA for PCR. The purified PCR product consisting of the HCS cDNA was treated with endonuclease as follows: for pEGFP-N1 constructs cDNA and plasmid were treated with *EcoR*I, for pEGFP-C1 constructs cDNA and plasmid were digested with *EcoR*I and *Xma*I. Fragments were ligated and transformed into DH5α *E. coli*. Clones found to be bearing the correct insert by restriction digest analysis were sequenced along the entire HCS coding sequence to ensure integrity of the insert. Primers used for sequencing HCS insert include B20, B72, B80, FW2, B16, B104, B105, B106, B107.

2.3.2 Generation of mammalian HCS expression plasmid

pEGFP-N1(Met^1-HCS) plasmid and pEFIRES plasmid (Hobbs *et al.*, 1998) were digested with *EcoRI*. The full length HCS fragment was ligated into the pEFIRES vector and colony PCR with primers B97 and EF-FOR employed to screen for clones bearing the insert in the correct orientation.

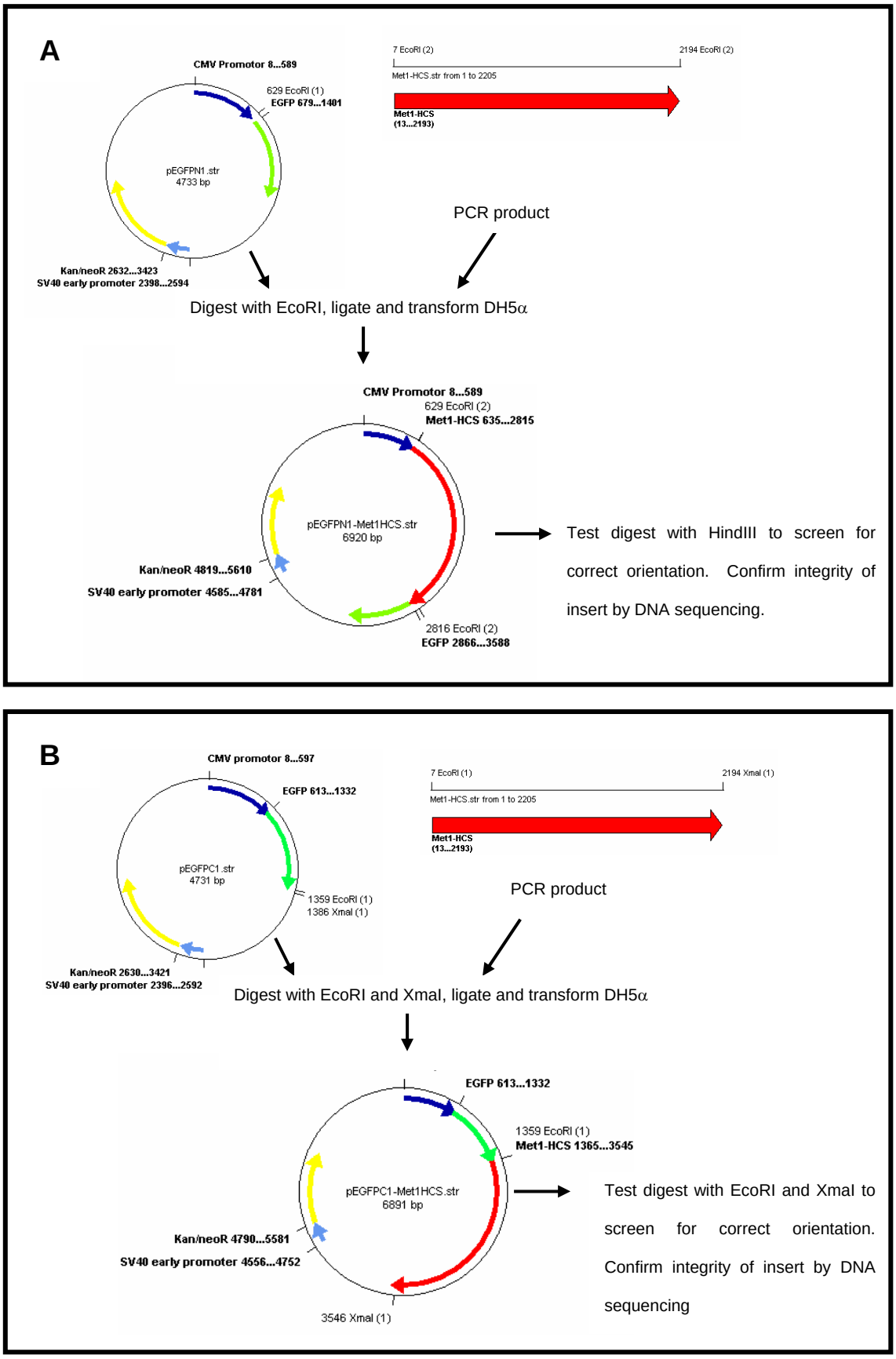

Figure 2.1 Cloning strategy for creation of GFP tagged HCS.
(A) HCS construct with a C-terminal GFP tag (B) HCS construct with an N-terminal GFP tag.

Production and Characterisation of polyclonal antibodies to examine HCS isoforms

3 Production and characterisation of polyclonal antibodies to examine HCS isoforms

3.1 Background

Prior to this study there had been only one report analysing HCS isoforms in cell and tissue lystates using antibodies. (Hiratsuka *et al.*, 1998). Currently there are no commercially available antibodies to HCS. As antibodies are useful tools for examining the properties of proteins, this part of the study aimed to generate a suite of HCS antibodies raised against various peptide epitopes of HCS. Polyclonal antibodies were chosen to be produced as a number of epitopes were selected in order to distinguish between cellular isoforms of HCS. Robust polyclonal antibodies have many uses, such as Western Blotting or Immunocytochemistry. Additionally, antibodies can be utilised for immunoprecipitation studies which may facilitate protein interaction, metabolic labelling and protein stability studies.

It has been shown previously that multiple isoforms of HCS exist. Diversity of protein products from a single gene can arise through multiple processes such as alternative splicing, alternative initiation of translation or proteolytic processing of mature transcripts. What controls the processing of HCS isoforms is unclear.

Alternative splicing

Alternative splicing of exons 5 and 6 of HCS results in an mRNA lacking the first two in frame AUG codons (Yang *et al.*, 2001). This results in a protein with the first initiation codon at Met^{58}. Different HCS splice variants have been detected in different tissue types, and hence there may be cell type specific regulation of mRNA processing (Yang *et al.*, 2001).

Alternative initiation of translation

Alternative use of initiation AUG codons provides another level of control over cellular translation. In eukaryotes factors such as mRNA length, secondary structure and context of nucleotides proximal to the AUG affect initiation (Cai *et al.*, 2006, Slusher, 1991).

The process by which alternative initiation sites are utilised is described as a "leaky scanning" mechanism. In the usual initiation process, the 40S ribosomal subunit attaches to the 5'mRNA followed by ATP dependent scanning for the initiator codon.(Cai *et al.*, 2006). Leakiness results when the first AUG is used inefficiently, which may be due to a poor Kozac consensus initiation sequence. Scanning can continue past the first AUG allowing for efficient recognition of a downstream AUG.

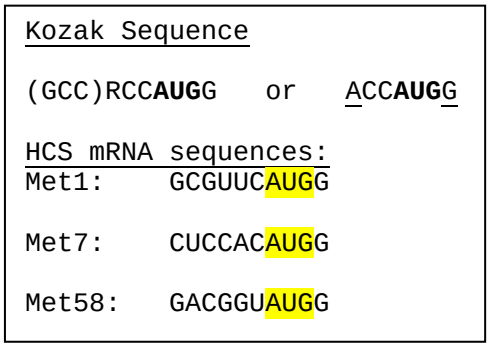

Figure 3-1 Comparison of HCS potential initiation codons to the Kozak consensus initiation sequence.

The most conserved features of the Kozac consensus sequence are the A at -3 and the G at +1. All three potential AUG codons contain the G at +1, the third codon (at Met^{58}) contains a purine (G) at -3 and most closely resembles the traditional Kozac sequence. However, many AUG sequence contexts for alternative initiation codons do not conform to the Kozak consensus.

Initiation codon usage can direct subcellular localisation. Cai et al, systematically analysed the consequences of alternative initiation of translation events and found that the majority (85.7%) were associated with alteration in subcellular localisation. They found most N-terminally truncated forms had significantly reduced isoelectic points targeting them to different cellular compartments, but retained their overall domain structure. An

example of this is the localisation of MOD5, a t-RNA modifying enzyme of *S.cerevisiae*. Two in-frame ATGs are used for initiation, the use of the first includes a mitochondrial targeting sequence which is absent in the peptide translated from the second initiation codon (Slusher *et al.*, 1991). Interestingly, many tRNA synthetases, which are evolutionarily related to HCS, have been identified to have alternative initiation of translation events (Cai *et al.*, 2006). Alternatively, use of alternative initiation codons may not alter localisation of the protein but may alter kinetic properties of enzymes. This has been shown for glutamine synthetase, where the long and short forms which arise due to alternative splicing of exon 1 have similar subcellular distributions but have different affinities for ATP. The dissociation constant for an inhibitor is also significantly altered, demonstrating that the N-terminal context can significantly change the conformation of the catalytic core of the enzyme altering substrate specificity (Shin and Park, 2004).

The sizes of HCS isoforms identified previously (Hiratsuka *et al.*, 1998) are consistent with alternative initiation of translation from the first three in frame AUG codons at Met^{1}, Met^{7} and Met^{58} (predicted Molecular weights of 81, 80 and 76 kDa respectively). Previously it has been shown that the activity of the HCS isoform starting at Met^{58} has only 40% the activity of the Met^{1} full length isoform. In order to try and discriminate between different HCS isoforms peptide eptitopes were chosen to differentiate between HCS species, with the aim of using these antibodies to identify altered properties of isoforms, such as the effect on subcellular localisation.

3.2 Specific methods

3.2.1 Production of polyclonal antibodies in rabbits

HCS peptides (N1, N2, N3 or CHCS), conjugated to Keyhole limpet hemocyanin (KLH) were used to immunise New Zealand white rabbits. Lyophilised peptides were reconstituted in sterile PBS. Peptides were diluted 1:1 in complete Freund's adjuvant for the first injection and in incomplete Freunds's adjuvant for subsequent injections. 150 μg of peptide were used per injection. Booster injections were repeated three times after four week intervals. Test bleeds were drawn from the animals and tested for antibody production by ELISA. Pre-immunisation sera were collected as negative controls. The animals were terminally bled 14 days after the final boost.

All experiments were approved by the University of Adelaide Animal Ethics Committee and conducted in accordance with the guidelines of the National Health and Medical Research Centre (NH&MRC) Australian Code of Practice for the Care and Use of Animals for Scientific Purposes.

3.2.2 Monitoring of antibody production by ELISA

Peptides were reconstituted to a concentration of 1 mg/ml in acetonitrile/water 50/50% (v/v). An aliquot (50 μl) of peptide solution was added to 10.5 ml Elisa Coating Buffer and 100 μl of the diluted peptide added per well to a 96 well Maxisorp plate (Nunc). Plates were incubated rocking overnight at 4°C to ensure complete coating. The plates were then blocked with 200 μl PAT Buffer per well for 30 minutes at room temperature. The plate was then washed with MilliQ water. Serial dilutions of rabbit sera in PAT buffer (refer section 2.1.11) were added to the plate (100 μl per well) and left for 1 hour on a rocking platform. The plate was then washed three times with MilliQ water and then probed with donkey anti-rabbit HRP antibody (Rockland) diluted in CAS Buffer 1:1000 for 1 hr. After final washing in MilliQ water the plate was developed with 200 μl OPD solution

per well. The colour development was quenched by addition of 100 μl of 1.0M H_2SO_4 per well before reading absorbance at 490 nm on a Labsystems Multiskan® Plate reader.

3.2.3 Antibody purification

3.2.3.1 Preparation of columns

Peptides used for immunisation contained a C-terminal cysteine residue to allow coupling via thiol linkage to SulfoLink resin (Pierce). Peptide (2.0 mg) was coupled to 1 ml of resin as per manufacturers' instructions. Columns were stored in PBS containing 0.05% sodium azide at 4°C.

3.2.3.2 Affinity purification

For affinity purification of antibodies aliquots of sera were thawed, diluted 1:2 in PBS+0.05%NaAzide and filtered through a 0.45μm membrane. The column was washed in 6 column volumes PBS+0.05%NaAzide and then the sera applied. Sera was re-applied over the column at least three times. The column was then washed in 12 column volumes PBS+0.05%NaAzide and antibodies eluted with 0.1M Glycine pH 2.5 into Eppendorf tubes containing 25 μL 1M Tris pH 9.0 as neutralisation buffer. Column was then regenerated in PBS+0.05%NaAzide and stored at 4°C. Fractions were pooled and buffer exchanged into PBS containing 10% glycerol using Amicon Spin Filters (Amicon). Antibody concentration was determined by taking an absorbance at 280nm where an OD of 1.35 represented 1 mg/ml.

3.2.4 Purification of HCS isoforms by affinity chromatography

3.2.4.1 Biotinylation of antibody

For biotin labelling of polyclonal antibodies a 50-fold excess of antibody: NHS biotin was used. NHS biotin was dissolved in DMSO and added to 1mg of antibody. The mixture

was incubated for two hours at room temperature with constant mixing before unreacted NHS biotin was removed using Amicon Spin Filters.

3.2.4.2 Coupling antibody to Streptavidin-Sepharose

Streptavidin-Sepharose (GE Healthcare) (500 μL) was packed in a disposable column (Bio-Rad) and equilibrated with PBS. Biotinylated antibody solution was added to the resin and the column capped and incubated for 1 hr at room temperature. Unbound material was washed from the column with PBS, followed by two column volumes 0.1M glycine pH 2.5. The column was then re-equilibrated in PBS pH 7.4.

3.2.4.3 Affinity purification of HCS isoforms

293T cells overexpressing HCS were harvested and lysed in RIPA buffer. Lysate was diluted 1:2 in PBS/0.05% (w/v) sodium azide and filtered through a 0.45 μm membrane. Lysate was added to the biotinylated antibody/streptavidin Sepharose column. The column was capped and placed on an Adams™ Nutator Mixer (BD Biosciences, NJ, USA) at 4°C for one hour. Flow through material was collected, the column washed with 2 x 5 mL PBS and HCS eluted with 2 mL 0.1M Glycine pH 2.5 into Eppendorfs containing 25 μL 1M Tris pH 9.0 as neutralisation buffer. HCS protein was concentrated and buffer exchanged into 50mM Tris pH 8.0 using Amicon Spin Filters. HCS isoforms were separated by SDS-PAGE and molecular weights determined by linear regression analysis of Rf values of Mark12 unstained protein markers. Estimation of molecular weight was determined from analysis of three independent purification processes.

3.2.4.4 Mass Spectrometry of HCS isoforms

Identification of HCS isoforms was performed by Dr Chris Bagley. Samples provided in a 10% glycine SDS-PAGE were excised from the gel and digested with 100 ng trypsin

under standardised low-salt conditions. Refer to Materials and Methods section 2.2.4 for details of mass spectrometry.

3.3 Results

3.3.1 Peptide design for immunisation

Peptides encompassing specific regions of HCS were ordered from Mimetopes, Australia, for generation of polyclonal antibodies in rabbits. The algorithm of Hopp and Woods (www.virus.kyoto.u.ac.jp, accessed 27/1/04) was used to predict antigenicity and therefore suitability of candidate sequences (Hopp and Woods, 1981). Four distinct peptides were designed against predicted immunogenic regions HCS molecule using this data and in consultation with Mimetopes, Australia. The peptides were also selected such that antibodies could be used to detect specific regions of the HCS molecule (table 3.1). Antibodies against N1 and N2 were designed to distinguish between isoforms of HCS potentially starting from different initiation of translation sites. N3 spans the proposed linker region between the N- and C-terminal halves of the protein. The CHCS peptide contains a GKGRGG motif that is highly conserved in the catalytic site of all BPLs (Wilson *et al.*, 1992).

Peptide	Amino Acid region	Amino Acid sequence
N1	1-15	MEDRLHMDNGLVPQK
N2	62-77	GRDDPKALGEEPKQRR
N3	304-318	QGHLENEDKDRMIVH
CHCS	499-510	AARQTEGKGRGG

Table 3-1 The four different peptide epitopes to which polyclonal antibodies to HCS were raised.

3.3.2 Analysis of antibody production by ELISA

Antibody titre was monitored by ELISA against the immunising peptide. The results are summarised in figure 3.2 where antibody titre for each of the peptides used is shown.

The graphs show a plot of whole serum binding to peptide antigen over a range of dilutions (Figure 3.2). All graphs indicate that anti-peptide antibodies are contained in the sera.

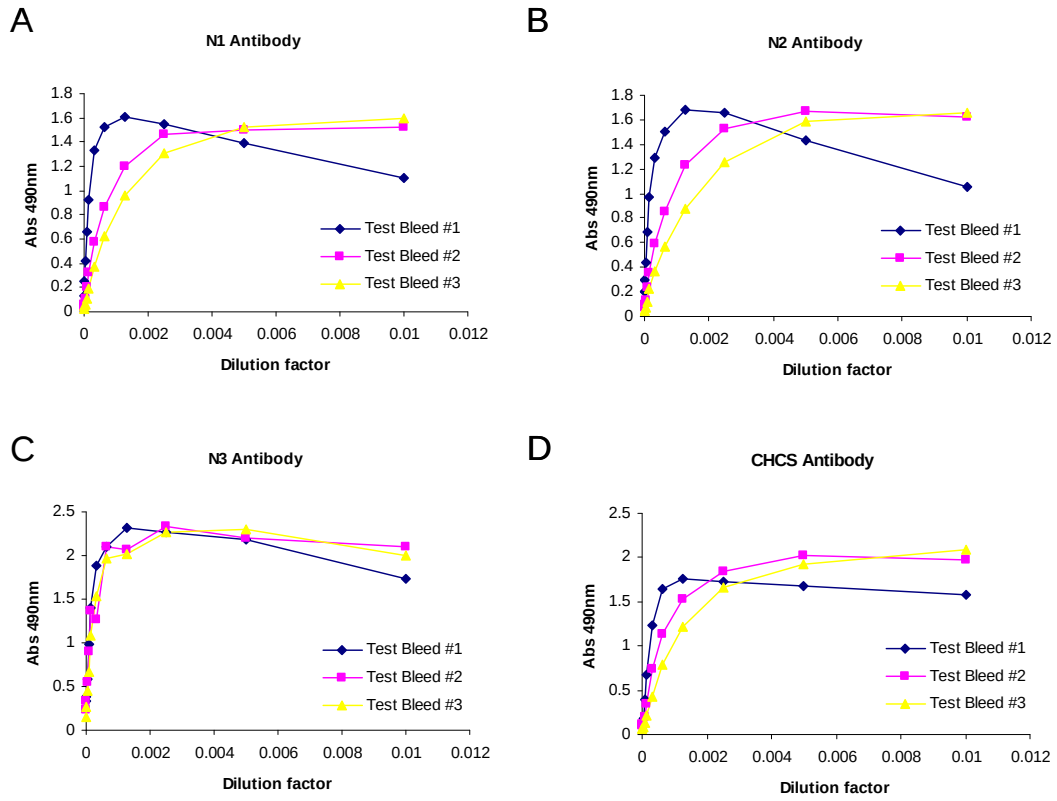

Figure 3-2 Titration of rabbit sera was determined by ELISA against the immunising peptide.
(A) N1 antibody (B) N2 antibody (C) N3 antibody (D) CHCS antibody.

3.3.3 Affinity purification of antibodies

Initially antibodies were purified using Protein A columns which have high affinity for the Fc region of rabbit immunoglobulins. Western Blot analysis on whole cell lysate from 293T human embryonic kidney cells revealed that these Protein A purified antibodies had cross-reactivity with multiple cellular proteins (data not shown). Hence, a strategy of affinity purification was employed. The peptides used for immunisation all contained a C-terminal cysteine residue which was utilised to couple the peptides to Sulfolink resin (PIERCE). A representative Coomassie stained gel of an antibody purification is shown in

figure 3.3. Antibodies were successfully purified to more than 95% purity as judged by coomassie staining.

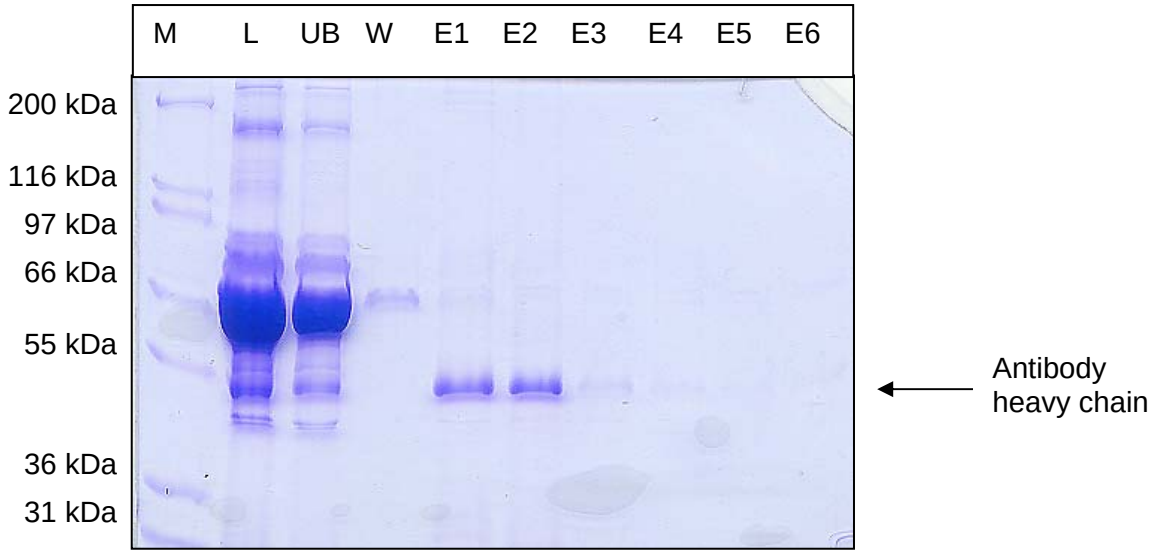

Figure 3-3. Affinity purification of ChBPL antibody.
10μL aliquots from the purification of anti-CHCS antibody over CHCS peptide column were run on a 10% SDS PAGE. The fractions analysed were (M) Marker, (L) Rabbit #10 serum (UB) Unbound material after passing over column, (W) Wash with PBS 0.05% sodium azide (E) Eluted fractions.

3.3.4 Characterisation of HCS with affinity purified antibodies

The HCS antibodies were used to analyse endogenous and recombinantly expressed HCS. 293T cells were selected as these cells are derived from human embryonic kidney, a tissue known to be rich in biotin and high in metabolic activity dependent on biotin-carboxylases (McMahon, 2002). Initial investigations by Western blotting indicated that only very low, barely detectable amounts of HCS were present in 293T cell lysates. Hence HCS was transiently transfected and overexpressed in 293T cells (figure 3.4). In this analysis only HCS specific bands were observed, indicating no cross reactivity with other cellular proteins. This highlighted the importance of affinity purification of the antibodies, as merely purifying the IgG fraction still resulted in a number of cross reacting bands.

Furthermore, multiple isoforms of HCS were detected in 293T cells (figure 3.4). The anti-N1 antibody, designed to interact with the very N-terminal 15 aa of HCS, detected a doublet, where the upper band (referred to as HCS-A) was approximately 86 kDa, and the lower band (referred to as HCS-B) 82 kDa. The estimated molecular weight for HCS starting at the first initiation methionine is 81 kDa. This was detected in both untreated cell lysate and in the overexpressed HCS lysate. The anti-N2 antibody, with an epitope of amino acids 62-77, detected both the upper two bands and an extra band at 72.4 kDa (referred to as HCS-C). A similar pattern was observed in the cells overexpressing HCS when probed with the anti-N3 antibody. The anti-CHCS antibody cross reacted with all HCS isoforms, including a product at approximately 55kDa. It should be noted that the molecular weight estimation for the CHCS band is less accurate, as this band could not be purified and analysed using unstained standards (Mark12, Invitrogen), and hence a less accurate method of estimating molecular weight using MagicMark standards (Invitrogen) had to be used. These results indicate that multiple isoforms of HCS are present in the cell, and these isoforms differ at their N-termini.

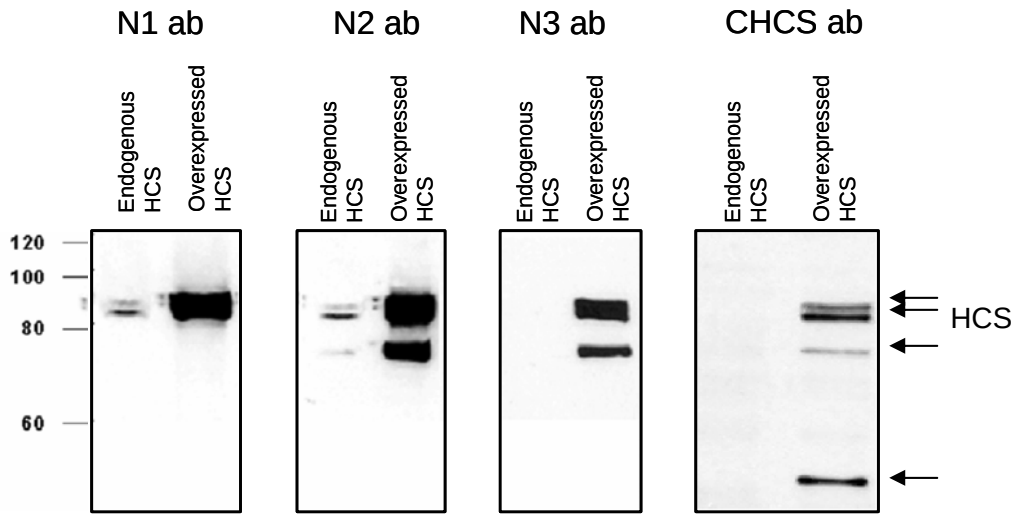

Figure 3-4. Detection of HCS isoforms in 293T cell lysate.
20 μg of cell lysate from untransfected cells (to examine endogenous amounts of HCS) and cells transiently transfected with pEFIRES(HCS) were run on a 10% Glycine SDS-PAGE and transferred to nitrocellulose. Blots were probed with 1.5 μg of HCS antibody indicated above the panel and detected by ECL.

To investigate whether the isoforms of HCS were unique to 293T cells, HeLa and HepG2 cells were also transfected with the pEFIRES(HCS) construct. Figure 3.5 is a Western Blot of cell lysates analysed 24 and 48 hours after transient transfection. Upregulated protein production of identical HCS isoforms were apparent in both HeLa and 293T cells. However, transfection of HepG2 cells was problematic, preventing analysis in this cell line despite several attempts (data not shown).

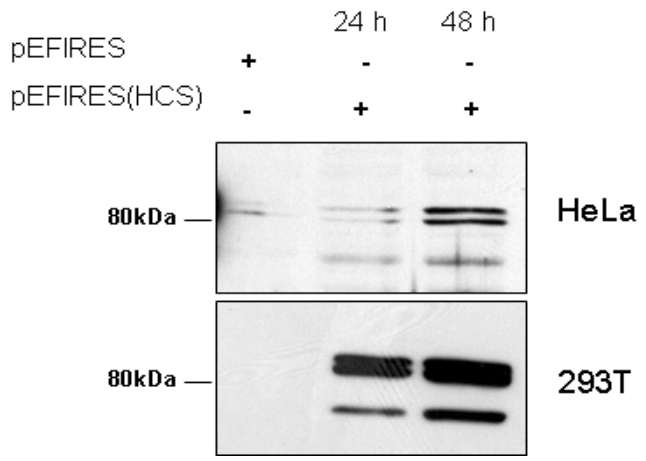

Figure 3-5 . Transient overexpression of HCS in HeLa and 293T cells.

Cells were transfected with pEFIRES(HCS) and harvested in RIPA buffer 24 and 48 hours post transfection. 20 μg of cell lysate was loaded per lane and Western Blotted with N2 antibody.

To examine these HCS isoforms further a stable cell line of 293T cells overexpressing HCS was generated by cultivating transfected cells in media containing puromycin containing media over a period of two weeks. A polyclonal pool of stably transfected clones was used for the remaining studies.

3.3.5 Mass spectrometry identification of HCS isoforms

Mass spectrometry was employed to confirm the identity of the immunoreactive bands observed in the Western Blots. Several methods for isolating HCS isoforms from 293T cells overexpressing HCS were trialled, including His-tag metal affinity chromatography, biotin affinity chromatography and coupling of anti-HCS antibodies to both Affigel and Sulfolink resins for affinity purification. However, the most effective method was a two

step procedure where HCS antibody N2 was first biotinylated, coupled to Streptavidin Sepharose and used for affinity purification. Successful purification of HCS isoforms A, B and C is shown in Figure 3.6.

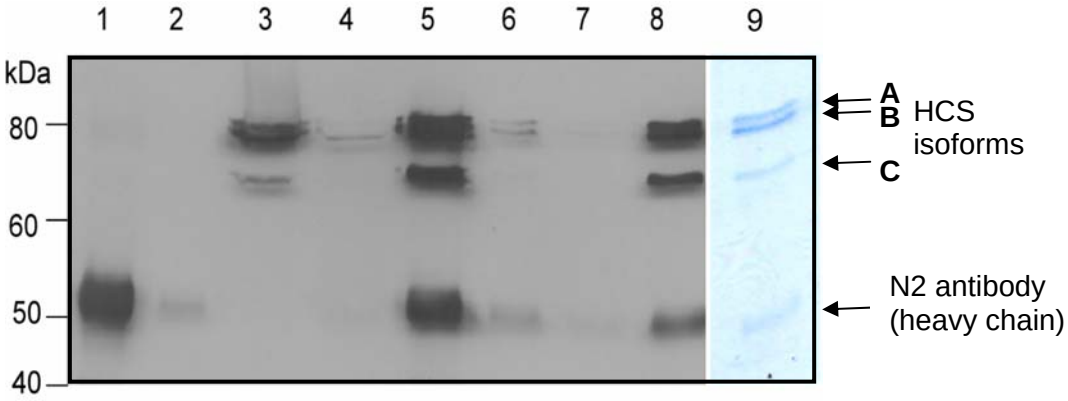

Figure 3-6 Affinity purification of HCS isoforms.
Lanes 1-8 N2 antibody Western Blot monitoring of HCS isoform purification. Lane 1- Biotinylated N2 antibody before binding to Streptavidin Sepharose. Lane 2 – unbound antibody. Lane 3 – 293T-HCS lysate. Lane 4- unbound lysate. Lanes 5-7 – Elution fractions 1-3. Lane 8 – Concentrated purified HCS. Lane 9 – Coomassie stained gel of purified HCS isoforms.

HCS samples A, B and C were subjected to in-gel tryptic digest and analysis by mass spectrometry (figure 3.7). Peptides with multiply charged ions were automatically detected and subjected to fragmentation. Fragmentation data were used to search the MASCOT database (Matrix Sciences) for protein identities. Matches were assigned if two or more sequenced peptides were identified in a protein in the database, and if the protein match was significant using probability based Mowse scoring (Pappin *et al.*, 1993). 22 peptides were identified from sample A, 10 from sample B and 18 from sample C, all of which matched HCS, confirming these bands as isoforms of HCS.

HCS band A

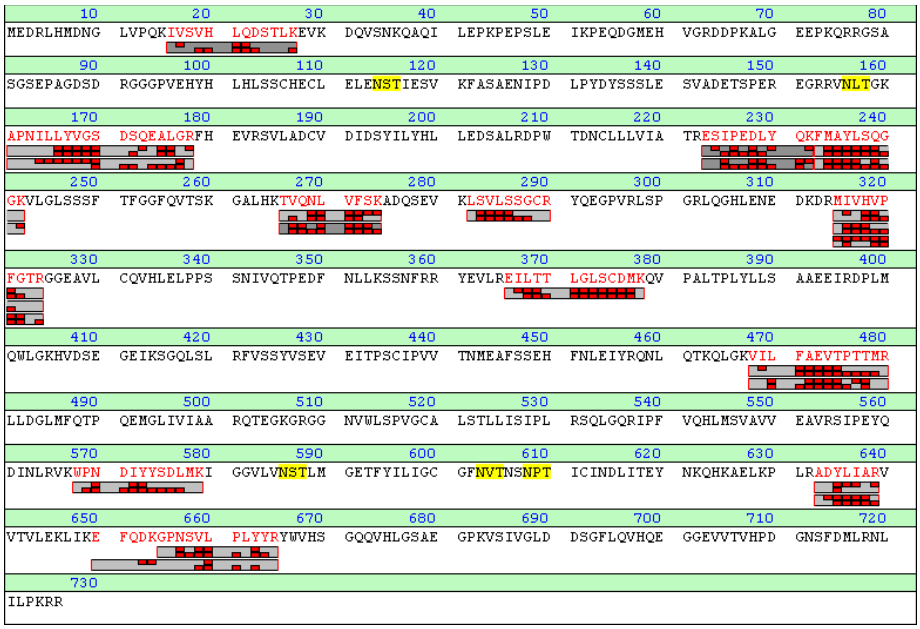

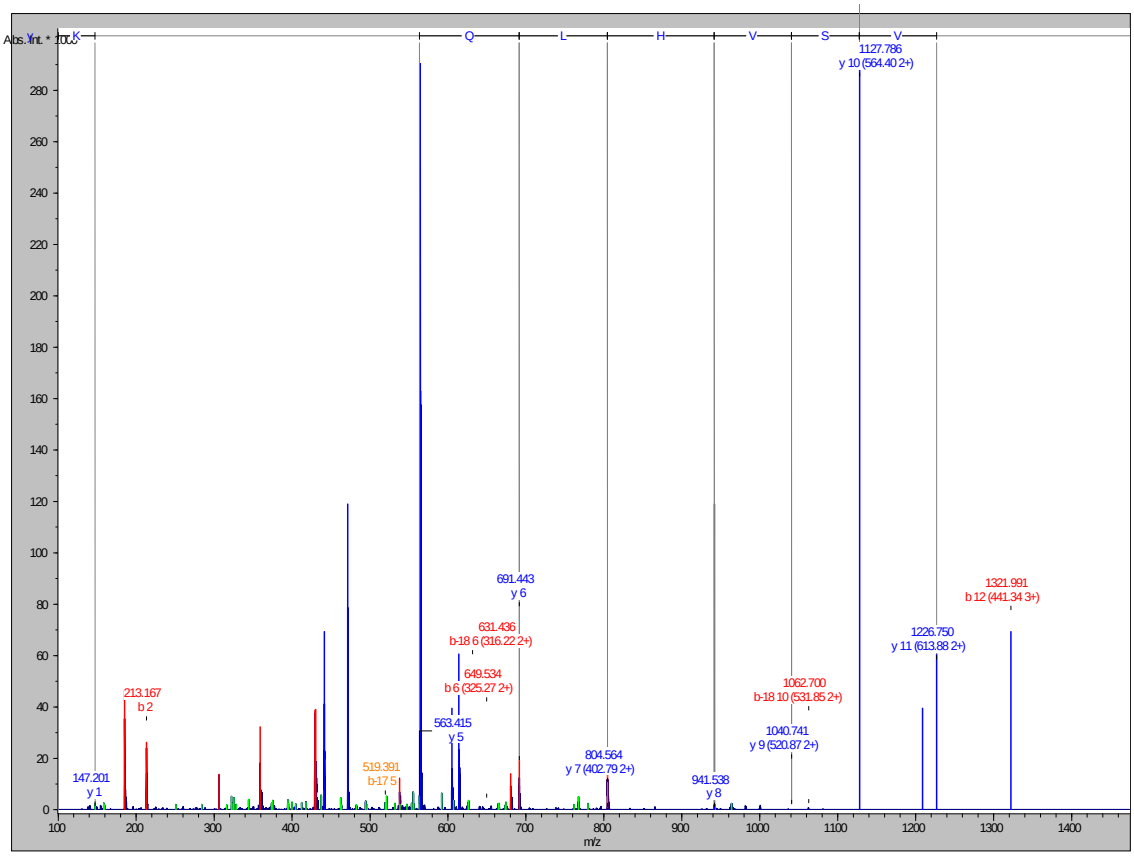

HCS band A: Most N-terminal peptide I[16-27]K

HCS band B

10	20	30	40	50	60	70	80
MEDRLHMDNG	LVPQKIVSVH	LQDSTLKEVK	DQVSNKQAQI	LEPKPEPSLE	IKPEQDGMEH	VGRDDPKALG	EEPKQRRGSA
90	**100**	**110**	**120**	**130**	**140**	**150**	**160**
SGSEPAGDSD	RGGGPVEHYH	LHLSSCHECL	ELENSTIESV	KFASAENIPD	LPYDYSSSLE	SVADETSPER	EGRRVNLTGK
170	**180**	**190**	**200**	**210**	**220**	**230**	**240**
APNILLYVGS	DSQEALGRFH	EVRSVLADCV	DIDSYILYHL	LEDSALRDPW	TDNCLLLVIA	TRESIPEDLY	QKFMAYLSQG
250	**260**	**270**	**280**	**290**	**300**	**310**	**320**
GKVLGLSSSF	TFGGFQVTSK	GALHKTVQNL	VFSKADQSEV	KLSVLSSGCR	YQEGPVRLSP	GRLQGHLENE	DKDRMIVHVP
330	**340**	**350**	**360**	**370**	**380**	**390**	**400**
FGTRGGEAVL	CQVHLELPPS	SNIVQTPEDF	NLLKSSNFRR	YEVLREILTT	LGLSCDMKQV	PALTPLYLLS	AAEEIRDPLM
410	**420**	**430**	**440**	**450**	**460**	**470**	**480**
QWLGKHVDSE	GEIKSGQLSL	RFVSSYVSEV	EITPSCIPVV	TNMEAFSSEH	FNLEIYRQNL	QTKQLGKVIL	FAEVTPTTMR
490	**500**	**510**	**520**	**530**	**540**	**550**	**560**
LLDGLMFQTP	QEMGLIVIAA	RQTEGKGRGG	NVWLSPVGCA	LSTLLISIPL	RSQLGQRIPF	VQHLMSVAVV	EAVRSIPEYQ
570	**580**	**590**	**600**	**610**	**620**	**630**	**640**
DINLRVKWPN	DIYYSDLMKI	GGVLVNSTLM	GETFYILIGC	GFNVTNSNPT	ICINDLITEY	NKQHKAELKP	LRADYLIARV
650	**660**	**670**	**680**	**690**	**700**	**710**	**720**
VTVLEKLIKE	FQDKGPNSVL	PLYYRYWVHS	GQQVHLGSAE	GPKVSIVGLD	DSGFLQVHQE	GGEVVTVHPD	GNSFDMLRNL
730							
ILPKRR							

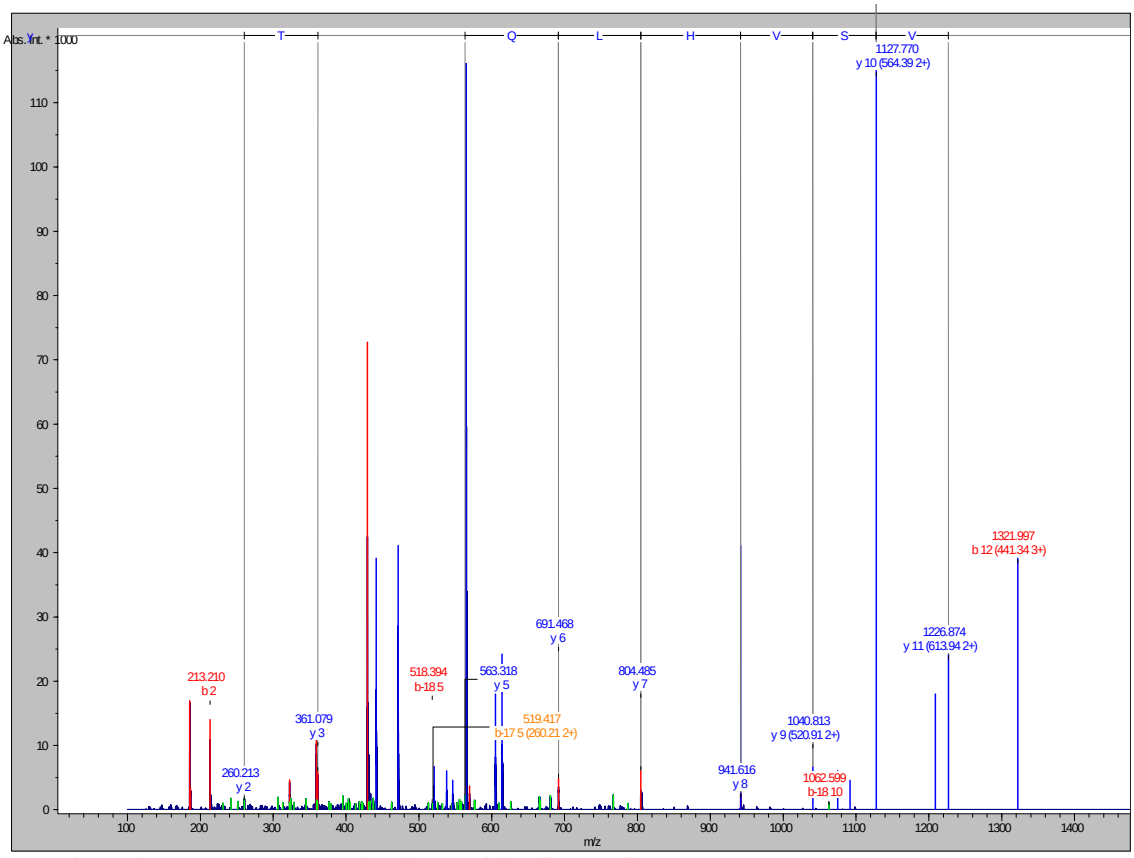

HCS band B: Most N-terminal peptide I[16-27]K

HCS band C

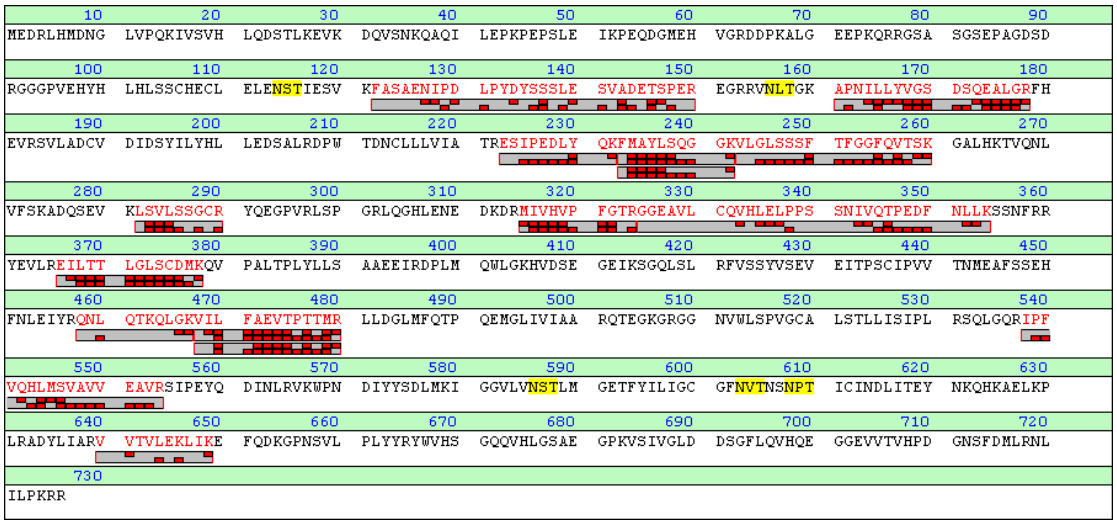

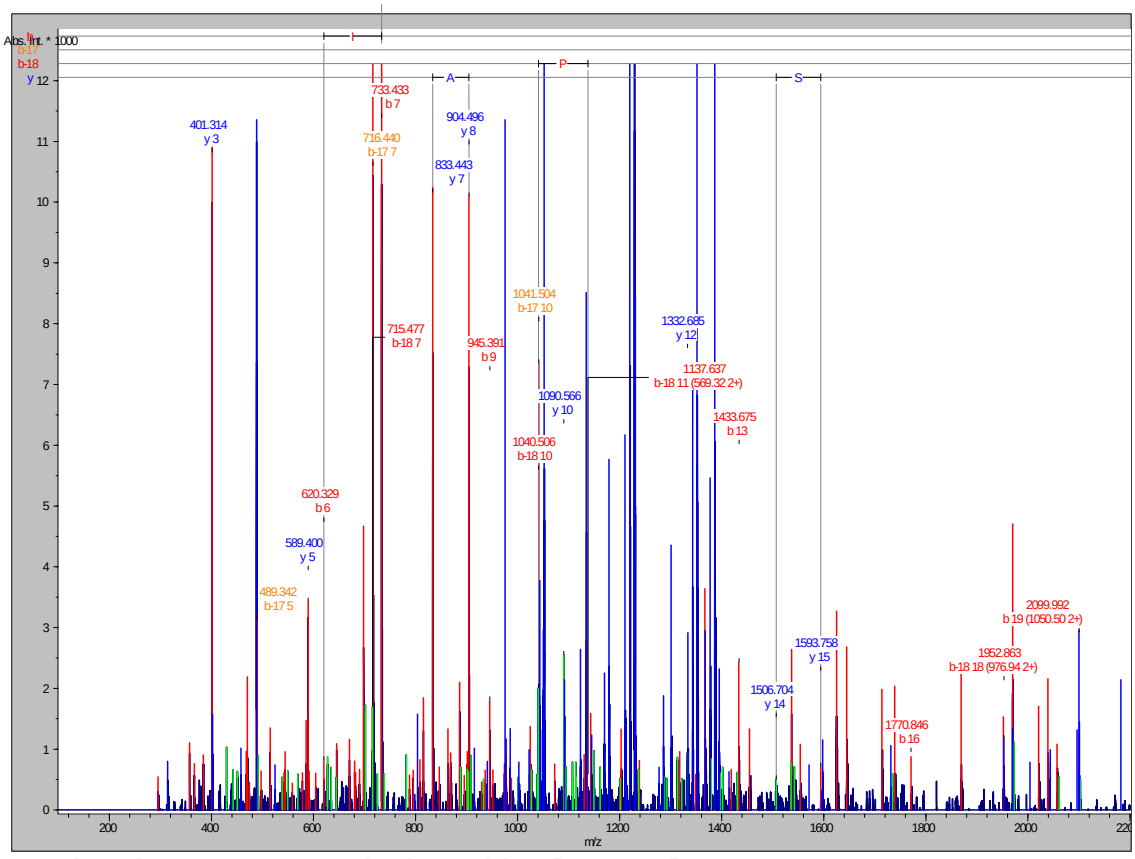

HCS band C: most N-terminal peptide F[122-150]R

Figure 3-7 LC-ESI Mass Spec analysis for each of the isolated HCS isoforms.
The upper panel shows the HCS sequence and corresponding tryptic peptides identified in the spectra (grey bars). The red boxes indicate matched sequence in peptides subjected to MS/MS analysis.The lower panel shows the MS/MS spectra for the most N-terminal peptides identified for each isoform. Blue peaks – y-ions, red peaks - b-ions, orange peaks, modified b-ions.

HCS A and HCS B both contained the peptide corresponding to amino acids 16-27 of HCS. Removal of amino acids 1-15 would only constitute a difference of 1,765 Da in molecular weight, which would not be clearly resolved under the SDS-PAGE conditions used. Similarly, the difference between initiation at Met^1 or Met^7 would also only produce a difference of 0.8 kDa. As the MS results did not allow definitive identification of the most N-terminal residue of the A and B samples, N-terminal sequencing was attempted. The HCS isoforms were purified and blotted onto PVDF membrane for N-terminal Edman degradation sequencing. Unfortunately this was unsuccessful despite several attempts both at the University of Adelaide and Monash University, Victoria. To resolve whether these different HCS species were the result of alternative initiation of translation, constructs were generated to express Met^1, Met^7 or Met^{58}-HCS in 293T cells. Comparison of the overexpressed proteins (Figure 3.8) showed that both the Met^1 and Met^7 HCS proteins resolved as a doublet by SDS-PAGE, ruling out the alternative initiation of translation from these two potential initiating methionines.

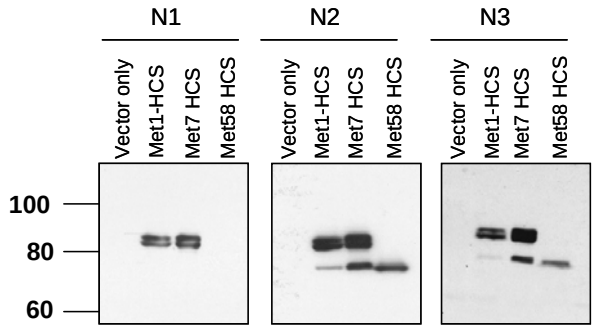

Figure 3-8 Expression of HCS from three potential initiation sites.

293T cells were transiently transfected with Met^1, Met^7 or Met^{58}-HCS. 20 μg of cell lysate were resolved by SDS-PAGE, and Western Blotted with the N-terminal HCS antibodies.

Possibly, the doublet represents forms of HCS containing a post-translational modification, altering mobility through the gel of the modified protein. Met^{58}-HCS was also slightly smaller than the fastest migrating product observed when Met^1-HCS was expressed (figure 3.8), suggesting that the isoforms observed are not a result of alternative initiation of translation.

The difference in mobility of HCS isoforms A and B may be due to post-translational modification. Phosphorylation can affect the migration of proteins through SDS-PAGE, by retarding migration through the gel, resulting in proteins that appear to have a larger molecular weight (Posada and Cooper, 1992). NetPhos 2.0 (http://www.cbs.dtu.dk/services/NetPhos/) predicts that there are potentially 25 serine, 10 threonine and 7 tyrosine residues that may be subject to phosphorylation in HCS. The predicted tyrosine phosphorylation sites include Tyr^{573} and Tyr^{574} which have been suggested to be sites of phosphorylation in HCS (Gravel, University of Calgary, personal communication).

However, analysis of the LC-ESI MS data showed that there were no peptides that corresponded to a mass difference expected for phosphorylation (+80) between HCS isoforms A, B or C. This does not imply that phosphorylation has not occurred, as the sequence coverage for each isoform was only 19.1%, 10.3% and 27.1% respectively. Interestingly, the peptide encompassing the proposed tyrosine phosphorylation sites Tyr^{573} and Tyr^{574} was sequenced for HCS isoform A and found to be unmodified, and no peptides corresponding to potential phophorylation at these sites were identified, ruling out these sites as phosphorylated residues in the largest isoform (HCS-A) observed.

3.3.6 Cross-reactivity of CHCS antibody

The CHCS peptide was specifically designed to span a conserved element in the catalytic domain, with the intention that this antibody would cross react with a number of other biotin protein ligases, making it a useful general BPL tool. To examine species cross-reactivity, recombinantly purified BPLs from either yeast (*S. cerevisiae* or *C. albicans*) or prokaryotes (*S. aureus* and *E. coli*) were assessed along with 293T cell lysate overexpressing HCS (proteins kindly supplied by Ms. Nicole Pendini and Dr. Steven Polyak in our laboratory). Proteins were fractionated by SDS-PAGE and investigated by Western blot (figure 3.9). The CHCS antibody (figure 3.9 B) failed to readily detect the

non-human BPL homologues, although increased ECL signal was detected with longer exposures to X-ray film. However at these exposures many non-specific bands were also detected in the 293T cell lysates. This low affinity interaction could be explained by examining sequence alignments of the catalytic region spanning the CHCS peptide eptitope (figure 3.9 C). Although the epitope contains the highly conserved GKGRGG motif at the C-terminus, there is sequence variation at the N-terminus which may reduce the affinity of the CHCS antibody for other species BPLs. Additionally, the epitope encompasses amino acids that form a flexible loop in the active site. This loop undergoes a disordered to ordered transition upon ligand binding, thereby closing over the active site and preventing hydrolysis of the reaction intermediate, biotinyl-5′-AMP (Weaver *et al.*, 2001b, Bagautdinov *et al.*, 2005). It is therefore likely that the conformational flexibility in the epitope prevented antibody binding to HCS and also the other species tested.

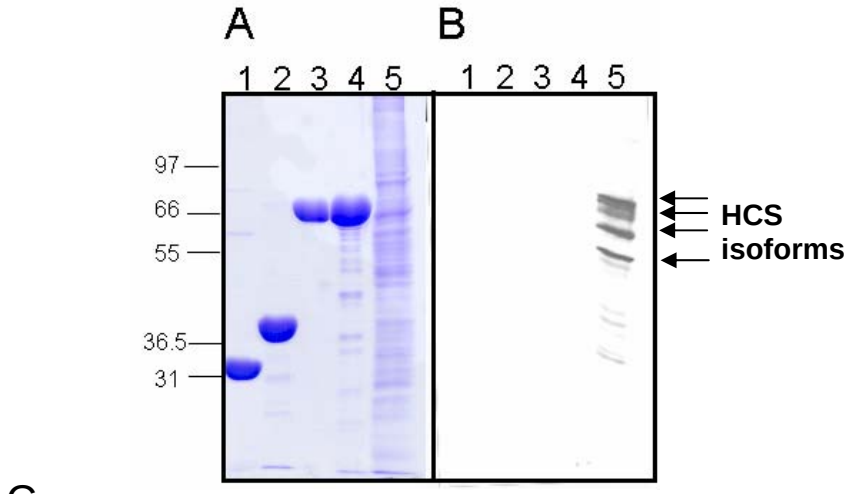

C

```
caBPL     G-FTITATTQIAGRGRGGNVWVNPRGVLATSVLFKIPPS  432
yBPL      STLLHVGTIQVSGRGRGGNTWINPKGVCASTAVVTMPLQ  448
HCS       MGLIVIAARQTEGKGRGGNVWLSPVGCALSTLLISIPLR  217
BirA      SGDACIAEYQQAGRGRRGRKWFSPFGANLYLSMFWRLEQ  141
saBPL     SSFFILSDEQTKGRGRFNRHWSSSKGQGLWMSVVLRPNV  145
                .  *  *:** .. * .. *      :.
```

Figure 3-9 Cross reactivity of CHCS antibody.
10 μg of recombinant BPL protein (lanes 1 -*E. coli* BirA, 2- *S. aureus* BPL, 3- *C. albicans* BPL 4- *S. cerevisiea* BPL) or 20 μg of whole cell lysate from 293T-HCS cells lane 5. A) Coomassie stained gel B) Western blot with CHCS antibody 1:1000 dilution. C) alignment of catalytic region of BPL species. The epitope used for the generation of the antibody is underlined and in bold.

3.3.7 Immunoprecipitation

Immunoprecipitation (IP) is a particularly useful method for detecting and enriching proteins in cell lysates. Antibodies that can successfully immunoprecipitate antigens enable protein:protein interaction experiments to be carried out (co-immunoprecipitation) and facilitate investigations into protein stability by metabolic labelling (pulse-chase experiments). To examine whether the suite of HCS antibodies generated here were suitable for immunoprecipitation, an IP was carried out with lysates from 293T cells and 293T cells stably overexpressing HCS. The results demonstrated that only the N1 and N2 antibodies are suitable for immunoprecipitation studies (figure 3.10). Both antibodies were able to immunoprecipitate HCS from stably transfected 293T cells (293T-HCS). The N1 antibody was able to IP the doublet of HCS (HCS-A and HCS-B) observed at ~81kDa. The N2 antibody was able to IP out the three HCS isoforms (A, B and C) detected in stably transfected 293T cells. The same HCS isoforms are able to be immunoprecipitated from 293T cells, confirming these HCS isoforms occur endogenously. However, neither the N1 or N2 antibody were capable of significantly enriching HCS. That is, the bands detected from 20 μg of cell lysate were of equal intensity to the bands immunoprecipitated from 2000 μg of cell lysate. Alternative ratios of antibody:antigen (5 μg: 200 μg) also demonstrated poor enrichment of HCS, Together, these data indicated that these antibodies are not ideal for co-immunoprecipitation and metabolic labelling studies.

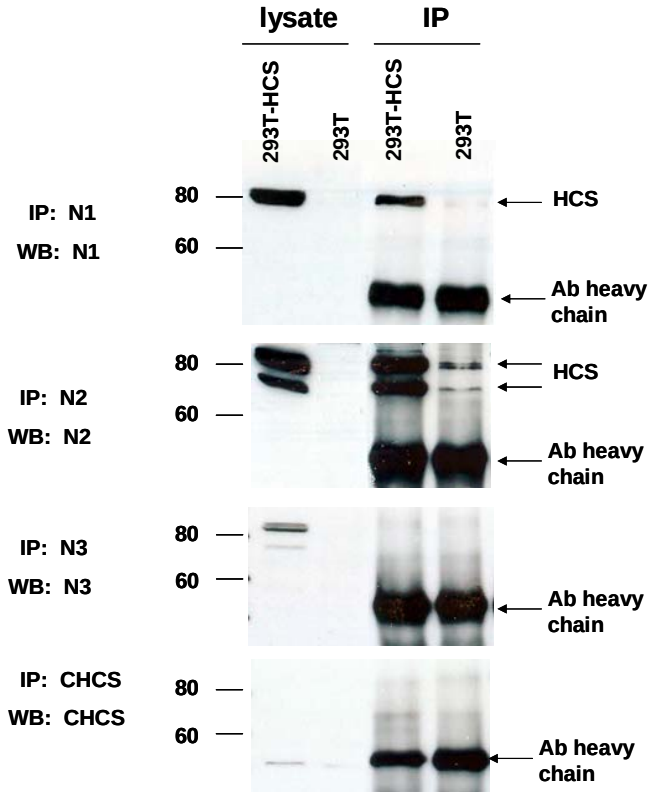

Figure 3-10 Immunoprecipitation with HCS antibodies in a variety of cell types.
2000 μg of whole cell lysate was immunoprecipitated with 5 μg of antibody. 20 μg of cell lysate and the immunoprecipitates were loaded onto the gel and subsequently blotted with 3 μg of the precipitating antibody.

3.3.8 Effect of antibodies on enzyme activity

To examine the effects of the antibodies on HCS activity a novel time-resolved fluorescence based HCS assay developed in our laboratory was employed. In this assay the apo-biotin domain comprising the C-terminal 104 amino acids from yeast pyruvate carboxylase (yPC-104) was used as a substrate. This was coupled to the surface of a 96-well plate. *In vitro* biotinylation of the substrate was performed and holo-yPC104 detected using Europium-labelled streptavidin (Eu^{3+}-Streptavidin) and time-resolved fluorescence. Due to the difficulties in purifying isoforms of HCS, the enzyme activity assays were performed using lysate from stably transfected 293T cells.

3.3.8.1 Validation of Assay

The sensitivity of the assay was investigated using standards of holo-yPC104. Detection of the biotinylated product was linear from 500 pg up to 100 ng (figure 3.11 A). Subsequenctly 100 ng of apo-yPC104 was coupled to each well of a 96-well plate and a standard curve of holo-yPC104 included to allow conversion of fluorescence intensity to product formed, and thus, HCS activity. Figure 3.11 B shows the activity of HCS in cell lysates of 293T cells and 293T cells stably overexpressing full length HCS. Endogenous HCS activity is barely detectable in this assay system, but activity in lysates from cells overexpressing HCS was measured in a dose-dependent manner. This indicated that the assay was suitable for detecting HCS activity, and that the isoforms of HCS observed in the overexpressed cells are indeed catalytically active. 50 μg of cell 293T-HCS lysate was used for subsequent assays.

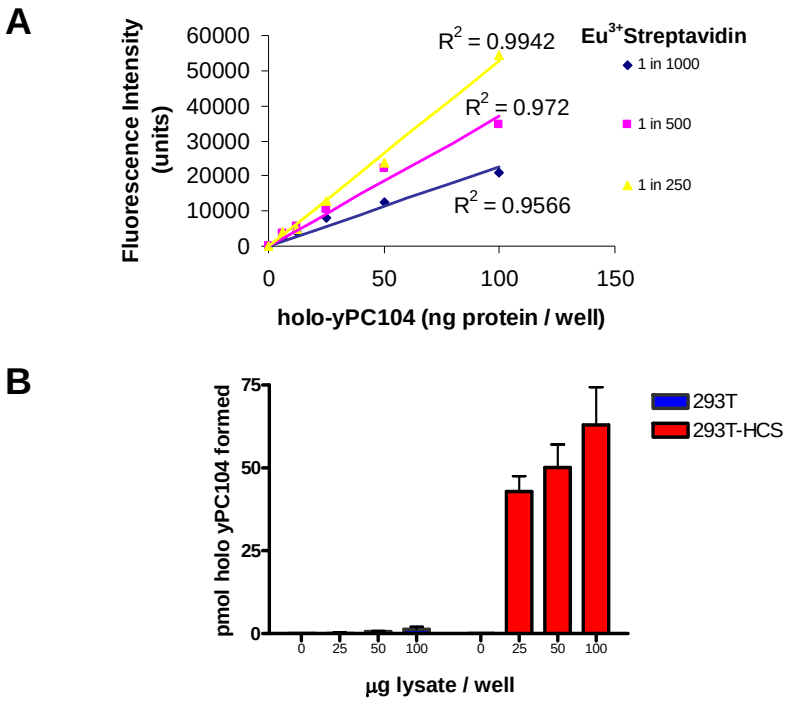

Figure 3-11 Optimisation of 96-well time resolved fluorescence assay for HCS activity.
(A) Detection of holo-yPC104 domain with varying concentrations of Europium labelled streptavidin. Detection is linear up to 100 ng/well.
(B) HCS activity of cell lysates. Endogenous HCS activity in 293T cells (blue bars) is barely detectable, but HCS activity in overexpressing cells (red bars) is readily detected. (Data shown +/- SEM from three experiments).

To examine the effect of the inhibitory properties of the antibodies on HCS activity, activity assays were performed. Cell lysates from 293T-HCS cells were incubated with increasing

amounts of antibody for one hour prior to *in vitro* biotinylation assay. An additional anti-HCS antibody (termed the Gravel anti-HCS antibody, further discussed in Chapter 4) was also included in this analysis. None of the HCS antibodies produced in this work were able to attenuate enzyme activity (figure 3.12). Conversely, the Gravel anti-HCS antibody (Narang *et al.*, 2004) (see Chapter 4) was able to inhibit HCS activity in a dose-dependent manner.

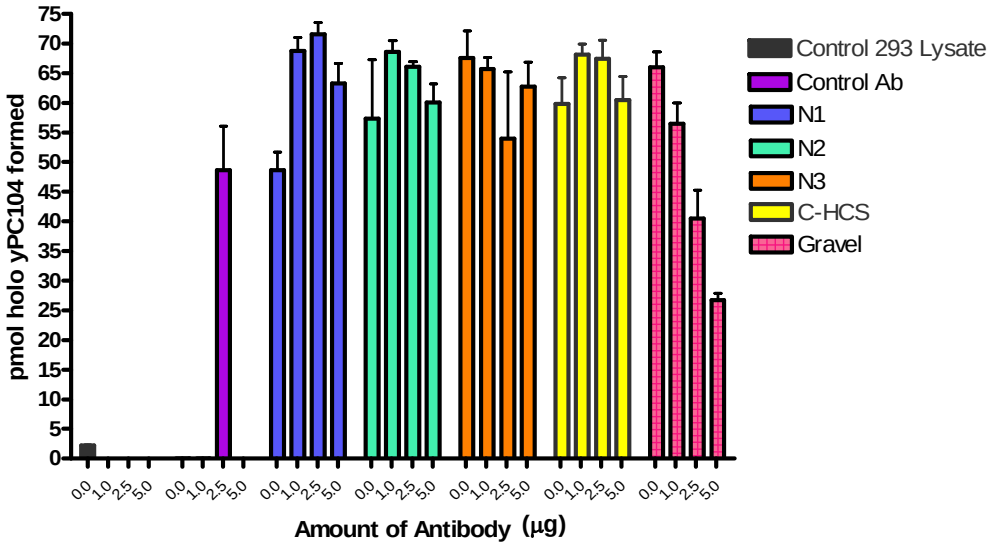

Figure 3-12 Effect of antibodies on HCS activity.
Cell lysate (50 µg) was assayed for HCS activity using apo-yPC104 as a substrate. Lysate from 293T cells acted as a negative control (black bar). An unrelated antibody (anti-rabbit secondary) was also used as a control (purple bar). Increasing concentrations of HCS antibodies were incubated with lysate for one hour prior to assaying for activity.

3.4 Discussion

To date there are no anti-HCS antibodies commercially available. The aim here was to create a suite of polyclonal antibodies (PAbs) that could be employed as tools for dissecting HCS structure and function.

In selecting whether to create monoclonal (MAb) or polyclonal (PAb) antibodies, a number of factors were taken into consideration. The production of PAbs is significantly more rapid and less costly than MAbs. Large quantities of PAbs were available within a few

months following the initial immunisation of rabbits, in contrast to the time, expertise and expense required to produce and characterise MAbs. Additionally, PAbs often have increased specificity because they are a product of multiple B cell clones each generating antibodies to a specific epitope, producing a pool of multiple antibodies with unique specificities (Lipman *et al.*, 2005). PAbs can also be more advantageous than MAbs in applications such as immunoprecipitation and immunocytochemistry as they recognise multiple epitopes, increasing the chances of binding available epitopes in samples. PAbs are also less susceptible to small changes in structure which may occur as a result of post-translational modification of the antigen (Lipman *et al.*, 2005). One disadvantage of producing PAbs is their non-renewable supply once terminal bleed sera have been utilised. However, for the quantities of antibody required for the current study, this was not a great concern. One important aspect to the design of this study was the production of four distinct PAbs against epitopes throughout the HCS protein. The peptides chosen for antibody production were selected to differentiate between HCS isoforms potentially arising from alternative initiation of translation or proteolytic processing.

The PAbs produced in this study were characterised for binding to HCS in a number of applications including Western Blotting, immunoprecipitation and effect on enzyme activity. Initial experiments suggested that the whole sera cross reacted non-specifically with several cellular proteins and so it was necessary to affinity purify these antibodies using a peptide affinity column. All four HCS antibodies generated were capable of binding HCS in Western Blot under denaturing conditions. Due to the linear nature of the peptide immunogen, polyclonal antibodies are more likely to bind to denatured protein. Two of the antibodies, N1 and N2, were capable of binding HCS in its native form as indicated by the immunoprecipitation results. In contrast, the N3 and CHCS antibodies were not useful for immunoprecipitation of native protein. This may be a product of antibody affinity for antigen, or the inability of the antibody to access the epitopes in the proteins folded state.

Western Blotting showed that four isoforms of HCS were present in 293T cells. The pattern obtained with the different antibodies indicated that these isoforms are differing at their N-termini (increased number of bands seen with more C-terminal epitope antibodies). This is consistent with previous reports (and other work in our laboratory) showing that whilst truncations into the N-terminus minimally disrupt HCS activity, truncations into the C-terminus are not tolerated (Campeau and Gravel, 2001). The absolute requirement for the C-terminus to remain intact has also been shown in other BPLs such as BirA (Chapman-Smith *et al.*, 2001). The HCS immunoreactive products seen in this study are consistent with the pattern of bands reported in human placental tissue (Hiratsuka *et al.*, 1998) (see also table 3.2). In the Hiratsuka study antibodies analogous to N1 and N2 described here were made, in addition to one raised against a fragment of HCS Ile^{128}-Pro^{398}. In the Hiratsuka study endogenous HCS could not be detected by Western blot in tissue lysates without prior enrichment of mitochondrial and cytosolic fractions over an ion-exchange column. This is consistent with the data presented here, indicating that there is a very low level of HCS present in mammalian cells, even in tissues which are highly metabolically active and rich in biotin-enzymes.

In both studies probing with the equivalent N1 antibodies detected a “doublet” of bands at estimated molecular weights of 86 and 82 kDa. The N2 antibody and Hiratsuka equivalent both detected a lower band at 74 kDa in cytosolic fractions. These products correspond approximately to the predicted molecular masses for initiation of translation at Met^{1}, Met^{7} and Met^{58} respectively. However, analysis of these HCS products by mass spectrometry and Western blot analysis performed in this study do not support the alternative initiation of translation hypothesis. Firstly, both bands of the doublet contain an identical peptide at 16-27 identified by LC-ESI MS. The difference in molecular weight of the first 16 amino acids (approximately 1.7 kDa) would not be sufficient to explain the altered mobility of these two forms through the SDS-PAGE. Secondly, recombinant

expression of Met^{1} and Met^{7}-HCS both produce identical doublets, indicating that the difference is not due to use of an alternative start of translation site. This contradicts the results reported in the Hiratsuka study, where an *in vitro* transcription/translation system showed all three isoforms were still observed, indicating that it was not post-translational processing (such as proteolytic cleavage) of the protein responsible. To rule out the possibility that the isoforms identified here were not just due to proteolytic degradation occurring as an artefact of cell lysis, precautions against proteolytic degradation of the samples were taken. A cocktail of protease inhibitors was used to prevent proteolysis upon cell lysis, and lysates were used fresh or stored at -20°C. It was observed that in the 293T-HCS cell lysates all isoforms remained stable even after repeated freeze thawing, wheras if these bands were present due to degradation it would be expected that the larger isoforms would be degraded after multiple freeze/thaw cycles. Ideally metabolic labelling would be employed to monitor the synthesis of HCS in the cell. However, this procedure requires good immunoprecipitating antibodies. The results obtained when using the antibodies developed during this project were not suitable for this process limiting this study.

In the Narang study, the presence of HCS as a doublet was accounted for as only the upper band was shown to contain biotin which was proposed to account for the differences in mobility between the two forms. In this study it appears that both bands of the doublet contain biotin (discussed in Chapter 4), and mass spectrometry analysis showed that there are unlikely to be significant differences in sequence between these two forms. Hence, it is speculated that the doublet identified in this study represents HCS in two different states of post-translational modification, accounting for altered mobility in SDS-PAGE. HCS contains many candidate phosphorylation sequences, and has been shown to contain two tyrosine phosphorylation sites (Gravel and colleagues, personal communication). While no phosphorylation sites were identified here, future work to to examine the phosphorylation state of HCS could include treatment of lysate with purified

phosphatases (eg. alkaline phosphatase) and examining the effect of this on migration of HCS isoforms. Alternatively, the reciprocal approach of incubating with $^{\gamma\text{-}32P}$ATP and purified kinase could also be trialled. The significance of post-translational modifications of HCS is yet to be elucidated.

The Hiratsuka paper also observed an isoform of HCS at ~62kDa, present in the mitochondrial fraction of human placenta. This is ~10 kDa larger than the size observed for the lowest HCS product detected with the CHCS antibody in this study, at ~55 kDa. This lower product detected by the CHCS antibody could not be purified due to the inability of this antibody to immunoprecipitate HCS, and also because this isoform is almost identical in size to the antibody heavy chain, making purification by immunoprecipitation or antibody affinity column difficult.

Immunogen	Purification	Western Blot (immunoreactive bands observed)	IP	Effect of Ab on HCS Activity	Subcellular localisation of HCS by Immuno-fluoresecne	Ref.
Peptide Met^{1}-Lys^{15}	Affinity	Doublet 82 and 86 kDa in cytosol	N/A	No effect	N/A	(Hiratsuka *et al.*, 1998)
peptide Met^{58}-Glu^{72}	Affinity	Doublet 82 and 86 kDa and 76 kDa in cytosol	N/A	No effect	N/A	(Hiratsuka *et al.*, 1998)
fusion protein Ile^{128}-Pro^{398}	Affinity	Doublet 82 and 86 kDa and 76 kDa in cytosol, 62 kDa band in mitochondria	IP reduced HCS activity of lysate	Reduced	N/A	(Hiratsuka *et al.*, 1998)
fusion protein Met^{58}-Arg^{726}	Whole serum	Doublet at 66 and 68 kDa, primarily nuclear (also cytosol)	Doublet at 66 and 68 kDa	Reduced*	Nuclear (nuclear lamina)	(Narang *et al.*, 2004)
peptide Met^{58}-Gly^{78}	Whole serum	Doublet at 66 and 68 kDa, primarily nuclear (also cytosol)	Doublet at 66 and 68 kDa	N/A	Nuclear (nuclear lamina)	(Narang *et al.*, 2004)
peptide Thr^{706}-Arg^{726}	Whole serum	Doublet at 66 and 68 kDa, primarily nuclear (also cytosol)	Doublet at 66 and 68 kDa	N/A	Nuclear (nuclear lamina)	(Narang *et al.*, 2004)
peptide Met^{58}-Arg^{77}	ProteinA IgG	N/A	N/A	N/A	Nuclear	(Chew *et al.*, 2006)

* This study

Table 3-2 Summary of properties of HCS antibodies reported in the literature.

In the 2004 study by Narang and colleagues three HCS antibodies were generated (table 3.2). These were used as whole serum (ie, not purified) in Western blotting and immunocytochemistry experiments. All three antibodies were reported to detect a doublet of ~66-68 kDa in cell lysate from multiple cell lines. Assuming the C-terminus of HCS is intact, a 66 kDa product would not immunoreact with an equivalent N2 antibody. As discussed in Chapter 4, I propose that these products are not HCS.

The effect of the antibodies on HCS activity was also assessed. The antibodies produced in this study had no effect on enzyme activity, mirroring the result reported by Hiratsuka and colleagues where antibodies corresponding to N1 and N2 were not inhibitory. Conversely, the Gravel anti-HCS antibody (further characterised in Chapter 4) showed a dose-dependent inhibition of HCS activity. This anti-HCS antibody was generated against recombinant fusion protein (Met^{58}-Arg^{726}). Similarly, the antibody in the Hiratsuka study, created using HCS fusion protein Ile^{128}-Pro^{398} as an immunogen, also abolished activity. This is consistent with the proposed structure of HCS, indicating that the very N-terminus is not critical for activity, but that the region corresponding to domain III (Gly^{159}-Arg^{314}) of the N-terminus (targeted by the Hiratsuka antibody) is necessary for catalysis. The epitope for the N3 antibody lies out this proposed domain III and in the proposed linker region. In retrospect, it would have been beneficial to design an antibody against the region of the N-terminus shown to be critical for enzyme activity (amino acids 160-266). Also, an antibody against a larger recombinant fusion protein would have increased the number of epitopes available which would be advantageous for immunoprecipitation studies. Unexpectedly, CHCS was not useful in immunoprecipitation or detecting BPLs of other species. In bacterial BPLs the amino acids in this epitope form a loop that is unstructured in the absence of ligand and only becomes ordered upon ligand binding (Weaver *et al.*, 2001b, Bagautdinov *et al.*, 2005). This may explain why this antibody was poor at binding native HCS.

In summary, this chapter has characterised the production and analysis of a suite of polyclonal antibodies against HCS. Four HCS isoforms were identified, three of which were confirmed to be HCS by mass spectrometry. The biological significance of the existence of multiple isoforms is yet to be determined. It is possible that these different forms of HCS have altered subcellular localisation, protein binding partners, stability, or substrate specificity. The subcellular distribution of these isoforms of HCS is the focus of the next chapter.

Subcellular localisation of HCS

4 Subcellular localisation of HCS

4.1 Introduction

Whilst recent studies (Chew *et al.*, 2006, Narang *et al.*, 2004) have described a predominantly nuclear localisation for HCS, at the time the present study was initiated no detailed examination of the subcellular distribution of HCS had been reported. As has been shown in chapter 4 several isoforms of HCS exist in mammalian cells, and this chapter examines the hypothesis that these isoforms, distinct at their N-termini, have altered subcellular localisations.

Control of subcellular localisation of a protein can occur through many mechanisms. A well known case is that for multiple mRNA transcripts arising from a single gene, by the process of alternative splicing. Splice variants in turn may contain (or lack) sequences encoding certain targeting peptides or motifs for translocation to multiple subcellular compartments (Danpure, 1995). Use of alternative initiation codons (discussed in section 3.1) can also lead to inclusion of different targeting motifs on protein products.

Mitochondrial targeting signals

The vast majority of mitochondrial proteins are synthesized in the cytosol and require translocation to the mitochondria. This is achieved through a mitochondrial targeting presequence at the N-terminus of the protein (reviewed in Pfanner and Geissler, 2001, Lithgow, 2000). The classical mitochondrial pre-sequence is a short region (around 20 amino acids) containing many positively charged, hydroxylated and hydrophobic residues. Importantly, this sequence forms an amphipathic helix necessary for recognition by components of the Translocase of the Outer Membrane complex. Upon import this peptide is cleaved by the mitochondrial processing peptidase (MPP) releasing the mature protein. Variations on this targeting peptide enable protein sorting to different compartments within the mitochondria. Proteins which are anchored in the outer

membrane, for example, consist of a non-cleavable matrix targeting peptide followed by a hydrophobic membrane anchoring sequence. Among the biotin-dependent enzymes, PC, PCC and MCC contain a classical 20 amino acid mitochondrial targeting peptide. In contrast the two forms of ACC have different N-terminal regions that effect subcellular localisation. ACC1 does not have a localisation peptide and is the only biotin enzyme found exclusively in the cytosol. The 200 amino acid N-terminus of ACC2 contains a putative mitochondrial targeting peptide anchoring it to the outer mitochondrial membrane (Abu-Elheiga *et al.*, 2000). Whilst biotinylation of all of these carboxylases is necessary for function, it is not known whether this post-translational modification occurs before or after entry into the mitochondria. A study of the alpha subunit of PCC in rat liver cells showed that the apo- precursor form can accumulate in the cytoplasm where it is biotinylated, before import into the mitochondria. However, apo-PCCα could also be imported into the mitochondria, where it was subsequently processed and biotinylated (Taroni and Rosenberg, 1991), suggesting that the mitochondrial carboxylases can be biotinylated in the cytosol or in the mitochondria. There have been several reports of HCS localised to the mitochondrial fraction (Hiratsuka *et al.*, 1998, Cohen *et al.*, 1985, Chang and Cohen, 1983). During the initial characterisation of the HCS cDNA a putative mitochondrial targeting sequence (PSKIVKWSDCCLPLACRPG) was identified upstream of Met^{1} (encoded by nt -120 to -64). However this sequence lacked an in-frame initiating methione residue (Leon-Del-Rio *et al.*, 1995). Alternative splicing of HCS mRNA can give rise to transcripts starting at Met^{1} or Met^{58} but this sequence is not characteristic of the amphipathic helices of mitochondrial pre-sequences. Hence, it is not known how HCS is targeted to the mitochondria, if indeed it is. The localisation of the different HCS isoforms has not previously been investigated.

Nuclear localisation signals

Proteins smaller than 45 kDa can enter the nucleus through the nuclear pore. Larger proteins must be actively translocated into the nucleus. Nuclear localisation signal (NLS)-

dependent trafficking is a common method of nuclear protein transport. NLS motifs are recognised by importins that contain adapter subunits with an affinity for the NLS and carrier subunits with affinity for nucleoporins in the nuclear pore complex (Jans and Hubner, 1996).

Nuclear localisation signals are unique amongst signalling motifs in that they are not cleaved off during translocation. Whilst there is no NLS consensus motif, all known NLS's are very hydrophilic and generally preceded by a beta-turn or random coil region (Jans and Hubner, 1996). An NLS can be classified as mono or bi-partite, where a mono-partite sequence contains a cluster of positively charged residues followed by a helix breaking residue. A bi-partite NLS consists of two clusters of basic residues separated by a 9-12 amino acid spacer (Nair *et al.*, 2003). Many factors can affect the NLS, for example its position in the protein is important as the NLS needs to be surface accessible to be functional. The presence of other targeting signals in the protein may also affect NLS function. For proteins that contain both nuclear and secretory signalling peptides the most N-terminal sequence seems to dominate (Jans and Hubner, 1996). Cell type specific differences of NLS efficacy have also been reported.

Green fluorescent protein

The ease of use of the green fluorescent protein (GFP) of jellyfish *Aequorea victoria* as a fusion protein for studying subcellular distribution of proteins makes it suitable for a first line of approach for the examination of protein localisation. When expressed in eukaryotic cells and excited by blue light GFP yields a bright green fluorescence easily observable using epifluorescent microscopes. The advantage of GFP to other fluorophore reporters is the fluorescence of GFP is intrinsic to the primary structure of the protein, and does not require a substrate or co-factor (Cubitt *et al.*, 1995). In using GFP as a fusion tag ideally both the fluorescence of the GFP and the functionality of the host protein would be preserved. There are a plethora of studies reporting the successful use

of GFP as a fusion protein for this purpose (Cubitt *et al.*, 1995, Chalfie and Kain, 2005). However, a critical point to consider is the position of the GFP fusion as either N-terminal or C-terminal to the host protein. In a systematic study to characterise a number of novel cDNAs from unknown transcripts (Simpson *et al.*, 2000), GFP was attached to both the N- and C-termini of expressed proteins. Many localisation patterns were only seen when the GFP tag was at a certain position. This was most striking for the mitochondrial proteins, where an N-terminal tag presumably interfered with mitochondrial targeting peptide recognition by the TOM machinery, resulting in nuclear and cytoplasmic staining more characteristic of GFP protein alone (Simpson *et al.*, 2000). In this study on human HCS the GFP tag has been placed at both the N- and C-terminal ends of the protein to overcome potential tag position artefacts. This study also employed the use of enhanced GFP (eGFP), a variant of wildtype GFP with improved folding and spectral properties to wild type GFP allowing for up to 35-fold more fluorescence intensity when excited at 488 nm compared to wildtype GFP (Cormack *et al.*, 1996).

This chapter therefore uses a variety of methods to investigate the subcellular localisation of isoforms of HCS, including bioinformatic analysis, GFP labelling, immunofluorescence and subcellular fractionation of cultured cells.

4.2 Methods

4.2.1 Transient transfection of GFP constructs

Cells were seeded into 6 well dishes containing poly-L-lysine coated glass coverslips at $2x10^5$ cells per/well in antibiotic-free DMEM containing 10% FCS. Cells were transfected with Lipofectamine reagent (Invitrogen) in a ratio of 1μg plasmid DNA : 2μL Lipofectamine reagent. After 24-48 hours cells were harvested by rinsing in PBS, and fixed in 4% paraformaldehyde for 30 minutes at room temperature. The coverslip was then washed twice in PBS and mounted in 10 μL antifade containing DAPI stain (5 ng/mL).

4.2.2 Immunofluorescence

Cells were seeded at $1x10^6$ cells per well onto poly-L-lysine coated coverslips in a six-well plate. After twenty-four hours cells were rinsed twice with PBS and then fixed by addition of 4% paraformaldehyde for 10 minutes at 4°C, followed by three 5 minute washes in PBS. Cells were then permeabilised with PBS containing 0.1% Triton-X100 for 3 minutes at 4°C and blocked in ImmunoCytochemistry (IC) blocking solution for 30 minutes at room temperature.

To probe cells, 5μg of primary antibody were diluted in IC blocking solution and added to cells for 1 hour. After three 5 minute washes in PBS secondary anti-rabbit Cy2 conjugated antibody (Jackson Immuno Research) was diluted 1:100 in blocking solution and incubated for 1 hour. After final washing the coverslip was mounted in Antifade solution containing DAPI (5 ng/mL) and sealed with black nail polish. Slides were stored at -20°C until viewed on the microscope. Microscopes used included a Nikon TE300 with images captured with V++ software for live cell imaging. A Leica Sp5 Spectral Confocal microscope (Adelaide Microscopy Facility, Adelaide) was used for co-localisation studies and images analysed with LeicaAS software. The advantage of confocal microscopy is

that it generates thin optical sections and so is able to eliminate confounding effects of out of focus fluorescence. Most importantly, confocal fluorescence microscopy allows quantification of the co-localisation of antigens. In images where more than one channel was analysed (multicolour) images were obtained by sequential scanning for each channel to eliminate the crosstalk of fluorophores and to ensure the reliable quantitation of co-localisation.

Two standard measurements to calculate co-localisation are Pearson's correlation and the overlap co-efficient. Pearson's correlation is a standard technique used in pattern recognition to describe the degree of overlap between the two patterns. It describes the correlation between signal intensities for each channel (Oheim and Li, 2007). The Overlap coefficient is often used to describe co-localisation as this measurement is less sensitive to differences in signal intensities. This is an advantage because it takes into account some of the limitations of fluorophores such as efficiency of probe hybridization (antibody affinity) or photobleaching. This value ranges from 0 to 1 where 1 is complete overlap of pixels in both channels (Oheim and Li, 2007). For determination of co-localisation, four separate fields of view were analysed using LeicaAF software with the threshold of detection set at 40 for both channels being analysed.

4.2.3 Subcellular fractionation

Cell lysate was separated into subcellular fractions using the QIAGEN QProteome Compartmentalisation Kit according to the manufacturer's instructions. An aliquot (250 μL) of each fraction was acetone precipitated and resuspended in 100 μL of 0.1% SDS. Samples were heated at 65°C for 10 minutes to redissolve the protein pellet. Concentrations were assayed using the BCA assay and the samples stored at -20°C until used.

4.3 Results for examining subcellular distribution of HCS

4.3.1 Localisation : a bioinformatic approach

A number of databases are available on the internet that can predict subcellular distribution of a protein depending on its sequence and the content of recognisable targeting motifs within that sequence. For all analysis the HCS sequence comprising Met^{1}-Arg^{726} was used as the input sequence (accession number NP_000402).

PSORTII (http://psort.ims.u-tokyo.ac.jp/), runs a user input sequence through a number of subprograms in order to make a prediction about a subcellular localisation. PSORTII did not identify a mitochondrial targeting peptide by MITDISC analysis which looks at the properties of the 20 most N-terminal amino acids to see if they comprise a mitochondrial targeting peptide. (Nakai and Kanehisa, 1992). It also reported a lack of consensus cleavage site for signal peptide removal (Gavel and von Heijne, 1990).

To determine if a recognisable mono-partite NLS is present in the input sequence PSORTII applies the NUCDISC algorithm to detect one of two patterns: either a four residue pattern of basic amino acids (ie lysines or arginines) or a seven amino acid pattern comprising of a proline followed within three residues by a basic lysine/arginine rich segment (3K/R residues out of 4) (http://psort.ims.u-tokyo.ac.jp/psort/helpwww2.html#nuc PSORT users manual). HCS contains a classical four residue NLS sequence PKRR at position 723 as well as the seven amino acid pattern PKQRRGS at position 73. There is no recognisable bi-partite NLS. The algorithm gave an NLS score of 0.21 (where greater than 0.2 indicates a tendancy for nuclear localisation over cytoplasmic). However when an additional scoring function, which is calculated based on the total amino acid composition of a protein, was taken into consideration a cytoplasmic localisation was predicted for HCS (Reinhardt and Hubbard, 1998).

TargetP (http://www.cbs.dtu.dk/services/TargetP/) is another database which predicts subcellular distribution of eukaryotic proteins based on the presence of N-terminal targeting peptides. This program also did not detect known signal peptides or mitochondrial targeting peptides in HCS.

Similarly, the NLS database (http://www.rostlab.org/db/NLSdb/), did not predict a NLS for HCS. This database searches for experimentally determined nuclear localisation signals within an input sequence (Nair *et al.*, 2003). LOCtree (http://cubic.bioc.columbia.edu/cgi/var/nair/loctree/query), another prediction package, also predited HCS to have a cytoplasmic localisation (Nair and Rost, 2005). In summary the predominant outcome of bioinformatic searches predicted a cytoplasmic localisation for full length HCS.

4.3.2 GFP labelled HCS localises to the cytoplasm

To examine the role of the potential alternative initiation of translation sites HCS-GFP constructs starting at Met^{1}, Met^{7} or Met^{58} were generated. When transiently expressed in 293T cells these constructs showed cytoplasmic distribution with fluorescence absent from the nuclei of cells (figure 4.1 A). This was the case for all three constructs. Figure 4.1 A and 4.1 B also demonstrate that there is no effect of paraformaldehyde fixation on HCS-GFP localisation. To ensure that the localisation of the fusion protein was not an artefact of the C-terminal GFP tag, an N-terminal fusion protein was also expressed (figure 4.1 B). Again cytoplasmic fluorescence was observed for this construct. A comparison of HCS-GFP to GFP alone implied that cytosolic localisation is a property of HCS as GFP alone was freely diffused throughout the cell (as it is small enough to enter through the nuclear pore complex). To ensure that fluorescence observed was from the HCS-GFP fusion proteins and not free GFP alone liberated by proteolysis a Western Blot

analysis with anti-GFP antibody was performed. This demonstrated GFP was indeed expressed as an intact fusion protein with HCS (Figure 4.1 C).

To examine whether the N-terminal half of HCS was implicated in HCS targeting, N-terminal constructs of HCS, missing the biotin-binding C-terminus, were analysed (figure 4.2). When the N-terminal domain of HCS (Met^{1}-Arg^{314}) was expressed as a GFP fusion protein (Met^{58}-nHCS-GFP) a predominantly cytoplasmic fluorescence signal was detected. This was also observed with the Met^{7}-nHCS-GFP construct. Despite several attempts at transfection the Met^{58}-nHCS-GFP construct had only a very low fluorescence signal, therefore making it difficult to definitively localise this protein.

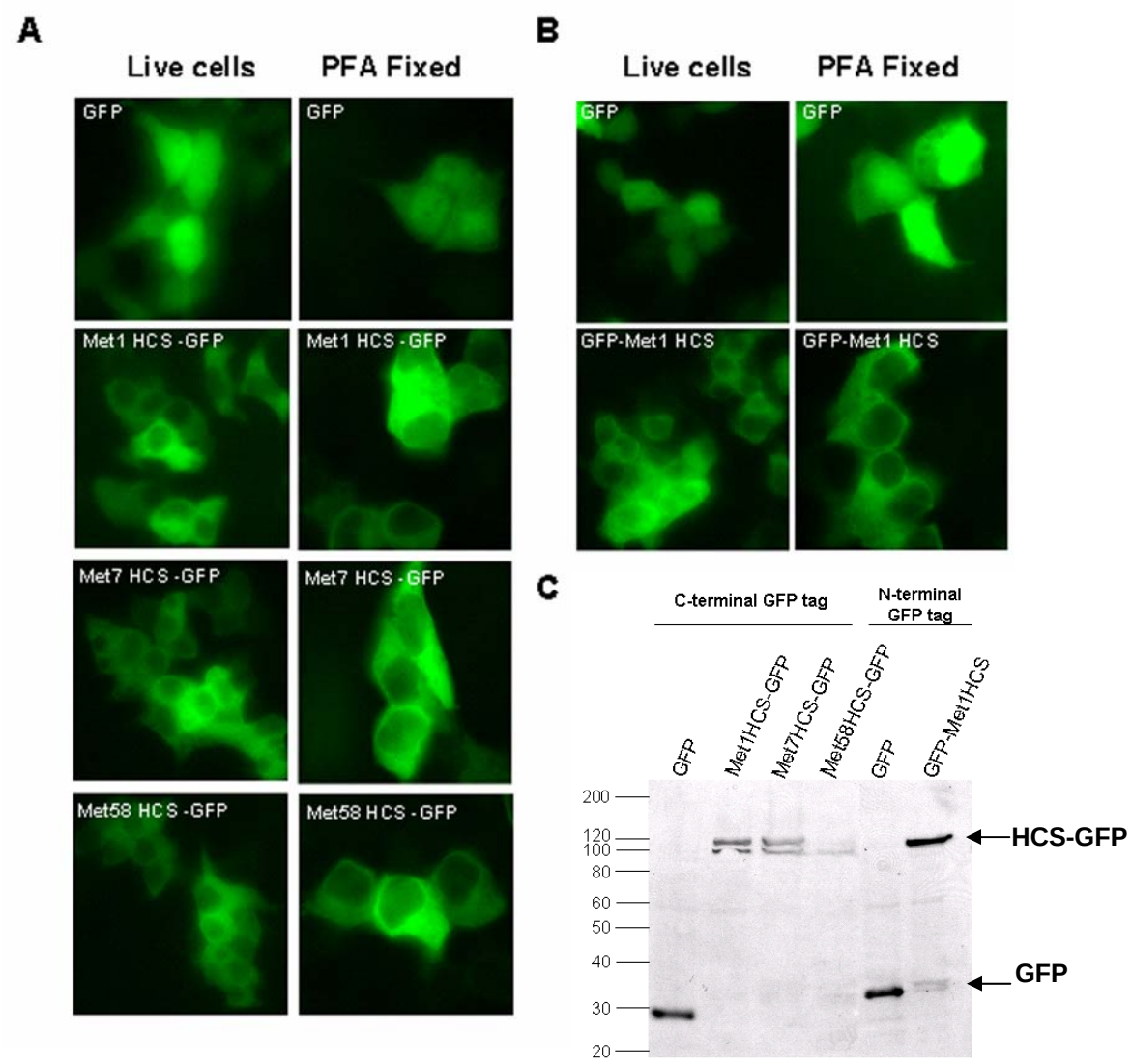

Figure 4-1 Localisation of GFP tagged HCS in 293T cells.

293T cells were transiently transfected for 24 hours with HCS-GFP constructs.
(A) Comparison of signal from live cells versus cells fixed in 4% paraformaldehyde. The GFP is attached as a C-terminal fusion to the various HCS constructs.
(B) Localisation of labelled HCS when the GFP is attached as an N-terminal fusion.
(C) Western Blot of 20 μg of whole cell lysate from transiently transfected cells probed with anti-GFP antibody. Position of tagged HCS and free GFP are indicated.

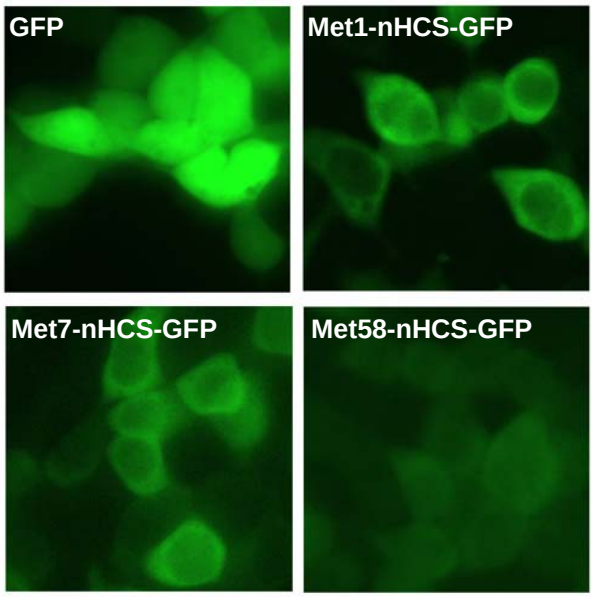

Figure 4-2. Localisation of the N-terminal domain of HCS is cytoplasmic.

N-terminal constructs of HCS (nHCS) consisting of the N-terminal domain up to Arg^{314} fused to GFP were transiently expressed for 24 hours in 293T cells. Cells were viewed live.

4.3.3 Suitability of antibodies for immunocytochemistry: Co-localisation of anti-HCS antibodies with HCS-GFP

Co-localisation of GFP tagged HCS with the anti-HCS antibodies described in chapter 3 was undertaken to examine the suitability of antibodies for immunocytochemistry. Firstly, the secondary antibody was tested to ensure it did not cross react with any cellular proteins. 293T cells, or 293T cells transiently transfected with vector expressing eGFP alone, were probed with anti-rabbit Cy3 conjugated secondary antibody (figure 4.3). The secondary antibody did not cross react with any endogenous proteins or GFP (lack of signal in Cy3 channel) and hence was used for all subsequent experiments.

To examine whether the antibodies created in the present study were suitable for immunocytochemistry, 293T cells were transfected with Met^{1}-HCS-GFP and then fixed prior to antibody staining and detection with Cy3 secondary antibody. Nuclei of cells were stained with DAPI (blue). The control (figure 4.4 A), transfected with Met^{1}-HCS-GFP and probed with Cy3 secondary antibody only, showed no cross reactivity of the secondary antibody with HCS, GFP or other endogenous cellular proteins. Antibodies N1-HCS and N2-HCS (figure 4.4 B and C respectively), co-localised with the HCS-GFP fusion protein as indicated by the yellow colour in the merged panel (lower right quadrant). Antibody N3-HCS (figure 4.4D) also co-localised with the HCS-GFP. The CHCS antibody showed a very low signal (Cy3, lower right panel of Figure 4.4 E) despite a large HCS-GFP fluorescence signal, indicating that this antibody may not be suitable for immunocytochemistry. LeicaAF software was used to calculate co-localisation of antibody staining and GFP fluorescence using Pearson's correlation or the Overlap co-efficient (see methods section 4.2.2, results table 4.1). The N2 antibody showed the highest degree of co-localisation by both Pearson's correlation and Overlap co-efficient. The N1 and N3 antibodies also showed high co-localisation. In contrast, the CHCS antibody did not show a high degree of co-localisation as measured by Pearson's correlation. Whilst the Overlap co-efficient was comparable to the N1 and N3 antibodies, the signal intensity

from the C-HCS antibody was at the minimum threshold of detection, and thus this antibody was not used for any subsequent localisation analyses.

Antibody	Pearson's correlation	Overlap co-efficient
N1	0.87	0.70
N2	0.88	0.84
N3	0.67	0.78
C-HCS	0.60	0.74

Table 4-1 Co-localisation values for HCS antibodies with GFP-HCS fluorescence.
Data is the average from 4 fields of view for each antibody. Analysed with LeicaAF software.

As the N2-HCS antibody was demonstrated to be the best candidate of for the detection of HCS by immunocytochemistry, the co-localisation of N2-HCS with the various HCS-GFP fusion proteins was examined (figure 4.5). Images were captured on a Leica Sp5 Confocal microscope. Here, some GFP signal was detected in the nucleus, but the majority of the signal was in the cytosol. Importantly, the N2-HCS antibody signal failed to co-localise with the nuclear signal. One explanation for this was the antibodies were unable to enter the nucleus. However, control experiments probing cells with an anti-Sox9 antibody (nuclear transcription factor) showed the expected nuclear staining indicating that the permeabilisation method used here was indeed suitable for nuclear detection . Therefore, the GFP signal observed in the nucleus is likely to be the free GFP cleaved from the fusion protein.

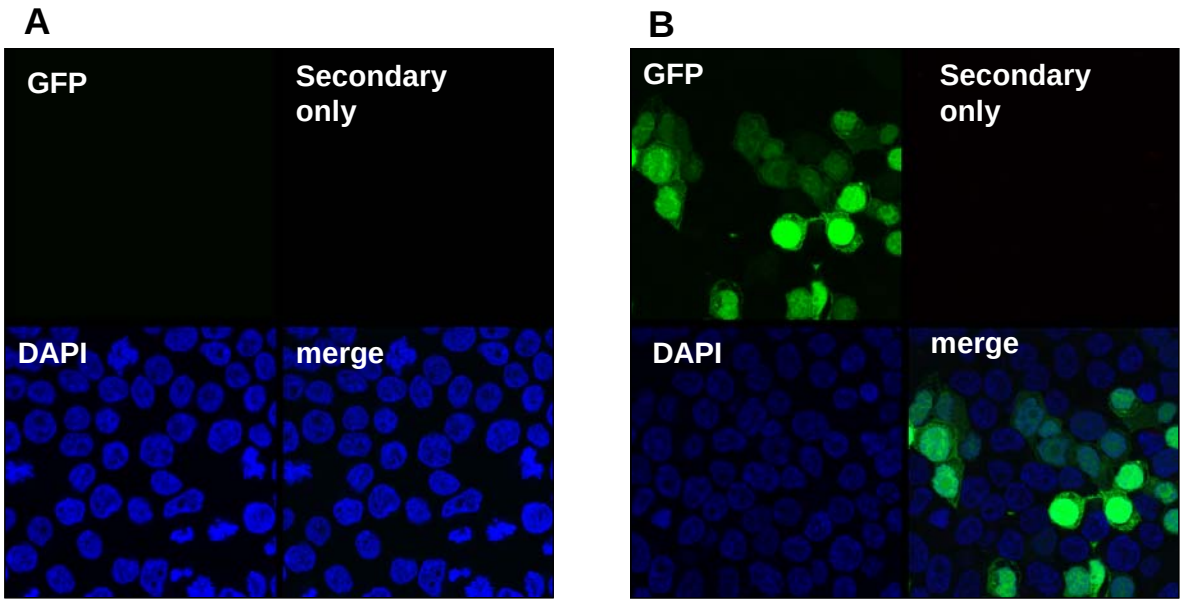

Figure 4-3 Validation of secondary antibody.

(A) Untransfected 293T cells probed with Cy3 conjugated anti-rabbit antibody. There was no cross reactivity with any endogenous proteins.
(B) 293T cells were transiently transfected with empty GFP vector only, and probed with secondary antibody. The secondary antibody does not react with GFP alone, validating its use in subsequent experiments. Nuclei were stained using DAPI.

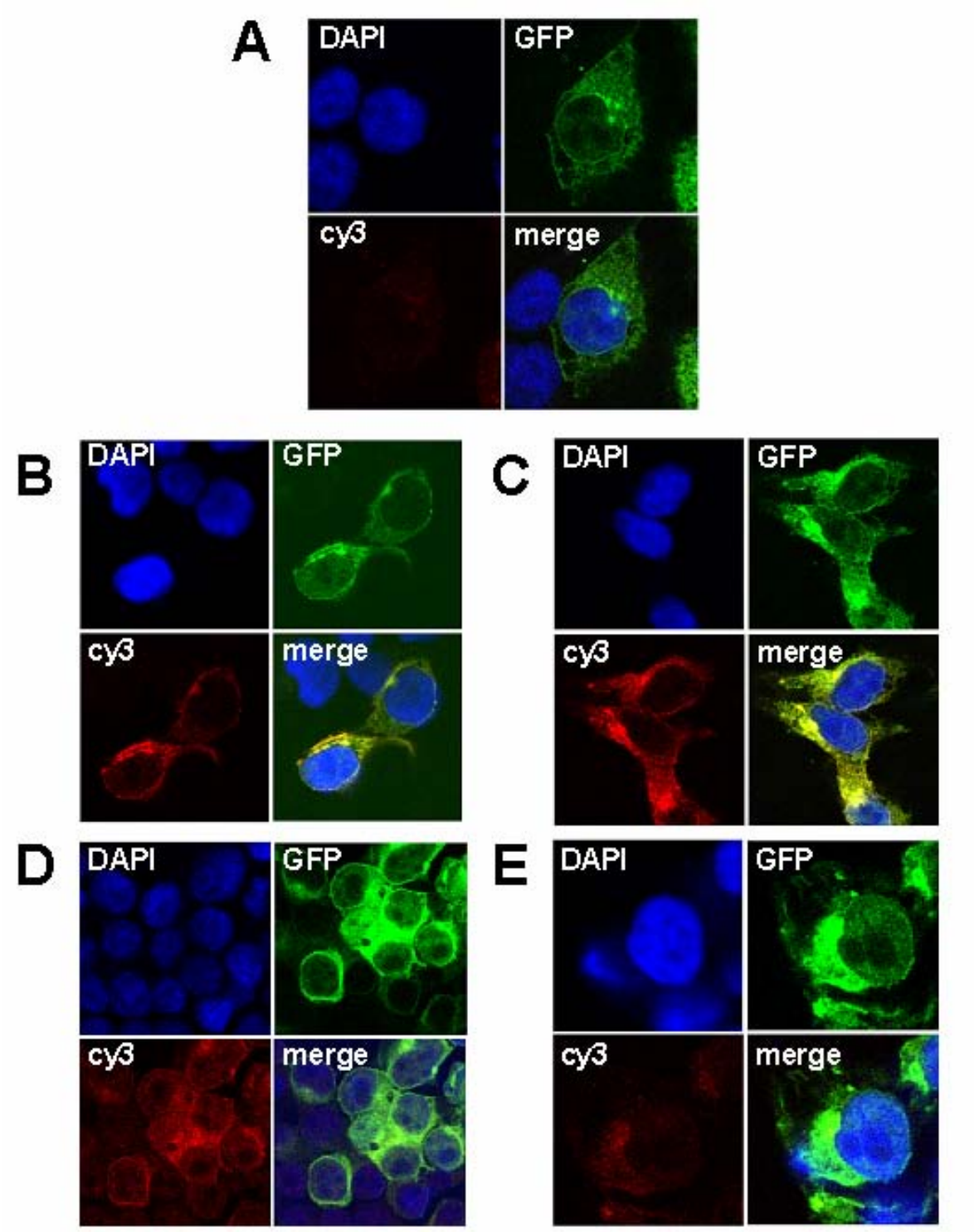

Figure 4-4 Co-localisation of GFP tagged HCS with HCS antibodies and secondary cy3 labelled antibody.

293T cells were transiently transfected for 24hours with HCS-GFP constructs, fixed and stained. Confocal images were captured. Nuclei are stained with DAPI (blue). (A) Cells probed with secondary Cy3 labelled antibody as a negative control, (B) Antibody N1, (C) Antibody N2, (D) Antibody N3, (E) Antibody CHCS.

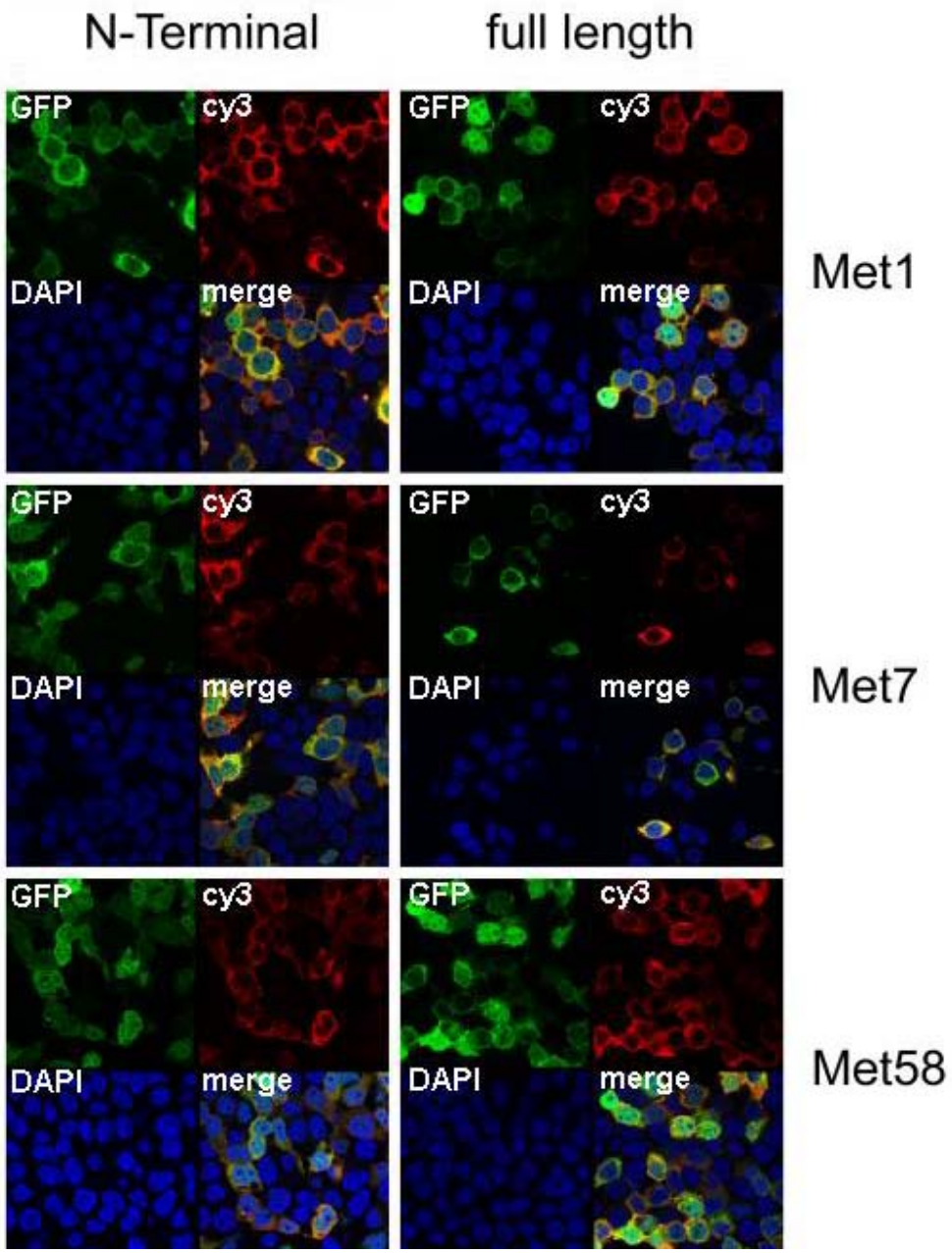

Figure 4-5. Co-localisation of HCS-GFP with cy3 labelled N2 antibody.
HCS-GFP fusion constructs (Met^{1}HCS-GFP, Met^{7}HCS-GFP and Met^{58}HCS-GFP) were transiently transfected and expressed in 293T cells for 24 hours. Following fixation, cells were probed with N2 antibody followed by Cy3 secondary antibody. Nuclei were stained with DAPI stain (blue).

4.3.4 Localisation of endogenous HCS

The localisation of endogenous HCS was then examined by immunofluorescence in several cell types. Figure 4.6 showed the localisation of HCS in 293T cells and 293T cells stably overexpressing HCS (293T-HCS) detected by the suite of HCS antibodies. Firstly, there are clear increases in staining intensity in the overexpressing cells compared to endogenous staining for the N1,N2 and N3-HCS antibodies. When the antibodies were used to probe 293T cells overexpressing HCS, a cytosolic staining was again observed (Figure 4.6, lower panel). Little fluorescence in the nuclei of the cells overexpressing HCS was observed. When endogenous levels of HCS were examined in 293T cells, the staining pattern was more diffuse. All three N-terminal antibodies show a punctate staining pattern, concentrated to perinuclear regions.

To exclude this staining pattern as cell type specific, HepG2 and HeLa cells were also analysed (figure 4.7). The most striking observation were the differences in staining with the N1-HCS and N2-HCS antibodies with these two cell types. The N1-HCS staining was exclusively in the cytoplasm in both HepG2 and HeLa cells, whereas the N2-HCS staining was localised throughout the cell. This pattern was similar in 293T cells where perinuclear staining with the N2-HCS and N3-HCS antibodies was seen. This result indicated differences in localisation between the full length and Met^{58}-HCS isoforms.

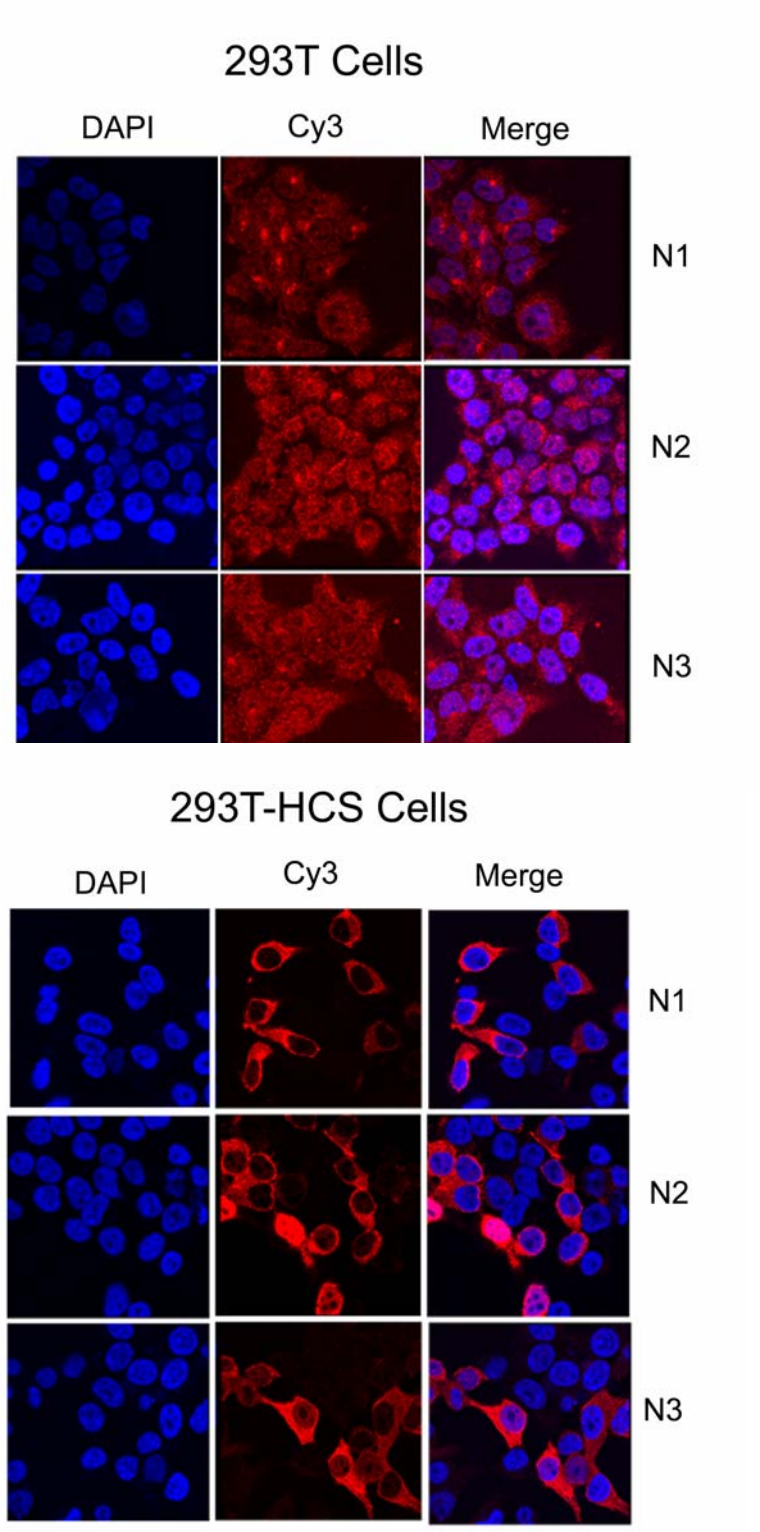

Figure 4-6 Localisation of endogenous and overexpressed HCS in 293T cells.

(A) 293T cells were fixed and probed with suite of N-terminal HCS antibodies.
(B) 293T cells stably expressed with HCS were probed as per (A). Nuclei were stained with DAPI.

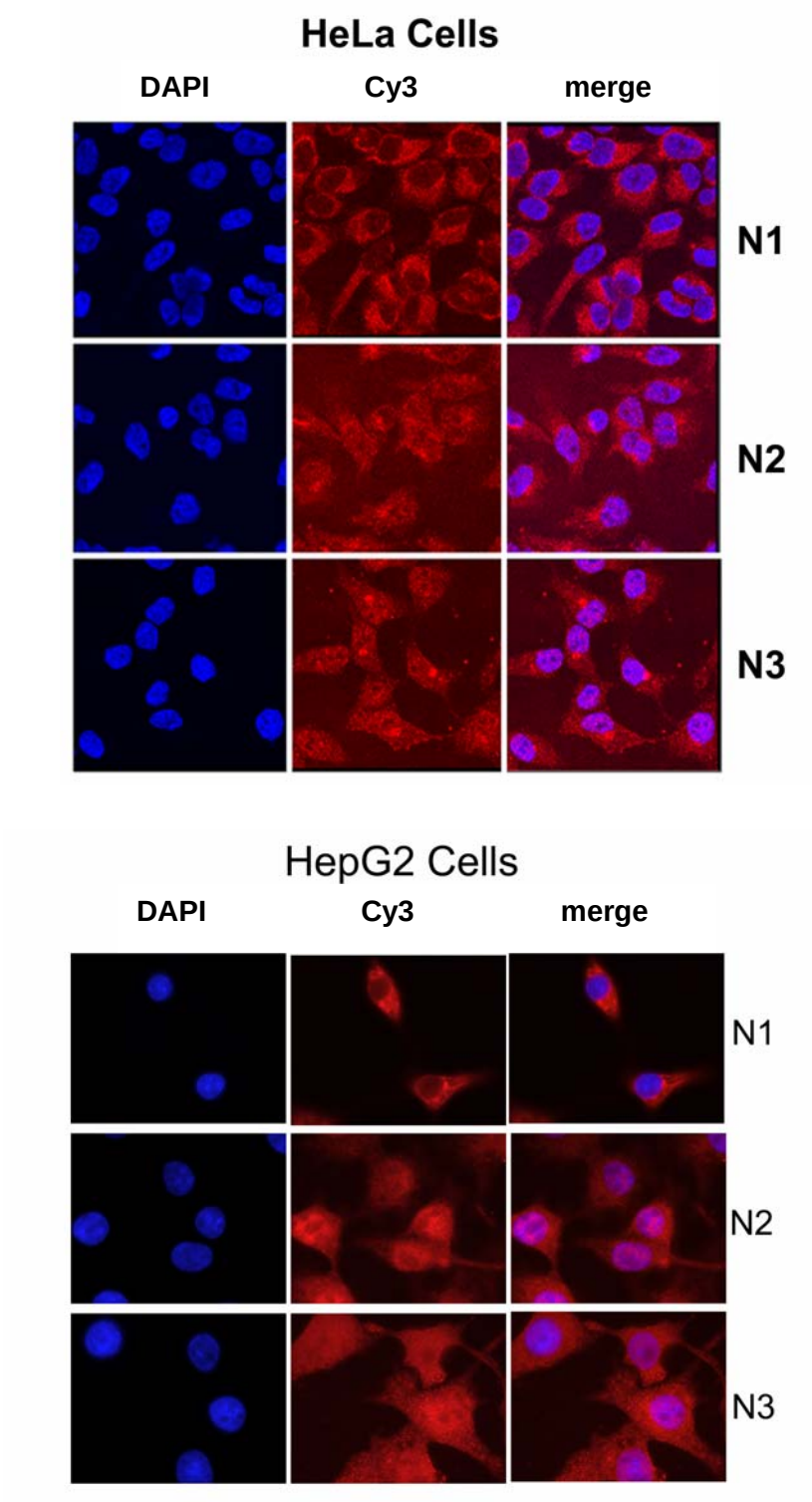

Figure 4-7 Localisation of endogenous HCS in HeLa and HepG2 cells.

(A) HeLa and (B) HepG2 cells. Cells were fixed and probed with suite of N-terminal HCS antibodies. Nuclei were stained with DAPI.

To examine this further, Met^{1}, Met^{7} and Met^{58} HCS expression constructs (containing no GFP tag) were transfected into 293T cells and probed with the three N-terminal HCS antibodies (Figure 4.8). The Met^{1}-HCS construct localises predominantly to the cytoplasm, as detected with all three anti-HCS antibodies (Figure 4.8 A). A similar result is seen with the Met^{7}-HCS construct (Figure 4.8 B). Although still primarily cytoplasmic, the Met^{58}-HCS construct did show an increased proportion of staining in the nucleus. No staining was observed when probed with the N1 antibody, as expected as the Met^{58}-HCS isoform lacks the epitope of the N1 antibody. When probed with N2 and N3 more nuclear staining was observed (Figure 4.8 C). The degree of co-localisation (Overlap coefficient) between the red channel (antibody stain) and blue channel (DAPI stain) was calculated, and found to be significantly increased in the Met^{58}-HCS construct compared to the Met^{1}-HCS construct ($P<0.05$) (Figure 4.8 D).

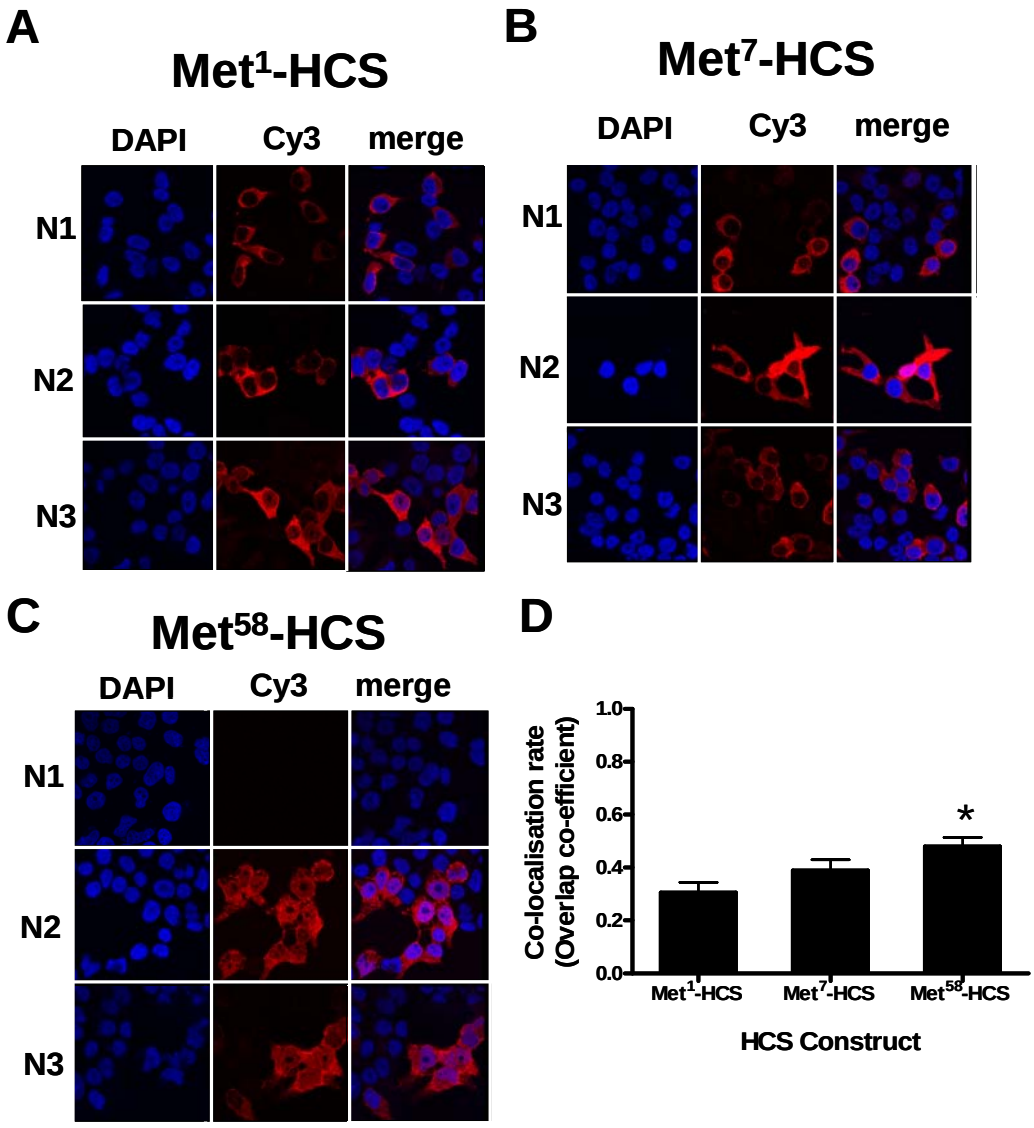

Figure 4-8 Localisation of untagged HCS isoforms in 293T cells.

293T cells were transiently transfected with pEFIRES containing (A) Met^{1}-HCS (B) Met^{7}-HCS or (C) Met^{58}-HCS. After 24 hours cells were fixed and probed with N-terminal HCS antibodies, detected with a Cy3 conjugated secondary antibody. Nuclei were stained with DAPI. (D) Co-localisation (Overlap Coefficient) of HCS staining (red channel) with nuclear staining (blue channel). P values were calculated by comparing co-localisation rates of Met^{7} and Met^{58} constructs to full length Met^{1}-HCS construct using unpaired t-tests. * $p<0.05$.

4.3.5 Subcellular fractionation analysis

An alternative strategy to examine the subcellular distribution of endogenous HCS was by subcellular fractionation and Western Blotting (figures 4.9 and 4.10). A QIAGEN compartmental extraction kit was used to separate cell lysate from HeLa and 293T cells into cytosolic, membrane bound (ie mitochondrial or endoplasmic reticulum), nuclear and cytoskeletal protein fractions. It is worth noting that the cytoskeletal fraction contains all the insoluble material from previous fractionation steps and some carry over from other protein fractions was observed (data not shown). Figure 4.9 is the result of fractionation of HeLa cells and 4.10 shows the results for 293T cells alone or overexpressing HCS. Probing the fractions with anti-PC antibody (known mitochondrial localisation) and anti-Sox9 antibody (nuclear transcription factor) confirmed the integrity of the fractionation procedure. To enhance the sensitivity of the N2-HCS antibody, which was otherwise limited in detecting low amounts of endogenous HCS, the antibody was first biotinylated and subsequently detected with streptavidin-HRP. This complicated the analysis as streptavidin-HRP cross reacts with endogenously biotinylated proteins such as PCC (77 kDa) and MCC (80 kDa). Hence a panel showing the result for streptavidin-HRP binding only was also included.

The three isoforms of HCS detected by the N2-HCS antibody are clearly visible in the cytosolic fraction of HeLa cells (figure 4.9). There is a weak band corresponding to the lowest molecular weight HCS isoform was visible in the nuclear fraction. Whilst this hasn't been confirmed by mass spectrometry to be the lower HCS isoform, it does correspond to the results seen in the overexpression studies where the Met^{58}-HCS construct showed increased HCS detection in the nucleus. A similar result is observed for endogenous HCS in 293T cells (figure 4.10 A). Fractionation of 293T-HCS cells (figure 4.10 B) markedly shows the absence of HCS from the nuclear fraction, consistent with the results seen with the GFP and immunocytochemical studies. Interestingly, evidence of

self-biotinylation of HCS is observed in panel 4.11 B, where a low level of biotinylation corresponding to the two largest HCS isoforms is visible.

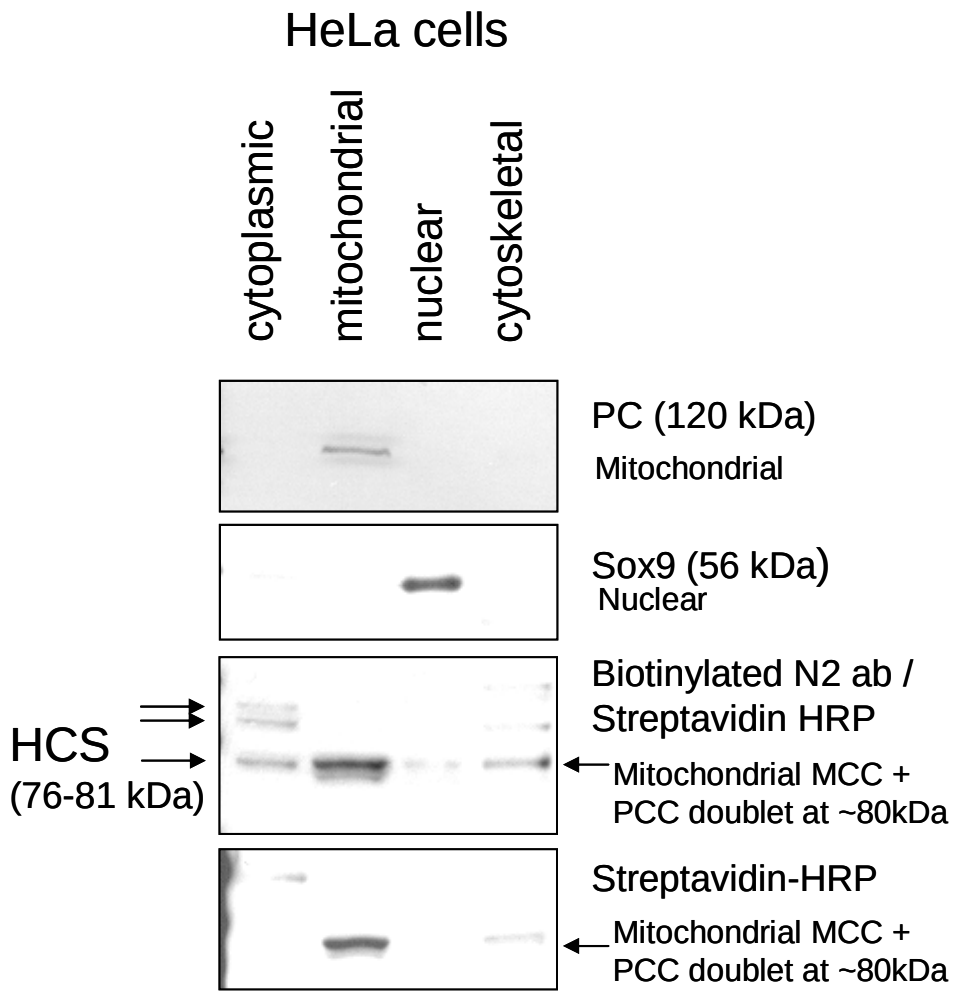

Figure 4-9 Subcellular fractionation of HeLa cells.

QIAGEN subcellular compartment kit was used to separate cellular fractions. 20 μg of protein were separated by SDS-PAGE. Westen Blotting with antibodies specific for mitochondrial pyruvate carboxylase (PC) and the nuclear transcription factor Sox9 confirmed integrity of fractionation procedure.
To probe for HCS the primary antibody (N2) was first biotinylated to enhance sensitivity. Biotinylated N2 ab was then detected with Streptavidin-HRP. The bottom panel showing background streptavidin HRP binding is included showing detection of carboxylases MCC and PCC (co-migrate at ~80kDa) in the mitochondrial fraction. The N2 antibody specifically detects the three HCS isoforms in the cytoplasmic fraction.

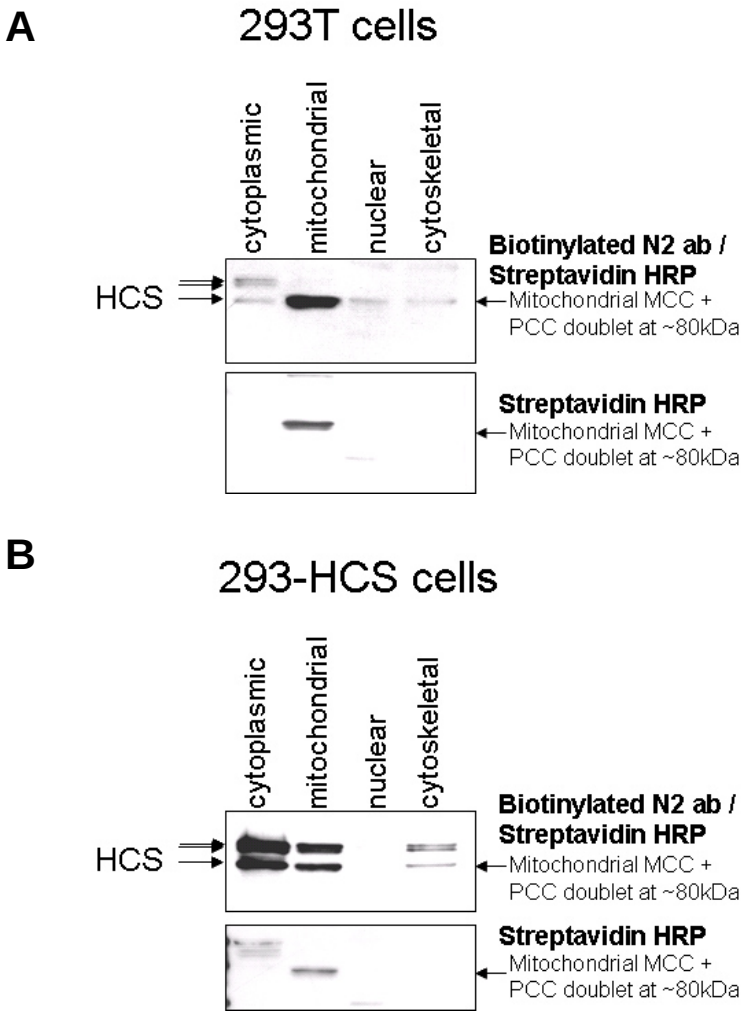

Figure 4-10 Subcellular fractionation of 293T cells (A) and 293T cells overexpressing HCS (B).
QIAGEN subcellular compartment kit was used to separate cellular fractions. 20 μg of protein were separated by SDS-PAGE. To probe for HCS the primary antibody (N2) was first biotinylated to enhance sensitivity. Biotinylated N2 ab was then detected with Streptavidin-HRP. The bottom panel showing background streptavidin HRP binding is included showing detection of carboxylases MCC and PCC (co-migrate at ~80kDa) in the mitochondrial fraction.

4.3.6 Evaluation of other HCS antibodies

The study by Narang *et al.*, 2004, reported predominantly nuclear localisation for HCS. This is in contrast with results presented in the present study. In order to evaluate this further, experiments were performed using the anti-HCS antibody used in the Narang study (henceforth termed Gravel anti-HCS antibody). This anti-serum was generated against recombinantly expressed HCS-Met^{58}-Arg^{726} and was not further purified.

The Gravel anti-HCS antibody had previously been reported to immunoprecipitate HCS from a wide variety of cell types as a doublet at 66-68 kDa. To confirm this result an immunoprecipitation was performed on lysates from HepG2, HeLa, 293T and 293T cells overexpressing HCS. Samples were fractionated and analysed by SDS-PAGE and Western blot (figure 4.11). The ~66kDa band was detected on the Coomassie stained gel in all lanes, however it did not appear as a doublet as previously reported. Western blot analysis with the N2 antibody did not detect any immunoreactive band at 66 kDa in any of the non-transfected cell lysates. Using lysates containing overexpressed HCS as a control, three HCS isoforms were immunoprecipitated by the Gravel anti-HCS antibody and detected by Western blot with N2 antibody. This indicated that the Gravel anti-HCS antibody was able to bind to the HCS isoforms recognised by the N2 antibody. However the 66 kDa band was not likely to be HCS.

Mass spectrometry was used to identify the 66kDa immunoprecipitated product from 293T cells. The protein was excised from a polyacrylamide gel stained with Coomassie blue, subjected to in-gel tryptic digestion and analysed by MALDI-TOF/TOF mass spectrometry at the Adelaide Proteomics Facility. In all, 35 peptides were detected and all matched to the sequence for rabbit serum albumin. This was significant as rabbit was the host animal for antibody production. Rather than indicating that the HCS antibody is binding specifically to rabbit albumin, the 66 kDa band observable in the immunoprecipitated

fraction is most likely albumin which has bound non-specifically to the resin during immunoprecipitation, and is not in fact an alternative isoform of HCS.

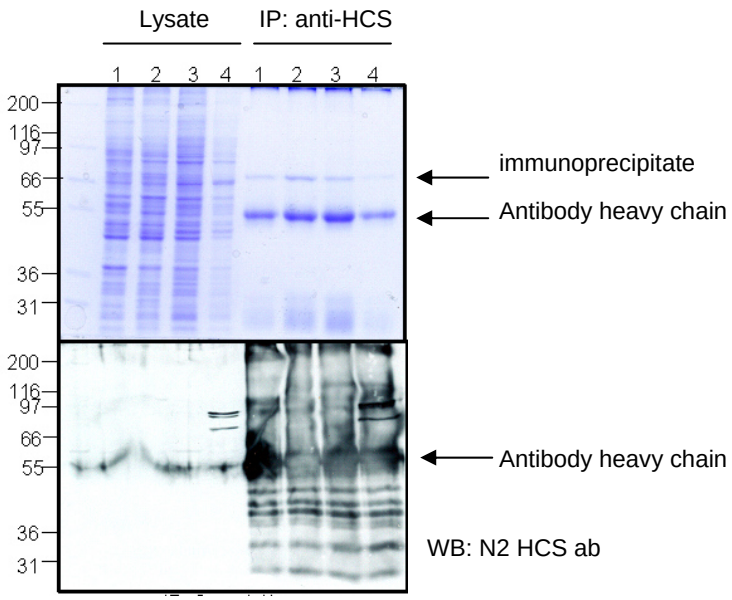

Figure 4-11 Immunoprecipitation of 200 μg of mammalian cell lysate with 10 μL anti-HCS antibody (Narang *et al.*, 2004).
Lane 1 – HeLa, Lane 2 – HepG2, Lane 3 – 293T, Lane 4 – 293T-HCS. Upper panel shows a coomassie stained SDS-PAGE. Lower panel represents a Western Blot with the N2-HCS antibody.

A further immunoprecipitation experiment was performed on 293T cells overexpressing HCS (figure 4.12). The Gravel polyclonal anti-HCS antibody was indeed capable of immunoprecipitating all the isoforms of HCS detected by antibodies generated in this study. This provided evidence that the Gravel antibody can recognise the HCS isoforms identified with the antibodies generated in the current study.

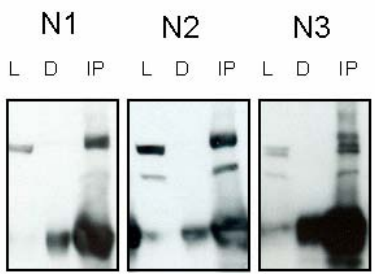

Figure 4-12 Immunoprecipitation with Gravel antibody on 293T-HCS cells.

200 μg of 293T-HCS lysate was immunoprecipitated with the Gravel anti-HCS antibody followed by Western Blotting with the N-terminal HCS antibodies prepared in the present study. L-lysate, D-immunodepleted fraction, IP- immunoprecipitate.

The Gravel antibody has reportedly been used to examine HCS by Western blotting. Initial attempts to use this antibody for this purpose resulted in very high background and cross-reactive binding to many cellular proteins. This is highlighted in figure 4.13. Subcellular fractions of HeLa cells were probed with Gravel anti-HCS. Even at high dilutions (1:16,000 in figure 4.13) there are many cross reacting cellular proteins (it should be noted that this is directly attributable to the primary antibody, as the secondary antibody was identical to that used in all previous Western blots). Interestingly there are several high intensity bands in the nuclear fraction. This may explain why nuclear localisation of HCS is reported when using this antibody in immunocytochemisty experiments.

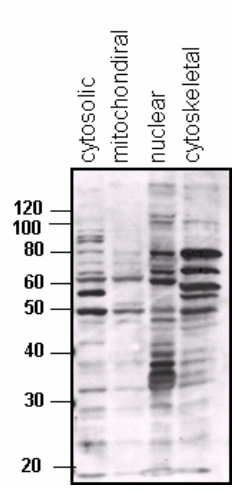

Figure 4-13 Western Blotting with Gravel anti-HCS serum on fractionated HeLa cell lysate.
Anti-serum was diluted at 1:16,000.

4.3.6.1 Immunocyotchemistry

The Gravel anti-HCS antibody has been used to demonstrate nuclear localisation of HCS in HeLa cells. This was confirmed here by probing HeLa cells with the Gravel anti-HCS antibody, followed by a Cy3 conjugated secondary antibody (Figure 4.14). As expected from the Western Blot above, this antibody produced nuclear staining, and contradict the results observed with the panel of antibodies described in this thesis. However, it has been shown here that the Gravel anti-HCS antibody is capable of immunoprecipitating the HCS isoform. To examine the binding of the Gravel anti-HCS antibody in another cell type, the antibody was used to probe 293T cells or 293T cells overexpressing GFP-HCS (Figure 4.15).

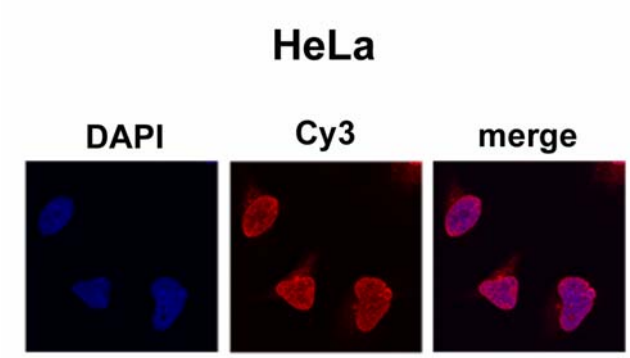

Figure 4-14 Gravel anti-HCS antibody shows nuclear staining of HeLa cells.
HeLa cells were probed with Gravel anti-HCS (Cy3) and nuclei stained with DAPI (blue).

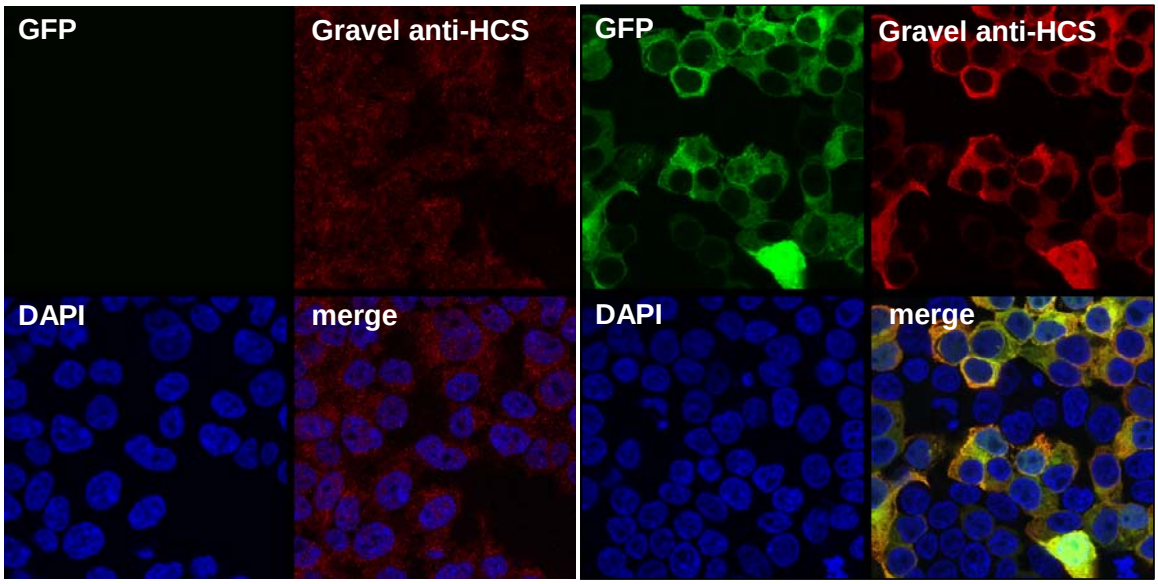

Figure 4-15 Gravel anti-HCS antibody binds to GFP labelled HCS.
Left panel - 293T cells. Right panel – 293T cells transiently overexpressing GFP-HCS (24 hour transfection). Nuclei are stained blue with DAPI.

In stark contrast to the result seen with HeLa cells, probing for endogenous HCS on 293T cells (Figure 4.15, left panel) with the Gravel anti-HCs antibody showed punctate staining throughout the cell, primarily in the cytoplasm. When the antibody is used to probe cells overexpressing GFP tagged HCS (Figure 4.15, right panel), a result similar to that observed with the N2 antibody was obtained (Figure 4.5 C). That is, GFP-HCS localises to the cytoplasm, and this co-localises with the staining for the antibody (Overlap coefficient 0.90).

These results suggest that the Gravel anti-HCS antibody is indeed capable of recognising and binding to the same isoforms of HCS as detected with my antibodies. However, there does appear to be a much higher degree of cross reactivity with other cellular proteins (as shown by Western Blotting), thereby preventing accurate analysis.

4.4 Discussion

The subcellular distribution of HCS is critical to understanding the role of HCS in biotin utilization in the cell. Bioinformatic analysis using several algorithms performed in this study indicated a likely cytoplasmic localisation for HCS, although a putative C-terminal NLS was indicated using the PSORTII NUCDISC algorithm. A potential mitochondrial targeting peptide has also been previously reported (Leon-Del-Rio *et al.*, 1995) but was not evident in this study (section 4.3.1). To determine empirically the localisation of HCS several methods including GFP labeling, immunocytochemistry and subcellular fractionation were employed.

The three approaches taken in this study to examine subcellular localisation of HCS consistently have shown a cytoplasmic localisation, not a concentrated nuclear localisation as previously reported (Narang *et al.*, 2004, Chew *et al.*, 2006). GFP labeling of HCS showed an almost exclusively cytoplasmic localisation for HCS. For immunostaining and co-localisation studies cells must first be fixed and permeabilised. Fixation with ethanol can cause leaking of GFP out of cells, whereas paraformaldehyde (PFA) fixation is compatible with GFP retention and fluorescence (Kalejta *et al.*, 1997). In this study 293T cells were viewed both live and fixed in PFA. This was important as PFA has been shown in several cell lines to increase the affinity of GFP for microfilaments, confounding localisation results (Schmitz and Bereiter-Hahn, 2001). In this study PFA had no effect on localisation. The constructs were made as both N- and C-terminal GFP fusions to investigate the proposition that targeting information was residing in the N-terminus. However, the position of the GFP tag did not affect the cytoplasmic localisation of labelled HCS.

The finding that HCS localised predominantly to the cytoplasm is consistent with the role of HCS in biotinylating cytosolic ACC1, and mitochondrial carboxylases prior to their import into the mitochondria (Taroni and Rosenberg, 1991). However, this was in contrast to

published results that showed HCS was predominantly nuclear (Chew *et al.*, 2006, Narang *et al.*, 2004). As overexpression of the protein and GFP tag may interfere with localisation signals, further investigations into localisation of endogenous protein were performed with the panel of anti-HCS antibodies described in Chapter 3. To determine the suitability of the antibodies for immunocytochemistry their co-localisation with the signal from GFP tagged HCS was calculated. If the antibodies showed a high degree of co-localisation with the GFP-HCS they were deemed suitable for use in immunocytochemistry experiments. The N2 antibody showed the highest co-localisation (table 4.2) and was subsequently used for the rest of the analysis. The N3 and CHCS antibodies displayed decreased co-localisation with the GFP labeled HCS protein (the CHCS antibody being excluded from further analysis). This is consistent with the results seen in Chapter 3, where these antibodies were not suitable for immunoprecipitation studies, indicating that these antibodies are unable to bind to the protein's native conformation.

Examination of endogenous HCS showed more diffuse staining patterns, where HCS staining was visible throughout the cell in a diffuse pattern (HepG2 cells) or concentrated at perinuclear regions in 293T and HeLa cells. The perinuclear staining of endogenous HCS is consistent with an association with the Golgi or endoplasmic reticulum, although further investigations using organelle markers would be required to support this conclusion.

Differences in localisation of HCS were observed using the N1 antibody compared to the N2 and N3 antibodies in both HeLa and HepG2 cells, indicating that there was some difference in localisation between full length (detected with N1) and shorter isoforms of HCS. Analysis of HCS overexpressed in 293T cells with no additional tags such as GFP showed that there was a statistically significant increase of HCS staining in the nucleus of cells transfected with the Met^{58}-HCS construct compared to full length HCS.

Fractionation studies showed that the majority of endogenous HCS (all three isoforms previously characterised in Chapter 3) was present in the cytoplasmic fraction. The shortest HCS isoform at ~76 kDa could not be resolved from the MCC and PCC subunits under these blotting conditions, so there may have been some of this isoform in the mitochondrial fraction, consistent with the punctate staining seen throughout the cell and with previous reports of HCS activity (Kosow *et al.*, 1962, Cohen *et al.*, 1985, Hiratsuka *et al.*, 1998). There was a faint band corresponding to the molecular weight of the lowest HCS isoform in the nuclear fraction of both HeLa and 293T cells, consistent with the immunofluorescence data showing an increased nuclear localisation of this isoform.

The 2004 Narang study was the first example of immunofluorescent localisation of HCS. This paper found that HCS was specifically localized to the core nuclear matrix, which was demonstrated by a combination of Western Blotting, Immunostaining and enzyme activity assay on subnuclear fractions. HCS protein and activity were tightly associated with the nuclear lamina in the core nuclear matrix. My results show that full length HCS is predominantly cytoplasmic. Only the 76 kDa isoform was detected in the nucleus. This leads to the hypothesis that the first 58 amino acids of HCS may be involved in a protein:protein interaction which anchors the protein in the cytoplasm. When this portion of the enzyme is absent, the potential NLS in the C-terminal fragment can be utilized, increasing nuclear localisation. This is consistent with the results seen in the Narang study, where the C-terminal half of HCS was found to localize to the nucleus. There are no recognisable protein binding motifs predicted in the first 58 amino acids of HCS sequence (when searched in PROSITE http://au.expasy.org/tools/scanprosite/ or MotifScan http://myhits.isb-sib.ch/cgi-bin/motif_scan). However very little is known about the structure of the N-terminus. It would be interesting to see if the potential NLS at the C-terminus of HCS is an effective NLS sequence by performing site directed mutagenesis on this region and seeing if this abolishes all nuclear localisation.

Particularly, why were there such contrasting differences between the results seen with antibodies produced in this study and the Gravel antibody on the localisation of HCS in HeLa cells? In the Narang study the polyclonal antibody was generated against recombinant fusion protein and serum employed as the source of antibody. Chapter 4 (4.3.4.6) demonstrated that this antibody is capable of inhibiting HCS activity, implying that some of the antibody binding sites are somewhere in or near the biotin binding site of the enzyme. Analysis of the Gravel antibody in this chapter has shown that the antibody is capable of binding and immunoprecipitating all the HCS isoforms. However, I have shown that this antibody (used in an unpurified, whole serum form) also cross reacts with other cellular proteins, including many in the nuclear fraction. This is in contrast to the antibodies developed in this study, which were affinity purified and showed no cross-reactivity to other cellular proteins by Western blot analysis. Hence, two possibilities may be occurring to explain this discrepancy in localisation. Firstly, the antibody may be cross reacting non-specifically with nuclear proteins, explaining the immunofluorescence data reported in the previous Narang *et al*. study. Alternatively, there may be yet other isoforms of HCS present which are not detected by the N-terminal antibodies generated in this study. In Chapter 4 the CHCS antibody, unfortunately unsuitable for localisation studies, showed detection of a smaller ~55kDa isoform of HCS (Figure 4.4). This band was at least as prominent as the other isoforms of HCS visible by Western Blotting, indicating that this isoform may be a significant proportion of HCS in the cell. This isoform was undetectable using the N-terminal HCS antibodies described in this work. The Gravel anti-HCS antibody may be able to detect this form of the enzyme, which may have a more predominantly nuclear localisation than the full length enzyme.

Another polyclonal antibody raised against an epitope identical to the N2-HCS epitope (Met^{58}-Arg^{77}) was generated by Chew et al (2005) and used to probe Jurkat cells, where nuclear immunostaining was again reported. The antibody reported in the Chew *et al.* paper was also subsequently used in (Camporeale *et al.*, 2006), where it was reported to

recognise *Drosophila* HCS (dHCS). However, of the 20 amino acids comprising the sequence of the epitope, only five are common to both species (figure 4.16). There has been no evidence presented on this antibody to support its specificity to either human HCS or dHCS. In the Camporeale 2006 study, chromosome spreads were probed with the anti-HCS antibody resulting in staining along the chromosome concentrated at "puffs" (sites of active transcription), some specific bands, and telomeres. The authors proposed the involvement of HCS in histone modification through nuclear localisation and association with chromatin. Given the lack of evidence provided to demonstrate binding specificity of this antibody, the nuclear localisation seen in their work could be due to any number of factors including those mentioned for the Gravel antibody.

In conclusion, the work presented here showed that HCS was predominantly localized to the cytoplasm, consistent with its role in biotinylation of carboxylase substrates. Nuclear localisation was observed to a lesser degree, due perhaps to information residing in the N-terminus of the enzyme.

Erratum

The absence of HCS from the MitoCarta dataset (published during the completion of this thesis, Paliarini et al, 2008, Cell 134:112-23) is an interesting observation. As the reviewer points out, however, my results do not exclude some mitochondrial localisation. Further elucidation of the exact subcellular localisation of HCS will require co-localisation studies with known mitochondrial markers. The attempt during this work to try and isolate protein-binding partners of HCS, whilst unsuccessful in this instance, would also help to confirm subcellular localisation. I maintain that the most important finding in this chapter was the observation that HCS resides primarily in the non-nuclear fraction.

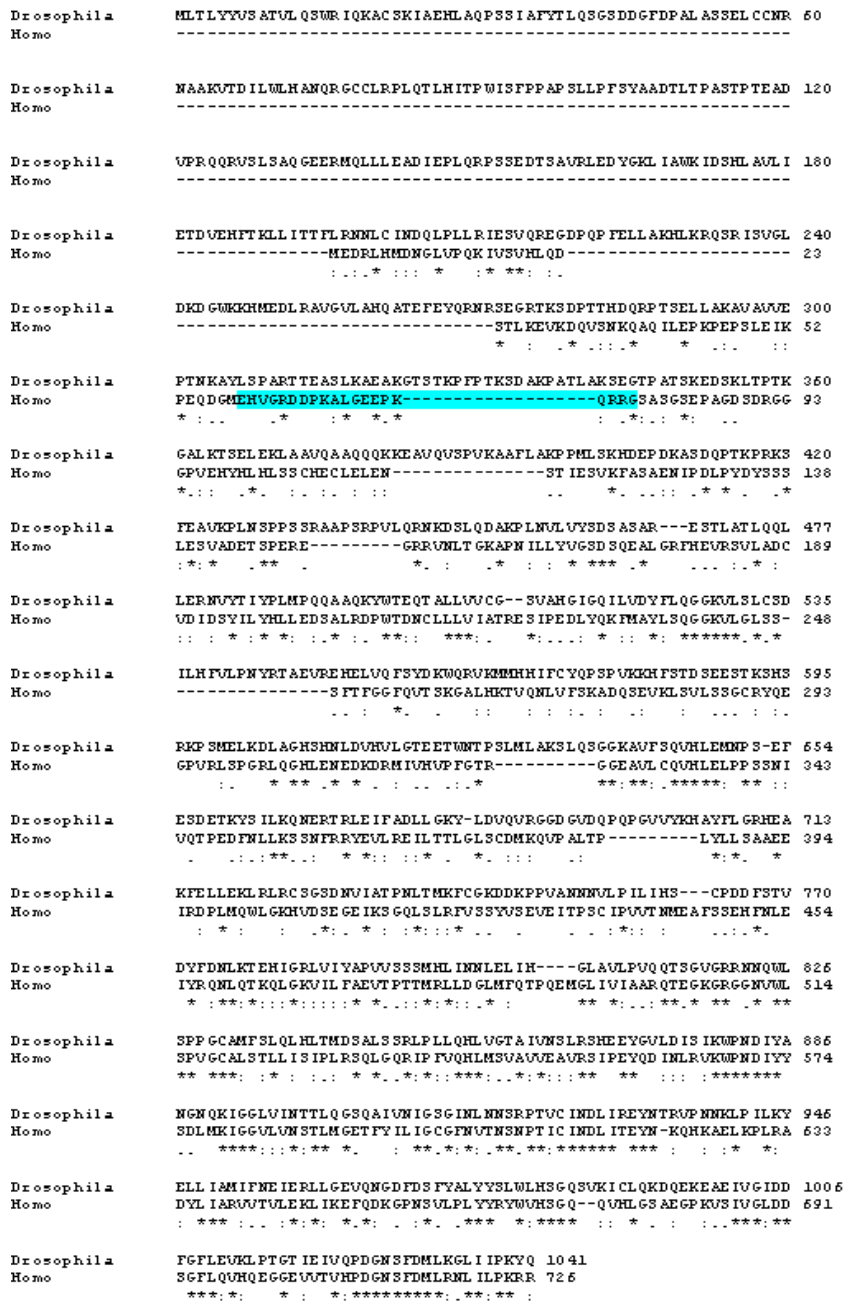

Figure 4-16 Alignment of holocarboxylase synthetase from *D. melanogaster* and *H.sapiens*. The epitope for the antibody against HCS described in (Chew *et al.*, 2006) is highlighted in blue. There is very little sequence homology between the two sequences in this portion of the enzyme.

Examination of HCS L216R in multiple carboxylase deficiency

5 Examination of HCS L216R in multiple carboxylase deficiency

5.1 Background

Multiple carboxylase deficiency (MCD) is caused by various defects in biotin metabolism. The severe neonatal form of MCD usually results from a reduced activity of holocarboxylase synthetase (HCS; MIM# 609018) and is characterised by severe lactic acidosis, cardiovascular compromise, encephalopathy and, without biotin supplementation, death (see Chapter 1 section 1.7). There are large number of mutations in HCS which result in MCD. For further background, please refer to our review analysing the structural mechanisms behind MCD 'Microbial biotin protein ligases aid in understanding holocarboxylase synthetase deficiency', attached as appendix A.2 to this thesis.

MCD Mutations can be classified as either K_M or V_{max} mutants. K_M mutations result in HCS with a decreased affinity for biotin. Patients with K_M mutations respond favourably to biotin therapy. In V_{max} mutants, the affinity for biotin is essentially unchanged but the activity of the enzyme is compromised and responsiveness to biotin therapy varies. These classes of mutation are discussed further in this section.

Table 5.1 is a summary of the known effects on the K_M for biotin and V_{max} for a selection of MCD mutations. It is clear that for mutations in the biotin-binding region of the enzyme (residues 336-726) the K_M for biotin is elevated 3 to 44 fold compared to the wildtype enzyme. Often these mutations leave the enzyme with higher residual activity than mutations in the N-terminal portion of the enzyme.

Mutation	Activity (% wildtype)	K_M Biotin (fold wildtype)	References
Wildtype	100	1	(Aoki *et al.*, 1999)
E42D	120	N.D.	(Yang *et al.*, 2001)
R183P	1.7	0.6	(Sakamoto *et al.*, 1999)
L216R	0.3	1.4	(Sakamoto *et al.*, 1999)
L237P	1.2-4.3	0.4-1.2	(Sakamoto *et al.*, 1999, Aoki *et al.*, 1997)
V333E	2-10	1.5	(Sakamoto *et al.*, 1999, Aoki *et al.*, 1999)
R360S	22.0	N.D.	(Yang *et al.*, 2001)
V363D	3.7	1.1	(Sakamoto *et al.*, 1999)
Y456C	0.2	N.D.	(Yang *et al.*, 2001)
T462I	<10	N.D.	(Aoki *et al.*, 1999)
L470S	4.3	N.D.	(Yang *et al.*, 2001)
R508W	34.5*	23*	(Burri *et al.*, 1985)
V547G	3.4	N.D.	(Yang *et al.*, 2001)
V550M	16.6	6.5	(Aoki *et al.*, 1997)
D571N	0.1	N.D.	(Aoki *et al.*, 1999)
G581S	<10	44.3	(Sakamoto *et al.*, 1999, Aoki *et al.*, 1999)
delT610	14	2.9	(Sakamoto *et al.*, 1999, Aoki *et al.*, 1999)
D634Y	12.0	N.D.	(Yang *et al.*, 2001)
Del(c.C2279)	0.1	N.D.	(Aoki *et al.*, 1999)
Del(c.T1876)	0.1	N.D.	(Aoki *et al.*, 1999)

*HCS activity measured in patient fibroblasts using apoPCC from rat liver as substrate
N.D Not determined.

Table 5-1 Effect of MCD mutations on HCS activity: Summary review from the literature. HCS activity was measured by expression of mutant HCS proteins in HCS deficient fibroblasts using apo-BCCP as a substrate unless indicated.

K_M mutants

There are many reports of MCD patients who show an elevated K_M for biotin, although the actual K_M values obtained vary widely between studies depending on the apo-carboxylase substrate used. (Burri *et al.*, 1981, Sakamoto *et al.*, 1999, Aoki *et al.*, 1997, Burri *et al.*, 1985, Morita *et al.*, 1998, Suzuki *et al.*, 1996, Dupuis *et al.*, 1999, Morrone *et al.*, 2002, Sakamoto *et al.*, 2000). In the cases where the mutation results in an elevated K_M for biotin, treatment with oral doses of biotin up to 10 mg/day is usually sufficient to resolve symptoms, as the increase in biotin concentration is enough to overcome the decreased affinity. Most of the mutations that result in increased K_M for biotin lie in the C-terminal catalytic portion of the enzyme, containing the biotin binding site.

The mutations that affect K_M cluster around the biotin and ATP binding sites of the enzyme, in areas of the enzyme which are highly evolutionarily conserved. This can be clearly seen when the analogous residues of the known structure of *P.horikoshii* BPL

(*Ph*BPL) are highlighted in comparison to the known biotin and ATP contacting residues (figure 5.1).

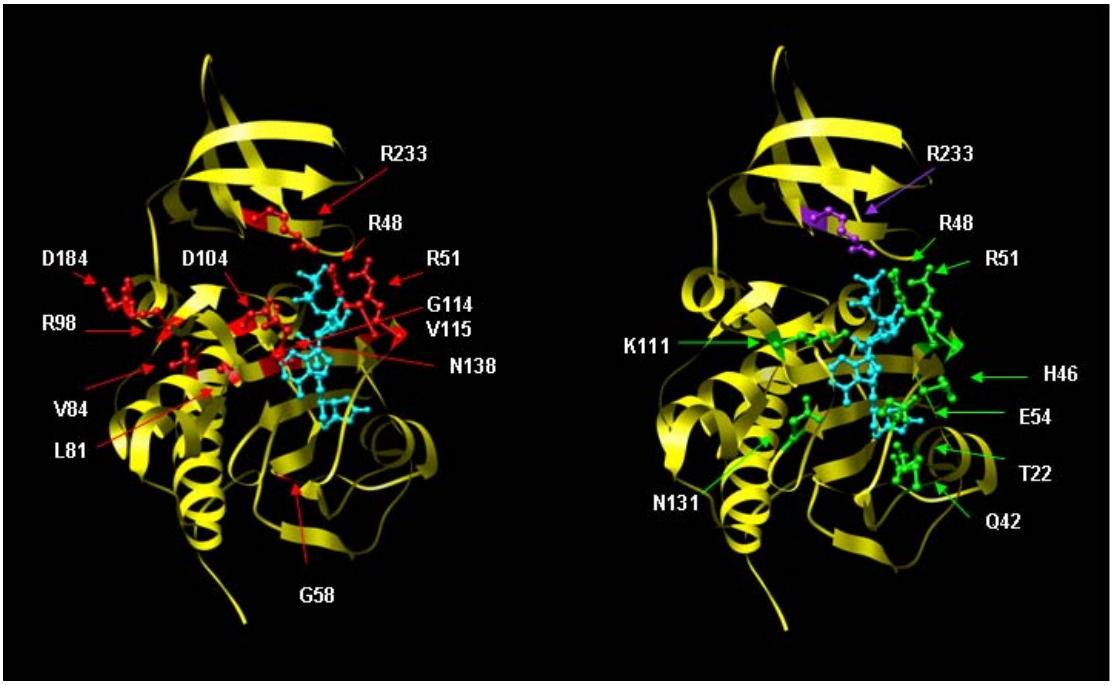

Figure 5-1 Crystal structure of BPL from *P.horikoshii* (yellow ribbon) shown in complex with biotinyl-5'AMP (blue) (Bagautdinov *et al.*, 2005), PDB 2DTO (Protein Data Bank, entry 2DTO).

Left: Equivalent residues in *P.horikoshii* structure which give rise to MCD in human HCS are highlighted in red.
Right: Residues shown to contact biotinyl-5-AMP' in the crystal structure of *P.horikoshii* (green). Residues shown to contact ADP in the crystal structure are highlighted in purple. Figure created using Chimera software (Pettersen et al. 2004).

The HCS-R508W mutation is a common allele in MCD present in a wide variety of ethnic groups. This arginine is located at a highly conserved position in the flexible loop which becomes structured upon binding of biotin and ATP (Wilson *et al.*, 1992). Mutation of the residue in BirA causes promiscuous biotinylation (Choi-Rhee et al., 2004). It is equivalent to Arg^{48} on *Ph*BPL structure above, and it is clear that a mutation to this residue would result in an altered affinity of the enzyme for biotin. Similarly, a number of mutations with altered K_M for biotin map to this region of the enzyme, for example HCS-N511K (Arg^{51} in *Ph*BPL). The HCS-D571N mutation occurs at a very highly conserved position within the KWPND motif present in all biotin ligases. This mutation, whilst not directly contacting biotin or ATP at the analogous position in the known crystal structures, is critical for activity as HCS-D571N protein showed barely detectable levels of activity (Aoki *et al.*,

1999). The analogous residue in the *Ph*BPL structure is essential for positioning of Lys^{111} in the binding pocket which plays a catalytic role in the synthesis of biotinyl-5'-AMP (Bagautdinov *et al.*, 2005). Asp^{615} in HCS (Asp^{138} in *Ph*BPL) occurs in the nucleotide binding site. Other mutations are not as easily explained but most likely result in subtle conformational changes that influence ligand binding or catalysis.

V_{max} mutants

The second group of HCS mutations do not alter the enzyme's affinity for biotin, and map to the N-terminal region of the enzyme, particularly to domain III of the N-terminus (residues Lys^{160}-Lys^{312} critical for enzyme activity (Campeau and Gravel, 2001, Swift, 2003). These mutations, namely R183P, L216R and L237P, vary in their responsiveness to biotin treatment. Interestingly, alignment of the BPL sequences from human, dog, horse, mouse, rat, chicken, *Danio* and *Fugu* show that the N-terminal extension is conserved amongst these vertebrate species. Furthermore, the equivalent amino acids at the positions L216 and L237 are invariant between these species (R183 is conserved amongst mammals), again highlighting their importance (Figure 5.2). There is no clinical information available on the one reported patient homozygous for the R183P mutation (Sakamoto *et al.*, 1998).

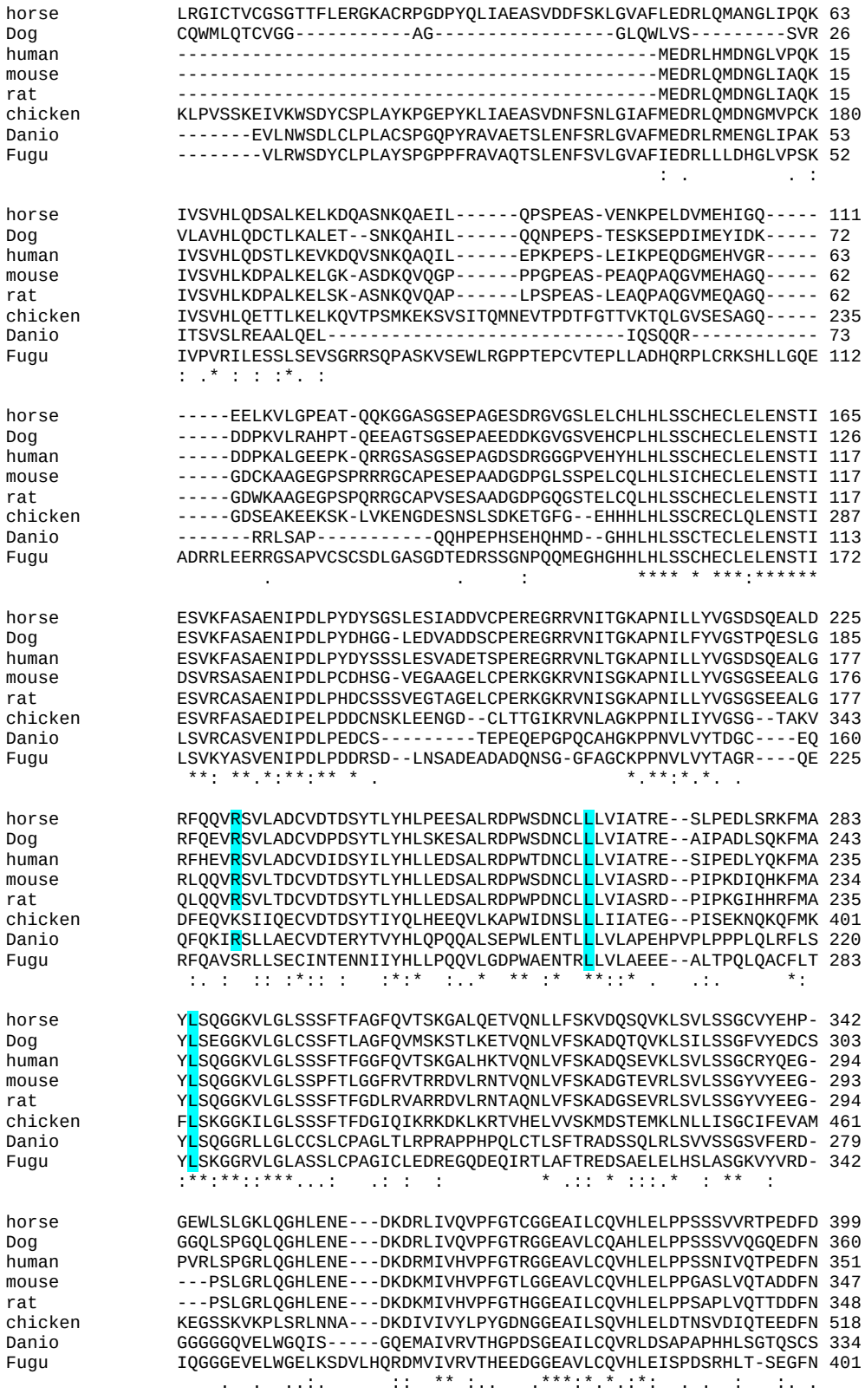

Figure 5-2 Alignment of the N-terminus of vertebrate holocarboxylases.
Sequences from human, dog, horse, mouse, rat, chicken, Danio and Fugu were aligned in ClustalW. Residues highlighted in blue show position of N-terminal mutations which give rise to MCD in human patients.

The L237P mutation was the first mutation reported outside of the catalytic domain (Aoki *et al.*, 1995). This enzyme, when expressed recombinantly, has severely reduced biotinylation activity (Sakamoto *et al.*, 1999, Aoki *et al.*, 1997). Yet despite impaired enzyme activity, the responsiveness of patients with this mutation to biotin therapy varies widely. Patient 2 from (Aoki *et al.*, 1995), a compound heterozygote where one allele contained the L237P mutation, the other a frameshift 780delG mutation resulting in an inactive truncation, required biotin treatment at 80 mg/day to control dermatological symptoms and showed delays in mental development at age 7. In contrast, Patient 1 from the same study was homozygous for the mutation. For Patient 1, treatment with 40mg biotin/day resolved all clinical and biochemical abnormalities and development was normal at 9 months. However, follow-up at 5 years showed a lowered IQ, for this patient who was otherwise symptom-free. Patients 1 and 3 from (Yang *et al.*, 2000) were heterozygous for L237P, with the other allele containing a truncated, non-functional protein. These patients died within the first five days of life (it is not clear whether biotin therapy was administered). Patient UW (Sakamoto *et al.*, 1998), homozygous for the L237P mutation, remained asymptomatic on 40mg biotin/day, despite urinary analysis revealing elevated excretion of 3-hydroxyisovaleric acid. These cases suggest that the L237P mutant does retain some small amount of biotinylation activity, although only one allele (expressed with a non-functional, truncated allele) is not sufficient to respond to biotin treatment. The proposed mechanism by which this mutation shows some form of biotin responsiveness is due to the actual biotin concentration in the cell (estimated at 1-10 nM) being far below the K_M for biotin (108 – 260 nM depending on the type of assay used). If the enzyme possesses any residual activity, it should be biotin responsive at higher biotin concentrations, resulting in enough enzyme activity to alleviate symptoms (Dupuis *et al.*, 1999). This suggests that V_{max} is an important factor in the pathology of the disease, and indeed there is a correlation between V_{max} and responsiveness to biotin therapy (Sakamoto *et al.*, 1999).

The L216R mutation was first identified in the heterozygous form (L216R/V363D) in patient VE (Dupuis *et al.*, 1996), who showed a good clinical response to biotin therapy (10-40 mg/day) (Dupuis *et al.*, 1999). This biotin responsiveness was attributed to the presence of the biotin responsive allele V363D. The first report of a patient homozygous for this mutation showed severe pathology, developing severe respiratory distress and metabolic acidosis within 12 hours of birth. Treatment with 20mg biotin/day yielded no clinical improvement. Treatment continued with 100mg biotin/day with 50mg carnitine/kg/day. However, there was little to no response to treatment over the next two years, and the patient suffered continued severe eczema (leading to conductive deafness in the auditory canals), recurrent fungal and bacterial infections, two episodes of metabolic decompensation and showed global developmental delay (Morrone et al., 2002).The most comprehensive review of patients with this mutation was presented by (Wilson *et al.*, 2005). This mutation appears to occur at a high frequency in the Samoan and Cook Island populations. Five of the seven patients reported homozygous for this mutation had died between 3 days to 3 years old. All patients presented within 24 hours of birth with severe acidosis. The two babies that did not receive biotin treatment died within seven days. Three of the patients, despite receiving high biotin doses, continued to show severe dermatological symptoms and recurrent septicemia followed by metabolic decompensation, and all died during one of these episodes. Patient 2 showed slow improvement with oral biotin treatment (20 mg/day) but showed moderate to severe developmental delay at age 18 months. Patient 7 at age 18 months had only mild developmental delay and “relatively normal” skin but had recurrent hospital admissions due to infections. Biochemically, this patient had an abnormal urine organic acid profile and persistent mild lactic acidosis (Wilson *et al.*, 2005). These babies also showed a lower mean birthweight (mean 2758g vs 3700g), indicating intrauterine growth retardation (IUGR), not reported for other cases of HCS deficiency. Due to the severity of this particular mutation, a collaboration was established with Dr Callum Wilson of the National Metabolic Service, Starship Children's Hospital, Auckland, New Zealand. We obtained patient fibroblasts from two patients with the L216R mutation

for analysis, with the aim to determine why this mutation leads to such drastic effects on enzyme activity and is associated with such severe pathology.

Patients in the present study

After obtaining appropriate human ethics approval, cell lines were obtained from patients PM and JW (referred to in the text as MCD-PM and MCD-JW). Patient JW is male, of Samoan origin born to non-consanguinous parents (refer to figure 5.3), born at term weighing 2920 g. At 1 hr after birth he had breathing difficulties and was hypotensive. Biochemical analysis showed acidosis. Cranial ultrasound showed bilateral subependymal cysts, which are found in other metabolic disorders such as Zellweger syndrome (Bats *et al.*, 2002) and have previously been reported in HCS deficiency (Squires *et al.*, 1997). Treatment with oral biotin and carnitine was commenced, and at 10 months he had recurrent bronchiolitis and persistent metabolic acidosis although growth and development profile was normal. Patient PM was born to non-consanguinous Samoan parents. She was unresponsive to biotin therapy and died.

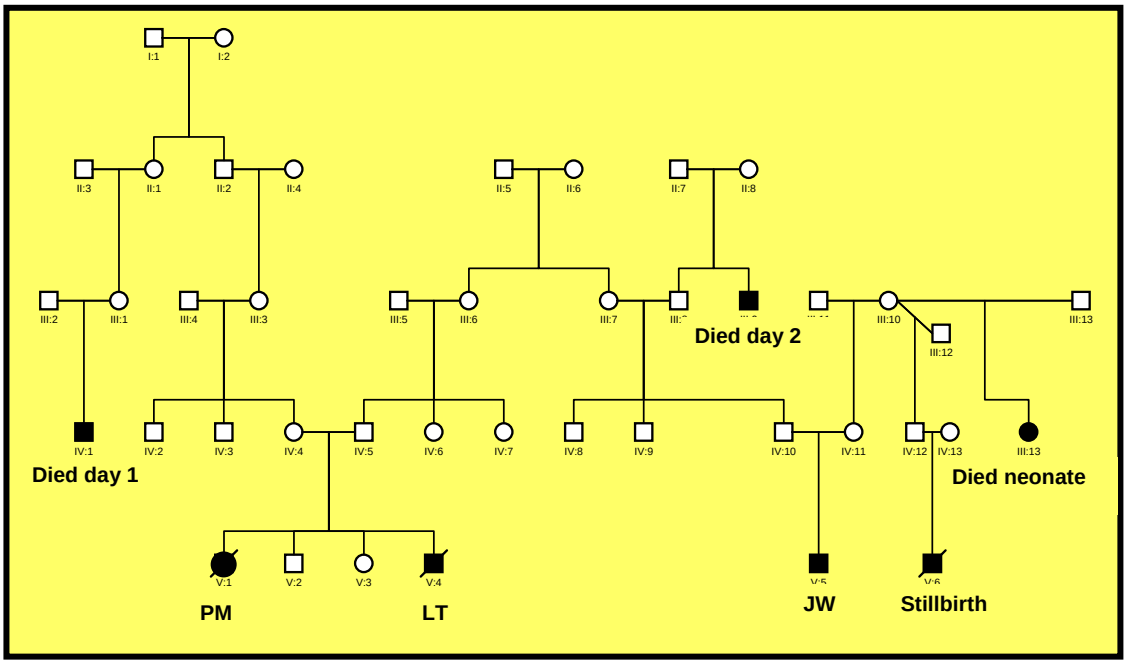

Figure 5-3 Family tree showing patients in the present study PM and JW.
Shaded boxes represent cases of MCD. The pattern of HCS deficiency follows classical Mendelian inheritance for an autosomal recessive disorder (Wilson, personal communication).

This study aimed to characterise the biochemical properties of the L216R mutant fibroblasts with the intention of examining the effects of the L216R on mRNA, protein stability and enzyme activity as well as protein subcellular localisation. The biological mechanism of biotin-responsiveness was investigated by cellular proliferation analysis.

5.2 Specific methods

5.2.1 Genotyping

The nucleotide substitution 647G>T in HCS cDNA results in the L216R amino acid substitution. To diagnose this, an oligonucleotide pair terminating one nucleotide from the mutation was designed to generate (or eliminate) a restriction site in combination witht he mutation. Cleavage of the PCR product with the corresponding restriction enzyme would reveal the presence or absence of the mutation. Cells were genotyped as previously reported (Dupuis *et al.*, 1996). Briefly, genomic DNA was isolated using a QIAGEN DNAeasy tissue extraction kit. A 245 bp amplicon of HCS was amplified with primers B176 and B177 which introduced an *HpaII* restriction site specifically into the PCR product bearing the L216R mutation. The PCR product was purified using QIAGEN PCR purification kit and approximately 1 μg of DNA was digested with *HpaII* at 37°C for two hours. Digestion of the L216R mutant results in two fragments (224 + 21bp) which could be resolved from the wildtype amplicons (245 bp) when resolved on a 2% agarose gel.

5.2.2 Reverse transcription PCR

Analysis was performed on the following cell lines: wildtype fibroblast cell line HFF, patient cell lines MCD-JW and MCD-PM, and control cell lines HepG2 and 293T. Cells from a 100 mm Petri dish were harvested in 1 mL of Trizol Reagent (Invitrogen) and RNA purified as per the manufacturer's instructions. To remove genomic DNA contamination 30 μL of RNA was treated with RNAse Free DNAseI for 30 minutes at 37°C in a 50 μL reaction containing 20 Units SuperIn RNAse inhibitor (Ambion), 10 mM Tris-HCl pH 8.0, 50 mM KCl and 1.5 mM $MgCl_2$. This was followed by phenol/chloroform (3:1) extraction, from which the upper aqueous phase was precipitated with 5 μL 3M sodium acetate pH 5.2 and 200 μL 100% ethanol. After precipitation at -80°C, RNA was pelleted, washed

om 70% ethanol and air dried. The purified RNA was dissolved in 20 μL DEPC H_2O and quantified by measuring absorbance at 260nm. RNA quality was assessed by calculating the OD 260 nm/280 nm ratio (where good quality was defined as a ratio of 1.8-2.0). cDNA synthesis was performed using 5 μg of RNA, 200 Units SuperscriptIII Reverse Transcriptase (Invitrogen) and 100 ng random hexamer primers according to the manufacturer's instructions in a total volume of 10 μL. 2 μL of the resulting cDNA was used as a template for PCR with the primers B106 and B107, with an annealing temperature of 55°C over 40 cycles (as outlined in section 2.2.4.11).

5.2.3 Biotin-deficient cell culture system

Biotin-deficient medium was prepared by incubation of FCS with streptavidin Sepharose (GE Healthcare, Buckinghamshire, England) overnight at 4°C. To calculate the amount of streptavidin Sepharose required, a titration with labelled ^{14}C biotin was performed to calculate the amount of streptavidin Sepharose required to remove a 50 fold excess of labelled biotin (ie 500 nM biotin). This is based on the estimation that FCS contains 10 nM biotin (Baumgartner *et al.*, 2004). 5 μL of 100 μM ^{14}C biotin was added to 1 mL of FCS, and a titration performed with streptavidin Sepharose. The capacity of the resin was defined as the minimal amount of resin capable of removing all the ^{14}C biotin in serum.

Biotin-depleted FCS was then sterilised through a 0.2 μm filter to remove the resin. Biotin deficient media were prepared with DMEM containing 10% biotin-depleted FCS and 100 ng/mL avidin. For labelling studies, cells were grown in biotin deficient media without avidin and supplemented with 100 nM ^{14}C biotin.

5.2.4 Cell proliferation assay

Cellular proliferation was measured by either trypan blue staining and counting (refer to section 2.2.1.2) or by CellTiter 96® AQ_{ueous} One Solution Cell Proliferation (MTS) Assay

(Promega). For the CellTiter 96 well assay, cells were plated at a density of 5000 cells/well in biotin-deficient media supplemented with appropriate concentrations of biotin as indicated. After 7 days growth, 20 μL of assay reagent was added per well and the plate incubated for one hour at 37°C, 5% CO_2. Absorbance was measured at 490 nM on a microplate reader (Molecular Devices, CA, USA).

5.2.5 Effect of L216R on subcellular localisation of HCS

pEGFP (L216R) was generated by R. Ivanov using QuickChange™ site-directed mutagenesis (Stratagene, CA,USA) using primers B156 and B157 upon the parental plasmid pK(hBPL). A *KpnI* fragment (containing the L216R mutation) was then subcloned into pET(hBPL). An *NcoI* / *XhoI* digest of pET(hBPL) was used to subclone the entire HCS gene into pGEM. Subsequently, pGEM(HCS-L216R) was digested with *EcoRI* to drop out the HCS cassette for subsequent cloning into the mammalian expression vectors pEGFP-C1 or pEFIRES. For analysis of subcellular localisation of HCS-L216R 24 hour transient transfections were carried out and cells viewed as outlined in section 5.2.1.

5.2.6 Tetracycline regulated expression of HCS

5.2.6.1 Cloning

pTR(HCS) was generated by introducing *an EcoRI* / *HindIII* fragment containing the HCS coding region into similarly treated pTR-YFP. To create the HCS-L216R mutant, an *EcoRI* / *BglII* fragment from pEGFP(HCS-L216R) was digested with *EcoRI* / *BglII* and ligated into similarly treated pTR (HCS). DNA sequencing confirmed the presence of wildtype or L216R mutant HCS forms, as appropriate.

5.2.6.2 Half-life study

To examine protein half-life, 1.5 μg of plasmid was transiently transfected into CHO AA8 Tet Off cells (Clontech) using Lipofectamine 2000, according to the manufacturer's

instructions. After 48 hours of transfection, the medium was changed, and medium containing doxycycline 4 μg/mL was added to cells. Cell lysates were harvested at time-points specified by addition of 250 μL of RIPA buffer as described in 2.2.2.1. Lysates were resolved by SDS-PAGE and Western Blotted with N2 antibody (Section 2.2.2).

5.3 Results

5.3.1 Genotyping of patient cells

The first part of this study was to confirm the presence of the mutation in the cell lines provided. Genotyping was performed on genomic DNA extracted from cells as described previously (Dupuis *et al.*, 1996). Genomic DNA was isolated directly from glycerol stocks of cells to avoid contamination. Plasmids encoding wildtype or L216R HCS were used as controls. Gel analysis of the DNA fragments obtained after *HpaII* digest show the HFF control fibroblasts are homozygous for the wildtype HCS allele as expected (figure 5.4). MCD-PM is homozygous for HCS L216R as expected. Surprisingly, the MCD-JW cells, which were indicated as heterozygous by our collaborators, appeared homozygous for the mutation. This confirmed that the cells were suitable for use in analysis of the HCS L216R mutation.

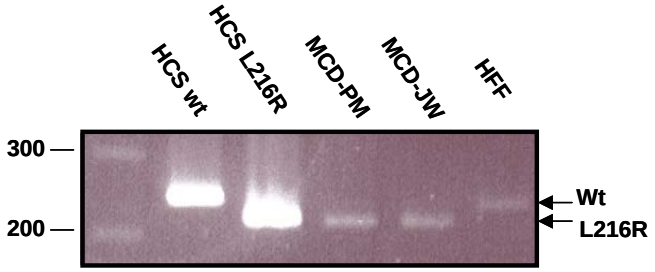

Figure 5-4 Genotyping to confirm presence of L216R mutation.
HCS wt and HCS-L216R plasmids were used as controls. MCD-PM and MCD-JW are homozygous for the L216R mutation. HFF is a control wildtype fibroblast cell line.

5.3.2 Effect of L216R HCS on cell proliferation

The patients from whom these cells were derived responded poorly to biotin therapy. To examine this property, a biologically significant output (cellular proliferation) was measured with varying biotin availability.

5.3.2.1 Cell proliferation in complete media

In an initial experiment growth rates of wildtype and mutant fibrolblast cells were compared when grown in complete media (figure 5.5). Cell number was determined by trypan blue exclusion staining and counting with a haemocytometer. Both MCD cell lines showed a significantly reduced cellular proliferation rate compared to wildtype cells.

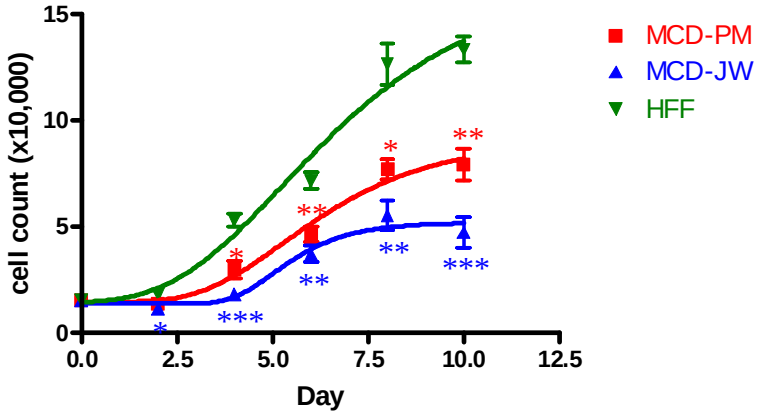

Figure 5-5 Growth curve of wildtype fibroblasts (HFF) compared to MCD L216R fibroblasts (MCD-PM and MCD-JW).
Cell number was measured by trypan blue exclusion staining and counted on a haemocytometer. Error bars are +/- SEM from 3 experiments. P values were determined by comparing growth of MCD cells at each time point to wildtype HFF cells using unpaired t-tests (Confidence Intervals 95%) by GraphPad Prism. * P <0.05, ** P <0.01, *** P<0.001

5.3.2.2 Optimisation of biotin deficient culture conditions

To examine the effect of biotin supplementation on the proliferation capacity of patient fibroblasts, it was important to define a biotin-deficient cell culture system.

Previous studies have shown that biotinylation of carboxylases is sensitive to biotin availability in cell culture medium (Rodriguez-Melendez *et al.*, 1999, Crisp *et al.*, 2004, Manthey *et al.*, 2002). Several methods for removing biotin from media have been reported in the literature. When using defined media, FCS is often the primary source of biotin in cell culture, typically at a concentration of 9 nM biotin (Baumgartner *et al.*, 2004). Standard DMEM does not contain biotin, therefore methods for reducing biotin content in culture have included the use of serum-free media (Rodriguez-Melendez *et al.*, 1999), dialysed FCS (Pacheco-Alvarez *et al.*, 2005, Pacheco-Alvarez *et al.*, 2002) and treatment of media with avidin (Manthey *et al.*, 2002, Griffin *et al.*, 2003, Crisp *et al.*, 2004). We found that treatment of FCS with streptavidin was necessary to completely deplete the biotin content. This latter method was employed in preference to the use of dialysed FCS as only biotin is specifically depleted rather than removing many low molecular mass molecules. A titration with labelled biotin was used to calculate the amount of streptavidin Sepharose required to remove up to 500 nM free biotin, i.e. 50 fold in excess of the reported biotin concentration in serum (Figure 5.6). Addition of 6.25 μL of 50% streptavidin Sepharose slurry per mL of serum was required to remove all detectable biotin from the system. For subsequent preparation of biotin deficient media 12.5 μL of streptavidin-Sepharose slurry was added per mL of serum to ensure complete removal of biotin.

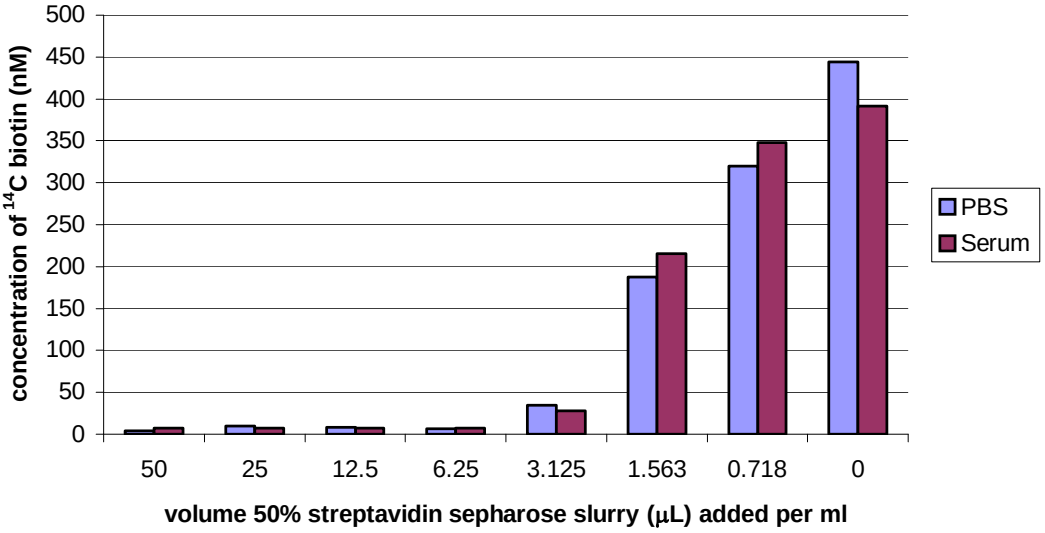

Figure 5-6 Titration of streptavidin Sepharose to optimise biotin-depletion of media.
The x axis represents the volume of streptavidin Sepharose added per mL of solution (PBS or serum), the y-axis shows the remaining concentration of ^{14}C labelled biotin in the supernatant after a one-hour incubation and removal of streptavidin Sepharose by centrifugation.

5.3.2.3 Effect of biotin supplementation on proliferation of HCS-L216R fibroblasts

To examine the effect of biotin availability on cellular proliferation, MCD and wildtype cells were grown in either complete or biotin-deficient media. Two alternative methods were used to examine cellular proliferation. Total cell number was determined by trypan blue staining and counting, or cellular proliferation was measured by the CellTitre 96® AQ_{ueous} One solution cell proliferation assay (Promega). This colourimetric assay measured the reduction of the tetrazolium salt MTS (3-(4,5-dimethylthiazol-2-yl)-5-(3-carboxymethoxyphenyl)-2-(4-sulfophenyl)-2H-tetrazolium) to formazan, giving an indication of the metabolic capacity of cells. Validation of the CellTitre AQ_{ueous} Assay confirmed that the quantity of formazan product measured by absorbance at 490 nm was

directly proportional to the number of living cells in the well up to 50,000 cells/well (figure 5.7-A).

Analysis of cellular viability after growth in biotin-deficient media for 7-10 days gave similar results for both methods tested (figure 5.7-B and 5.7-C). Both the MCD cell lines showed significantly reduced proliferation compared to wildtype cells when grown in complete media ($P<0.001$). There was a significant effect of biotin depletion on the growth of wildtype HFF cells as measured by both counting ($P<0.001$) and CellTitre Assay ($P<0.05$). However, there were no significant differences between growth of MCD cells in complete or biotin-deficient media.

To examine if proliferation of MCD cells could be rescued by addition of supra-physiological amounts of biotin, a cell viability assay was carried out using the CellTitre AQueous assay. Cells were first grown for two weeks in biotin-deficient media to induce a state of biotin stress. Starved cells were then plated at a density of 1,000 cells per well and grown for seven days in complete media, or biotin deficient media supplemented with a range of biotin concentrations (0.01 nM -1 mM). The results are shown in Figure 5.8.

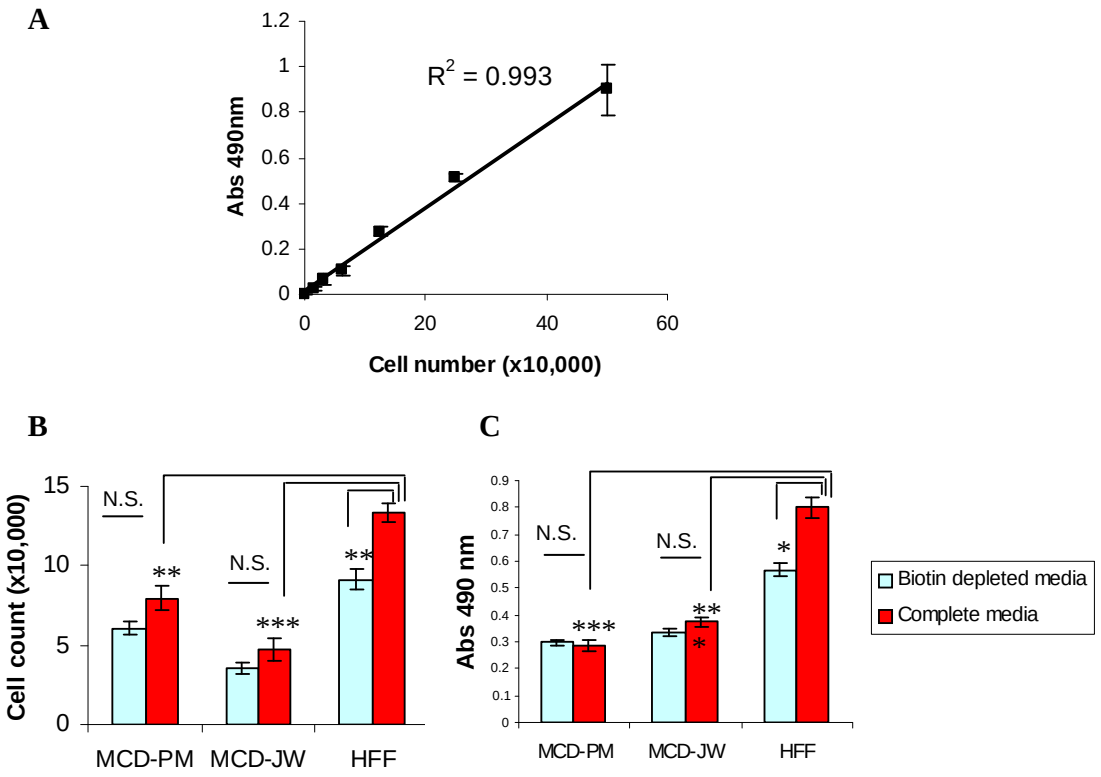

Figure 5-7. Effect of biotin depletion on cell proliferation.

(A) Validation of CellTiter 96® AQueous One assay showing linear relationship between metabolic activity (MTS reduction) and cell number (result for MCD-JW cells shown, n=3 Error bars +/-SEM). Subsequently, cells were grown in complete or biotin deficient media for 7 days (B) or 10 days (C) and then growth measured.
B) Number of live cells as measured by trypan blue staining
C) Number of live cells as measured by CellTiter 96® AQueous One Solution Cell Proliferation Assay (Promega).
Error bars are +/- SEM from three experiments. P values were calculated by comparing biotin depleted to complete media for each cell type and comparing growth in complete media of HCS L216R cells (MCD) to wildtype (HFF) cells using unpaired t-tests (Confidence intervals 95%) by GraphPad Prism Software. N.S not significant $P>0.05$, * $P < 0.05$, ** $P < 0.01$, *** $P < 0.001$.

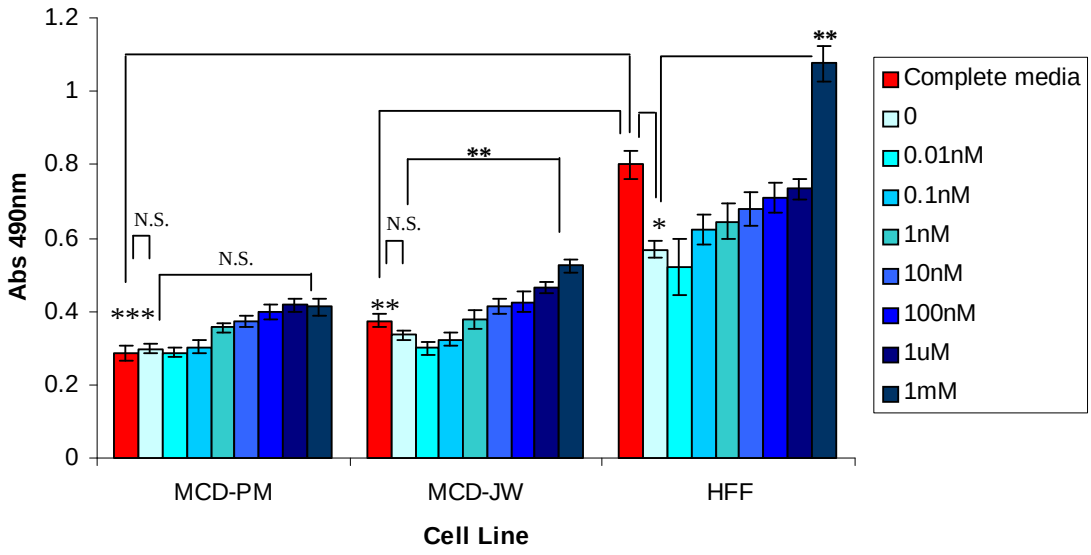

Figure 5-8 Effect of biotin supplementation on proliferation of HCS-L216R fibroblasts.

Cells were grown for two weeks in biotin deficient media before plating into a 96 well plate in either complete, biotin deficient, or biotin deficient media with re-addition of biotin from 0.01nM to 1mM. Cells were grown for one week and then cellular proliferation measured using the CellTiter 96® AQueous One Solution Cell Proliferation Assay (Promega). Error bars are +/- SEM from three experiments. P values were calculated by comparing biotin depleted to complete media for each cell type and comparing growth in complete media of HCS L216R cells (MCD) to wildtype (HFF) cells using unpaired t-tests (Confidence intervals 95%) by GraphPad Prism Software.
N.S. not significant P>0.05, * P < 0.05, ** P < 0.01, *** P < 0.001.

As shown in figure 5.7, MCD cells have reduced proliferation compared to wildtype cells and biotin starvation reduces growth of wildtype cells but has little effect on MCD cells (figure 5.8). Addition of exogenous biotin is able to restore proliferation of wildtype cells, or indeed increase proliferation as seen in the maximum stimulation of proliferation at 1 mM biotin. Addition of biotin to MCD cells results in a non-significant trend of increasing proliferation. However, even at maximal biotin concentrations of 1 mM (clinically unachievable levels) proliferation still fails to match that of wildtype cells in complete media (MCD-PM 51% of HFF, MCD-JW 66% of HFF).

5.3.3 Analysis of HCS-L216R expression and activity

5.3.3.1 Effect of HCS-L216R on mRNA expression

One hypothesis to explain the lack of biotin responsiveness of the L216R mutant is that there is lack of expression of the protein due to a deleterious effect of the mutation on transcription, translation, or stability of the mRNA. To determine if there was any effect, the expression of HCS-L216R in MCD fibroblasts was compared to expression of wildtype HCS in control fibroblasts using RT-PCR.

First, transcription was investigated. Pilot experiments were performed to optimise the amount of input cDNA and PCR cycles to ensure that the threshold of detection of the PCR products was in the linear range. Analysis of wildtype and patient fibroblasts (HFF and MCD-PM and MCD-JW respectively), as well as HepG2 and 293T cell lines (known to be rich in biotin-enzymes) revealed no significant differences in HCS expression (figure 5.9).

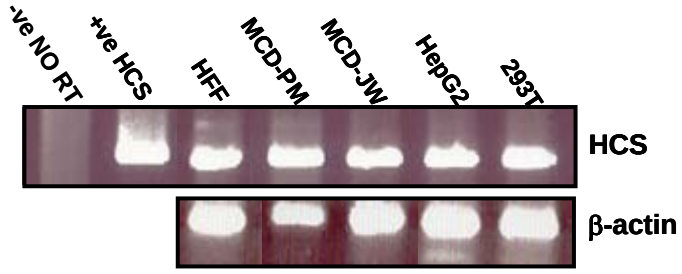

Figure 5-9 Analysis of HCS mRNA expression by RT-PCR in wildtype and MCD cell lines.
pEFIRES(HCS) plasmid was used as a template for the positive control lane. Negative control contains no RT. A 658bp product was amplified with B106 and B107 primers.

5.3.3.2 Analysis of HCS protein in wildtype and L216R HCS fibroblasts

As expression of the HCS mRNA had been confirmed in the patient cells, the presence of HCS protein was subsequently analysed. To increase the sensitivity of detection a biotinylated form of the N2 antibody was used to probe Western Blots of whole cell extracts. Due to the use of the biotinylated N2 antibody and subsequent detection with Streptavidin-HRP, analysis of the 76 kDa isoform of HCS could not be performed as this band was indistinguishable from the alpha-chains of MCC and PCC detected with the Streptavidin at 77 and 80 kDa. Hence all analysis was performed on full length (80 kDa) protein. Figure 5.10 showed there was no detectable full length HCS protein in the patient cells.

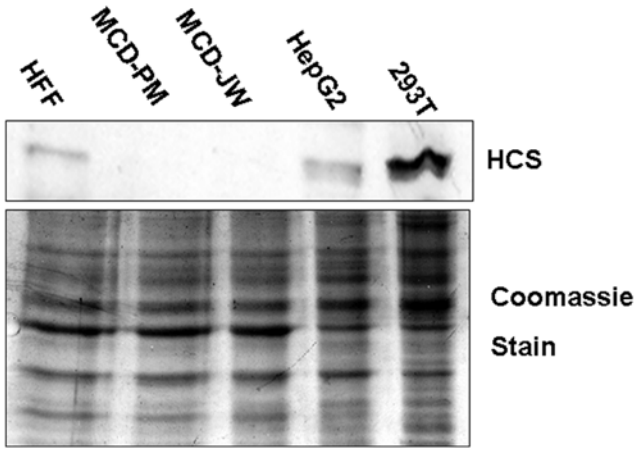

Figure 5-10 Western blot of full length HCS protein in wildtype and MCD cells.

20 μg of protein was probed with biotinylated N2 antibody and detected with streptavidin-HRP. The lower panel shows equal loading of samples on a Coomassie stained gel.

5.3.3.3 Effect of L216R on HCS activity

Two methods were subsequently employed to assay HCS activity in cell lysates. The incorporation of ^{3}H biotin onto an acceptor substrate is the most sensitive method for measuring HCS activity, and was employed for measuring endogenous HCS activity in cell lysates. A novel 96-well assay (described in section 2.2.4.2), using Europium labelled streptavidin and time-resolved fluorescence developed in our laboratory, was used for

analysis of lysates from overexpressing cells. This assay is much easier to manipulate, contains no radioactivity and is much more high-throughput, although less sensitive than the ^{3}H biotin incorporation assay.

Firstly, lysates from patient and control fibroblasts, as well as HepG2 and 293T cells, were analysed for HCS activity. Negligible HCS activity was detected in the patient cells, even though HCS activity in the wildtype fibroblasts was lower compared to the HepG2 and 293T cells (table 5.2) .

Cell type	HCS activity (pmol/min/mg)
HFF	118.2
MCD-PM	7.9
MCD-JW	5.7
HepG2	215.3
293T	508.4

Table 5-2 Activity of endogenous HCS in various cell lines.
Lysate (70 μg) was assayed for ^{3}H-biotin incorporation onto apo-yPC104 for one hour at 37ºC.

However, as full length protein could not be detected in the MCD cell lysates (figure 5.10), it could not be determined whether the mutation caused the protein to be inactive, or whether the loss of activity was due to the absence of protein.

To resolve this, constructs were generated to overexpress both wild-type and L216R HCS in mammalian cells (using a tetracycline-responsive expression system, discussed in section 5.3.7 below). Activity of cell lysates was measured over a range of biotin concentrations ranging from 0-1000 nM (Figure 5.11). HCS-L216R was inactive at all biotin concentrations (Figure 5.11 B). Activity remained at basal levels even in 1 mM biotin (data not shown). Western Blotting of cell lysates confirmed expression of the protein.

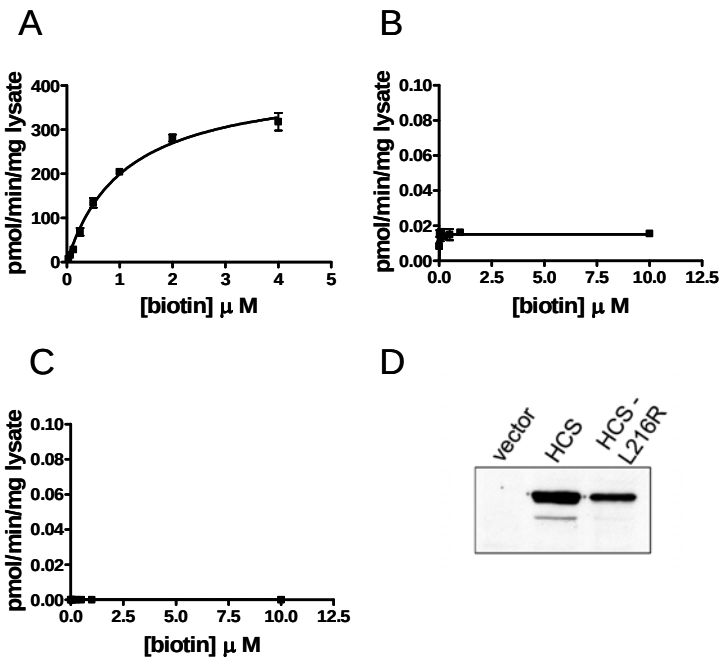

Figure 5-11 Enzymatic analysis of HCS and HCS-L216R.

CHO AA8 tet-off cells were transfected with pTRE, pTR(HCS) or pTR(HCS-L216R). After 48 hours transfection cells were harvested, and cell lysates assayed with increasing concentrations of biotin. Samples included in the kinetic analysis were (A) overexpressed wildtype HCS, (B) overexpressed HCS-L216R and (C) empty vector control. Error bars are +/- from three experiments. (D) Protein expression was confirmed by analysing 10 mg of cell lysate by Western blot probed with N2-HCS antibody.

5.3.4 Effect of L216R mutation on protein stability

As full length HCS protein could not be detected by Western blotting of whole cell extracts (figure 5.10), it was hypothesized that the L216R mutation causes a reduction in protein stability or affects protein folding, leading to increased turnover.

Currently there have been no studies into the regulation of HCS degradation or stability. There are several methods commonly used to examine the half-life of a protein. Metabolic pulse-chase labelling is widely used, but this method requires the use of suitable immunoprecipitating antibodies. As the antibodies developed in the present study were not suitable for such experiments, cycloheximide, a protein synthesis inhibitor, was employed. Cycloheximide was added to 293T cells overexpressing either the wildtype or mutant HCS protein and whole cell extracts prepared over a 48 hour

timecourse. However, no alteration of HCS levels was observed over this period, indicating that the protein was not rapidly turned over (figure 5.12). As cycloheximide is toxic to cells, rapidly inducing apoptosis and reducing cell viability, is not suitable for determining protein half-lives over 24 hours (Blom *et al.*, 1999, Alessenko *et al.*, 1997, Croons *et al.*, 2007). Hence cycloheximide could not be used for determining the half life of HCS.

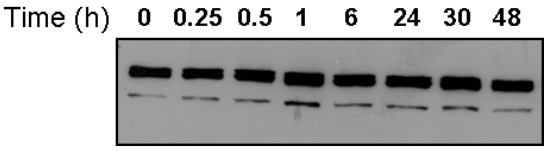

Figure 5-12 HCS stability assayed by cycloheximide study.

293T-HCS cells were treated with 10 μM cycloheximide and cells harvested at the time points indicated. HCS was detected by Western Blotting 10 μg of whole cell extract with N2-HCS ab.

An alternative approach using a tetracycline repressible expression system was then employed to examine the relative stability of the wildtype and mutant protein. In this system the tetracycline-controlled transactivator (tTA) was constitutively expressed in CHO AA8 Tet Off cells (Clontech). Constructs bearing the target gene HCS or HCS-L216R were generated under the control of a minimal CMV promoter downstream of the tet operator sequence of *E. coli* (tetO). In this system, when both plasmids are present in the mammalian cell in the absence of the regulating agent (tetracycline or its analogue doxycycline), tTA is produced and able to bind to tetO, thereby driving expression of the target gene from the CMV promoter. When doxycycline is added to the media, tTA undergoes a conformational change, dissociating from tetO and blocking transcription. This is the so-called “Tet-Off” transcription system (figure 5.13 A) (Zhu *et al.*, 2002). This system is advantageous for the present study in that only transcription of the gene of interest is switched off, leaving the rest of the cell to function normally. This enabled long time-courses to be monitored without concern about toxicity to the cell from global translational inhibitors, such as cycloheximide. Additionally, overexpression of HCS

allowed for easy detection by Western Blotting with antibodies, avoiding the need for an immunoprecipitation step.

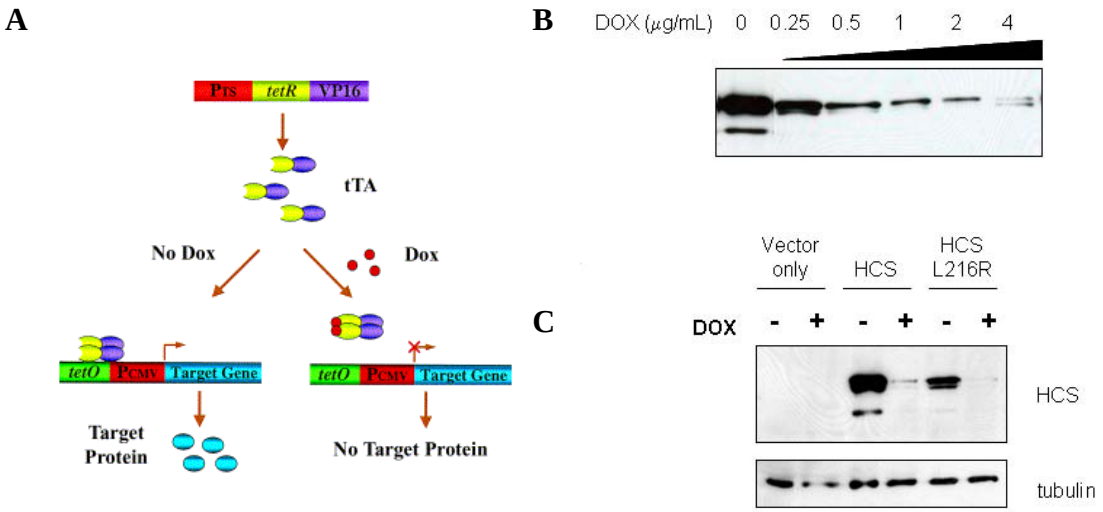

Figure 5-13 Tet-Off expression system used for controlled expression of HCS.

(A) Tetracycline-controlled transcriptional activator (tTA) system: "Tet-Off." Tissue- or cell type-specific promoter directs the expression of tTA, a fusion protein of tetracycline repressor of *E. coli* (TetR) and the transcription activation domain of viral protein 16 of herpes simplex virus (VP16). In the absence of regulating agent doxycycline (DOX), tTA binds the responsive elements tetracycline-resistance operon of *E. coli* transposon Tn10 (*tetO*) and activates minimum promoter from human cytomegalovirus (pCMV) leading to transcription and expression of downstream target gene. In the presence of Dox, tTA dissociates from *tetO* and terminates transcription of the target gene, in this case HCS. (Zhu *et al.*, 2002)
(B) Western Blot demonstrating tetracycline controlled expression of HCS. CHO AA8 Tet-Off cells were transfected with 1.5 μg of plasmid pTR(HCS) with increasing amounts of DOX present in the media and allowed to express for 48 hours. 10 μg of whole cell lysate was analysed by Western Blotting with N2 antibody.
(C) Transfections were performed as for B, with cells grown in presence or absence of 4 μg/mL DOX. Lysate (10 μg) was Western Blotted with N2 antibody or anti-tubulin antibody as a loading control. Appropriate expression / repression of HCS and HCS-L216R were observed.

Initial studies were performed to validate the doxycycline (Dox) controlled expression of HCS in this system. Figure 5.13.B shows the dose-dependent response of HCS expression to Dox concentration. For subsequent experiments Dox at 4 μg/mL was used. Tight regulation of HCS expression could be achieved by the presence or absence of Dox in the culture media (figure 5.13.C). Endogenous HCS was not detectable (as shown in the vector only lanes).

For determination of protein half-life, cells were treated as outlined in section 5.2.6.2. When whole cell extracts were analysed by Western Blotting (figure 5.10.A). Coomassie staining of gels confirmed equal loading of samples (data not shown). A clear reduction in protein stability was observed in the L216R mutant protein compared to wildtype. Densitometry on the full-length (81 kDa) band was performed and the half-life calculated by plotting the log value of the protein intensity against time.

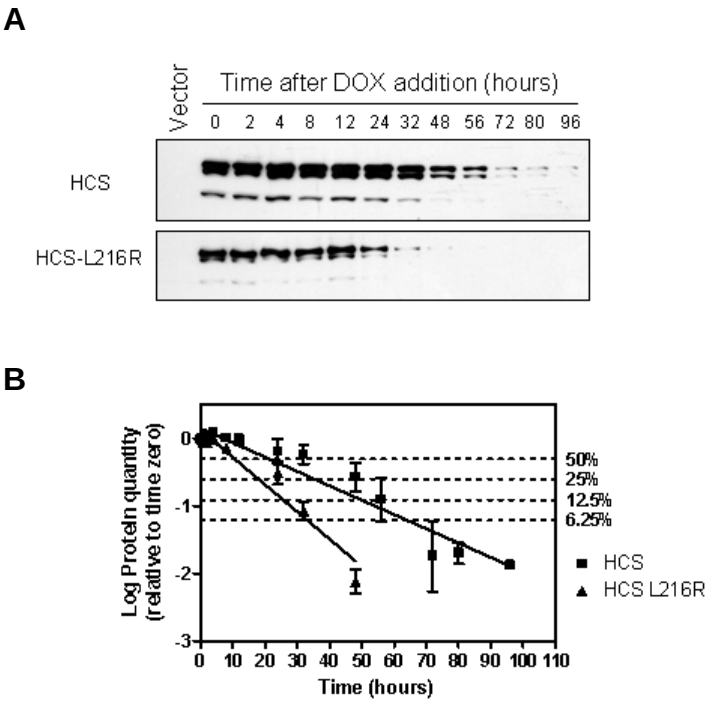

Figure 5-14 Stability of HCS L216R is reduced compared to wildtype protein.

Wildtype (HCS) and mutant (HCS L216R) protein were transiently transfected into CHO AA8 Tet Off cells. After 48 hours expression, DOX was added. Cells were harvested at appropriate timepoints post DOX addition.
(A) Whole cell lysate (10 μg) was analysed by Western Blotting with N2 antibody. A representative blot is shown.
(B) Densitometry on full length HCS protein (81kDa) was calculated and expressed relative to time zero. To calculate half-life the log value of protein intensity was plotted against time. Linear regression lines for wildtype and mutant are shown (r^2 =0.9209 and 0.8979 respectively, n=3). Horizontal dashed lines indicate 50% decreases in protein on a log scale, representing four half-lives. No time points past 48 hours are indicated for the mutant protein as no bands were detectable past this time point.

	HCS	HCS-L216R
Half Life (hours)	16.80	8.52
Fold Difference	1.00	0.51

Table 5-3 Half-Life calculation for wildtype and L216R HCS using the Tet-Off expression system.

The results indicated that the HCS-L216R protein is significantly less stable than the wildtype protein (figure 5.14), the half-life values indicating this protein is turned over twice as quickly in the cell (table 5.3).

Interestingly, this experimental system also allowed investigation into the relative stabilities of the HCS isoforms detectable by Western Blotting. Quantification separating the upper two bands (the doublet) was too difficult, but comparisons between the full length isoform and the lower ~76 kDa isoform were able to be performed on the wildtype enzyme (Figure 5.15)

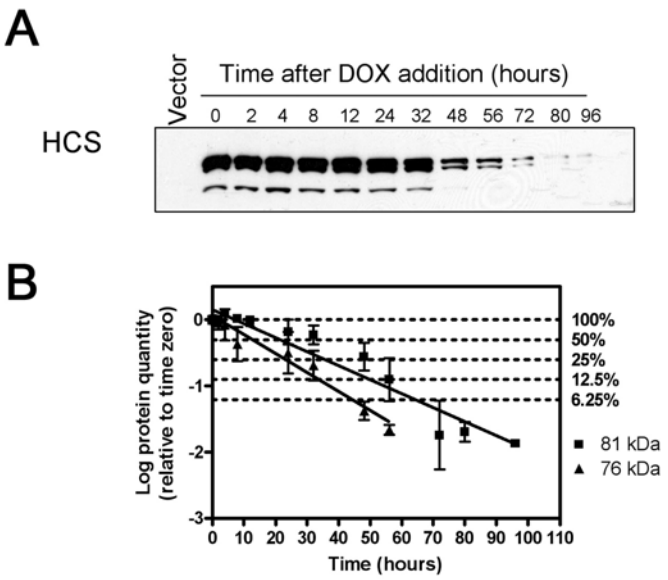

Figure 5-15 Stability of the 76 kDa isoform of HCS is reduced compared to the full length 81 kDa isoform.

pTR(HCS) was transiently transfected into CHO AA8 Tet Off cells. After 48 hours expression, DOX was added. Cells were harvested at appropriate timepoints post DOX addition.
(A) Whole cell lysate (10 μg) was analysed by Western Blotting with N2 antibody. A representative blot is shown.
(B) Densitometry on full length HCS protein (81kDa) and lower isoform of 76 kDa was calculated and expressed relative to time zero. To calculate half life the log value of protein intensity was plotted against time. Linear regression lines for wildtype and mutant are shown (r^2 =0.9209 and 0.8979 respectively, n=3). Horizontal dashed lines indicate 50% decreases in protein on a log scale, representing four half-lives. No time points past 48 hours are indicated for the mutant protein as no bands were detectable past this time point.

	HCS 81kDa	HCS 76kDa
Half Life (hours)	16.80	11.58
Fold Difference	1.00	0.69

Table 5-4 Half-Life calculation for wildtype and L216R HCS using the Tet-Off expression system.

These results indicated the smaller isoform of HCS was less stable than the full length isoform.

5.3.5 Localisation of L216R HCS

We predicted that the L216R mutation may result in altered cellular localisation of the protein, hence explaining the lack of biotinylation of the carboxylases resident in the mitochondria and cytoplasm. Due to the low levels of endogenous protein in even the wildtype fibroblasts, a GFP labelling approach (as described in Chapter 4) was used to examine whether the localisation of HCS-L216R was affected. Figure 5.16 shows that the subcellular distribution of the GFP tagged HCS-L216R displayed a similar cytosolic localisation to the wildtype enzyme.

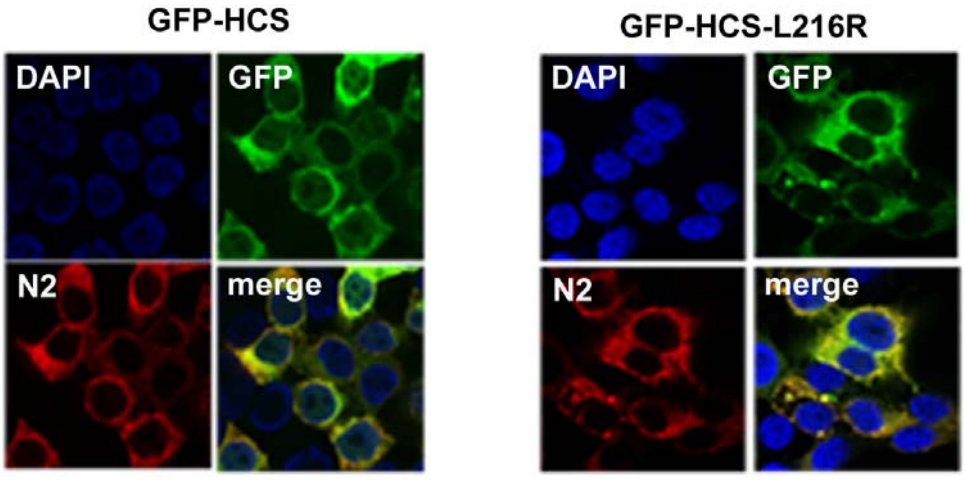

Figure 5-16 HCS L216R and wildtype HCS have a similar cytosolic localisation.

293T cells were transiently transfected with GFP-HCS or GFP-HCS-L216R. Cells were fixed and probed with N2 Ab, detected with a Cy3 secondary (red). Nuclei were stained with DAPI (blue). Co-localisation of N2 ab and GFP are shown in the merge panel (yellow).

5.3.6 Effect of L216R mutation on biotinylation of histones

Given the lack of HCS activity in the MCD patient cells, and previous studies indicating the importance of HCS in the biotinylation of histones (Narang *et al.*, 2004), the biotinylation status of histones from the MCD patient cell lines was examined. I predicted that histones from MCD patients would contain less biotin than wildtype cells, due to the lack of HCS activity. Analysis of histone extracts by streptavidin blotting (figure 5.17) showed no detectable differences in biotinylation status between wildtype and HCS-L216R fibroblast histone extracts, as judged by streptavidin blotting.

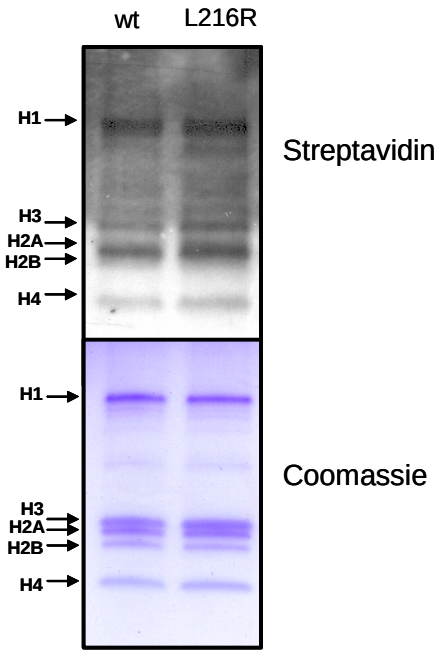

Figure 5-17 Biotinylation of histones in wildtype vs HCS-L216R fibroblasts.

5 μg of histone proteins were separated by SDS-PAGE.
Upper panel – Western Blot with streptavidin-HRP.
Lower panel – Coomassie stained gel confirming equal loading of samples. Positions of histone proteins are indicated by arrows.

5.4 Discussion

5.4.1 Effect of HCS-L216R on cellular proliferation: examining the non-biotin responsive phenotype of patient cells

Initial experiments showed that the MCD patient cells had a significantly reduced proliferation capacity compared to wildtype cells when grown in standard media (DMEM + 10% fetal calf serum, Figure 5.5). It is widely accepted that this media contains approximately 10 nM biotin (from the serum component), which is already much higher than the reported serum concentrations of biotin in humans of 0.24 nM (Mock *et al.*, 1995).

Subsequently, growth in biotin-deficient media was trialled. In the wildtype cells there was a significant decrease in proliferation (figure 5.7 and 5.8) in biotin-deficient media. There are mixed reports in the literature on the effects of biotin availability on cellular proliferation. No effects of low biotin (<0.2 nM) or high biotin (10 μM) were seen on cultured outer root sheath cells from human hair follicles, contrary to anecdotal evidence suggesting beneficial effects of biotin on hair and nail condition (Limat *et al.*, 1996). Similarly, there was no effect on proliferation of NCI-H69 small cell lung cancer cells grown in low (25 pM), physiological (250 pM) or pharmacological (10 nM) biotin containing media (Scheerger and Zempleni, 2003). Crisp and colleagues (2004) found that proliferation of JAr carcinoma cells showed a modest response to biotin levels, with proliferation decreased to 70% that of controls in biotin-deficient media (25 pM vs 250 pM). Proliferation increased 161% when cells were grown in high biotin (10 nM) media (Crisp *et al.*, 2004). Conversely, despite lymphocytes *in vitro* showing increased biotin uptake early in the cell cycle in response to proliferation (Stanley *et al.*, 2002), *in vivo* biotin supplementation in humans (resulting in plasma biotin levels 7.4 times higher than controls) led to a decrease in lymphocyte proliferation, postulated to be due to interference of cellular uptake of pantothenic acid through the Sodium-Dependent

Multivitamin Transporter (SMVT). Pantothenic acid is also required for cellular proliferation (Zempleni *et al.*, 2001). The present study suggests that biotin deficiency does reduce cellular proliferation, which is consistent with the essential role of ACC in fatty acid synthesis required for membrane biogenesis. However, increasing biotin concentration did not appear to significantly increase proliferation rates unless at extremely high (and clinically impossible to achieve) levels of 1 mM (Figure 5.8).

Both MCD cell lines tested showed little effect of biotin on proliferation. There was no significant difference between cells grown in complete or biotin deficient media (measuring either total cell number or metabolic capacity as indicators of proliferation) (Figure 5.7). Proliferation rate of these cells could not be increased to wildtype levels even at exceedingly high biotin concentrations (Figure 5.8). However, some increases in proliferation were seen, suggesting that there is perhaps a very basal level of HCS activity in these cells which can respond to biotin, but not in a way that can restore proliferation to that of controls. This is consistent with previous reports measuring effects of HCS deficiency such as PCC activity in MCD patient cells with N-terminal domain mutations. In the study by Sakamoto and colleagues (1999) MCD lymphoblasts and fibroblasts containing the R183P and L237P mutations had severely compromised PCC activity (<10% controls). This activity could not be restored even at 100 μM biotin. R183P-HCS, which has a higher V_{max} than L237P, was able to restore PCC activity to 65% controls at the highest biotin concentration, whilst L237P-HCS was able to only increase activity to 20% that of controls at 100 μM biotin. A similar result was confirmed in a separate study, where PCC activity could not be restored to normal levels even at 50 μM biotin in L237P-HCS cells (Aoki *et al.*, 1997). This is in contrast to the G581S mutant tested in the Sakamoto study, where PCC activity was <10% in the basal low biotin media but could be completely restored to full activity at high levels of biotin. This agrees with the elevated K_M for biotin of this mutant. It would be interesting to examine the proliferation response of a K_M mutant in the assay used in the present study. One would predict that proliferation

would be restored to control levels at high biotin concentrations, in contrast to the results seen with the L216R fibroblasts.

The curious result from this study was the ability of the L216R cells to proliferate at all, given the complete lack of activity of this mutant, and the presumably critical role of HCS in cellular viability. To date there are no reports of HCS knock-out mice in the literature. Knock outs of ACC1 are embryonic lethal in mice, Arabidopsis and yeast. (Abu-Elheiga *et al.*, 2005, Baud *et al.*, 2003, Hasslacher *et al.*, 1993). However, most cells grown in culture derive most of their lipid requirement from serum in the media and have a reduced requirement for endogenous fatty acid biosynthesis, and therefore ACC and HCS activity (Jacobs *et al.*, 1973). Skin fibroblasts grown in media composed of 15% lipid-deficient FCS showed 70-80% increased ACC activity compared to growth in 15% normal FCS. (Jacobs *et al.*, 1973). Addition of free fatty acids palmitic acid, stearic acid, oleic acid or arachidonic acid all were able to block this increase in ACC activity. I would predict that MCD cells would be non-viable in a chemically-defined lipid free media. It would be interesting to examine the effect of fatty acid supplementation on these cell's growth, and ability to bypass the critical role of HCS. This also helps explain why this mutation is not always lethal *in utero*, as most fatty acids required during foetal development are maternally derived (Larque *et al.*, 2002).

5.4.2 Expression, production, activity and localisation of HCS-L216R

Genotype analysis shows that the two patients in this study were homozygous for the L216R mutation, the most pathologically severe form of MCD so far identified.

Mutations can affect the way mRNAs are edited, i.e. where mutations can introduce or alter splicing sites resulting in exon skipping or creation of cryptic splice sites. Such is the case with the mutation 1519+5G>A (IVS10+5G>A), a commonly occurring HCS allele in the Faroese population, and present in a number of European cases of MCD. This

mutation occurs at +5 of a splice donor site in intron 10 of the HCS gene, leading to skipping of exon 10 resulting in a frameshift and premature termination of the protein, lacking the entire catalytic domain. mRNA analysis of these patients showed that both normally and abnormally spliced mRNA's were produced, resulting in patients who remain asymptomatic for many years due to the activity of the HCS translated from the normally spliced mRNA (Sakamoto *et al.*, 2000). The L216R mutation (caused by a T647→G mutation) occurs in the centre of exon 7 (translation begins in exon 6), and the position of the mutation is not at a potential splicing site (Suzuki *et al.*, 2005). mRNA analysis by RT-PCR showed no discernible effect on expression of HCS mRNA.

Both protein and activity are compromised by the L216R substitution.

Endogenous levels of HCS are low in the cell (discussed in section 4.4), so to detect endogenous amounts of HCS biotinylated N2 antibody was used to probe whole cell extracts. Full length HCS was undetectable in the patient cell lines (Figure 5.10). This led to the subsequent investigations into protein stability. Endogenous HCS activity was barely detectable in both patient cell lines. As protein could not be detected in either patient cell line, activity of HCS-L216R overexpressed in CHO AA8 cells was also measured. Western Blot analysis showed that the protein was expressed and produced the three isoforms detected by the N2 antibody characterised in Chapter 3. Similar results have been seen in previous studies where HCS mutants have been overexpressed to assay activity (Aoki *et al.*, 1997, Aoki *et al.*, 1999). In these previous studies none of the point mutations tested resulted in altered levels or size of protein detected by Western Blotting. In the present study, there was consistently a lower amount of HCS-L216R expressed as detected by Western blot, but this was not quantified by using an internal transfection control.

The activity of the HCS-L216R enzyme could not be detected (over controls), either in MCD fibroblast cell lysates or when overexpressed. This is consistent with previous

reports showing the severe effect of this mutation on enzyme activity. In a previous study by Dupuis and colleagues, a number of HCS mutants were overexpressed and HCS activity measured by ^{3}H biotin incorporation onto BCCP substrate. The L216R mutation showed no detectable activity, but in that case expression of the protein had not been confirmed (Dupuis *et al.*, 1999). A similar study also showed that the L216R mutant had the lowest activity of all mutants tested (0.3% activity compared to wildtype) (Sakamoto *et al.*, 1999).

Whilst the localisation of HCS remains controversial, my studies have consistently shown a predominantly cytoplasmic localisation. It would be expected that if this particular mutation caused protein misfolding it may be possible to see an alteration of subcellular localisation as the proteins accumulate in the ER or are targeted for degradation in the proteasome. Alternatively, mutations in this region of the protein may interfere with protein-protein interactions mediating localisation. GFP labelling of L216R and overexpression in the same system employed in Chapter 5 showed there was no significant difference in subcellular localisation of this mutant. HCS-L216R showed a similar cytosolic pattern to the wildtype enzyme.

Together these results indicate that the L216R mutation does not affect expression of the HCS gene or localisation of the protein. Overexpression studies show that the protein can be translated and processed to similarly sized wildtype isoforms, although full length protein can not be detected in patient cells. The L216R mutation renders the protein catalytically inactive.

Initial results obtained with preliminary investigations into biotinylation of histones in HCS-L216R fibroblasts were quite surprising. Previous reports have indicated the critical role of HCS in biotinylation of histones by examination of histones from HCS-deficient MCD

cells (Narang *et al.*, 2004). Further analysis of biotinylation of histones is examined and discussed in the following chapter.

5.4.3 Reduced stability of HCS-L216R : a possible mechanism for disease severity

Increased turnover of HCS in MCD patients was first hypothesized by Suormala and colleagues in 1997, after examination of a patient who showed a normal K_M for biotin but greatly reduced V_{max} consistent with an N-terminal mutation (the genotype of the patient was not examined). However, there have been no quantitative data reported to test this hypothesis. Examination of the relative half-lives of wild type and mutant HLCS using the tetracycline-repressible expression system confirmed the reduced stability of the p.L216R protein in cultured cells.

Previously, limited work on the stability of HCS activity in MCD patient fibroblasts has been reported. In an early study, a patient with the HCS exhibiting a K_M for biotin similar to wildtype, but with a reduced V_{max} (patient MC, genotype not specified (Burri *et al.*, 1985)), HCS activity was more heat labile when tested at 48°C. This contrasted with patient JR (shown in a later study to contain the active site mutation R508W), where K_M was elevated and HCS activity was actually more stable at 48°C compared to controls (Burri *et al.*, 1985). These data indicated that MCD mutations can cause structural perturbations affecting enzyme stability. There have been several mutations in BirA identified in temperature-sensitive *E.coli* strains which result in decreased protein stability (Wilson *et al.*, 1992). These include V83G and I207S, both of which are shielded from solvent in the protein core. Interestingly, Arg^{235} is implicated in decreasing protein stability, as mutations at this residue disrupt a salt bridge between Arg^{235} and Glu^{110}. The analogous residue in HCS, Asp^{634}, is also a mutant MCD allele.

To date, no investigations into the regulation of HCS stability and turnover in mammalian cells have been performed. The only investigation into the half-life of any of the biotin protein ligases was a by-product of a recent large-scale study examining the half life of more than 3,750 proteins of the budding yeast proteome. These authors calculated a half life for BPL1 (yeast BPL) at 23 minutes (Belle *et al.*, 2006). However, the authors of this study caution against interpreting individual protein measurements due to experimental errors in the data. In this study, we were able to compare relative stability between wildtype and mutant HCS proteins. The absolute half-life of the endogenous protein may not agree with the value obtained here, due to overexpression of the protein and consequent flooding of the degradation machinery. Optimally, a metabolic pulse-chase labelling experiment would provide more accurate information on the turnover of endogenous protein levels. However this approach required immunoprecipitation with high affinity antibodies which were unavailable. Alternatively, the Tet-Off system has been used for estimations of protein half-life where suitable immunoprecipitating antibodies are unavailable (Gao *et al.*, 2002).

It perhaps should not be surprising that the substitution of the hydrophobic, non-polar leucine residue by a strongly basic, positively charged hydrophilic arginine residue at position 216, in the critical domain III region of the N-terminus of HCS, would cause disruption to the protein's structure, rendering it more susceptible to degradation. The transfections showed that the HCS-L216R protein can be expressed, and a similar pattern (doublet at 81kDa and lower 76 kDa band) was observed, indicating that the processing necessary to obtain these isoforms was unaffected, although the 76 kDa isoform is less prevalent in the L216R mutant.

A molecular explanation for the role of L216R in catalysis has been proposed from truncation analysis of HCS (Campeau and Gravel, 2001). Mutant HCS N-terminal deletions up to L166 were able to complement conditional lethal birA strains of *E. coli* (see

figure 1.9A). Of particular significance were HCS mutants with deletions to Ala^{235} or Thr^{266}, which were inactive or only weakly active, whereas further deletions up to Lys^{378} restored activity. Deletions into the catalytic domain (up to Leu^{460} or Pro^{569}) were inactive as expected. This indicates that the region between Leu^{166} and Arg^{290} may interact with the catalytic domain, and that deleting this region impeded the reaction (Campeau and Gravel, 2001). This is consistent with the results seen previously in previous domain mapping of HCS in our laboratory (see figure 1.9B) (Swift et al., 2004), and this study, where the L216R mutation resulted in compromised enzyme activity and reduced stability.

The work described in this chapter aids in explaining the clinical findings whereby the patients are extremely unstable biochemically, respond only moderately to high doses of biotin and, if they survive the neonatal period, are prone to recurrent episodes of metabolic decompensation during times of intercurrent illness and increased demands on the biotin cycle.

Erratum

The HFF fetal foreskin fibroblasts employed here were obtained from a neonatal male. Great care was taken to ensure that the passage-number of all primary cell lines (control and patient lines) was kept as low as reasonably possible, no experiments were carried out on cell lines past passage 20. Whilst it would be optimal to have several control lines for comparison this was not feasible in the project undertaken due to lack of available cell lines.

I also agree with the reviewer that full genomic sequencing would be optimal to confirm patient genotypes. The reviewer states that semi quantitative RT-PCR was not an adequate method and that qPCR should have been employed. Q-PCR is a more quantitative method, however the time and resources to invest in setting up this Q-PCR (not used in our laboratory at the time) would have been proportionately too great an investment for the result obtained.

The reviewer asks for clarification of figure 5.12 and details of the transfection process, which are outlined on p141 (5.2.6.2). Cells were transfected, left for 48 hours in transfection medium (no DOX), before the media was replaced with fresh media containing varying concentrations of DOX.

Artefactual detection of biotin on histones with streptavidin

6 Artefactual detection of biotin on histones with streptavidin

6.1 Background

There are five classes of histones, H1, H2A, H2B, H3 and H4, which mediate the packaging of DNA into chromatin. An octamer of core histones consisting of a H3-H3-H4-H4 tetramer and two H2A-H2B dimers form the nucleosomal core particle around which DNA is wrapped. Histone H1 then functions as a linker connecting nucleosomes. There are many post-translational modifications made to histone proteins, collectively known as the "histone code" (Strahl and Allis, 2000, Jenuwein and Allis, 2001). The type of modifications, and the interplay of these modifications, has an important impact on chromatin architecture, and hence the accessibility of DNA for replication, repair or transcription.

It has been reported that biotin is attached to all classes of histone proteins (Hymes *et al.*, 1995, Stanley *et al.*, 2001). Both holocarboxylase synthetase and biotinidase have been implicated in this process, although the biological significance of such a modification remains unclear. The detection of biotin on molecules is greatly facilitated by the wide variety of (strept)avidin-based technologies exploiting the extremely strong non-covalent interaction of (strept)avidin for biotin, with a Ka of 10^{15} M. Streptavidin is widely used as it has several advantages over avidin. Avidin is a heavily glycosylated protein, rich in basic residues with a pI around 10. This is in comparison to streptavidin which contains no carbohydrate and has a lower pI of 7. Streptavidin is employed in many biotin detection studies as it shows lower background binding to other cellular components compared to avidin (Diamandis and Christopoulos, 1991). Hence, many studies examining biotinylation of histones have employed detection with streptavidin (Stanley *et al.*, 2001, Manthey *et*

al., 2002, Peters *et al.*, 2002, Camporeale *et al.*, 2004, Crisp *et al.*, 2004, Landenberger *et al.*, 2004, Kobza *et al.*, 2005, Kothapalli *et al.*, 2005, Camporeale *et al.*, 2006, Chew *et al.*, 2006, Camporeale *et al.*, 2007). In this chapter I show that the binding of streptavidin to histones appears to occur independently of the biotin-binding site on streptavidin. Hence, caution should be used when employing a streptavidin-based detection system to infer biotinylation.

6.2 Specific materials and methods

6.2.1 Histone extraction

Histone extracts were prepared from 293T, HeLa or HepG2 cells as described in (Stanley *et al.*, 2001), with the following modifications to reduce carry through of labelled biotin in the procedure. After acid extraction, histones were precipitated with TCA and washed twice in acidified acetone (0.1% HCl) and then twice in acetone. Precipitated histones were reconstituted in water, and protein concentration assessed by BCA assay (Pierce, Rockford, IL, USA) using commercially available histones (from calf thymus) as a standard.

6.2.2 Biotinylation of yPC-104 domain

The apo-biotin domain consisting of the C-terminal 104 amino acids of yeast PC (yPC-104) was purified as described previously (Val *et al.*, 1995). For biotinylation with ^{14}C-biotin an in vitro biotinylation reaction using recombinant yeast BPL (Polyak *et al.*, 1999) was performed overnight at 37°C in a 100 μL reaction mix containing 7 μM (20 μg) apo-yPC104, 50 mM Tris pH 8.0, 3 mM ATP, 5.5 mM $MgCl_2$, 0.1 mg/mL BSA, 0.1 μM DTT, 10 μM ^{14}C biotin and 3.4 nM yeast BPL.

6.3 Results

6.3.1 Biotinylation of carboxylases was sensitive to biotin availability but biotinylation of histones was not.

Cells were cultured in complete or biotin-deficient media as described in Chapter 5 (section 5.2.4). To examine whether both the biotin-carboxylases and histones were sensitive to biotin availability, cells were passaged five times over 3 weeks in complete media or biotin-deficient media. Biotin deficiency caused severe effects on cellular morphology and viability with increased numbers of rounded and detached cells, readily observable after two weeks (figure 6.1A). Proliferation rates, as determined by cell counting through the time course, were also reduced with the treatment (data not shown).

Streptavidin blot analysis of whole cell lysates from 293T cells revealed that at the end of the three week biotin starvation period, biotinylation of PC, PCC and MCC was abolished (figure 6.1B). ACC was not detected in the conditions used here. Importantly, the presence of apo-PC protein was confirmed by Western Blot (figure 6.1B, lower panel). Thus, the reduced biotinylation status of carboxylases in the biotin-deficient cells was due to a reduction in the biotinylation of PC, not decreased PC protein expression.

Histones were extracted from 293T cells grown under these conditions and analysed by streptavidin blot. In contrast to the biotin carboxylases, the amount of streptavidin reactive material on histones was not affected by biotin starvation (figure 6.1C). Streptavidin binding was observed equally to all classes of histones extracted under all growth conditions. SDS-PAGE analysis confirmed equal loading of samples. These experiments were all repeated with HeLa and HepG2 cells with both cell lines producing the same results (data not shown).

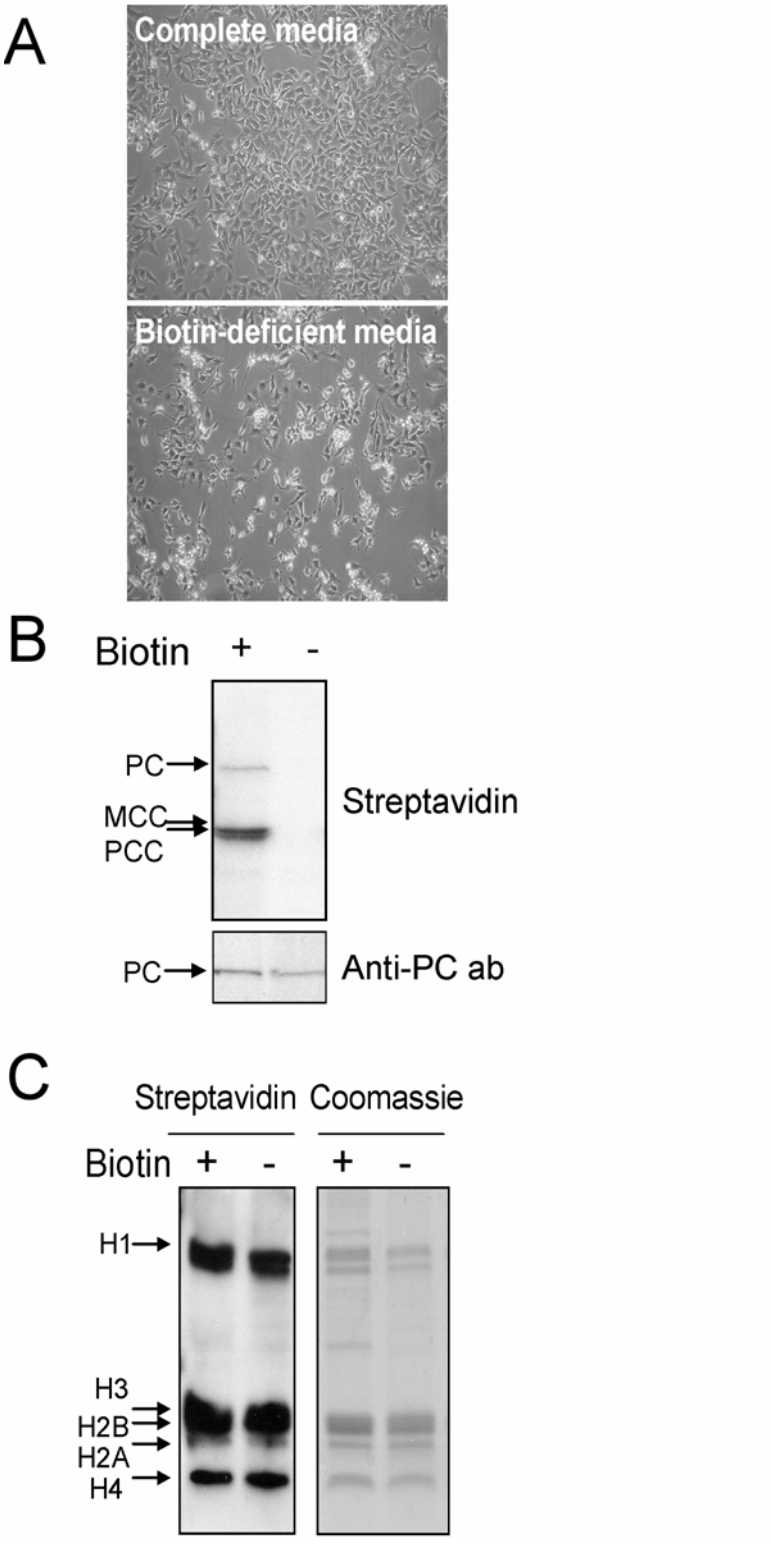

Figure 6-1 Biotinylation of carboxylases was sensitive to biotin availability but biotinylation of histones was not in several cell lines. Cells were cultured in complete media (+) or biotin-deficient media (-).
(A) Reduced cellular proliferation and changes to cellular morphology after growth in biotin deficient media for two weeks (HeLa cells, 100X magnification).
(B) Detection of biotinylated carboxylases in lysates from 293T cells. PC (120 kDa) and the alpha subunits of MCC and PCC which co-migrate as a doublet at ~80 kDa were detected by probing with streptavidin-HRP. Detection of total PC protein was determined by anti-PC antibody blot.
(C) Detection of biotinylated histones in 293T cells cultured as above. A Coomassie-stained gel (right) acts as a loading control.

6.3.2 Streptavidin interacts with histones independent of the biotin binding site of the streptavidin.

To address whether the interaction between streptavidin and biotin was indeed dependent upon biotin, a biotin-blocking experiment was performed. Commercially available calf thymus histones, histones from 293T cells and the biotinylated PC were resolved by SDS-PAGE together with biotinylated protein molecular weight markers. These proteins were then transferred to nitrocellulose and probed with either non-treated or biotin-treated streptavidin. When blocked with free biotin, the streptavidin failed to bind to the biotinylated markers and to biotinylated PC protein. However, binding to histones was unaffected (see figure 6.2A). The non-specific interaction of streptavidin with histones was further confirmed by dot-blot analysis (figure 6.2B). The biotin domain of yeast PC (holo-yPC104, *Mr* 11322 Da) was chosen due to the similar molecular mass of histone proteins. Furthermore, we have previously reported the isolation of the biotinylated domain and confirmed by mass spectroscopy that one molecule of biotin is attached per protein molecule (Val *et al.*, 1995, Polyak *et al.*, 1999). 500 ng of holo-yPC104 or 500 ng histones were spotted onto nitrocellulose and probed with streptavidin pre-treated with increasing amounts of free biotin. As expected, free biotin reduced streptavidin binding to holo-yPC104 in a concentration-dependent manner. Conversely, there was no effect of biotin concentration on binding of streptavidin to histones. Quantification of dot blot intensity (Figure 6.2C) confirmed that pre-blocking streptavidin with increasing concentrations of biotin inhibited binding to holo-yPC104 but had no effect on binding to histones.

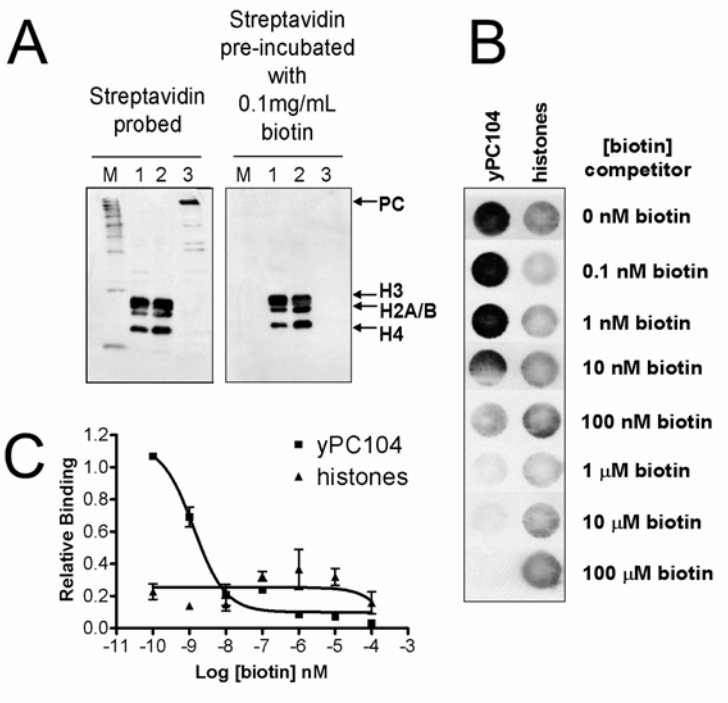

Figure 6-2 Streptavidin interacts with histones independently of the biotin binding site of streptavidin.

(A) Western Blot probed with streptavidin-HRP (left) or streptavidin-HRP pre-incubated with 0.1mg/mL biotin (right). Lane M, Biotinylated protein marker; Lane 1, 5 μg histones from 293T cells; Lane 2, 5 μg calf thymus histones; Lane 3, recombinant yeast PC.
(B) Dot Blot of 500 ng yeast PC biotin domain (yPC-104) or 500 ng calf thymus histones probed with streptavidin-HRP pre-incubated with varying amounts of biotin as indicated. (C) Densitometry was performed on dot blots and graphed showing the summary of results of three experiments. Results are plotted as mean (relative to holo-yPC104 binding) ± SEM.

6.3.3 ^{14}C biotin fails to be incorporated onto histone proteins but is incorporated into carboxylase proteins.

The data above demonstrated that streptavidin binding to histones was occurring independently of biotin. In order to ascertain the biotinylation status of histones, alternative methodologies were required that did not involve streptavidin. Western analysis, using anti-biotin antibodies or avidin-HRP, were attempted but the sensitivity here was at least 20-fold lower than the Streptavidin-blot and could not readily detect histone proteins (data not shown). However, incorporation of radiolabelled biotin and phosphorimager analysis did produce better sensitivity than the Streptavidin blot. Whole cell extracts and histones

were prepared from 293T cells that were passaged five times during three weeks, cultured in either complete media or biotin-deficient media supplemented with ^{14}C-biotin as the sole biotin source. Biotinylation of carboxylases was confirmed by streptavidin blotting (Figure 6.3A) and incorporation of labelled biotin (Figure 6.3A, right panel lane labelled ^{14}C). As observed previously, histone extracts showed a strong signal when probed with streptavidin (Figure 6.3B). Even when histones were overloaded onto the gel to increase the likelihood of detection using the ^{14}C label, there was no evidence of attachment of labelled biotin onto histone proteins. As a positive control for detection of biotinylated proteins, a serial dilution of ^{14}C-holo-yPC104 was analysed on the same blot with the histone extracts. The PhosphorImager detection was more sensitive than the streptavidin blot, and shown to be capable of measuring 1 pmol of protein-bound biotin (15 ng of holo-yPC104, equal to 1 pmol protein). There is a 1:1 stoichiometry of biotin to yPC104 biotin domain. Hence, 50 μg histones failed to incorporate more than 1 pmol of C^{14} biotin over the time-course. Assuming that the 50 μg extract contained equal ratios of histone proteins (i.e. 10 μg each of H1, H2A, H2B, H3 and H4), this is equivalent to a total of ~3 nM of histones. As the threshold of detection was 1 pmol of biotin, this indicates that biotinylation of histones is a very rare event. Here, this represents <0.03% of histones modified by radio-labelled biotin in this analysis. Liquid scintillation counting of histone extracts also showed no difference between histone extracts prepared from normal or ^{14}C-biotin labelled media (data not shown).

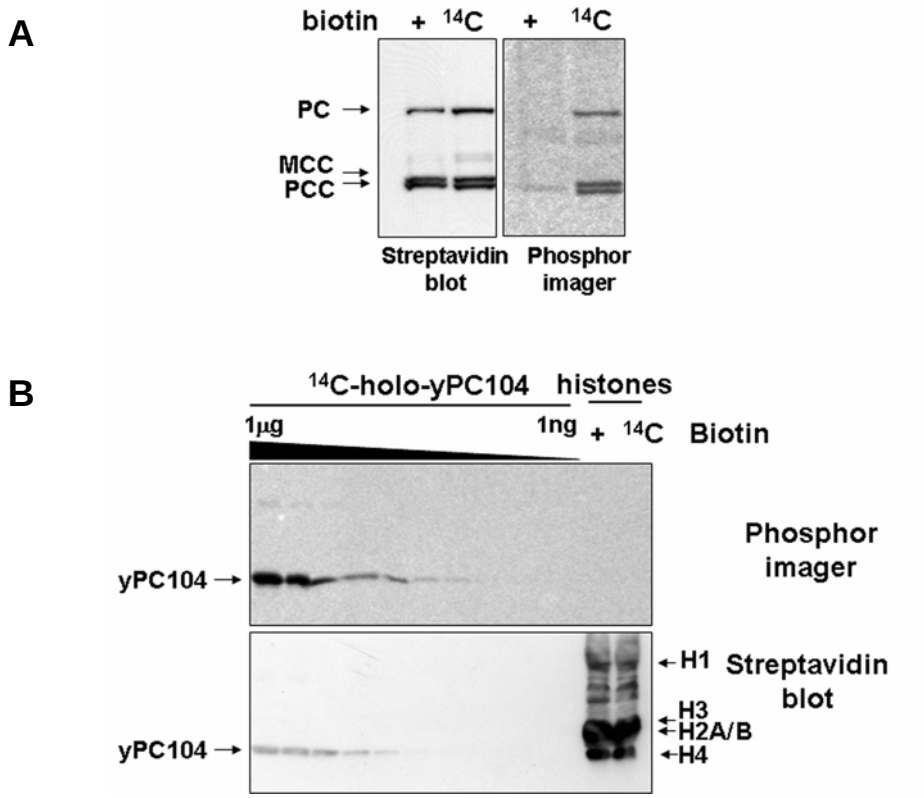

Figure 6-3 ^{14}C biotin fails to be incorporated onto histone proteins but is incorporated onto carboxylase proteins.

(A) Carboxylases were isolated from lysates of 293T cells grown for three weeks in complete media (+) or biotin-deficient media containing 100 nM ^{14}C biotin (^{14}C). Biotinylated carboxylases were visualised by Western blotting with streptavidin-HRP (left panel). Incorporation of labelled biotin was confirmed by PhosphorImaging (right panel).
(B) Histones were purified from 293T cells grown under identical conditions to (A), and 50 µg histones separated by SDS-PAGE. Streptavidin binding was observed on all classes of histones by Western Blotting (lower panel) but there was no detection of incorporated ^{14}C biotin onto histones (upper panel). A standard curve showing a serial (1:2) dilution of holo-^{14}C-yPC104 (1 µg to 1 ng) was a positive control for detection of ^{14} C label showing a detection limit of 1 pmol of C^{14} biotin (15.6 ng holo-^{14}C-yPC104).

6.4 Discussion

Early investigations into the localisation of biotin observed that the vitamin is found not only in the cytoplasm and mitochondria associated with biotin-dependent carboxylases, but also within the nucleus. Dakshinamurti and Mistry were the first to report biotin in the nucleus when they injected both rats and chicks with radio-labelled biotin and analysed cellular fractions (Dakshinamurti and Mistry, 1963b). The study found that 23% of observed radioactivity in chick livers was nuclear, 29% was associated with the

mitochondria and 40% in the cytosolic fraction. For rats, the results were similar, with 15% of radioactivity being nuclear, 18% mitochondrial and 53% being cytoplasmic. Following this, Petrelli *et al* also examined rat liver tissue for subcellular localisation of biotin (Petrelli *et al.*, 1979). In direct contrast to the report by Dakshinamurti and Mistry, Petrelli *et al* found the vast majority of biotin in rat tissue was cytosolic (91%) or mitochondrial (3.54%). The proportion of biotin observed in the nuclei of rats was only 0.30%. The differences in nuclear localisation of biotin observed by these two groups may be due to the different methods of cellular fractionation used. Dakshinamurti and Mistry washed the isolated nuclei from rat livers 12 times, thereby decreasing the radioactivity from 15.1% to 0.1%. This suggests that the high proportion of radioactivity initially observed in the nuclear fraction was due to contamination of the nuclei with cytosol, which was subsequently removed by thorough washing. A more recent analysis of cellular distribution of biotin (Stanley *et al.*, 2001) agrees that only 1% of total biotin is nuclear. The data from the current study also implies that the amount of biotin attached to histones from cultured cells is low, below the threshold of our radio-labelling system (1 pmol protein-bound biotin).

The first reports of histones being the site of biotin attachment appeared over ten years ago (Hymes *et al.*, 1995). Since then there have been numerous reports investigating this addition to histone modifications. However, in order to detect small amounts of nuclear biotin, sensitive detection techniques have been required. Streptavidin blotting has been the technique of choice in the majority of studies. Recent studies have employed anti-biotin antibodies to show incorporation of biotin onto histones. Furthermore, several specific anti-biotinylated histone antibodies have been generated in an attempt to precisely define the biotinylation sites (Camporeale *et al.*, 2004, Kobza *et al.*, 2005, Chew *et al.*, 2006). In light of the data presented here, further analysis of histone biotinylation should proceed with the alternative immunochemical techniques. Standard streptavidin-biotin techniques should be avoided when assessing biotinylation status. Ideally, studies

determining the site of biotinylation of histones in vivo, using a “top down” approach should precede using methods that do not rely on secondary detection systems. For example mass spectrometry would be a powerful tool for providing evidence of histone biotinylation.

Whilst detection of biotin using streptavidin probes indicates that all classes of histones contain biotin (Stanley *et al.*, 2001) only recently have studies been aimed at determining specific sites of biotinylation. These studies have all been based on the *in vitro* biotinylation of synthetic peptides representing histone N- or C-terminal tails by human serum (as a source of biotinidase) and biocytin. Peptides were then resolved by electrophoresis and probed with streptavidin to monitor biotinylation (Chew *et al.*, 2006, Kothapalli *et al.*, 2005, Camporeale *et al.*, 2004). Whilst these studies have provided evidence for biotinylation sites mediated by biotinidase in vivo through the production of modification specific antibodies, HCS has also been shown to be responsible for histone biotinylation (Narang *et al.*, 2004). Whether HCS has similar or distinct biotinylation sites to biotinidase remains to be determined.

The incorporation of radio-labelled substrates is one of the classical methods for analysing histone modifications (Villar-Garea and Imhof, 2006). It also provides an alternative to using streptavidin for investigating biotinylation. There have been very few studies where this technique has been employed to investigate histone biotinylation in cell culture or animal systems. Narang and co-workers (Narang *et al.*, 2004) showed incorporation of ^{14}C biotin onto calf thymus histones in vitro using recombinant HCS. However the specificity of HCS under in vitro conditions should be considered as it has been shown that *E. coli* biotin protein ligase is capable of biotinylating non-natural substrates, such as BSA (Choi-Rhee *et al.*, 2004). In the present study incorporation of labelled biotin onto histones in cell culture was undetectable despite passaging cells in culture five times over three weeks with ^{14}C biotin as the only source of biotin. It seems unlikely after multiple cycles of

cell proliferation that biotinylated proteins would not incorporate the radio-labelled factor. Indeed, under these conditions the biotin-carboxylases were readily modified with the label. However, histone biotinylation could not be detected by liquid scintillation or PhosphorImager analysis, sensitive to 1 pmol of ^{14}C-biotin. In the work of Stanley and co-workers (2001), incorporation of ^{3}H labelled biotin onto the histones of peripheral blood mononuclear cells was measured by liquid scintillation counting of histone extracts. In the current study the protocol for histone extraction was similar to that of Stanley *et al.*, 2001, with modification of a trichloroacetic acid precipitation step and acetone wash after histone extraction. As an increased uptake of labelled biotin in proliferating cells has been reported (Stanley *et al.*, 2002), this additional clean up step reduces the likelihood of carry through of labelled biotin in contaminating cytosol from cells. Whilst modest increases in radiolabel were observed in the histone extracts in the Stanley study, it was not specifically shown that this was due to incorporation directly onto histone proteins.

The mechanism by which streptavidin interacts independently of biotin with histones is unknown. A number of non-biotinylated peptides that bind to streptavidin have been identified by phage display (Devlin *et al.*, 1990, Lam *et al.*, 1991). A clear consensus sequence of His-Pro-Gln (to a lesser extent His-Pro-Met) was observed in all isolated streptavidin binding peptides. These peptides have been used as so called “Strep-tags” (AWR**HPQ**FGG and NWS**HPQ**FEK) to assist in protein purification (see review, Skerra and Schmidt, 1999). Murine prion protein 90-231 has also been shown to bind to streptavidin, which is mediated by a minimal peptide substrate THNQWNKP, lacking the His-Pro sequence critical in the peptides isolated by phage display (Boetel *et al.*, 2006). The nano-tag, another streptavidin binding peptide (fMDVEAWL) has also been used as a tag for protein purification (Lamla and Erdmann, 2004). The mechanism of prion peptide binding to streptavidin is unknown, however in all these cases the binding of the peptide to streptavidin can be competed with biotin, indicating that the biotin binding site is involved in the interaction, as has been shown in crystallographic studies of strep-tag and nano-tag

binding to streptavidin (Schmidt *et al.*, 1996, Perbandt *et al.*, 2007). Sequence analysis of histones showed no clearly defined conserved motifs between all classes of histones that would account for streptavidin binding, and histones contain very few histidine residues which are critical for “strep-tag” binding. The binding site and mechanism of the interaction of streptavidin with histones is yet to be determined.

In studies examining the effect of biotin availability in histone biotinylation, the extent of histone biotinylation has been monitored by streptavidin blotting (Manthey *et al.*, 2002, Landenberger *et al.*, 2004, Crisp *et al.*, 2004). In all these cases there were no visibly significant differences in the amount of “histone biotinylation” observed. The results of the present study indicate that the use of streptavidin for probing the dynamics of biotin transfer on and off histone proteins is not a suitable method as streptavidin appears to bind independently of biotin. Similarly, studies examining the response of histone biotinylation to stimuli such as UV irradiation (Peters *et al.*, 2002) also employed streptavidin probing. Only moderate differences in the amount of streptavidin reactive material was observed under various experimental conditions. Our work indicates that caution should be shown when interpreting these studies given the non-specific interaction of streptavidin with histones.

Final Discussion

7 Final Discussion

A detailed discussion of results arising from each collection of experiments can be found at the conclusion of each chapter. In this section of the thesis I will highlight new findings with significance to this work, and discuss what future strategies may be useful to refine results in this study and answer some of the remaining questions surrounding HCS.

7.1 HCS structure

It is clear that the elucidation of an X-ray crystal structure will ultimately assist in understanding structure and function relationships in HCS, particularly the role of the N-terminal extension in catalysis. This study has shown how comparative analysis using structures of bacterial isozymes can provide an understanding of the effect of MCD-inducing point mutations on HCS structure and function. The recent structural analysis of the bacterial *Staphylococcus aureus* BPL by my colleague adds to the growing collection of known biotin ligase structures (Pendini *et al.*, 2008). However, a high-resolution structure of a large eukaryotic BPL has yet to be elucidated. One outcome arising from this knowledge can be in the development of new antipathogenic agents, such as anti-fungal therapies, using the BPL as a drug target. Rational drug design can be employed with structural biology to develop agents that target pathogen without inhibiting the host's BPL. This requires a detailed understanding of the structural similarities and differences and employing this knowledge towards a pathogen specific inhibitor.

One novel finding from these studies was the demonstration of an interaction between the N- and C-terminal halves of the HCS protein using yeast two hybrid experiments (refer to appendix A.1). Following this, it would be beneficial to map the site(s) of interaction by truncation and mutational analysis. This work is currently underway and initial results indicate that a minimal N-terminal fragment of HCS encompassing residues 159-314 is required for the intra-molecular interaction (personal communication, L.Mayende,

University of Adelaide, Australia). Mutational and structural studies are progressing. Together these data will be required in order to understand the catalytic mechanism of HCS at a molecular level.

7.2 HCS modifications

This work attempted to look for post-translational modification sites in HCS using mass spectrometry (Chapter 4). There are over 40 potential sites of phosphorylation in the HCS sequence (as analysed using the NetPhos algorithm at http://www.cbs.dtu.dk/services/NetPhos/), and there are unpublished reports of phosphorylation of tyrosines in the conserved ^{567}KWPNDIYY^{574} motif in HCS (personal communication, R.A. Gravel, University of Calgary, Canada). Analysis of peptides encompassing Tyr^{573} and Tyr^{574} by MALDI-MS in this study showed no mass change corresponding to phosphorylation (data not shown). However the Adelaide Proteomics Centre is currently validating a method for analysis of phosphopeptides from complex mixtures. This technique could be used in future studies of HCS modification. Western Blotting with phospho-specific antibodies, or SDS-PAGE analysis using a phospho-specific stain(s) could provide initial evidence. Analysis of factors affecting phosphorylation, and the role of phosphorylation (or other modifications) on enzyme activity, localisation, and interaction with substrates and, possibly, other protein binding partners is yet to commence.

7.3 HCS localisation and correlation with biological function

This study reported the successful generation of four affinity-purified polyclonal anti-HCS antibodies that detected HCS with high specificity. These provided valuable tools for a thorough investigation of the cellular localisation of HCS. By combining Western blot analysis and immunolocalisation with GFP reporter studies a clear relationship between HCS localisation and function was established. These experiments have helped to

address conflicting data in the literature. Unlike other immunolocalisation studies we have demonstrated that only a small fraction of HCS resides in the nucleus. In addition, we showed that histone biotinylation is a rare event, if it occurs at all. At the time of writing it has been over ten years since the initial description of biotinylation of histones, yet conclusive evidence in the form of mass spectrometry of native histones showing the appropriate mass shift is yet to be published. These two findings have forced reassessment of the mechanism of biotin-induced gene regulation. The proposal in the literature has been that global gene expression can be controlled by histone biotinylation. Alternative mechansims should now be considered. Here we can look to other systems. For example, recent analysis of the HCS1 and HCS2 genes in *Arabidopsis* has indicated that of the two identified HCS genes, only HCS1 is essential, and responsible for biotinylation of the biotin-dependent enzymes (Puyaubert *et al.*, 2008). HCS2 was postulated to be an inactive pseudogene in the *Arabidopsis* genome. This study showed that alternative splicing of the 5'-UTR of HCS1 resulted in a change in initiation of translation codon. This could help explain how the HCS1 protein is targeted to the three compartments of the plant cell, cytosol, mitochondria and plastid. The HCS1 sequence does not contain a known transit peptide sequence, and while Western Blot analysis by Puyaubert and colleagues showed that HCS1 was present in all three compartments, analysis of GFP constructs did not show mitochondrial localisation (Puyaubert *et al.*, 2008). They postulated that this may be due to lack of sensitivity of the GFP assay, inability to detect dual localisations of the protein (the most abundant localisation signal impeding detection of the minor locale) or lack of cis-acting elements needed for mitochondrial targeting. All the reasons cited above may also help to explain why lack of nuclear staining was observed in the GFP experiments reported in this study (Chapter 4).

In Puyaubert *et al.*, (2008) the authors also postulate that the HCS2 gene in plants may have a role as a non-transcribed RNA, controlling the stability of other RNA species. The

role of regulatory RNA species such as micro-RNAs in the regulation of gene expression by biotin have not been investigated, but it is possible that metabolites of biotin may interact directly with RNA to regulate activity. The mechanism by which biotin exerts its effects on transcription have been characterised in both prokaryotic and eukaryotic cells. There is a well described mechanism of transcriptional regulation by BirA (Beckett, 2007), and there has been a description of a biotin responsive element in the yeast genome vhr1p, which also requires the activity of the yeast BPL (Pirner and Stolz, 2006, Weider *et al.*, 2006). The yeast biotin responsive sequence (AATCA-N8-TGAYT) does not appear to function as a response element in the human genome, but at this stage no efforts have been made to elucidate whether a comparable mechanism occurs in mammals.

To date there have been no publications characterising factors which influence HCS expression, although it has been demonstrated that biotin availability affects transcription (Solorzano-Vargas *et al.*, 2002). Experiments such as promoter mapping, to test for cis-acting regulatory elements upstream of the HCS ORF using reporter-gene assay systems followed by chromatin immunoprecipitation assay (ChIP) to analyse for specific transcription factor binding, would help in answering this question. Two of the Sp/Kruppel-like factor family of transcription factors (Sp1 and Sp3) have been shown to respond to biotin levels (Griffin *et al.*, 2003). However it is not known if HCS itself is a target. Examination of the regulatory elements governing HCS expression will aid in understanding potential other roles of HCS in the cell. Similarly, analysing temporal and spatial expression of HCS mRNA during development, for example in a zebrafish model, may help determine the mechanism by which biotin deficiency is teratogenic in many species.

7.4 New directions for HCS deficiency-therapeutics

The work here has described a mechanism for reduced HCS activity in patients with the L216R-HCS mutation of MCD, due to increased turnover of the destabilised protein. This observation partially explains why these patients do not respond to biotin therapy. However, more work is required to identify new and better treatments. Future work in this area could involve the examination of nutritional supplementation. The addition of fatty acids may help overcome the cell's requirement of HCS (and subsequent ACC) activity. It is not clear whether supplementation with fatty acids to substitute for ACC activity and aspartate to substitute PC activity could be clinically useful for treatment in patients with the non-biotin responsive L216R mutation. Future work in this field could start with *in vitro* analysis of nutritional supplementation to the MCD fibroblast cell lines described here.

Another potential avenue for new therapeutics is small molecular chaperones. These function by increasing the half life of proteins that are otherwise unstable. This approach has been used to treat inherited enzyme disorders such as lysosomal storage disease (Fan, 2008). MCD may also be a candidate for this type of treatment, as only low levels of functional protein need to be restored to alleviate symptoms. Furthermore, examination of the structural properties of the N-terminus of HCS will greatly enhance our understanding of why this particular mutation is so deleterious. If the proposed N and C-terminal domain interaction ("cap") does indeed occur, it may be that the L216 residue is critical in that interaction, and thus a candidate for treatment with a site-specific pharmacological chaperone. Ultimately crystallographic studies of the entire HCS protein will be beneficial to examine why this mutation has such drastic effects on enzyme activity. Together this knowledge has the potential to provide new treatments for those patients who are poorly responsive to the only available current treatment, biotin therapy.

Appendices

Appendix 1 – Novel protein interactions of HCS

Protein "interaction traps" are useful to understand the biology of a particular protein of interest by examining the proteins with which it interacts. One initial aim of the work described in this thesis was to examine interactions between HCS and novel partner proteins. It was envisaged this would implicate HCS in novel cellular pathways, such as biotin-regulated gene expression or signal transduction. Specifically, this part of the study proposed that the N-terminal domain could mediate unique functions for HCS through specific protein-protein interactions. Here I employed two alternative techniques for identifying interacting proteins. Firstly, a Yeast Two-Hybrid assay, and secondly a unique promiscuous biotinylation approach.

A.1 Yeast Two-Hybrid approach

This study used the Matchmaker LexA based Yeast Two Hybrid system (Clontech). The bait protein consisted of the full length HCS protein, or an N-terminal fragment of HCS Met^{1}-Arg^{314} (nHCS) which was screened against a commercially available human liver cDNA library. Liver was chosen as this tissue is known to express HCS and is rich in biotin-dependent enzymes such as pyruvate carboxylase (Suzuki *et al.*, 1994). As a positive control the biotin domain of human PC was cloned into the prey plasmid. This has previously been shown in our laboratory to be biotinylated by HCS both *in vitro* and *in vivo.* As expected, the yeast two-hybrid system was indeed capable of detecting the protein:protein interaction between HCS and a biotin domain.

The Yeast Two-Hybrid system was optimised and several rounds of screening carried out. Unfortunately it was unsuccessful in isolating any novel protein interaction partners. This was primarily due to the poor quality of the cDNA used for constructing the library. Additionally, the Yeast Two-Hybrid assay was also used to examine the interaction of the N- and C-terminus of HCS. Yeast were co-transformed with nHCS (amino acids Met^{1}-

Arg^{314}) and cHCS (amino acids Met^{315}-Arg^{726}) and grown on selective media to test activation of reporter genes (kindly performed by Ms Lungisa Mayende, see figure A.1). There was strong activation of both reporters when yeast were co-transformed with bait plasmid pLexA(cHCS) and prey plasmid pB42AD(nHCS). However, this was not observed in the reciprocal screen where the bait and prey positions were reversed. This result is the first direct evidence to support an interaction between the two halves of HCS. This result is being further investigated in our laboratory by Ms Mayende as part of her doctoral project investigating the structure of HCS.

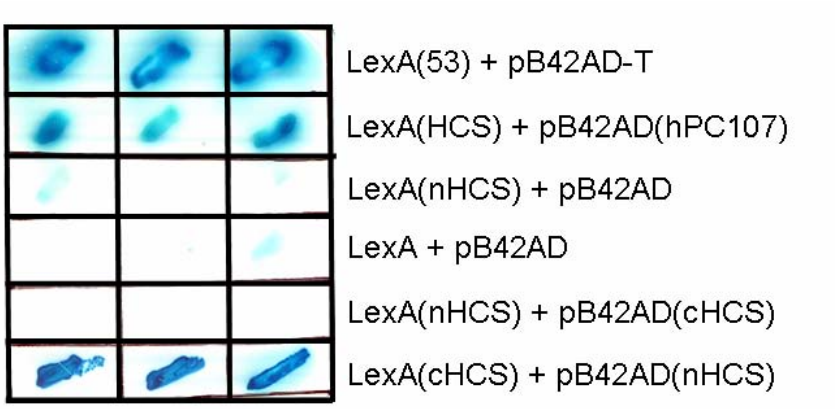

Figure A-1 Interaction of the N- and C-terminus of HCS as examined by yeast two hybrid assay.
Grid shows three independent clones plated on induction/selection media (galactose, -ura, -his, -trp, -LEU, +X-gal). Growth and blue colour indicates dual activation of LEU2 and LacZ reporter genes. Positive controls- row 1- interaction of p53 and T antigen, row 2- interaction of HCS and human PC biotin domain. Negative controls – Row 3 and 4. Experimental – rows 5 and 6 N- and C-terminal HCS.

A.2 Promiscuous biotinylation approach

Due to the inability of the Yeast Two Hybrid system to successfully isolate novel interacting partners of HCS an alternative approach was employed. This was based on the work of Choi-Ree et al, 2004, who first demonstrated that the BirA variant R118G exhibited a promiscuous biotinylation phenotype. In BirA, the side chain of the arginine at position 118 forms a salt bridge with the side chain of the aspartic acid at position 176 (in

the highly conserved KWPND motif), closing over the biotin binding site and sequestering the biotinyl-5'-AMP in the active site (figure A.2). Removal of the arginine side chain by replacement with a glycine abolishes this salt bridge, opening up the active site and increasing dissociation of the intermediate (Kwon and Beckett, 2002) (figure A.2).

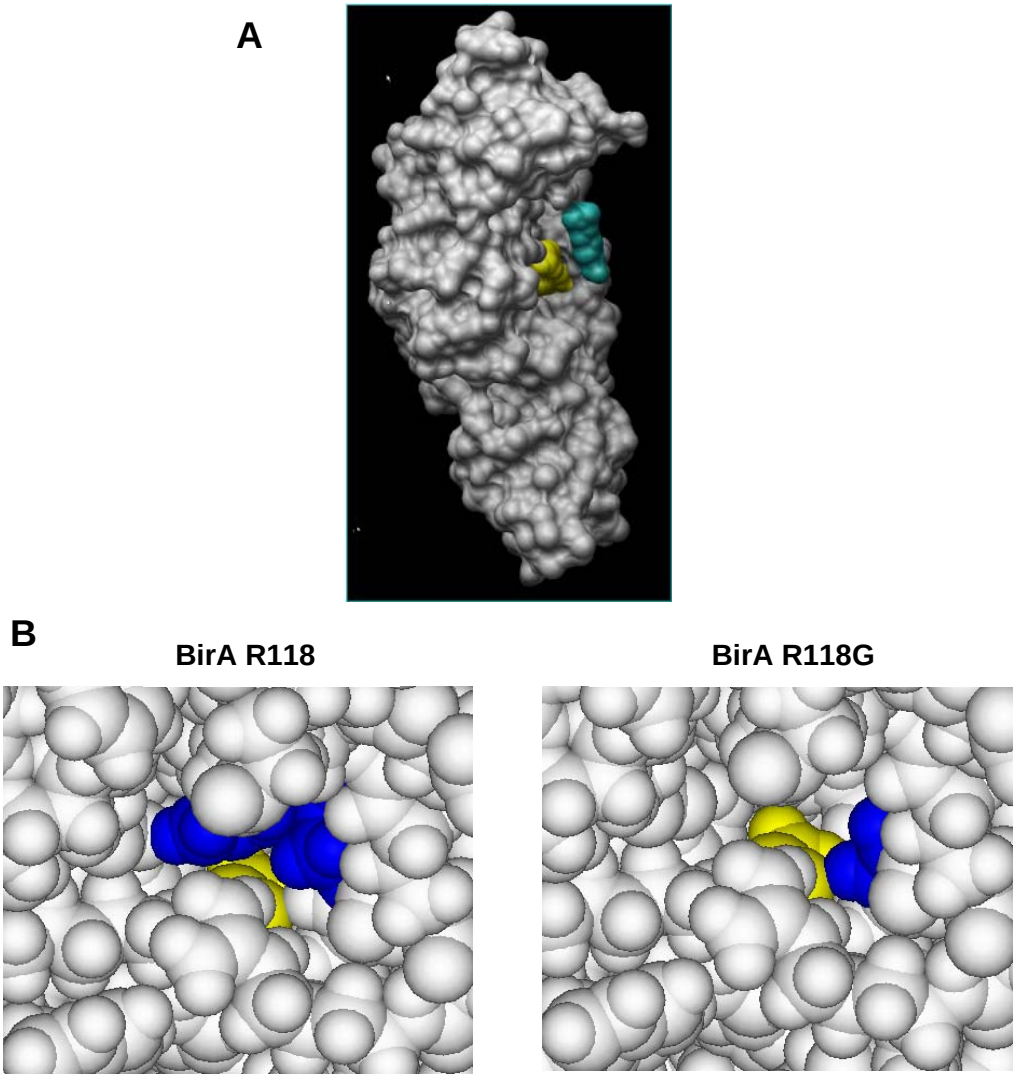

Figure A-2 Structural basis for BirA-R118G promiscuous biotinylation

(A) Model of BirA generated in Chimera using the structures of Wilson et al, 1992 and Weaver et al, 2001. BirA Arginine 118 Biotin.
(B) Model showing the difference in structure at the biotin binding pocket in the wildtype R118 enzyme (left) compared to the promiscuous mutant R118G (right). Biotin is more available to solvent in the mutant. BirA amino acid at 118 Biotin.
(Models courtesy Mr. Cvetan Stokowski, University of Adelaide).

In order to engineer a HCS variant exhibiting promiscuous biotinylation, the analogous arginine residue of HCS (Arg^{508}) was substituted with a glycine residue by site directed mutagenesis. The work I carried out followed on from initial characterisation of bacterially expressed HCS-R508G by Ms. Lisa Clarke, honours student (Clarke, 2005). Following on from Ms. Clarke's initial creation of the mutant and expression in bacterial cells, I subcloned the mutant into mammalian expression vectors to examine the effects in mammalian cells.

Additionally, a series of chimeric proteins was engineered consisting of the N-terminus of HCS (Met^{1}-Arg^{314}) fused to the catalytic domain of BirA (Pro^{61}-Lys^{321}) joined by the short three amino acid linker (Pro-Glu-Pro) (figure A.3). The purpose of generating these chimeras was twofold: firstly, if the analogous mutation in HCS (R508G) did not produce a "leaky" phenotype, then fusion to the characterised "leaky" catalytic domain of BirA to the N-terminus of HCS would engineer a "leaky" phenotype. Secondly, the chimera would provide an insight into the structure of HCS, by analysing potential self-biotinylation. If the HCS N-terminus does form a "cap" over the active site, then it would be predicted that lysines in the N-terminus would be in close proximity to the biotin binding site and hence targets for promiscuous, proximity dependent biotinylation.

To assess the promiscuous biotinylation activity of the wildtype and mutant proteins they were recombinantly expressed in 293T cells. Cell lysates were harvested 24 hours following transfection and analysed by SDS-PAGE and Western blot probed with avidin. Initial analysis with cells grown in normal complete media (DMEM+10% FCS) failed to show any promiscuous biotinylation (data not shown).

Figure A-3 Schematic of proteins expressed in 293T cells to examine promiscuous biotinylation.
Wildtype and mutant BirA and HCS proteins were generated by Quickchange mutagenesis. Chimeric proteins consisting of the three N-terminal domains of HCS fused to the catalytic domain of BirA were produced by PCR overlap extension {Clarke, 2005 #311}.

The equivalent mutation R508G does not result in promiscuous biotinylation, but self-biotinylation of HCS and nHCS:BirA chimera proteins was observed

Shown below (figure A.4) is the analysis of promiscuous biotinylation by the HCS and BirA mutants as well as the chimeric proteins when grown in additional biotin (10 nM). Panel A shows detection of biotinylated proteins in lysate with avidin-AP. All lanes would be expected to show bands corresponding to the sizes of known biotinylated proteins, ie PC (120 kDa), PCC and MCC (which often appear as a doublet at 77 and 80 kDa) and ACC at 260 kDa. ACC is not detected by Western blotting under these conditions. A marked increase in the number of proteins biotinylated by the BirA-R118G mutant was observed under these conditions (figure A-4, lane 5), implying promiscuous biotinylation activity. The analogous mutation in HCS does not result in promiscuous biotinylation (figure A.4, lane 3). However, self biotinylation of HCS is observed in panel A. Interestingly, self-

biotinylation of the nHCS:BirA chimera but not of the nHCS:BirA-R118G chimera is observed. Equivalent expression of the HCS and chimeric proteins was confirmed by Western Blotting with N2 antibody. An antibody for BirA was unavailable to confirm expression of these proteins but the promiscuous biotinylation clearly observed in figure A.4, lane 5 indicates that BirA-R118G was also expressed. Further work is required to identify the site(s) of biotinylation by mass spectroscopy.

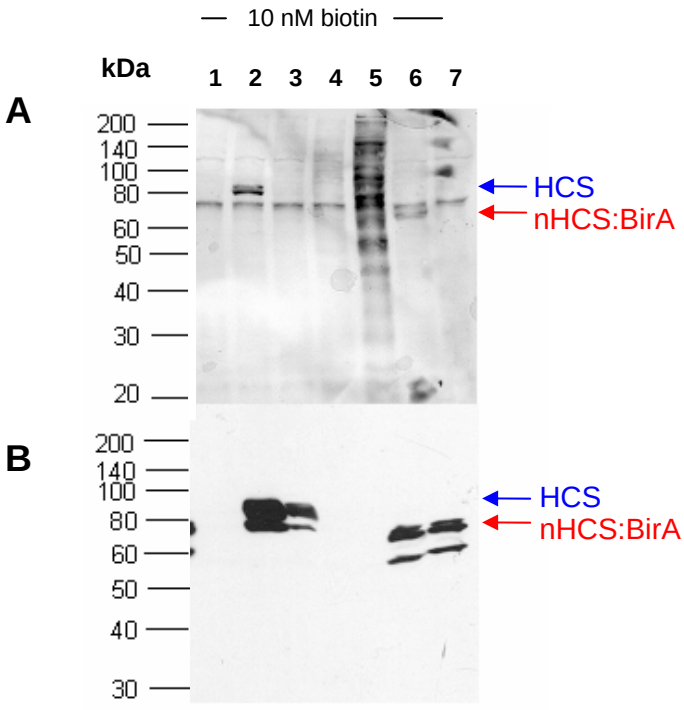

Figure A-4 Analysis of mutants confirms promiscuous biotinylation by BirA-R118G, but not of HCS-R508G.

293T cells were transiently transfected and grown in media supplemented with 10nM biotin for 24 hours. Cells were harvested and 20 μg of lysate loaded onto 10% SDS-PAGE gels. Lane 1- Empty vector, 2- HCS, 3- HCS-R508G, 4- BirA, 5- BirA-R118G, 6- nHCS:BirA chimera, 7- nHCS:BirA-R118G chimera. Panel A) probed with Avidin-AP B) N2 antibody. Arrows indicate position of HCS (blue) and chimeric (red) protein.

When the analogous mutation was created in HCS in this study, promiscuous biotinylation was not observed. Interestingly the "leaky" BirA phenotype was only observed when additional biotin (10 nM) was added to the media, which may be due to the enzymes reduced affinity for biotin (Kwon *et al.*, 2002).

A.3 Discussion

Promiscuous biotinylation is one potentially useful way to investigate inter and intramolecular protein:protein interactions in HCS. Unexpectedly, the mutation of Arg^{508} to Gly did not produce the same phenotype as that observed in BirA. Interestingly, the chimeric protein nHCS:BirA and wildtype HCS both showed self-biotinylation. Self-biotinylation has previously been reported for HCS (Narang *et al.*, 2004). The finding of self-biotinylation of the chimeric protein was surprising, particularly given that the chimeric protein bearing the BirA-R118G mutation did not show self biotinylation or promiscuous biotinylation. We predicted that the chimeric protein bearing the BirA-R118G mutation would result in increased dissociation of the biotinyl-5'-AMP and hence biotinylation of nearby lysine residues. The hypothesis that the N-terminus of HCS is directly interacting with the biotin-binding C-terminal half of the enzyme predicts that lysine residues in the N-terminus of HCS may therefore be sites of self-biotinylation. Self-modification of adenylating enzymes has been previously reported for other enzymes such as methionyl-tRNA synthetases, where the activated methionine-5'-AMP has been shown to modify the lysine chains closest to the adenylated intermediate (Hountondji *et al.*, 2000). Self-biotinylation of wildtype BirA was also reported in the Choi-Ree *et al*. study. Self-modification of methionyl-tRNA synthase is repressed by addition of the tRNA acceptor substrate, indicating that self-biotinylation seen in this study may be a consequence of overexpression of the protein. Self-biotinylation was only observed when additional biotin was added to the media.

Previous studies in our lab have shown that the R508G mutation in HCS decreases the stability of the enzyme when it is recombinantly expressed in *E. coli* (Clarke, 2005). It may be that other mutations in the active site, or a combination of mutations, are required to produce a "leaky" phenotype. The complete removal of the charged Arg at 508 and substitution with glycine may perturb the overall structure to such an extent that the first partial reaction can not proceed. A more conservative substitution such as lysine could be

examined. Whilst a single amino-acid substitution at Arg^{118} in BirA causes rapid dissociation of the biotinyl-5'-AMP intermediate, further work could be done mutating other residues in HCS that are analogous to residues in the loop between the β2 and β3 strands which have shown to be critical for biotin binding. One such residue would be Gly^{505}. For the analogous residue in BirA (Gly^{115}), it has been shown that the dissociation rate of biotinyl-5'-AMP was increased 3000 fold when Gly^{115} was mutated to a serine residue (Kwon *et al.*, 2002). Arg^{116} and Gly^{117} have been shown to interact with biotin in the BirA structure, and are also sites which could be mutated in HCS (Lys^{506} and Gly^{507}). Arg^{118} forms a salt bridge with Asp^{176}, and mutation of this aspartic acid residue could be trialled to change the charge on this residue, abolishing the salt bridge which could result in a "leaky" HCS variant.

In conclusion, no novel protein interactions were identified using the two approaches described in this appendix. However, this study provides the first direct evidence for intermolecular interactions occurring between the N- and C-terminus of HCS. This forms the basis for continued studies by others in our group.

Appendix 2 – Review: Microbial biotin protein ligases aid in understanding holocarboxylase synthetase deficiency

Pendini, N.R., Bailey, L.M., Booker, G.W., Wilce, M.C., Wallace, J.C. and Polyak, S.W. (2008) Microbial biotin protein ligases aid in understanding holocarboxylase synthetase deficiency.
Biochimica et Biophysica Acta (BBA) – Proteins & Proteomics, v.1784 (7/8), pp. 973 - 982, July/August 2006

References

References

Abu-Elheiga, L., Brinkley, W. R., Zhong, L., Chirala, S. S., Woldegiorgis, G. and Wakil, S. J. (2000) The subcellular localization of acetyl-CoA carboxylase 2, *Proc Natl Acad Sci U S A,* 97**,** 1444-9.

Abu-Elheiga, L., Matzuk, M. M., Kordari, P., Oh, W., Shaikenov, T., Gu, Z. and Wakil, S. J. (2005) Mutant mice lacking acetyl-CoA carboxylase 1 are embryonically lethal, *Proc Natl Acad Sci U S A,* 102**,** 12011-6.

Alban, C. (2000) Is plant biotin holocarboxylase synthetase a bifunctional enzyme?, *C R Acad Sci III,* 323**,** 681-8.

Alessenko, A. V., Boikov, P., Filippova, G. N., Khrenov, A. V., Loginov, A. S. and Makarieva, E. D. (1997) Mechanisms of cycloheximide-induced apoptosis in liver cells, *FEBS Lett,* 416**,** 113-6.

Ames, B. N., Elson-Schwab, I. and Silver, E. A. (2002) High-dose vitamin therapy stimulates variant enzymes with decreased coenzyme binding affinity (increased K_M): Relevance to genetic disease and polymorphisms, *Am J Clin Nutr,* 75**,** 616-58.

Aoki, Y., Li, X., Sakamoto, O., Hiratsuka, M., Akaishi, H., Xu, L., Briones, P., Suormala, T., Baumgartner, E. R., Suzuki, Y. and Narisawa, K. (1999) Identification and characterization of mutations in patients with holocarboxylase synthetase deficiency, *Hum Genet,* 104**,** 143-8.

Aoki, Y., Suzuki, Y., Li, X., Sakamoto, O., Chikaoka, H., Takita, S. and Narisawa, K. (1997) Characterization of mutant holocarboxylase synthetase (HCS): A K_M for biotin was not elevated in a patient with HCS deficiency, *Pediatr Res,* 42**,** 849-54.

Aoki, Y., Suzuki, Y., Sakamoto, O., Li, X., Takahashi, K., Ohtake, A., Sakuta, R., Ohura, T., Miyabayashi, S. and Narisawa, K. (1995) Molecular analysis of holocarboxylase synthetase deficiency: A missense mutation and a single base deletion are predominant in Japanese patients, *Biochim Biophys Acta,* 1272**,** 168-74.

Arcuri, C., Giambanco, I., Bianchi, R. and Donato, R. (2002) Subcellular localization of s100a11 (s100c, calgizzarin) in developing and adult avian skeletal muscles, *Biochim Biophys Acta,* 1600**,** 84-94.

Artymiuk, P. J., Rice, D. W., Poirrette, A. R. and Willet, P. (1994) A tale of two synthetases, *Nat Struct Biol,* 1**,** 758-60.

Athappilly, F. K. and Hendrickson, W. A. (1995) Structure of the biotinyl domain of acetyl-coenzyme A carboxylase determined by MAD phasing, *Structure,* 3**,** 1407-19.

Attwood, P. V. and Wallace, J. C. (2002) Chemical and catalytic mechanisms of carboxyl transfer reactions in biotin-dependent enzymes, *Acc Chem Res,* 35**,** 113-20.

Bagautdinov, B., Kuroishi, C., Sugahara, M. and Kunishima, N. (2005) Crystal structures of biotin protein ligase from *Pyrococcus horikoshii* ot3 and its complexes: Structural basis of biotin activation, *J Mol Biol,* 353**,** 322-33.

Ballard, T. D., Wolff, J., Griffin, J. B., Stanley, J. S., van Calcar, S. and Zempleni, J. (2002) Biotinidase catalyzes debiotinylation of histones, *Eur J Nutr,* 41**,** 78-84.

Bartel, P., Chien, C. T., Sternglanz, R. and Fields, S. (1993) Elimination of false positives that arise in using the two-hybrid system, *Biotechniques,* 14**,** 920-4.

Bats, A. S., Molho, M., Senat, M. V., Paupe, A., Bernard, J. P. and Ville, Y. (2002) Subependymal pseudocysts in the fetal brain: Prenatal diagnosis of two cases and review of the literature, *Ultrasound Obstet Gynecol,* 20**,** 502-5.

Baud, S., Guyon, V., Kronenberger, J., Wuilleme, S., Miquel, M., Caboche, M., Lepiniec, L. and Rochat, C. (2003) Multifunctional acetyl-CoA carboxylase 1 is essential for very long chain fatty acid elongation and embryo development in Arabidopsis, *Plant J,* 33**,** 75-86.

Baumgartner, E. R. and Suormala, T. (1997) Multiple carboxylase deficiency: Inherited and acquired disorders of biotin metabolism, *Int J Vitam Nutr Res,* 67**,** 377-84.

Baumgartner, M. R., Dantas, M. F., Suormala, T., Almashanu, S., Giunta, C., Friebel, D., Gebhardt, B., Fowler, B., Hoffmann, G. F., Baumgartner, E. R. and Valle, D. (2004) Isolated 3-methylcrotonyl-CoA carboxylase deficiency: Evidence for an allele-specific dominant negative effect and responsiveness to biotin therapy, *Am J Hum Genet,* 75**,** 790-800.

Beckett, D. (2007) Biotin sensing: Universal influence of biotin status on transcription, *Annu Rev Genet,* 41**,** 443-64.

Belle, A., Tanay, A., Bitincka, L., Shamir, R. and O'Shea, E. K. (2006) Quantification of protein half-lives in the budding yeast proteome, *Proc Natl Acad Sci U S A,* 103**,** 13004-9.

Berger, S. L. (2002) Histone modifications in transcriptional regulation, *Curr Opin Genet Dev,* 12**,** 142-8.

Blom, W. M., de Bont, H. J., Meijerman, I., Mulder, G. J. and Nagelkerke, J. F. (1999) Prevention of cycloheximide-induced apoptosis in hepatocytes by adenosine and by caspase inhibitors, *Biochem Pharmacol,* 58**,** 1891-8.

Boetel, T., Bade, S., Schmidt, M. A. and Frey, A. (2006) Prion protein 90-231 contains a streptavidin-binding motif, *Biochem Biophys Res Commun,* 349**,** 296-302.

Bommer, U. A. and Thiele, B. J. (2004) The translationally controlled tumour protein (tctp), *Int J Biochem Cell Biol,* 36**,** 379-85.

Borden, K. L. (2002) Pondering the promyelocytic leukemia protein (pml) puzzle: Possible functions for pml nuclear bodies, *Mol Cell Biol,* 22**,** 5259-69.

Briones, P., Ribes, A., Vilaseca, M. A., Rodriguez-Valcarcel, G., Thuy, L. P. and Sweetman, L. (1989) A new case of holocarboxylase synthetase deficiency, *J Inherit Metab Dis,* 12**,** 329-30.

Burri, B. J., Sweetman, L. and Nyhan, W. L. (1981) Mutant holocarboxylase synthetase: Evidence for the enzyme defect in early infantile biotin-responsive multiple carboxylase deficiency, *J Clin Invest,* 68**,** 1491-5.

Burri, B. J., Sweetman, L. and Nyhan, W. L. (1985) Heterogeneity of holocarboxylase synthetase in patients with biotin-responsive multiple carboxylase deficiency, *Am J Hum Genet,* 37**,** 326-37.

Cai, J., Huang, Y., Li, F. and Li, Y. (2006) Alteration of protein subcellular location and domain formation by alternative translational initiation, *Proteins,* 62**,** 793-9.

Campeau, E. and Gravel, R. A. (2001) Expression in Escherichia coli of N- and C-terminally deleted human holocarboxylase synthetase. Influence of the N-terminus on biotinylation and identification of a minimum functional protein, *J Biol Chem,* 276**,** 12310-6.

Camporeale, G., Giordano, E., Rendina, R., Zempleni, J. and Eissenberg, J. C. (2006) Drosophila melanogaster holocarboxylase synthetase is a chromosomal protein required for normal histone biotinylation, gene transcription patterns, lifespan, and heat tolerance, *J Nutr,* 136**,** 2735-42.

Camporeale, G., Shubert, E. E., Sarath, G., Cerny, R. and Zempleni, J. (2004) K8 and K12 are biotinylated in human histone H4, *Eur J Biochem,* 271**,** 2257-63.

Camporeale, G., Zempleni, J. and Eissenberg, J. C. (2007) Susceptibility to heat stress and aberrant gene expression patterns in holocarboxylase synthetase-deficient drosophila melanogaster are caused by decreased biotinylation of histones, not of carboxylases, *J Nutr,* 137**,** 885-9.

Chalfie, M. and Kain, S. (2005) *Green fluorescent protein, properties applications and protocols, vol. 47, 2nd edition (methods of biochemical analysis).* John Wiley & Sons Inc.

Chang, H. I. and Cohen, N. D. (1983) Regulation and intracellular localization of the biotin holocarboxylase synthetase of 3T3-l1 cells, *Arch Biochem Biophys,* 225**,** 237-47.

Chapman-Smith, A. and Cronan, J. E., Jr. (1999a) The enzymatic biotinylation of proteins: A post-translational modification of exceptional specificity, *Trends Biochem Sci,* 24**,** 359-63.

Chapman-Smith, A. and Cronan, J. E., Jr. (1999b) Molecular biology of biotin attachment to proteins, *J Nutr,* 129**,** 477S-484S.

Chapman-Smith, A., Morris, T. W., Wallace, J. C. and Cronan, J. E., Jr. (1999) Molecular recognition in a post-translational modification of exceptional specificity. Mutants of the biotinylated domain of acetyl-CoA carboxylase defective in recognition by biotin protein ligase, *J Biol Chem,* 274**,** 1449-57.

Chapman-Smith, A., Mulhern, T. D., Whelan, F., Cronan, J. E., Jr. and Wallace, J. C. (2001) The C-terminal domain of biotin protein ligase from *E. coli* is required for catalytic activity, *Protein Sci,* 10**,** 2608-17.

Che, P., Weaver, L. M., Wurtele, E. S. and Nikolau, B. J. (2003) The role of biotin in regulating 3-methylcrotonyl-coenzyme A carboxylase expression in Arabidopsis, *Plant Physiol,* 131**,** 1479-86.

Cherbonnel-Lasserre, C. L., Linares-Cruz, G., Rigaut, J. P., Sabatier, L. and Dutrillaux, B. (1997) Strong decrease in biotin content may correlate with metabolic alterations in colorectal adenocarcinoma, *Int J Cancer,* 72**,** 768-75.

Chew, Y. C., Camporeale, G., Kothapalli, N., Sarath, G. and Zempleni, J. (2006) Lysine residues in N-terminal and C-terminal regions of human histone H2A are targets for biotinylation by biotinidase, *J Nutr Biochem,* 17**,** 225-33.

Choi-Rhee, E., Schulman, H. and Cronan, J. E. (2004) Promiscuous protein biotinylation by Escherichia coli biotin protein ligase, *Protein Sci,* 13**,** 3043-50.

Clarke, L. K. (2005) Novel variants of biotin protein ligase (honours thesis) *School of Molecular and Biomedical Science* University of Adelaide, Adelaide.

Cohen, N. D., Thomas, M. and Stack, M. (1985) The subcellular distribution of the holocarboxylase synthetase of the rat liver, *Annals of the New York Academy of Sciences,* 447**,** 393-395.

Collins, J. C., Paietta, E., Green, R., Morell, A. G. and Stockert, R. J. (1988) Biotin-dependent expression of the asialoglycoprotein receptor in HepG2, *J Biol Chem,* 263**,** 11280-3.

Cormack, B. P., Valdivia, R. H. and Falkow, S. (1996) FACS-optimized mutants of the green fluorescent protein (GFP), *Gene,* 173**,** 33-8.

Crisp, S. E., Griffin, J. B., White, B. R., Toombs, C. F., Camporeale, G., Said, H. M. and Zempleni, J. (2004) Biotin supply affects rates of cell proliferation, biotinylation of carboxylases and histones, and expression of the gene encoding the sodium-dependent multivitamin transporter in JAr choriocarcinoma cells, *Eur J Nutr,* 43**,** 23-31.

Cronan, J. E., Jr. (1989) The E. coli bio operon: Transcriptional repression by an essential protein modification enzyme, *Cell,* 58**,** 427-9.

Cronan, J. E., Jr. and Wallace, J. C. (1995) The gene encoding the biotin-apoprotein ligase of Saccharomyces cerevisiae, *FEMS Microbiol Lett,* 130**,** 221-9.

Croons, V., Martinet, W., Herman, A. G., Timmermans, J. P. and De Meyer, G. R. (2007) Selective clearance of macrophages in atherosclerotic plaques by the protein synthesis inhibitor cycloheximide, *J Pharmacol Exp Ther,* 320**,** 986-93.

Cubitt, A. B., Heim, R., Adams, S. R., Boyd, A. E., Gross, L. A. and Tsien, R. Y. (1995) Understanding, improving and using green fluorescent proteins, *Trends Biochem Sci,* 20**,** 448-55.

Dakshinamurti, K. and Mistry, S. P. (1963a) Amino acid incorporation and biotin deficiency, *J Biol Chem,* 238**,** 297-301.

Dakshinamurti, K. and Mistry, S. P. (1963b) Tissue and intracellular distribution of biotin-C-14-00H in rats and chicks, *J Biol Chem,* 238**,** 294-6.

Danpure, C. J. (1995) How can the products of a single gene be localized to more than one intracellular compartment? *Trends in Cell Biology,* 5**,** 230-238.

Denis, L., Grossemy, M., Douce, R. and Alban, C. (2002) Molecular characterization of a second copy of holocarboxylase synthetase gene (hcs2) in Arabidopsis thaliana, *J Biol Chem,* 277**,** 10435-44.

Devlin, J. J., Panganiban, L. C. and Devlin, P. E. (1990) Random peptide libraries: A source of specific protein binding molecules, *Science,* 249**,** 404-6.

Diamandis, E. P. and Christopoulos, T. K. (1991) The biotin-(strept)avidin system: Principles and applications in biotechnology, *Clin Chem,* 37**,** 625-36.

Dupuis, L., Campeau, E., Leclerc, D. and Gravel, R. A. (1999) Mechanism of biotin responsiveness in biotin-responsive multiple carboxylase deficiency, *Mol Genet Metab,* 66**,** 80-90.

Dupuis, L., Leon-Del-Rio, A., Leclerc, D., Campeau, E., Sweetman, L., Saudubray, J. M., Herman, G., Gibson, K. M. and Gravel, R. A. (1996) Clustering of mutations in the biotin-binding region of holocarboxylase synthetase in biotin-responsive multiple carboxylase deficiency, *Hum Mol Genet,* 5**,** 1011-6.

Estojak, J., Brent, R. and Golemis, E. A. (1995) Correlation of two-hybrid affinity data with in vitro measurements, *Mol Cell Biol,* 15**,** 5820-9.

Fan, J. Q. (2008) A counterintuitive approach to treat enzyme deficiencies: Use of enzyme inhibitors for restoring mutant enzyme activity, *Biol Chem,* 389**,** 1-11.

Feldman, G. L., Hsia, Y. E. and Wolf, B. (1981) Biochemical characterization of biotin-responsive multiple carboxylase deficiency: Heterogeneity within the bio genetic complementation group, *Am J Hum Genet,* 33**,** 692-701.

Fuchshuber, A., Suormala, T., Roth, B., Duran, M., Michalk, D. and Baumgartner, E. R. (1993) Holocarboxylase synthetase deficiency: Early diagnosis and management of a new case, *Eur J Pediatr,* 152**,** 446-9.

Gao, M. H., Bayat, H., Roth, D. M., Yao Zhou, J., Drumm, J., Burhan, J. and Hammond, H. K. (2002) Controlled expression of cardiac-directed adenylylcyclase type VI provides increased contractile function, *Cardiovasc Res,* 56**,** 197-204.

Gavel, Y. and von Heijne, G. (1990) Cleavage-site motifs in mitochondrial targeting peptides, *Protein Eng,* 4**,** 33-7.

Griffin, J. B., Rodriguez-Melendez, R. and Zempleni, J. (2003) The nuclear abundance of transcription factors sp1 and sp3 depends on biotin in Jurkat cells, *J Nutr,* 133**,** 3409-15.

Gudi, T., Huvar, I., Meinecke, M., Lohmann, S. M., Boss, G. R. and Pilz, R. B. (1996) Regulation of gene expression by cGMP-dependent protein kinase, *J. Biol. Chem.,* 271**,** 4597-4600.

Hasslacher, M., Ivessa, A. S., Paltauf, F. and Kohlwein, S. D. (1993) Acetyl-CoA carboxylase from yeast is an essential enzyme and is regulated by factors that control phospholipid metabolism, *J Biol Chem,* 268**,** 10946-52.

Hiratsuka, M., Sakamoto, O., Li, X., Suzuki, Y., Aoki, Y. and Narisawa, K. (1998) Identification of holocarboxylase synthetase (HCS) proteins in human placenta, *Biochim Biophys Acta,* 1385**,** 165-71.

Hobbs, S., Jitrapakdee, S. and Wallace, J. C. (1998) Development of a bicistronic vector driven by the human polypeptide chain elongation factor 1alpha promoter for creation of stable mammalian cell lines that express very high levels of recombinant proteins, *Biochem Biophys Res Commun,* 252**,** 368-72.

Holme, E., Jacobson, C. E. and Kristiansson, B. (1988) Biotin-responsive multiple carboxylase deficiency in an 8-year-old boy with normal serum biotinidase and fibroblast holocarboxylase-synthetase activities, *J Inherit Metab Dis,* 11**,** 270-6.

Hopp, T. P. and Woods, K. R. (1981) Prediction of protein antigenic determinants from amino acid sequences, *Proc Natl Acad Sci U S A,* 78**,** 3824-8.

Hountondji, C., Beauvallet, C., Pernollet, J. C. and Blanquet, S. (2000) Enzyme-induced covalent modification of methionyl-tRNA synthetase from Bacillus stearothermophilus by methionyl-adenylate: Identification of the labeled amino acid residues by matrix-assisted laser desorption-ionization mass spectrometry, *J Protein Chem,* 19**,** 563-8.

Hymes, J., Fleischhauer, K. and Wolf, B. (1995) Biotinylation of histones by human serum biotinidase: Assessment of biotinyl-transferase activity in sera from normal individuals and children with biotinidase deficiency, *Biochem Mol Med,* 56**,** 76-83.

Hymes, J. and Wolf, B. (1999) Human biotinidase isn't just for recycling biotin, *J Nutr,* 129**,** 485S-489S.

Jacobs, R. A., Sly, W. S. and Majerus, P. W. (1973) The regulation of fatty acid biosynthesis in human skin fibroblasts, *J Biol Chem,* 248**,** 1268-76.

Jans, D. A. and Hubner, S. (1996) Regulation of protein transport to the nucleus: Central role of phosphorylation, *Physiol Rev,* 76**,** 651-85.

Jenuwein, T. and Allis, C. D. (2001) Translating the histone code, *Science,* 293**,** 1074-80.

Jitrapakdee, S. and Wallace, J. C. (2003) The biotin enzyme family: Conserved structural motifs and domain rearrangements, *Curr Protein Pept Sci,* 4**,** 217-29.

Johnston, A. J., Hoogenraad, J., Dougan, D. A., Truscott, K. N., Yano, M., Mori, M., Hoogenraad, N. J. and Ryan, M. T. (2002) Insertion and assembly of human Tom7 into the preprotein translocase complex of the outer mitochondrial membrane, *J Biol Chem,* 277**,** 42197-204.

Kalejta, R. F., Shenk, T. and Beavis, A. J. (1997) Use of a membrane-localized green fluorescent protein allows simultaneous identification of transfected cells and cell cycle analysis by flow cytometry, *Cytometry,* 29**,** 286-91.

Kim, K.-H. (1997) Regulation of mammalian acetyl-Coenzyme A carboxylase, *Annual Review of Nutrition,* 17**,** 77-99.

Kobza, K., Camporeale, G., Rueckert, B., Kueh, A., Griffin, J. B., Sarath, G. and Zempleni, J. (2005) K4, K9 and K18 in human histone H3 are targets for biotinylation by biotinidase, *FEBS J,* 272**,** 4249-59.

Kosow, D. P., Huang, S. C. and Lane, M. D. (1962) Propionyl holocarboxylase synthesis. I. Preparation and properties of the enzyme system, *J. Biol. Chem.,* 237**,** 3633-3639.

Kothapalli, N., Sarath, G. and Zempleni, J. (2005) Biotinylation of K12 in histone H4 decreases in response to DNA double-strand breaks in human JAr choriocarcinoma cells, *J Nutr,* 135**,** 2337-42.

Kwon, K., Streaker, E. D. and Beckett, D. (2002) Binding specificity and the ligand dissociation process in the E. coli biotin holoenzyme synthetase, *Protein Sci,* 11**,** 558-70.

Laemmli, U. K. (1970) Cleavage of structural proteins during the assembly of the head of bacteriophage T4, *Nature,* 227**,** 680-5.

Lam, K. S., Salmon, S. E., Hersh, E. M., Hruby, V. J., Kazmierski, W. M. and Knapp, R. J. (1991) A new type of synthetic peptide library for identifying ligand-binding activity, *Nature,* 354**,** 82-4.

Lamla, T. and Erdmann, V. A. (2004) The nano-tag, a streptavidin-binding peptide for the purification and detection of recombinant proteins, *Protein Expr Purif,* 33**,** 39-47.

Landenberger, A., Kabil, H., Harshman, L. G. and Zempleni, J. (2004) Biotin deficiency decreases life span and fertility but increases stress resistance in Drosophila melanogaster, *J Nutr Biochem,* 15**,** 591-600.

Larque, E., Demmelmair, H. and Koletzko, B. (2002) Perinatal supply and metabolism of long-chain polyunsaturated fatty acids: Importance for the early development of the nervous system, *Ann N Y Acad Sci,* 967**,** 299-310.

Leon-Del-Rio, A., Leclerc, D., Akerman, B., Wakamatsu, N. and Gravel, R. A. (1995) Isolation of a cDNA encoding human holocarboxylase synthetase by functional complementation of a biotin auxotroph of Escherichia coli, *Proc Natl Acad Sci U S A,* 92**,** 4626-30.

Li, B. and Fields, S. (1993) Identification of mutations in p53 that affect its binding to sv40 large T antigen by using the yeast two-hybrid system, *FASEB J,* 7**,** 957-63.

Li, S. and Cronan, J., Jr (1992) The gene encoding the biotin carboxylase subunit of Escherichia coli acetyl-CoA carboxylase, *J. Biol. Chem.,* 267**,** 855-863.

Limat, A., Suormala, T., Hunziker, T., Waelti, E. R., Braathen, L. R. and Baumgartner, R. (1996) Proliferation and differentiation of cultured human follicular keratinocytes are not influenced by biotin, *Arch Dermatol Res,* 288**,** 31-8.

Lipman, N. S., Jackson, L. R., Trudel, L. J. and Weis-Garcia, F. (2005) Monoclonal versus polyclonal antibodies: Distinguishing characteristics, applications, and information resources, *ILAR J,* 46**,** 258-68.

Lithgow, T. (2000) Targeting of proteins to mitochondria, *FEBS Lett,* 476**,** 22-6.

Lund, A. M., Joensen, F., Hougaard, D. M., Jensen, L. K., Christensen, E., Christensen, M., Norgaard-Petersen, B., Schwartz, M. and Skovby, F. (2007) Carnitine transporter and holocarboxylase synthetase deficiencies in the Faroe islands, *J Inherit Metab Dis*.

Malvagia, S., Morrone, A., Pasquini, E., Funghini, S., la Marca, G., Zammarchi, E. and Donati, M. A. (2005) First prenatal molecular diagnosis in a family with holocarboxylase synthetase deficiency, *Prenat Diagn,* 25**,** 1117-9.

Manthey, K. C., Griffin, J. B. and Zempleni, J. (2002) Biotin supply affects expression of biotin transporters, biotinylation of carboxylases and metabolism of interleukin-2 in jurkat cells, *J Nutr,* 132**,** 887-92.

Marenholz, I., Heizmann, C. W. and Fritz, G. (2004) S100 proteins in mouse and man: From evolution to function and pathology (including an update of the nomenclature), *Biochem Biophys Res Commun,* 322**,** 1111-22.

McMahon, R. J. (2002) Biotin in metabolism and molecular biology, *Annu Rev Nutr,* 22**,** 221-39.

Meisinger, C., Wiedemann, N., Rissler, M., Strub, A., Milenkovic, D., Schonfisch, B., Muller, H., Kozjak, V. and Pfanner, N. (2006) Mitochondrial protein sorting: Differentiation of beta-barrel assembly by tom7-mediated segregation of mdm10, *J Biol Chem,* 281**,** 22819-26.

Merkel, A. (2002) Pleckstrin homology and Tec homology domains link Tec kinase signalling to the cytoskeleton (Thesis), *School of Molecular and Biomedical Science,* University of Adelaide, Adelaide.

Michaelson, J. S. (2000) The Daxx enigma, *Apoptosis,* 5**,** 217-20.

Mock, D. M., Lankford, G. L. and Mock, N. I. (1995) Biotin accounts for only half of the total avidin-binding substances in human serum, *J Nutr,* 125**,** 941-6.

Mock, D. M., Mock, N. I., Stewart, C. W., LaBorde, J. B. and Hansen, D. K. (2003) Marginal biotin deficiency is teratogenic in ICR mice, *J Nutr,* 133**,** 2519-25.

Mock, D. M., Quirk, J. G. and Mock, N. I. (2002) Marginal biotin deficiency during normal pregnancy, *Am J Clin Nutr,* 75**,** 295-9.

Mock, D. M. and Stadler, D. D. (1997) Conflicting indicators of biotin status from a cross-sectional study of normal pregnancy, *J Am Coll Nutr,* 16**,** 252-7.

Mock, D. M., Stadler, D. D., Stratton, S. L. and Mock, N. I. (1997a) Biotin status assessed longitudinally in pregnant women, *J. Nutr.,* 127**,** 710-716.

Mock, N., Malik, M., Stumbo, P., Bishop, W. and Mock, D. (1997b) Increased urinary excretion of 3-hydroxyisovaleric acid and decreased urinary excretion of biotin are sensitive early indicators of decreased biotin status in experimental biotin deficiency, *Am J Clin Nutr,* 65**,** 951-958.

Morita, J., Thuy, L. P. and Sweetman, L. (1998) Deficiency of biotinyl-AMP synthetase activity in fibroblasts of patients with holocarboxylase synthetase deficiency, *Mol Genet Metab,* 64**,** 250-5.

Morrone, A., Malvagia, S., Donati, M. A., Funghini, S., Ciani, F., Pela, I., Boneh, A., Peters, H., Pasquini, E. and Zammarchi, E. (2002) Clinical findings and biochemical and molecular analysis of four patients with holocarboxylase synthetase deficiency, *Am J Med Genet,* 111**,** 10-8.

Nair, R., Carter, P. and Rost, B. (2003) Nlsdb: Database of nuclear localization signals, *Nucleic Acids Res,* 31**,** 397-9.

Nair, R. and Rost, B. (2005) Mimicking cellular sorting improves prediction of subcellular localization, *J Mol Biol,* 348**,** 85-100.

Nakai, K. and Kanehisa, M. (1992) A knowledge base for predicting protein localization sites in eukaryotic cells, *Genomics,* 14**,** 897-911.

Narang, M. A., Dumas, R., Ayer, L. M. and Gravel, R. A. (2004) Reduced histone biotinylation in multiple carboxylase deficiency patients: A nuclear role for holocarboxylase synthetase, *Hum Mol Genet,* 13**,** 15-23.

Oheim, M. and Li, D. (2007) In *Imaging cellular and molecular biological functions* (Eds, Shorte, S. L. and Frischknecht, F.) Springer Berlin Heidelberg.

Pacheco-Alvarez, D., Solorzano-Vargas, R. S. and Del Rio, A. L. (2002) Biotin in metabolism and its relationship to human disease, *Arch Med Res,* 33**,** 439-47.

Pacheco-Alvarez, D., Solorzano-Vargas, R. S., Gonzalez-Noriega, A., Michalak, C., Zempleni, J. and Leon-Del-Rio, A. (2005) Biotin availability regulates expression of

the sodium-dependent multivitamin transporter and the rate of biotin uptake in HepG2 cells, *Mol Genet Metab 2005 May 16;.* 85**,** 301-7.

Pappin, D. J., Hojrup, P. and Bleasby, A. J. (1993) Rapid identification of proteins by peptide-mass fingerprinting, *Curr Biol,* 3**,** 327-32.

Patton, D. A., Johnson, M. and Ward, E. R. (1996) Biotin synthase from Arabidopsis thaliana. cDNA isolation and characterization of gene expression, *Plant Physiol,* 112**,** 371-8.

Pendini, N. R., Bailey, L., Polyak, S. W., Swift, R., Wilce, M. and Wallace, J. C. (2006) Probing the importance of the N-terminal region of human Biotin Protein Ligase, In *31st Lorne Proteins Conference* Lorne, Victoria, Australia, pp. Poster 220.

Pendini, N. R., Polyak, S. W., Booker, G. W., Wallace, J. C. and Wilce, M. C. (2008) Purification, crystallization and preliminary crystallographic analysis of biotin protein ligase from Staphylococcus aureus, *Acta Crystallogr Sect F Struct Biol Cryst Commun,* 64**,** 520-3.

Perbandt, M., Bruns, O., Vallazza, M., Lamla, T., Betzel, C. and Erdmann, V. A. (2007) High resolution structure of streptavidin in complex with a novel high affinity peptide tag mimicking the biotin binding motif, *Proteins,* 67**,** 1147-53.

Perham, R. N. (2000) Swinging arms and swinging domains in multifunctional enzymes: Catalytic machines for multi-step reactions, *Annual Review of Biochemistry,* 69**,** 961-1004.

Peters, D. M., Griffin, J. B., Stanley, J. S., Beck, M. M. and Zempleni, J. (2002) Exposure to UV light causes increased biotinylation of histones in Jurkat cells, *Am J Physiol Cell Physiol,* 283**,** C878-84.

Petrelli, F., Moretti, P. and Paparelli, M. (1979) Intracellular distribution of biotin-14-C-OOH in rat liver, *Mol Biol Rep,* 4**,** 247-52.

Pettersen EF, Goddard TD, Huang CC, Couch GS, Greenblatt DM, Meng EC, Ferrin TE.(2004) UCSF Chimera--a visualization system for exploratory research and analysis. *J Comput Chem.* 25,1605-12.

Pfanner, N. and Geissler, A. (2001) Versatility of the mitochondrial protein import machinery, *Nat Rev Mol Cell Biol,* 2**,** 339-49.

Pirner, H. M. and Stolz, J. (2006) Biotin sensing in Saccharomyces cerevisiae is mediated by a conserved DNA element and requires the activity of biotin-protein ligase, *J Biol Chem,* 281**,** 12381-9.

Polyak, S. W., Bailey, L. and Wallace, J. C. (2002) Analysis of biotin domains as subtrates for biotin protein ligase In *ComBio 2002*, Vol. 34 Proceedings of the Australian Society for Biochemistry and Molecular biology, Sydney, Australia., pp. POS-TUE-012.

Polyak, S. W., Chapman-Smith, A., Brautigan, P. J. and Wallace, J. C. (1999) Biotin protein ligase from Saccharomyces cerevisiae. The N-terminal domain is required for complete activity, *J Biol Chem,* 274**,** 32847-54.

Polyak, S. W., Chapman-Smith, A., Mulhern, T. D., Cronan, J. E., Jr. and Wallace, J. C. (2001) Mutational analysis of protein substrate presentation in the post-translational attachment of biotin to biotin domains, *J Biol Chem,* 276**,** 3037-45.

Posada, J. and Cooper, J. A. (1992) Requirements for phosphorylation of map kinase during meiosis in Xenopus oocytes, *Science,* 255**,** 212-5.

Puyaubert, J., Denis, L. and Alban, C. (2008) Dual targeting of Arabidopsis holocarboxylase synthetase1: A small upstream open reading frame regulates translation initiation and protein targeting, *Plant Physiol,* 146**,** 478-91.

Reche, P., Li, Y. L., Fuller, C., Eichhorn, K. and Perham, R. N. (1998) Selectivity of post-translational modification in biotinylated proteins: The carboxy carrier protein of the acetyl-CoA carboxylase of Escherichia coli, *Biochem J,* 329 (Pt 3)**,** 589-96.

Reche, P. and Perham, R. N. (1999) Structure and selectivity in post-translational modification: Attaching the biotinyl-lysine and lipoyl-lysine swinging arms in multifunctional enzymes, *EMBO J,* 18**,** 2673-82.

Reche, P. A. (2000) Lipoylating and biotinylating enzymes contain a homologous catalytic module, *Protein Sci,* 9**,** 1922-9.

Reinhardt, A. and Hubbard, T. (1998) Using neural networks for prediction of the subcellular location of proteins, *Nucl. Acids Res.,* 26**,** 2230-2236.

Roberts, E. L., Shu, N., Howard, M. J., Broadhurst, R. W., Chapman-Smith, A., Wallace, J. C., Morris, T., Cronan, J. E., Jr. and Perham, R. N. (1999) Solution structures of apo- and holo-biotinyl domains from acetyl coenzyme A carboxylase of Escherichia coli determined by triple-resonance nuclear magnetic resonance spectroscopy, *Biochemistry,* 38**,** 5045-53.

Rodionov, D. A., Mironov, A. A. and Gelfand, M. S. (2002) Conservation of the biotin regulon and the BirA regulatory signal in eubacteria and archaea, *Genome Res,* 12**,** 1507-16.

Rodriguez-Melendez, R., Camporeale, G., Griffin, J. B. and Zempleni, J. (2003) Interleukin-2 receptor-gamma -dependent endocytosis depends on biotin in Jurkat cells, *Am J Physiol Cell Physiol,* 284**,** C415-21.

Rodriguez-Melendez, R., Cano, S., Mendez, S. T. and Velazquez, A. (2001) Biotin regulates the genetic expression of holocarboxylase synthetase and mitochondrial carboxylases in rats, *J Nutr,* 131**,** 1909-13.

Rodriguez-Melendez, R., Perez-Andrade, M. E., Diaz, A., Deolarte, A., Camacho-Arroyo, I., Ciceron, I., Ibarra, I. and Velazquez, A. (1999) Differential effects of biotin deficiency and replenishment on rat liver pyruvate and propionyl-CoA carboxylases and on their mRNAs, *Molecular Genetics and Metabolism,* 66**,** 16-23.

Rodriguez-Melendez, R. and Zempleni, J. (2003) Regulation of gene expression by biotin (review), *The Journal of Nutritional Biochemistry,* 14**,** 680-690.

Rohde, M., Lim, F. and Wallace, J. C. (1991) Electron microscopic localization of pyruvate carboxylase in rat liver and Saccharomyces cerevisiae by immunogold procedures, *Arch Biochem Biophys,* 290**,** 197-201.

Romero-Navarro, G., Cabrera-Valladares, G., German, M. S., Matschinsky, F. M., Velazquez, A., Wang, J. and Fernandez-Mejia, C. (1999) Biotin regulation of pancreatic glucokinase and insulin in primary cultured rat islets and in biotin-deficient rats, *Endocrinology,* 140**,** 4595-600.

Said, H. M. (1999a) Biotin bioavailability and estimated average requirement: Why bother? *Am J Clin Nutr,* 69**,** 352-3.

Said, H. M. (1999b) Cellular uptake of biotin: Mechanisms and regulation, *J Nutr,* 129**,** 490S-493S.

Sakaguchi, M., Miyazaki, M., Takaishi, M., Sakaguchi, Y., Makino, E., Kataoka, N., Yamada, H., Namba, M. and Huh, N. H. (2003) S100c/A11 is a key mediator of Ca^{2+}-induced growth inhibition of human epidermal keratinocytes, *J Cell Biol,* 163**,** 825-35.

Sakamoto, O., Suzuki, Y., Aoki, Y., Li, X., Hiratsuka, M., Yanagihara, K., Inui, K., Okabe, T., Yamaguchi, S., Kudoh, J., Shimizu, N. and Narisawa, K. (1998) Molecular analysis of new Japanese patients with holocarboxylase synthetase deficiency, *J Inherit Metab Dis,* 21**,** 873-4.

Sakamoto, O., Suzuki, Y., Li, X., Aoki, Y., Hiratsuka, M., Holme, E., Kudoh, J., Shimizu, N. and Narisawa, K. (2000) Diagnosis and molecular analysis of an atypical case of holocarboxylase synthetase deficiency, *Eur J Pediatr,* 159**,** 18-22.

Sakamoto, O., Suzuki, Y., Li, X., Aoki, Y., Hiratsuka, M., Suormala, T., Baumgartner, E. R., Gibson, K. M. and Narisawa, K. (1999) Relationship between kinetic properties of mutant enzyme and biochemical and clinical responsiveness to biotin in holocarboxylase synthetase deficiency, *Pediatr Res,* 46**,** 671-6.

Salomoni, P. and Khelifi, A. F. (2006) Daxx: Death or survival protein? *Trends Cell Biol,* 16**,** 97-104.

Samols, D., Thornton, C. G., Murtif, V. L., Kumar, G. K., Haase, F. C. and Wood, H. G. (1988) Evolutionary conservation among biotin enzymes, *J Biol Chem,* 263**,** 6461-4.

Saunders, M., Sweetman, L., Robinson, B., Roth, K., Cohn, R. and Gravel, R. A. (1979) Biotin-response organicaciduria. Multiple carboxylase defects and complementation studies with propionicacidemia in cultured fibroblasts, *J Clin Invest,* 64**,** 1695-702.

Schagger, H. and Von Jagow, G. (1987) Tricine-sodium dodecyl sulfate-polyacrylamide gel electrophoresis for the separation of proteins in the range from 1 to 100 kDa, *Anal Biochem,* 166**,** 368-79.

Scheerger, S. B. and Zempleni, J. (2003) Expression of oncogenes depends on biotin in human small cell lung cancer cells NCI-H69, *Int J Vitam Nutr Res,* 73**,** 461-7.

Schmidt, T. G., Koepke, J., Frank, R. and Skerra, A. (1996) Molecular interaction between the strep-tag affinity peptide and its cognate target, streptavidin, *J Mol Biol,* 255**,** 753-66.

Schmitz, H. D. and Bereiter-Hahn, J. (2001) GFP associates with microfilaments in fixed cells, *Histochem Cell Biol,* 116**,** 89-94.

Serebriiskii, I. G., Khazak, V. and Golemis, E. A. (2001) Redefinition of the yeast two-hybrid system in dialogue with changing priorities in biological research, *Biotechniques,* 30**,** 634-6, 638, 640.

Shin, D. and Park, C. (2004) N-terminal extension of canine glutamine synthetase created by splicing alters its enzymatic property, *J Biol Chem,* 279**,** 1184-90.

Simpson, J., Wellenreuther, R., Poustka, A., Pepperkok, R. and Weimann, S. (2000) Systematic subcellular localization of novel proteins identified by large-scale cDNA sequencing, *EMBO reports,* 1**,** 287-292.

Singh, I. N. and Dakshinamurti, K. (1988) Stimulation of guanylate cyclase and RNA polymerase II activities in HeLa cells and fibroblasts by biotin, *Mol Cell Biochem,* 79**,** 47-55.

Skerra, A. and Schmidt, T. G. (1999) Applications of a peptide ligand for streptavidin: The strep-tag, *Biomol Eng,* 16**,** 79-86.

Slusher, L., Gillman, E., Martin, N. and Hopper, A. (1991) mRNA leader length and initiation codon context determine alternative AUG selection for the yeast gene MOD5, *PNAS,* 88**,** 9789-9793.

Solorzano-Vargas, R. S., Pacheco-Alvarez, D. and Leon-Del-Rio, A. (2002) Holocarboxylase synthetase is an obligate participant in biotin-mediated regulation of its own expression and of biotin-dependent carboxylases mRNA levels in human cells, *Proc Natl Acad Sci U S A,* 99**,** 5325-30.

Spence, J. T. and Koudelka, A. P. (1984) Effects of biotin upon the intracellular level of cGMP and the activity of glucokinase in cultured rat hepatocytes, *J Biol Chem,* 259**,** 6393-6.

Squires, L., Betz, B., Umfleet, J. and Kelley, R. (1997) Resolution of subependymal cysts in neonatal holocarboxylase synthetase deficiency, *Dev Med Child Neurol,* 39**,** 267-9.

Stanley, J. S., Griffin, J. B. and Zempleni, J. (2001) Biotinylation of histones in human cells. Effects of cell proliferation, *Eur J Biochem,* 268**,** 5424-9.

Stanley, J. S., Mock, D. M., Griffin, J. B. and Zempleni, J. (2002) Biotin uptake into human peripheral blood mononuclear cells increases early in the cell cycle, increasing carboxylase activities, *J Nutr,* 132**,** 1854-9.

Stockert, R. J. and Ren, Q. (1997) Cytoplasmic protein mRNA interaction mediates cGMP-modulated translational control of the asialoglycoprotein receptor, *J Biol Chem,* 272**,** 9161-5.

Strahl, B. D. and Allis, C. D. (2000) The language of covalent histone modifications, *Nature,* 403**,** 41-5.

Streaker, E. D. and Beckett, D. (2006) Nonenzymatic biotinylation of a biotin carboxyl carrier protein: Unusual reactivity of the physiological target lysine, *Protein Sci,* 15**,** 1928-35.

Suormala, T., Fowler, B., Duran, M., Burtscher, A., Fuchshuber, A., Tratzmuller, R., Lenze, M. J., Raab, K., Baur, B., Wick, H. and Baumgartner, R. (1997) Five patients with a biotin-responsive defect in holocarboxylase formation: Evaluation of responsiveness to biotin therapy in vivo and comparative biochemical studies in vitro, *Pediatr Res,* 41**,** 666-73.

Suzuki, Y., Aoki, Y., Ishida, Y., Chiba, Y., Iwamatsu, A., Kishino, T., Niikawa, N., Matsubara, Y. and Narisawa, K. (1994) Isolation and characterization of mutations in the human holocarboxylase synthetase cDNA, *Nat Genet,* 8**,** 122-8.

Suzuki, Y., Aoki, Y., Sakamoto, O., Li, X., Miyabayashi, S., Kazuta, Y., Kondo, H. and Narisawa, K. (1996) Enzymatic diagnosis of holocarboxylase synthetase deficiency using apo-carboxyl carrier protein as a substrate, *Clin Chim Acta,* 251**,** 41-52.

Suzuki, Y., Yang, X., Aoki, Y., Kure, S. and Matsubara, Y. (2005) Mutations in the holocarboxylase synthetase gene hlcs, *Hum Mutat,* 26**,** 285-90.

Swift, R. (2003) Domain Mapping and functional analysis of human biotin protein ligase (honours thesis) *School of Molecular and Biomedical Science* University of Adelaide, Adelaide, p. 84.

Swift, R., Norman, M., Jitrapakdee, S., Wallace, J. C. and Polyak, S. W. (2004) Domain mapping and functional analysis of the N-terminal region of human holocarboxylase synthetase, In *Australian Health And Medical Research Congress*, poster 1146.

Tang, N. L., Hui, J., Yong, C. K., Wong, L. T., Applegarth, D. A., Vallance, H. D., Law, L. K., Fung, S. L., Mak, T. W., Sung, Y. M., Cheung, K. L. and Fok, T. F. (2003) A genomic approach to mutation analysis of holocarboxylase synthetase gene in three Chinese patients with late-onset holocarboxylase synthetase deficiency, *Clin Biochem,* 36**,** 145-9.

Taroni, F. and Rosenberg, L. E. (1991) The precursor of the biotin-binding subunit of mammalian propionyl-CoA carboxylase can be translocated into mitochondria as apo- or holoprotein, *J Biol Chem,* 266**,** 13267-71.

Tissot, G., Douce, R. and Alban, C. (1997) Evidence for multiple forms of biotin holocarboxylase synthetase in pea (Pisum sativum) and in Arabidopsis thaliana: Subcellular fractionation studies and isolation of a cDNA clone, *Biochem J,* 323 (Pt 1)**,** 179-88.

Toby, G. G. and Golemis, E. A. (2001) Using the yeast interaction trap and other two-hybrid-based approaches to study protein-protein interactions, *Methods,* 24**,** 201-17.

Touma, E., Suormala, T., Baumgartner, E. R., Gerbaka, B., Ogier de Baulny, H. and Loiselet, J. (1999) Holocarboxylase synthetase deficiency: Report of a case with onset in late infancy, *J Inherit Metab Dis,* 22**,** 115-22.

Val, D. L., Chapman-Smith, A., Walker, M. E., Cronan, J. E., Jr. and Wallace, J. C. (1995) Polymorphism of the yeast pyruvate carboxylase 2 gene and protein: Effects on protein biotinylation, *Biochem J,* 312 (Pt 3)**,** 817-25.

Villar-Garea, A. and Imhof, A. (2006) The analysis of histone modifications, *Biochim Biophys Acta,* 1764**,** 1932-9.

Waldrop, G. L., Rayment, I. and Holden, H. M. (1994) Three-dimensional structure of the biotin carboxylase subunit of acetyl-coA carboxylase, *Biochemistry,* 33**,** 10249-56.

Wallace, J. C., Jitrapakdee, S. and Chapman-Smith, A. (1998) Pyruvate carboxylase, *Int J Biochem Cell Biol,* 30**,** 1-5.

Watanabe, T. (1983) Teratogenic effects of biotin deficiency in mice, *J Nutr,* 113**,** 574-81.

Watanabe, T. and Endo, A. (1984) Teratogenic effects of avidin-induced biotin deficiency in mice, *Teratology,* 30**,** 91-4.

Watanabe, T. and Endo, A. (1990) Teratogenic effects of maternal biotin deficiency on mouse embryos examined at midgestation, *Teratology,* 42**,** 295-300.

Weaver, L. H., Kwon, K., Beckett, D. and Matthews, B. W. (2001a) Competing protein:protein interactions are proposed to control the biological switch of the E.coli biotin repressor, *Protein Sci,* 10**,** 2618-22.

Weaver, L. H., Kwon, K., Beckett, D. and Matthews, B. W. (2001b) Corepressor-induced organization and assembly of the biotin repressor: A model for allosteric activation of a transcriptional regulator, *Proc Natl Acad Sci U S A,* 98**,** 6045-50.

Weider, M., Machnik, A., Klebl, F. and Sauer, N. (2006) Vhr1p, a new transcription factor from budding yeast, regulates biotin-dependent expression of vht1 and bio5, *J Biol Chem,* 281**,** 13513-24.

Wiedmann, S., Eudy, J. D. and Zempleni, J. (2003) Biotin supplementation increases expression of genes encoding interferon-gamma, interleukin-1beta, and 3-methylcrotonyl-CoA carboxylase, and decreases expression of the gene encoding interleukin-4 in human peripheral blood mononuclear cells, *J Nutr,* 133**,** 716-9.

Wiedmann, S., Rodriguez-Melendez, R., Ortega-Cuellar, D. and Zempleni, J. (2004) Clusters of biotin-responsive genes in human peripheral blood mononuclear cells, *The Journal of Nutritional Biochemistry,* 15**,** 433-439.

Wilson, C. J., Myer, M., Darlow, B. A., Stanley, T., Thomson, G., Baumgartner, E. R., Kirby, D. M. and Thorburn, D. R. (2005) Severe holocarboxylase synthetase deficiency with incomplete biotin responsiveness resulting in antenatal insult in Samoan neonates, *The Journal of Pediatrics,* 147**,** 115-118.

Wilson, K., Shewchuk, L., Brennan, R., Otsuka, A. and Matthews, B. (1992) Escherichia coli biotin holoenzyme synthetase/bio repressor crystal structure delineates the biotin- and DNA-binding domains, *PNAS,* 89**,** 9257-9261.

Wolf, B., Grier, R. E., Allen, R. J., Goodman, S. I. and Kien, C. L. (1983) Biotinidase deficiency: the enzymatic defect in late-onset multiple carboxylase deficiency, *Clin Chim Acta,* 131**,** 273-81.

Wolf, B., Heard, G. S., Weissbecker, K. A., McVoy, J. R., Grier, R. E. and Leshner, R. T. (1985) Biotinidase deficiency: Initial clinical features and rapid diagnosis, *Ann Neurol,* 18**,** 614-7.

Xu, Y. and Beckett, D. (1996) Evidence for interdomain interaction in the Escherichia coli repressor of biotin biosynthesis from studies of an N-terminal domain deletion mutant, *Biochemistry,* 35**,** 1783-92.

Yang, X., Aoki, Y., Li, X., Sakamoto, O., Hiratsuka, M., Gibson, K. M., Kure, S., Narisawa, K., Matsubara, Y. and Suzuki, Y. (2000) Haplotype analysis suggests that the two predominant mutations in Japanese patients with holocarboxylase synthetase deficiency are founder mutations, *J Hum Genet,* 45**,** 358-62.

Yang, X., Aoki, Y., Li, X., Sakamoto, O., Hiratsuka, M., Kure, S., Taheri, S., Christensen, E., Inui, K., Kubota, M., Ohira, M., Ohki, M., Kudoh, J., Kawasaki, K., Shibuya, K., Shintani, A., Asakawa, S., Minoshima, S., Shimizu, N., Narisawa, K., Matsubara, Y. and Suzuki, Y. (2001) Structure of human holocarboxylase synthetase gene and mutation spectrum of holocarboxylase synthetase deficiency, *Hum Genet,* 109**,** 526-34.

Zempleni, J., Helm, R. M. and Mock, D. M. (2001) In vivo biotin supplementation at a pharmacologic dose decreases proliferation rates of human peripheral blood mononuclear cells and cytokine release, *J. Nutr.,* 131**,** 1479-1484.

Zempleni, J. and Mock, D. (1999) Biotin biochemistry and human requirments, *Journal of nutritional biochemistry,* 10**,** 128-138.

Zempleni, J. and Mock, D. M. (2000) Marginal biotin deficiency is teratogenic, *Proc Soc Exp Biol Med,* 223**,** 14-21.

Zhu, Z., Zheng, T., Lee, C. G., Homer, R. J. and Elias, J. A. (2002) Tetracycline-controlled transcriptional regulation systems: Advances and application in transgenic animal modeling, *Semin Cell Dev Biol,* 13**,** 121-8.